Geoarchaeological contributions to the study of the initial settlement of the southern Peruvian Andes

Dissertation

der Mathematisch-Naturwissenschaftlichen Fakultät

der Eberhard Karls Universität Tübingen

zur Erlangung des Grades eines

Doktors der Naturwissenschaften

(Dr. rer. nat.)

vorgelegt von

Sarah Ann Meinekat

aus Bad Neuenahr-Ahrweiler

Tübingen

2025

Gedruckt mit Genehmigung der Mathematisch-Naturwissenschaftlichen Fakultät der Eberhard Karls Universität Tübingen.

Tag der mündlichen Qualifikation:	19.12.2025
Dekan:	Prof. Dr. Thilo Stehle
1. Berichterstatter:	Prof. Dr. Christopher E. Miller
2. Berichterstatter:	Assoc. Prof. Dr. Kurt Rademaker
3. Berichterstatterin	Assoc. Prof. Dr. Ximena Villagran

For and thanks to my family and friends.

Contents

Figures

Tables

Abbreviations

µFTIR	micro-Fourier Transform Infrared Spectroscopy
µXRF	micro-X-Ray Fluorescence Spectroscopy
EH	Early Holocene
LH	Late Holocene
LMH	Late Middle Holocene
masl	Meters above sea level
QJ-280	Quebrada-Jaguay-280
SEM	Scanning Electron Microscope
TP	Terminal Pleistocene

Abstract

Cuncaicha rock shelter and Quebrada Jaguay-280 are pivotal sites for understanding the initial settlement of the southern Peruvian Andes and coast during the Terminal Pleistocene and Early Holocene. Prior to this dissertation, no detailed geoarchaeological study focused on site formation processes at sites dated to the period of initial settlement of the region, leaving critical questions unresolved regarding the formation history of deposits, the preservation and interpretation of anthropogenic materials, and the nature of occupation and inter-site relations between the coast and the high Puna.

This study establishes a microcontextual framework for understanding site formation processes, (micro-) stratigraphy, and human-environment interactions at Cuncaicha rock shelter and Quebrada Jaguay-280. Through an integrated analytical approach combining soil and sediment micromorphology, micro-Fourier Transform Infrared Spectroscopy (μFTIR), and micro-X-Ray Fluorescence (μXRF), this research characterises the (micro-) stratigraphic sequences and depositional histories of both localities. Complementary experimental studies examining fuel resource exploitation in the high Puna environment provide reference data for identifying and interpreting anthropogenic activities preserved in the stratigraphic record.

The resulting high-resolution stratigraphic framework provides the contextual foundation necessary for interpreting archaeological assemblages, refining radiocarbon-based chronologies, and directing future geoarchaeological research at these sites. This microcontextual methodology enables precise documentation of anthropogenic and natural depositional processes, offering critical insights into the temporal and spatial patterning of human occupation and paleoenvironmental conditions.

By addressing these issues, this dissertation not only advances our understanding of the early human occupation of the region but also proposes an advanced methodological approach for interpreting complex archaeological sites in contrasting environmental contexts.

Zusammenfassung

Cuncaicha und Quebrada Jaguay-280 stellen Schlüsselfundstätten für die Erforschung der initialen Besiedlung der südperuanischen Anden und Küstenregion im späten Pleistozän und frühen Holozän dar. Bis zur vorliegenden Dissertation fehlte eine detaillierte geoarchäologische Untersuchung der Fundplatzgenese in dieser frühesten Besiedlungsphase, sodass wesentliche Fragen zur Sedimentationsgeschichte, zur Erhaltung und Interpretation anthropogener Hinterlassenschaften sowie zu Besiedlungsmustern und den Beziehungen zwischen Küsten- und Puna-Fundstätten in der Region unbeantwortet blieben.

Die vorliegende Arbeit entwickelt einen mikrokontextuellen Analyserahmen zur Erfassung von Fundplatzgenese, (Mikro-)Stratigraphie und Mensch-Umwelt-Interaktionen in Cuncaicha und Quebrada Jaguay-280. Mittels eines integrativen analytischen Ansatzes, der Boden- und Sedimentmikromorphologie, Mikro-Fourier-Transform-Infrarotspektroskopie (μFTIR) und Mikro-Röntgenfluoreszenz (μXRF) verbindet, charakterisiert diese Forschung die (mikro-)stratigraphischen Sequenzen und Ablagerungsgeschichten beider Fundplätze. Eine ergänzende experimentalarchäologische Studie zur Nutzung von Brennstoffressourcen in der Puna-Landschaft liefert Referenzdaten für die Identifizierung und Interpretation anthropogener Aktivitäten im stratigraphischen Befund.

Das hieraus resultierende hochauflösende stratigraphische Modell bildet die kontextuelle Basis für die Interpretation archäologischer Funde, die Präzisierung von Radiokarbon-Chronologien und die Ausrichtung zukünftiger geoarchäologischer Forschungen an diesen Fundstätten. Der mikrokontextuelle Ansatz ermöglicht eine präzise Dokumentation anthropogener und natürlicher Sedimentationsprozesse und liefert wesentliche Erkenntnisse zu den zeitlichen und räumlichen Mustern menschlicher Besiedlung sowie zu paläoökologischen Rahmenbedingungen.

Durch die Bearbeitung dieser Fragestellungen leistet die Dissertation nicht nur einen Beitrag zum vertieften Verständnis der frühen menschlichen Besiedlung der Region, sondern entwickelt zugleich einen fortgeschrittenen methodischen Ansatz für die Interpretation komplexer archäologischer Fundstätten in heterogenen Umweltkontexten.

Resumen

El abrigo rocoso de Cuncaicha y Quebrada Jaguay-280 son contextos arqueológicos claves para la comprensión del poblamiento inicial de los Andes y la región costera del sur de Perú, durante el Pleistoceno Final y el Holoceno Temprano. Hasta la publicación de esta tesis doctoral, no existía un estudio geoarqueológico enfocado en los procesos de formación de sitios datados para el periodo de poblamiento tempranos en esta región, quedando sin respuesta cuestiones fundamentales sobre la historia de la formación de los depósitos, la conservación e interpretación de los materiales antropogénicos, la naturaleza de la ocupación y las relaciones entre los yacimientos costeros y los de la alta Puna.

La presente investigación establece un marco de análisis microcontextual para la comprensión de los procesos de formación de sitios, la (micro)estratigrafía y las interacciones desarrolladas entre el ser humano y el ambiente en Cuncaicha y Quebrada Jaguay-280. Mediante un enfoque analítico integrador que combina micromorfología de suelo y sedimentos, espectroscopía infrarroja por transformada de Fourier (μFTIR) y fluorescencia de rayos X (μXRF), este trabajo caracteriza las secuencias (micro)estratigráficas y las historias deposicionales de ambos sitios. s. Un estudio arqueológico experimental complementario examina el uso de recursos combustibles en el paisaje de la alta Puna, proporcionando datos de referencia para la identificación e interpretación de las actividades antropogénicas en el registro estratigráfico de Cuncaicha.

El resultado de este modelo estratigráfico de alta resolución constituye una base contextual para la interpretación de conjuntos arqueológicos, precisando las cronologías de radiocarbono y orientando las futuras investigaciones geoarqueológicas en estos yacimientos. La metodología microcontextual permite precisar el registro de los procesos de depositación antropogénicos y naturales, ofreciendo información crítica sobre los patrones temporales y espaciales de ocupación humana y sobre las condiciones paleoecológicas.

Al abordar estas temáticas, esta tesis doctoral no solo profundiza en la comprensión de los primeros asentamientos humanos de la región, sino que también propone un enfoque metodológico avanzado para la interpretación de sitios arqueológicos complejos en contextos ambientales contrastantes.

List of Publications for Cumulative Dissertation

This section presents the publications published, submitted, or in preparation for fulfilment of a cumulative dissertation at the Faculty of Science at the University of Tübingen. The requirement is at least two manuscripts accepted for publication.

Numbers in parentheses at the end of each citation present the percentage extent and significance of my personal contribution **(scientific idea/ data generation/ analysis and interpretation/ paper writing)** in this dissertation, in accordance with § 6,2 of the Doctoral Degree Regulations of the Faculty of Science at the University of Tübingen.

Published Manuscripts:

Paper 1 **Meinekat SA**, Miller C, and Rademaker K, 2021. A site formation model for Cuncaicha rock shelter: Depositional and post-depositional processes at the high-altitude keysite in the Peruvian Andes. Geoarchaeology 37: 304–331. **(70/90/90/80)**

Paper 2 **Meinekat SA**, Milton EBP, Furlotte B, Zarrillo S, and Rademaker K, 2023. Fire as High-Elevation Cold Adaptation: An Evaluation of Fuels and Terminal Pleistocene Combustion in the Central Andes. Quaternary Science Reviews 316, 108244.
(80/70/90/80)

Paper 3 **Meinekat SA**, Milton EBP, Osorio D, Mentzer SM, Miller CE, Sandweiss DH, and Rademaker K. Microstratigraphy and site formation processes at Quebrada-Jaguay 280 (Peru). Geoarchaeology 41: e70054.
(90/80/90/90)

List of Additional Publications

Paper 4 Marcazzan D and **Meinekat SA** (2022) Creating Qualitative Datasets in Geoarchaeology: An easy-applicable description template for archaeological thin section analysis using Stoops 2003. *MethodsX*, 101663.

Chapter 1: Introduction

This doctoral thesis presents the first systematic geoarchaeological investigation of two interconnected sites in the Central Andes of southern Peru, both of which date to the period of initial peopling of the region. The geoarchaeological work focuses on the sites of Cuncaicha rock shelter in the high Andes, and Quebrada Jaguay-280 which lies on the arid Pacific coast. These studies are complemented by an experimental study that furthers our understanding of the (paleo-)landscape and resources therein.

Although – or perhaps precisely because - Cuncaicha rock shelter and Quebrada Jaguay-280 occupy opposite ends of a challenging environmental spectrum, their connection provides a unique framework for examining early settlement systems during the first human dispersals across South America.

Initial Human Settlement

The initial human settlement of South America remains a central topic in archaeological research, particularly in the Andes region, with increasing evidence supporting a Late Pleistocene occupation dating to after 13 ka, despite ongoing debate over exact chronologies, with some earlier dates (Borrero, 2016; Borrero & Santoro, 2022a; Goebel et al., 2008; Pitblado & Rademaker, 2024; Politis et al., 2016; Prates et al., 2020; Rademaker, 2024; Steele & Politis, 2009; Waters, 2019).

A recent comprehensive study of radiocarbon chronologies demonstrates that during the period of initial occupation, the Terminal Pleistocene (>11.7 ka) and the first two millennia of the Early Holocene (11.7-8.8 ka), archaeological evidence in Peru is clustered in two groups: 1) Archaeological sites along the Pacific coast, and 2) archaeological sites in the Andean highlands above 2,500 masl (Rademaker, 2024).

In the Pacific coastal and Central Andean regions of South America, early human settlers were confronted with exceptionally diverse and often extreme environmental conditions, ranging from hyperarid coastal deserts and to high elevation zones exceeding 4,000 masl (Pulgar Vidal, 1987; Troll, 1958, 1968) (Figure 1).

Those environments pose specific frame conditions to human lifeways.

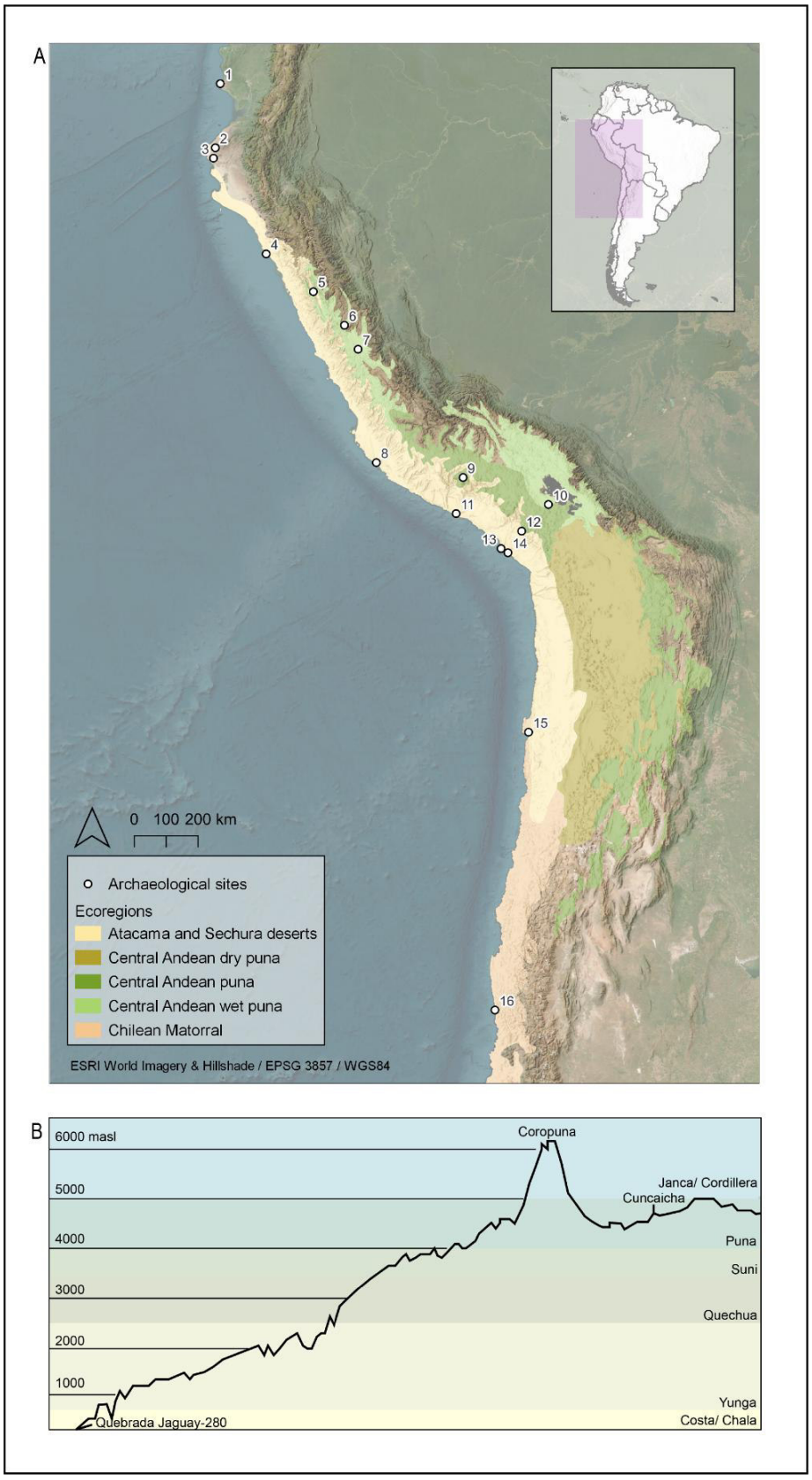

Figure 1: A: Map of the Central Andes with ecoregions after Dinerstein et al. (2017) and archaeological sites named in the following section. 1 – Las Vegas, 2 – Siches sites, 3 – Paiján sites, 4 – Huaca Prieta, 5 – Guitarrero Cave, 6 – Lauricocha,, 7 – Pachamachay, 8 – La Yerba, 9 – Cuncaicha, 10 – Soro Mik'aya Patjxa, 11 – Quebrada Jaguay-280, 12 – Asana, 13 – Ring Site, 14 – Quebrada Tacahuay, 15 – La Chimba 13, 16 – Quebrada Santa Julia. B: Vertical ecoregions of Peru after Pulgar Vidal (1987). Transect between Quebrada Jaguay-280 and Cuncaicha, summit of Nevado Coropuna shown.

The distribution and the chronology of early sites prompt key questions regarding human adaptation to diverse environments and the extent to which coastal and highland sites formed components of local, broader, and contemporaneous settlement networks (Santoro et al., 2019; Santoro & Núñez, 1987). These issues fundamentally concern subsistence, mobility, and interzonal connectivity at the landscape level (Santoro et al., 2019; Santoro & Núñez, 1987).

Theories on Subsistence and Adaptation

Several hypotheses regarding human adaptation to coastal versus highland settings, and the links between these zones, have previously been proposed in the archaeological literature.

Along the Pacific coast in South America, early coastal adaptations have been understood largely in terms of reliance on maritime resources, as evidenced by the faunal remains at early coastal sites (Engel, 1957, 1970; Prieto & Sandweiss, 2020; Sandweiss, 2014).

Maritime subsistence has been argued to have played a critical role in laying the groundwork for the development of Andean civilisations (Maritime Foundations of Andean Civilization (MFAC)) (Moseley, 1975), though recent investigations have reevaluated the degree of dietary dependence on maritime resources.

While marine resource exploitation appears widespread and the primary dietary resource across some early coastal sites such as Quebrada-Jaguay-280 (Sandweiss et al., 1998), Quebrada Tacahuay (deFrance, 2009; Keefer et al., 1998), the Ring Site (Sandweiss et al., 1989) and La Chimba 13 (Llagostera et al., 2000), certain locations exhibit divergent or more heterogeneous patterns of subsistence strategies during the early preceramic (*sensu* Sandweiss (2014), ~TP-EH), such as Las Vegas (Stothert, 1985; Stothert et al., 2003), the Paiján sites (Chauchat, 1988; Dillehay et al., 2003), Huaca Prieta (J. B. Bird et al., 1985; Dillehay et al., 2012), the Siches sites (Piperno, 2011), and during later preceramic periods, *e.g*. at La Yerba (Beresford-Jones et al., 2018). The archaeological assemblage from Quebrada Santa Julia, located further south along the coast of Chile, notably lacks indicators of maritime subsistence exploitation (Jackson et al., 2007). This absence stands in contrast to the maritime adaptations documented at other sites within the same coastal region (Jackson et al., 1999, 2007).

So, while the MFAC theory has been nuanced, the viability of fisher-(hunter-gatherer) subsistence strategies in early coastal environments as a successful adaptation to the coast is broadly acknowledged.

Highland adaptations and subsistence strategies of early Andean hunter-gatherers, on the other hand, have been examined through multiple, occasionally conflicting, theoretical perspectives, centring on whether highland occupations were contemporaneous with, or subsequent to lowland sites. Underlying this debate is the dichotomy of the presumed (in)habitability of the highlands, given the ecological and biological constraints of life at high-elevation (Aldenderfer, 1998), versus the resource richness of the Dry Puna (Núñez & Santoro, 1988; Osorio et al., 2017) and the Wet Puna (Rick, 1980).

It has been suggested that highland settlement followed lowland occupations, proceeding slowly as populations adapted biologically to the new environment as suggested from sites like Asana and Soro Mik'aya Patjxa (Aldenderfer, 1998, 2006; Haas et al., 2017). Others have proposed that highland habitation occurred gradually, reflecting a process of landscape learning for early sites in the south-central Atacama (Loyola et al., 2019), or following climatic shifts that created more favourable conditions but then was persistent in the Argentinian Puna (Yacobaccio, 2017). Further, transhumance with seasonal, high residential mobility between low and high elevation zones has been suggested especially for Central Peruvian site complexes, among those for example Guitarrero Cave (Lanning, 1967; Lavallée, 2000; Lynch, 1971). Some researchers have anticipated an immediate and continuous use of the highlands in Peru at sites such as Lauricocha and Pachamachay (Cardich, 1964; Rick, 1980), enabled by rich resource availability, especially in terms of food (“virtual meat larder” (Rick, 1980, p. 3)), with only shelter and fuel (*Author’s note: keep in mind for later*) being argued to be scarce (Rick, 1980, p. 25).

Although no consensus exists regarding the most probable model, it is anticipated that early populations employed a complex mobility system incorporating both inter- and intra-zonal connections (Borrero & Santoro, 2022; Osorio et al., 2017; Santoro & Núñez, 1987).

The issue is exacerbated by a persistent research bias favouring coastal over highland excavations (Santoro & Núñez, 1987; Schiappacasse & Niemeyer, 1975), though at

the same time, some coastal sites may have been subjected to fluctuating paleoshorelines (Richardson, 1981).

Additionally, it remains unclear whether comparable adaptive strategies should be expected across such a wide latitudinal span as the Andes, or even just the Central Andean Puna(s), or whether such generalisations obscure important ecological and cultural differences and more regional approaches are sensible (López Mendoza et al., 2024).

Core Research Objectives

To better understand these processes – at least in the Central Andes of southern Peru – a twofold archaeological approach is required:

1) Site-level investigations, which generate high-resolution data necessary for constructing reliable radiocarbon chronologies and for obtaining detailed information on site formation processes and functional site use
2) Inter-site-level investigations, which examine networks of contemporaneous early sites across coastal and highland regions

By applying a geoarchaeological approach to the deposits at Quebrada Jaguay-280 and Cuncaicha rock shelter, we aim to generate high-resolution, contextual data to clarify the contexts of the deposits and within their respective environmental settings, as well as to situate them within broader temporal and spatial patterns of human occupation.

1.1 Case Studies: Quebrada Jaguay-280 and Cuncaicha rock shelter

1.1.1 Quebrada Jaguay-280

Quebrada Jaguay-280 (QJ-280), a multicomponent site on the hyper-arid southern Peruvian coast (Figure 2), has been a key site for understanding Terminal Pleistocene–Early Holocene maritime adaptations and early coastal settlement in South America (Sandweiss et al., 1998). The site has produced data that document early coastal resource use, lithic technology, and interzonal connections to the highlands (Sandweiss et al., 1998).

Figure 2: Map of southern Peruvian coast with location of Quebrada Jaguay-280 and perennial and intermittent/ephemeral stream systems in the region (top). Photograph of the site (bottom).

Excavations and chronology

Excavations at QJ-280 during the 1990s were organised into four sectors (I–IV), with primary investigations focused on Sectors I and II (Sandweiss et al., 1998; Tanner, 2001). Sector I is characterised mainly by shell midden deposits that overlie and fill a circular, semi-subterranean Early Holocene house structure that intrude into an earlier Terminal Pleistocene midden (Tanner, 2001). Sector II consists of shell midden deposits with pit features and postholes, which may represent a rectangular structure dating to the Terminal Pleistocene (Tanner, 2001).

Sandweiss et al. (1998) identified a Terminal Pleistocene (13–11 ka), an Early Holocene I (10.6–10 ka), and an Early Holocene II (~8.7–8.2 ka) component at QJ-280 based on conventional radiocarbon ages. Later, Jones et al. (2019) documented an additional mid-Holocene component.

Subsistence and seasonality

The interpretation of a maritime adaptation at QJ-280 derives from the scarcity of terrestrial fauna and the abundance of marine remains (McInnis, 1999; Reitz et al., 2016, 2017; Sandweiss et al., 1998). Analysis of these faunal remains by Reitz et al. (2016, 2017) indicates that specialised fishing practices were in place from the site's earliest occupations. Sandweiss et al. (1998) proposed a seasonal occupation of QJ-280 during the Terminal Pleistocene and Early Holocene, linked to the availability of water during the austral summer.

Recent studies of marine shell isotopes narrow the timing of occupation to February and March (Gruver, 2018). A recent study of macrobotanical remains at the site by Furlotte (2024) suggests that the occupants of the site broadened their subsistence strategy by incorporating plants into their diets, some of which suggest site visits beyond the previously proposed season due to plant part seasonality.

Lithics, cacti, and interzonal connection

Finds of non-coastal materials at QJ-280 indicate links with regional, intermediate, and highland zones as early as the Terminal Pleistocene (Sandweiss et al., 1998; Sandweiss & Rademaker, 2011). The macrobotanical study at QJ-280 (Furlotte, 2024) finds connections to the lomas zone between 200-1000 masl that provides plant resources during the austral winter (July-September), when the coastal fog (*garúa*) is

most prominent (Dillon et al., 2003, 2011). Further, *Opuntia* sp. (prickly pear cactus) seeds, a plant that in Peru grows above 2,000 meters, have been found at the site, strengthening the intermediate elevation inland connections (Sandweiss & Rademaker, 2011).

In addition, the earliest deposits contain tools made from Alca-1, Alca-4, and Alca-5 obsidian, which is sourced from the highlands (Rademaker et al., 2013, 2022).

New excavations

Fieldwork in 2017 revisited intact deposits and old excavation profiles. Besides the novel macrobotanical evidence from QJ-280, and the occupational seasonality study based on *mesodesma donacium* geochemical analysis (Gruver, 2018), the most recent fieldwork aimed at a new radiocarbon chronology based on short-lived botanical remains (Furlotte, 2024). Beyond redating the site, another goal of the 2017 fieldwork was to better understand the stratigraphy and micro-context of QJ-280.

Critiques and Debates

QJ-280 is a renowned site supporting an early (TP-EH) maritime adaptation during the time of initial settlement of the continent, along with other sites along the Pacific coast in Peru (*e.g.*, Huaca Prieta, Ring site, Quebrada Tacahuay, Quebrada de los Burros) and Chile (*e.g.*, La Chimba 13 and Punta Ñagué) (deFrance, 2009; Dillehay et al., 2012, 2017; Jackson & Méndez, 2005; Keefer et al., 1998, 2003; Lavallée et al., 2011; Llagostera et al., 2000; Reitz et al., 2016).

However, a recent review of radiocarbon chronologies in Peru has highlighted the dire need to redate early coastal sites due to general issues with the dating materials and methods, number of ages obtained, and the high chance of a severe old wood effect (Rademaker, 2024), applying to some sites more (Dillehay et al., 2012, 2017) than to others.

Further, no geoarchaeological investigation at QJ-280 focusing on site formation and micro-context has been conducted yet. However, a study of the site stratigraphy and stratigraphic integrity is a necessary first step to obtain any reliable material for dating – at QJ-280, as well as at other sites. Further, many of the previous interpretations at QJ-280 rely on stratigraphic field observations (Sandweiss et al., 1998; Tanner, 2001). These interpretations require a more detailed, microcontextual investigation to verify.

1.1.2 Cuncaicha rock shelter

Cuncaicha Rockshelter, located at 4,480 masl in the Pucuncho Basin in the Dry Puna of the southern Peruvian Andes (Figure *3*), is one of the highest known Pleistocene archaeological sites in the world (Rademaker, 2014; Rademaker et al., 2014). Excavations at Cuncaicha have yielded compelling evidence of early high-altitude human occupation, beginning as early as 12.4 ka, challenging long-standing assumptions about the timing and nature of the initial human settlement of high Andean environments (Rademaker et al., 2014).

Early Occupation

Rademaker et al. (2014) reported more than 20 radiocarbon dates older than 11.5 ka from Cuncaicha. Continuous refinement of the original radiocarbon chronology (Rademaker & Hodgins, 2018) of the site yielded 23 ages dating to the Late Pleistocene (>11.7 ka), eleven ages dating to the Early Holocene (11.7-8.8 ka), three ages dated to the Early to Early-Middle Holocene (8.8-7.8 ka), six ages dating to the Late-Middle-Holocene (5.5-4.2 ka), and an additional two ages dating to the Late Holocene (<4.2 ka) (Rademaker, 2024; Rademaker & Hodgins, 2018). The thorough dating of ultra-filtered and XAD-purified faunal bone collagen creates one of the most robust radiocarbon chronologies in Peru, especially for the Late Pleistocene and Early Holocene occupations (Rademaker, 2024).

Technology, Subsistence, and High-Elevation Adaptation

While the location of the site in the Puna >4000 masl has repeatedly been claimed harsh and inhospitable (Capriles et al., 2016), analysis of the extensive archaeological record at Cuncaicha—particularly comparisons of its lithic and faunal assemblages with those from other high-altitude Andean sites—suggests that the location may have functioned as a residential base camp as early as the Terminal Pleistocene (Rademaker & Moore, 2019). On-going analyses focus on lithic technologies (Osorio et al., in prep.). Mobility and subsistence studies based on stable isotope analyses have been conducted (Chala-Aldana et al., 2018; Haller von Hallerstein, 2017), and have been refined and corrected in recent years, indicating a subsistence based on highland resources and mobility within the high-elevation landscape (>4,000 masl) (Milton et al., 2022, in prep.).

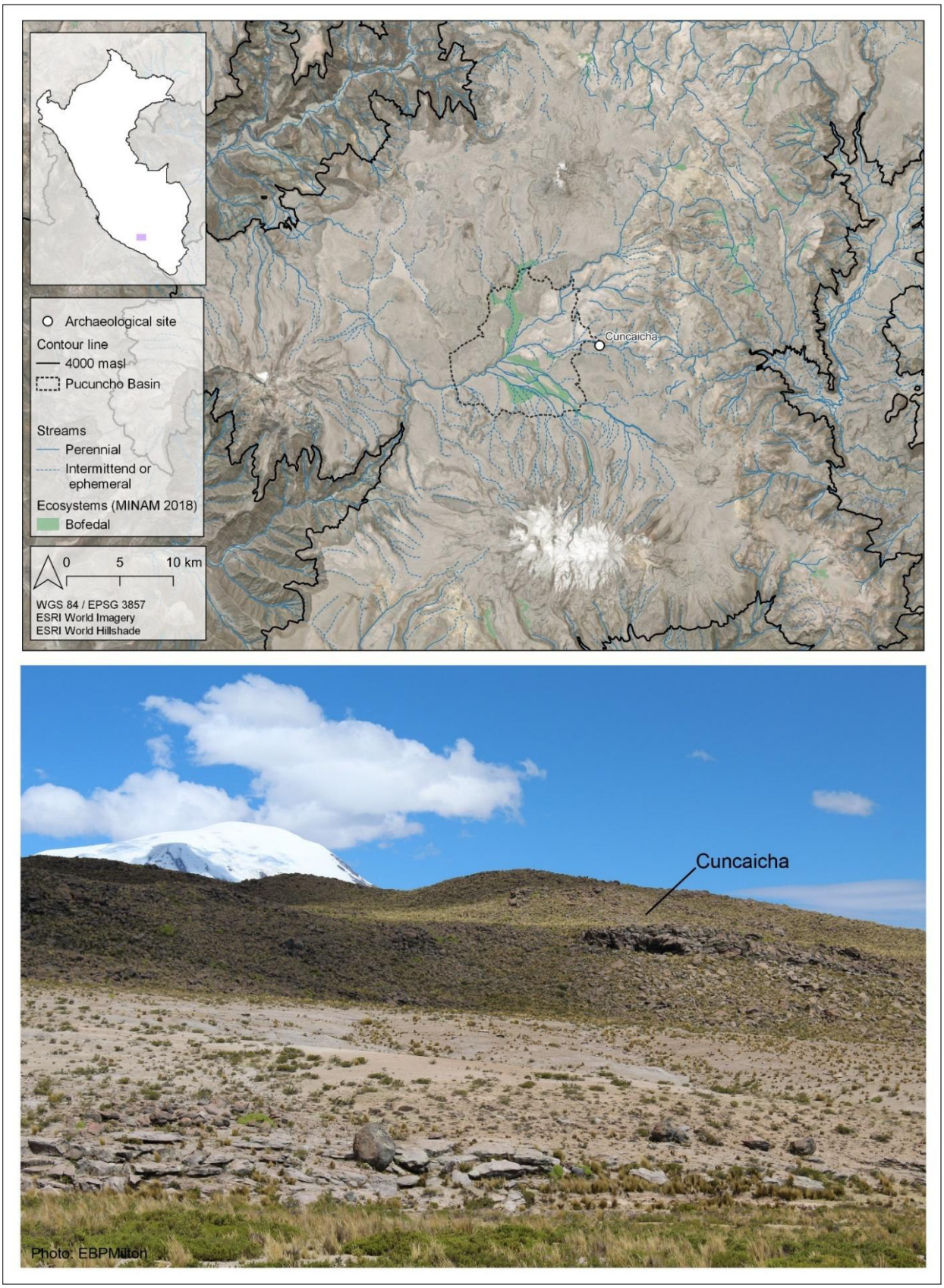

Figure 3: Map of the Pucuncho Basin in the Central Andes of southern Peru with location of Cuncaicha rock shelter, perennial and intermittent/ephemeral stream system, and high-elevation wetland ecosystems (*bofedal*) (top). Photograph of the site (bottom).

Human Skeletal Remains

Cuncaicha also contains some of the oldest human skeletal remains known from the Andean highlands, with five individuals buried at the site, dating to the Early Holocene (n=3) and Late Holocene (n=2) (Francken et al., 2018; Rademaker & Hodgins, 2018). Francken et al. (2018) conducted a comprehensive osteological analysis of these remains, which span from the Early to the Late Holocene. The study documented variation in cranial and post-cranial morphology, indicators of habitual activity (*e.g.*, osteoarthritis), and general health status (Francken et al., 2018). The remains suggest a physically active lifestyle consistent with high-altitude foraging and mobility (Francken et al., 2018). The mortuary contexts, though simple, are significant for their antiquity and provide rare insight into early Andean lifeways (Francken et al., 2018). Further studies focus on manual activities hinting at habitual and forceful precision grasping tasks (Karakostis et al., 2021), as well as a cranial study of one of the Early Holocene individuals comparing east-west skull patterns in South America (Menéndez et al., 2019).

Ancient DNA and Population History

Cuncaicha has also contributed to the emerging picture of South American population history through ancient DNA studies. Samples from the site were included in Posth et al. (2018) and subsequent studies (Nakatsuka et al., 2020), which examined genomic data from nearly 50 ancient individuals across Central and South America. These studies found that early individuals at Cuncaicha and elsewhere in the Andes carry ancestry closely related to early North American, before populations were replaced or admixed with other lineages across much of the continent, although the high Andes—including Cuncaicha—may have retained greater genetic continuity (Nakatsuka et al., 2020; Posth et al., 2018). The genetic data also support the emergence of Andean-specific genetic structure by the mid-Holocene, with evidence of long-term continuity and gene flow within the highlands and between the highlands and Pacific coast (Nakatsuka et al., 2020; Posth et al., 2018).

Critiques and Debates

Despite its robust dataset, Cuncaicha has not been without critique. Capriles et al. (2016) have argued for more conservative interpretations of high-altitude Pleistocene occupation, emphasising the extreme physiological and ecological constraints of these

environments, which is directly related to contrasting theories about the initial settlement process (Aldenderfer, 1998). While the proposed consistent and diverse use of local resources and residential features at Cuncaicha argue against a purely short-term occupation, this remains an open question warranting further studies at Cuncaicha.

What remains lacking to date in support of this argument are a comprehensive analysis of the deposit, the stratigraphic integrity, and site formation. Further studies concerning lithic technology, the faunal remains, provenance of materials, and an integrated synthesis of the archaeological assemblage will contribute greatly to our understanding of Pleistocene peopling of the Puna.

1.2 Geoarchaeology: Site Formation Processes, Anthropogenic Features, Micro-Context, and Experimental Geoarchaeology

This thesis aims to contribute to the above questions pertaining to the initial settlement of the southern Peruvian Andes, by using a geoarchaeological approach to study the site formation at Cuncaicha rock shelter and Quebrada Jaguay-280.

Geoarchaeology, in general, tries to answer archaeological questions by applying concepts and methods from the geosciences (Miller, 2011). It is a very broad field, people have tried to narrow down the definition and name, but ultimately we are always linking some kind of geo-data to past human activities (Goldberg & Macphail, 2006; Pollard, 1999; Rapp & Hill, 2006).

As befits any geoarchaeological thesis - and at the risk of disciplinary cliché - I reference Renfrew's (1976) foundational observation that "every problem in archaeology starts as a problem in geoarchaeology." – a maxim as frequently quoted as it is valid. This principle calls for a methodological shift from material culture studies to holistic examination of the stratigraphic matrix, “the deposit”, and its inherent complexities.

1.2.1 Site Formation Processes

Understanding the deposit as part of the archaeological record (Miller, 2011), is tightly linked to questions of site formation processes, including depositional and post-depositional processes (Goldberg et al., 1993; Karkanas & Goldberg, 2018; Schiffer, 1972, 1987; Stein, 1987, 2001).

Michael B. Schiffer established the fundamental distinction between cultural formation processes (c-transforms), and natural formation processes (n-processes) (Schiffer, 1972, 1987). The objective of c-transforms is to understand the processes through which artefacts were incorporated into the depositional context in which they are found, differentiating between primary (where used) and secondary (moved from location of use) deposition, systemic (active use) and archaeological (deposited) context (Schiffer, 1972, 1987). The objective of n-transforms is to understand the processes that affect the artefacts after deposition, through post-depositional modifications by natural agents, such as bioturbation, pedogenesis, erosion, chemical weathering and trampling (Schiffer, 1972, 1987).

The study of site formation processes were expanded by integrating soil and sediment, aka the entire deposit (aside from classical “artefacts”) into considerations (Stein, 1987, 2001). A key aspect of this work involves distinguishing between natural and cultural sediment inputs, adopting a multi-scalar approach to the study of deposits, and recognizing that deposits are dynamic systems shaped by the ongoing interaction of both natural and cultural processes (Stein, 1987, 2001).

Advocating a holistic approach to the archaeological deposit, the systematic application of micromorphology has become a key method to study the deposit – with foundational work by Cornwall (1953) and Dalrymple (1958) in the 1950s. Micromorphology as a primary analytical approach for examining site formation processes (depositional and post-depositional) at the microscopic level, providing critical insights into stratigraphic preservation, the origin of, and the integrity within deposits has become more established in Prehistoric archaeology since the 1980s (Goldberg, 1979; Goldberg et al., 1993). A comprehensive discussion of micromorphological methodology and its foundational applications in archaeological research is provided in Chapter 3.2.1 Micromorphology.

1.2.2 Anthropogenic Features

Aside from understanding “natural” processes of deposition and post-deposition that affect the deposit and artefacts therein, another focus of geoarchaeological studies of site formation is the examination of features, *i.e*. horizontally and vertically constrained, depositional or erosional contexts (Eggert, 2008; Miller, 2011). Anthropogenic features are part of the deposit and site formation, and connect natural and cultural processes as they relate to human activities, in which human (= anthropogenic) agency is the main driver of deposition (or erosion), allowing for inferences about human behaviour (Courty, 2001; Miller, 2011). Anthropogenic features relate to a variety of human behaviours, *e.g*. middens and dumping (Schiegl et al., 2003; Shillito et al., 2011), bedding (Goldberg et al., 2009), trampling (Banerjea et al., 2015; Marcazzan et al., 2023; Rentzel et al., 2017), and combustion (Goldberg et al., 2009; Haaland et al., 2021; Leierer et al., 2020; Mallol et al., 2013a; Marcazzan et al., 2022, 2023; Meignen et al., 2007).

Given the central role of fire in human evolution and archaeological research (Chazan, 2017; Clark & Harris, 1985; Karkanas et al., 2007; Kuhn & Stiner, 2019; Murphree & Aldeias, 2022; Sandgathe, Dibble, Goldberg, McPherron, & Hodgkins, 2011; Sandgathe, Dibble, Goldberg, McPherron, Turq, et al., 2011; Sandgathe & Berna, 2017; Shimelmitz et al., 2014; Sorensen, 2017, 2019), fire and its recognition has received considerable attention in geoarchaeological research (Canti, 2025; Goldberg et al., 2017; Stahlschmidt et al., 2020). The microanalytical identification and classification of combustion features reveals complexity and variability in combustion signatures and fire residues, related to burning conditions, fuel sources, and post-depositional modifications (Aldeias, 2017; Goldberg et al., 2017; Mallol et al., 2013a; Mallol et al., 2017; Mentzer, 2012; Miller et al., 2010; Théry-Parisot, 2002).

1.2.3 Micro-Context

A main goal of this thesis is to generate contextual information, or - shifting to the microscopic scale – microcontextual information. The microcontextual approach combines micromorphology, a method to allow analysis of an artefact/ feature/ deposit in its association with its provenience and surrounding matrix, with other high-

resolution micro-analytical techniques, such as *e.g*. µFTIR, µXRF, SEM, phytoliths and organic petrology, in which the results of those additional analyses directly link to the contextual frame provided by micromorphology (Goldberg et al., 2017; Goldberg & Berna, 2010; Mentzer & Quade, 2013). The microcontextual approach is implemented across a diverse array of archaeological sites spanning different chronological and geographical contexts, yielding a wealth of information about site formation, and on combustion features in particular (Berna et al., 2012; Goldberg et al., 2001, 2017; Haaland et al., 2021; Karkanas et al., 2007; Leierer et al., 2020; Marcazzan et al., 2022, 2023; Miller et al., 2013; Shahack-Gross et al., 2014; Stahlschmidt et al., 2015; Villagran et al., 2017; Wadley et al., 2011).

1.2.4 Experimental Geoarchaeology

The use of experimental frameworks to generate comparative reference data for identifying anthropogenic signatures within sedimentary sequences is a widely adopted methodological approach in geoarchaeological research. Experimental geoarchaeological research has addressed diverse topics, including for example identifying activity areas (Banerjea et al., 2015), examining the effect of animal trampling (Eren et al., 2010), lime plaster identification (Karkanas, 2007), stabling deposits (Macphail et al., 2004), bedding constructions (Miller & Sievers, 2012), ash composition (Shahack-Gross & Ayalon, 2013), and shell midden deposits (Villagran et al., 2011a).

Fire has emerged as a focal topic in experimental geoarchaeology as well, with studies aimed at characterising combustion signatures, understanding the formation, and taphonomic processes governing their expression and preservation in archaeological deposits (Aldeias, 2017). Mallol et al. (2013) and Miller et al. (2010) have studied the effect of different human actions on combustion structures. Aldeias et al. (2016) examined how heat alters underlying deposits. Aldeias et al. (2019) investigate the microarchaeological record of shellfish roasting. Haaland et al. (2017) show how experimental burning of glauconite minerals can be employed as a proxy for heat distribution in a deposit.

Considerable research effort has centred specifically on experimental studies examining different fuel sources and their resulting combustion residues (for example (Buonasera et al., 2019; Costamagno et al., 2005; Mentzer, 2009; Théry-Parisot et al., 2005).

Chapter 2: Objectives of the Study

Cuncaicha rock shelter and Quebrada Jaguay-280 are key sites for understanding the initial settlement of the southern Peruvian Andes.

No detailed geoarchaeological study focused on site formation processes has been conducted before, leaving open key questions concerning the formation history of the deposits, the presence, preservation, and interpretation of anthropogenic materials and features, and the type of occupation and inter-site relations.

The aim of this doctoral dissertation is to provide **basic yet crucial** information about the (micro-) stratigraphy, site formation, and human-environment dynamics for both sites. Through this, I aim to establish a foundational framework to guide subsequent analyses of archaeological materials, the development of accurate radiocarbon chronologies, and future geoarchaeological investigations.

Objective 1

How did the archaeological sites form?

Objective 1 addresses the investigation of site formation processes, focusing on the natural and cultural factors that shape the formation and preservation of archaeological deposits. Cuncaicha rock shelter and Quebrada Jaguay-280 represent distinctly contrasting sites, suggesting different processes affecting the sites. The methodological framework however remains consistent:

- First, each site is situated within its **geomorphological and ecological contexts** to establish the broader environmental framework of occupation, deposition, and preservation
- Subsequently, the stratigraphic sequences are examined in detail, with attention to the identification of **strata, micro-units, and constituent components**
- The following step involves the characterisation of **depositional processes** responsible for the accumulation of sediments and anthropogenic materials
- Finally, **post-depositional processes** are identified and evaluated, providing insight into the integrity and taphonomic history of the deposits

Objective 2

What was the sites' function?

This objective engages with the broader archaeological discourse on the routes and dynamics underlying the initial human settlement of the Andes. Positioned at opposite extremes of an altitudinal transect from the Pacific coast to the high Andes, Quebrada Jaguay-280 and Cuncaicha rock shelter offer a unique opportunity to investigate variability in site function across distinct ecological zones. The geoarchaeological analysis centres on the identification of sedimentary signatures that inform interpretations of site function:

- At both sites, I investigate the presence of **anthropogenic components and features**, assess their state of preservation, and evaluate their association with specific **human activities**
- I evaluate whether based on the presence and spatial distribution of anthropogenic features, the arrangement and variability of components, their spatio-temporal dynamics, and the **inferred human actions** behind deposition inferences can be drawn regarding **patterns of site use and occupation intensity**

Objective 3

How did early settlers use locally available resources and how did that affect the settlement process?

Successful human settlement is contingent upon the availability and strategic utilisation of local resources. Quebrada Jaguay-280 and Cuncaicha rock shelter occupy particularly challenging environments: one situated on the hyperarid coast, and the other positioned above 4,000 meters in the high Andes, providing contrasting contexts to examine adaptive strategies. At Quebrada Jaguay-280, the exploitation of maritime resources for subsistence has been a central focus and recent studies explore the use of plant resources. At Cuncaicha, the high-elevation Puna environment is frequently depicted as an inhospitable environment, purportedly challenging human settlement through resource scarcity. Investigating this perception provides an opportunity to

assess adaptive strategies in highland contexts. Our geoarchaeological investigation focuses on fuel as a critical resource enabling the use of fire at high elevation.

- First, this study aims to investigate the range of **fuel resources potentially available** within the Puna landscape surrounding Cuncaicha that are then systematically **compared with combustion remains** recovered at the site
- This approach aims at the identification of resources exploited by early occupants, providing first insights into **strategies of resource selection**, procurement, and management within a high-altitude environment
- Lastly, we explore whether a potential **variability in successful resource exploitation** yields divergent theoretical explanations for patterns of site occupation between the two sites

Chapter 3: Material and Methods

3.1 Field Methods and Materials

A significant part of the work for this doctoral thesis was the participation in fieldwork over several years (2017, 2019, 2021-2022, 2022) during the term of the overarching projects (www.paleoandes.com). Fieldwork focussed on 1) excavation, 2) archaeological and geological survey, and 3) assemblage work.

While a lot of time, work, and effort has been invested in the general fieldwork, here I focus on fieldwork, -methods, and samples specific to the geoarchaeological investigations, and I provide a **documentation of all sediment samples** for future reference and studies (**Appendix I**).

3.1.1 Sediment Sampling

Sediment sampling focused on the collection of oriented block samples for micromorphology. Sampling strategy followed a combined approach 1) to cover the whole stratigraphic sequence and all archaeological strata present in the excavated units at the sites, and 2) to focus on special features identified in the field during excavation. Samples for micromorphology were either placed in the excavation profiles or sampled as a monolith within the excavation unit. For sampling, we used plaster bandages, as this allows us to adjust to challenging deposits at archaeological sites, unlike the use of a Kubiëna box (Karkanas & Goldberg, 2018). Block samples are annotated with a site abbreviation, followed by the year of sampling (short year), and a serial number.

In addition, we collected loose samples of bulk sediment. On the one hand, loose samples were collected surrounding the sites for reference of geological components, on the other hand, some loose samples were collected from the back of the micromorphological samples to allow for microarchaeological analyses linking to specific micro-units and layers within the block sample (Karkanas & Goldberg, 2018). Those bulk samples are annotated with the block sample ID, followed by a lower-case letter in alphabetical order (top to bottom).

Sediment samples analysed in **Paper I** all derive from field seasons in 2012, 2014, and 2015, preceding the work of this thesis. Meinekat et al. (2021) provide an overview of samples from Cuncaicha rock shelter in the paper.

In 2017, our team excavated Quebrada Jaguay-280. All samples presented in **Paper III** were collected during that field season. Beyond the two block samples that are the subject of **Paper III**, additional samples were collected for future studies and are hosted in the Geoarchaeology Working Group, Institute for Archaeological Sciences, University of Tübingen (Appendix I, Table 3).

Samples for geoarchaeological investigations deriving from fieldwork in 2019 (Excavations at Pachamachay and Panaulauca, Appendix I, Table 4 and Table 5) are not part of this thesis. All block samples for micromorphology from these sites from the year 2019 were sampled, documented, and partially processed in the laboratory by the author. All samples are hosted in the Geoarchaeology Working Group, Institute for Archaeological Sciences, University of Tübingen for future studies.

In 2022, our team conducted an archaeological and geological survey for provenance studies. Further, we conducted a combustion experiment. The results of the experiment are summarized in **Paper II**. After the experimental combustion, we sampled ash and charcoal of each of the fires. Ash smear slides, as well as bulk ash and charcoal samples that were not use during the analysis for **Paper II**, are hosted in the Geoarchaeology Working Group, Institute for Archaeological Sciences, University of Tübingen for future studies (Appendix I, Table 6).

3.2 Laboratory methods

3.2.1 Micromorphology

Micromorphology is a method deriving from the soil sciences, in particular from the field of micropedology (Kubiëna, 1938, 1956, 1967, 1970). In the soil sciences, Kubiëna's micromorphology concept was adapted and further developed (Bullock et al., 1985; Fitzpatrick, 1993; Stoops, 2021).

Micromorphology, a method to study undisturbed, oriented soil and sediment block samples in thin sections, was soon applied in archaeology, as it allows for investigation of the context of an archaeological deposit under the microscope (Courty et al., 1989). Micromorphology is an integral part within geoarchaeology (Goldberg & Macphail, 2006; Karkanas & Goldberg, 2018; Macphail & Goldberg, 2018). In geoarchaeology, and archaeology in general, micromorphology is used to disentangle complex depositional and post-depositional processes that lead to site formation, and the contextual nature of the method is what may allow us to reconstruct the archaeological site (Karkanas & Goldberg, 2018).

For micromorphological analyses, thin sections are produced by mounting an undisturbed, dried, then resin-impregnated sediment sample on a slide and grinding the sample down to 30µm thickness. The thin section is then studied using a petrographic microscope, in this case a Zeiss Axio Imager petrographic microscope and a Motic petrographic microscope, with at least plane-polarized light (PPL), and cross-polarized light (XPL), and in with addition oblique incident light (OIL), and fluorescence (blue light and ultraviolet).

The analysis of thin sections follows the descriptive terminology and interpretations of several publications (Bullock et al., 1985; Courty et al., 1989; Nicosia & Stoops, 2017; Stoops et al., 2010; Stoops, 2021). Marcazzan and Meinekat (2022) created a description template to facilitate documentation of mostly qualitative thin section data in archaeology in a reproducible way.

3.2.2 Sediment Smear Slides

Smear slides are a fast way to analyse the microscopic composition of loose samples, *e.g*. ash samples (Martinez Dyrzo & Mentzer, in prep.; Rothwell, 1989). Smear slides are produced by using a covering agent, like Entellan®, on a slide with a very small amount of sample (Rothwell, 1989). The sample is dispersed with the mounting agent and then covered with a cover slip (Rothwell, 1989). If too many components above silt size are included, air bubbles impede analysis (Rothwell, 1989). After drying, the slides are analysed using - in this case - a Zeiss Axiometer petrographic microscope

using 10x, 20x, and 40x magnification under plane-polarized and crossed-polarized light.

3.2.3 (μ)FTIR

Fourier Transform Infrared Spectroscopy (FTIR) is a technique for mineral identification that is based on the identification of functional groups in organic and inorganic compounds (Berna, 2017; Toffolo, 2025).

Infrared radiation is a type of electromagnetic radiation, either presented with the wavelength (length of wave in nm or μm) or with its wavenumber (number of waves per centimetre in cm^{-1}) (Toffolo, 2025). Infrared radiation ranges between 700nm and 1nm, sub-divided into the near-infrared (NIR) range (700-2,500nm / 14,000-4,000cm^{-1}), the mid-infrared (MIR) range (2,500-25,000nm / 4,000-400cm^{-1}), and the far-infrared (FIR) range (25,000-100,000nm / 400-10cm^{-1}) (Mentzer, 2022; Toffolo, 2025).

The infrared absorption in a sample reflects interactions between the molecular bonds and infrared radiation (vibrations); mostly the MIR range is used as it is suited for investigation of molecular vibrations across a broad spectrum of organic and inorganic compounds (Mentzer, 2022; Toffolo, 2025). Vibrations of functional groups in molecules have different modes (vibrational modes) (Toffolo, 2025).

Infrared absorption is measured over a range of wavelengths, resulting in an interferogram (Berna, 2017; Toffolo, 2025). In a second step, the interferogram are then transformed with a mathematical algorithm, the Fourier transform, into the infrared spectrum (Berna, 2017; Toffolo, 2025). The spectrum shows the relative amount of infrared energy that is absorbed by the sample at each wavelength (Mentzer, 2022). As different minerals have unique spectra, or fingerprint, regions, these spectra can then be used for mineral identification, by comparing the sample spectra to reference spectra, for example from an online spectral database (Mentzer, 2022). For an overview of online available spectral databases see Mentzer (2022).

One way of conducting FTIR analyses in archaeology is by using a bench instrument on a loose sample (Berna, 2017; Mentzer, 2022; Weiner, 2010). A second way for FTIR analyses is micro-FTIR or μFTIR analysis (Berna, 2017; Mentzer, 2022). Here,

measurements can be conducted on a thin section directly and non-destructively (Berna, 2017; Mentzer, 2022).

In (geo-)archaeology, the use of FTIR as a quantitative method of distinguishing mineralogical compositions of archaeological sediments and materials is widespread (Toffolo, 2025; Weiner, 2010; Weiner et al., 2007), though the application of FTIR in archaeology bears potential beyond mineral identification (Lebon et al., 2010; Pothier Bouchard et al., 2019; Pucéat et al., 2004).

3.2.4 µXRF

X-ray fluorescence (XRF) spectroscopy is a technique used to analyse the elemental composition of materials by measuring the intensity and energy of characteristic radiation emitted when the sample is exposed to X-rays (Mentzer, 2017). When high-energy X-ray radiation excites atoms within a sample, electrons are shot from the inner oribtals (Mentzer, 2017). Outer electrons, from a higher energy level, fill the inner shell vacancies, emitting X-ray fluorescence radiation (photons) in the process (Mentzer, 2017). This radiation is specific to an element, allowing for elemental identification (Mentzer, 2017).

Microscopic X-ray fluorescence spectroscopy (micro-XRF/µ-XRF) focuses the X-rays on a limited spatial area of a sample, enabling analysis on thick and thin sections and block samples (Mentzer, 2017; Mentzer & Quade, 2013).

Besides XRF spectra that include information about elemental abundance through relative peak intensity, elemental distribution maps are another valuable output of the method (Mentzer, 2017). These results can be compared to micromorphological observations directly, making it especially useful in a microcontextual approach.

Recently, XRF data processing utilising vector based graphic software for visualisation of archaeological information has opened a new perspective in µXRF application in archaeology.

Chapter 4: Results and Discussion

This cumulative dissertation is based on three distinct studies.

The first study, **Meinekat et al.** (2021), follows a multi-method geoarchaeological approach to investigate the stratigraphy and site formation at Cuncaicha rock shelter (**Paper 1**).

The second study, **Meinekat et al.** (2023), follows up on the first paper and investigates resource availability and use. We apply an experimental approach to understand combustion practices at Cuncaicha rock shelter with a focus on fuel (**Paper 2**).

The third study, **Meinekat et al.** (subm.), shifts the regional focus to the coast of Peru. We apply a micro-contextual approach to investigate the micro-stratigraphy and site formation at Quebrada Jaguay-280 (**Paper 3**).

The papers are attached as **Appendix II, III, and IV**.

Paper 1 - A site formation model for Cuncaicha rock shelter

Title	**A site formation model for Cuncaicha rock shelter: Depositional and postdepositional processes at the high-altitude keysite in the Peruvian Andes**
First Author	Sarah A. Meinekat
Co-authors	Christopher E. Miller, Kurt Rademaker
DOI	10.1002/gea.21889
Journal	Geoarchaeology
Status	published

We study the deposit at the Cuncaicha rock shelter (4480 masl) in the southern Peruvian Andes, focusing on how depositional and post-depositional processes have shaped the sedimentary and archaeological record at the site.

The aim of the study is to formulate a site formation model that disentangles natural versus anthropogenic contributions, to evaluate preservation and stratigraphic integrity, and thus inform interpretation of occupation and behaviour in this high-altitude environment. In addition, we investigate if the deposit at the site may yield links to paleoenvironmental changes.

Stratigraphy and sedimentary components (**Objective 1**)

We identify five archaeological strata and a sterile substratum with sedimentary and occupational hiatuses evident between stratigraphic units. Stratum VI is the archaeologically sterile substratum, Stratum V corresponds to the Terminal Pleistocene occupation phase (~12.3 – 11.1 ka, n=23), Stratum IV comprises the Early Holocene occupation phase (~9.6 – 9.2 ka, n=7), Stratum III encompasses the Late-Middle-Holocene occupation phase (~5.9 – 4.8 ka, n=6), and Stratum II (~2.1 – 1.9 ka, n=1) and Stratum I (~0.8 – 0.6 ka, n=1) link to Late Holocene occupations, see also Rademaker and Hodgins (2018). Human burials date into the Early Holocene hiatus and the hiatus following the Late-Middle-Holocene occupation (Rademaker & Hodgins, 2018).

The Cuncaicha deposit comprises decimetre-scale strata that were differentiated during excavation based on field observations of chromatic variation and anthropogenic inclusion type and density. The present study enables refined distinctions:

We observe a mix of geogenic, biogenic and anthropogenic components, forming the deposit at the site. The predominant geogenic components shift from tufa-related carbonate precipitation during the Terminal Pleistocene to aeolian deposited sediments during the Holocene. The biogenic components, humified organic matter, peak in the Middle Holocene, where we identify the formation of a soil A-horizon. The anthropogenic components interbedded with these natural sediments reflect the macroscopic archaeological findings on a micro-scale, with high abundance of lithic debitage and bone fragments.

Moreover, micromorphological analysis has enabled the identification of anthropogenic inputs that remain archaeologically invisible at macroscopic scales, particularly microscopic ash remains.

Post-depositional Processes (**Objective 1**)

Micromorphological analysis revealed several processes that have modified the deposits after initial deposition. Such processes are the weathering of bone, dissolution of carbonates and precipitation of secondary carbonates, and the recrystallization of tufa into a phosphatic mineral, which we relate to the formation of a soil A-horizon during the Mid-Holocene.

Further, we identify localized mixing of sediments due to bioturbation. Larger-scale bioturbation, such as krotovinas, were identified during excavation and material separated for analysis and interpretation. Other intrusive features impacting the stratigraphic sequence are related to burial pits linked to the presence of five human interments at the site.

We observe variation in the presence of post-depositional processes that relate to changing paleoenvironmental conditions through time.

Paleoenvironmental Links (**Objective 1**)

The data demonstrate a positive correspondence between paleoenvironmental dynamics and sedimentary accumulation processes at the archaeological site.

During the Terminal Pleistocene we identify tufa formation that is related to moist conditions at the site. Contemporaneously, a wet phase (CAPE II) has widely been recognised in the region (Baker et al., 2001; Baker & Fritz, 2015; Betancourt et al., 2000; Maldonado et al., 2005; Nunnery et al., 2019; Pfeiffer et al., 2018; Placzek et al., 2006; Pueyo et al., 2011; Quade et al., 2008). As the CAPE II event coincides with the Terminal Pleistocene occupation documented in the Cuncaicha deposit, we propose that enhanced moisture regimes during this interval generated exceptionally favourable ecological conditions around Cuncaicha rock shelter, thereby promoting Terminal Pleistocene settlement at the site.

A documented shift to drier conditions with the beginning of the Holocene (Baker & Fritz, 2015; B. W. Bird et al., 2011; Bush et al., 2005; Bustamante et al., 2016; Cheng et al., 2013; Ekdahl et al., 2008; Hillyer et al., 2009; Ramirez et al., 2003; Seltzer et al., 2000; Thompson et al., 1995, 1998; van Breukelen et al., 2008), is coeval with an occupation hiatus at the site, dated from 11.1 – 9.6 ka.

The deposit continues with the Early Holocene occupation in which – with prevailing drier conditions - we observe a reduction in tufa formation and increase in aeolian deposition at Cuncaicha rock shelter, representative of the climatic shift.

Another occupation hiatus is dated to ~9.2 – 5.9 ka, coinciding with the driest period documented in the region (Abbott et al., 2003; Baker et al., 2001; Bush et al., 2005; Moreno et al., 2009; Pueyo et al., 2011; Rigsby et al., 2005; Seltzer et al., 2000; Thompson et al., 1998; Vining et al., 2019).

During the Late-Middle Holocene, another wet phase, around the time of termination of LMH occupation, has been identified in the Andes region (Abbott et al., 2003; B. W. Bird et al., 2011; Bustamante et al., 2016; Cross et al., 2000; Ekdahl et al., 2008; Hillyer et al., 2009; Vining et al., 2019). We propose this shift towards wetter conditions in combination with a thick deposit triggered the formation of a soil A-horizon in the site.

We do not observe archaeologically sterile strata that deposited during the times of non-occupation. Erosion could explain occupation hiatuses with unconformity in deposition, however, no indicators for erosional events were detected at the site.

The repetitive pattern of paleoclimatic change and occupation cessation may suggest that the micro-regional ecosystem was – and likely is - highly sensitive to climatic variability, thereby significantly affecting human settlement patterns in the region, though the burials at the site, and subsequent analysis demonstrating highland locality of the humans (Milton et al., in prep.), indicate that the broader Puna region remained hospitable.

Anthropogenic Features (**Objective 2**)

Analysis of anthropogenic features at Cuncaicha rock shelter prioritised the identification and characterisation of combustion features, given the prevalence of thermally altered materials throughout the stratigraphic sequence. (Almost) Intact, constrained combustion features are limited to the Late Holocene strata, in which we observe stacked combustion features.

Stacked combustion features, as seen in Strata I and II, exhibit superimposed layers of rubified sediment, charcoal, and ashes. These features are indicative of multiple burning events in the same place, *i.e*. when a new fire is built on top of the remains of a previous fire (Mentzer, 2012).

The other strata do not exhibit such preserved constrained combustion features. However, that does not signify lack of combustion. In contrast, human fire making is evidenced throughout the occupation sequence, as all strata contain burnt bones, charred organic matter, and ashes. The general mixing of components, also with unburnt materials, as well as the loss of the original combustion morphology, are indicative of reworking (Mentzer, 2012). Further, the identified plant ash remains are ash oxalate pseudomorphs, a common component in plant ashes (Canti, 2003; Canti & Brochier, 2017). Now, while ash oxalate pseudomorphs are not taxon-specific

(Aldeias, 2017; Canti & Brochier, 2017), the distinctive round shape of the pseudomorphs discovered in the Cuncaicha ashes suggests at least some species specific links.

Occupation Intensity and Site Use (**Objective 2**)

The question of occupation intensity and site use at Cuncaicha cannot be answered by geoarchaeology alone. Yet, feature preservation – or lack thereof – is able to tell us something about site use and occupation intensity.

Miller et al. (2013) and Karkanas et al. (2015) correlate the presence of single, preserved hearths to low-intensity occupation, or short-term site visits, during which no maintenance practices took place. Given the lack of microstratigraphic resolution and the remaining insecurities concerning sedimentary hiatuses at Cuncaicha, this is a tentative comparison.

However, in the Andes, the comprehensive comparison of occupation intensity through artefact density between early sites (Rademaker & Moore, 2019), together with reviewing combustion evidence at early sites above 2,500 masl (Meinekat et al., 2023) similarly suggests that combustion features tend to be preserved at sites indicating short-term, or ephemeral occupations. Rick (1980, p. 80) explicitly suggests, that the absence of hearths in the lower part of the sequence at Pachamachay may be related to dispersal “by intensive human activity in the site.”

Archaeological Implications

Our investigations at Cuncaicha rock shelter provide the framework for subsequent artefact analyses by identifying archaeological strata, phases of deposition and stasis, and the impact of bioturbation and resulting material mixing.

Beyond that, our study highlights that the archaeological site also serves as a paleoenvironmental archive, linking to significant paleoclimatic events.

Further, our findings relate to overall questions of intensity of site occupation and can (should) be integrated with the results of material studies relating to the proposed residential use of the site.

Paper 2 - Fire as high-elevation cold adaptation

Title	Fire as high-elevation cold adaptation: An evaluation of fuels and Terminal Pleistocene combustion in the Central Andes
First Author	Sarah A. Meinekat
Co-authors	Emily B.P. Milton, Brett Furlotte, Sonia Zarrillo, Kurt Rademaker
DOI	https://doi.org/10.1016/j.quascirev.2023.108244
Journal	Quaternary Science Reviews
Status	published

In this paper, we explore how fire use functioned as an adaptive strategy in high-elevation Andean environments during the Terminal Pleistocene, focusing especially on how proposed resource constraints at altitude influence fuel selection, combustion performance, and the archaeological visibility of combustion residues and features.

Through a combination of a thorough literature review, experimental combustions and residue analyses, and comparison to an archaeological case study (Cuncaicha rock shelter), we test whether multiple fuel types could have supported effective fire in the Puna, and how that may shape our interpretations of past human occupations at high elevation.

Fire up high (**Objective 3**)

In a first step, we compiled all accessible evidence for fire use and fuel identification at Terminal Pleistocene and Early Holocene (first millennium) sites in the Andes at sites above 2,500 masl (Table 1 and Table 2).

Table 1: Archaeological sites >2500 masl from the central and southern Andes radiocarbon dated to the Terminal Pleistocene (TP). Summarized, for full table see Meinekat et al. 2023.

Site	Elevation (masl)	^{14}C BP	SHCal20 95% cal BP	Dated material	Combustion	Combustion features / description	Fuel ID
Guitarrero Cave	2580	10,240 ± 45	12,013-11,648	cordage, wood artifacts, charcoal	yes	no	no
Tres Ventanas	3810	10,030 ± 170	12,432-10,879	charcoal	yes	no	no
Jaywamachay	3350	10,280 ± 170	12,600-11,319	charcoal	yes	Hearth and charcoal floor at base of Stratum J3	no
Cuncaicha	4480	10,380 ± 100	12,603-11,786	ultrafiltered bone	yes	no	present study

				collagen; charcoal			
Cueva Bautista	3935	*10,917 ± 69	12,972-12,729	dispersed charcoal. bone collagen	yes	two shallow hearths in Zone O	no
Alero El Pescador	3300	10,310 ± 130	12,606-11,349	charcoal	yes	yes	no
San Lorenzo 1	2950	*10,400 ± 130	12,683-11,728	charcoal	yes	no	no
Salar de Punta Negra 6	2975	10,260 ± 60	12,432-11,638	charcoal	yes	no	no
Tulan 109	2950	*10,590 ± 150	12,751-11,953	charcoal	yes	no	no
Cueva de Yavi	3430	*10,450 ± 55	12,598-12,019	charcoal	yes	no	no
Pintoscayoc 1	3780	*10,720 ± 150	12,969-12,090	charcoal	yes	no	no
Inca Cueva 4	3650	*10,620 ± 140	12,760-11,999	uncarbonized *Hypsocharis* sp. leaves	yes	hearths in Layer 2	*Polylepis* sp.
Peña de las Trampas	3580	10,190 ± 190	12,142-11,289	charcoal	yes	yes	no
Agua de la Cueva	2905	*10,950 ± 90	13,070-12,736	charcoal	yes	hearths in Subunit 2b	no

Table 2: Archaeological sites >2500 masl from the central and southern Andes radiocarbon dated to the first radiocarbon millennium of the Early Holocene (EH). Summarized, for full table see Meinekat et al. 2023.

Site	**Elevation (masl)**	**^{14}C BP**	**SHCal20 95% cal BP**	**Dated material**	**Combustion**	**Combustion features / description**	**Fuel ID**
Lauricocha (L-2)	3930	9525 ± 260	11,629-9975	charcoal mixed with burned and unburned bone	yes	no	no
Pachamachay	4300	9010 ± 285	11,066-9429	charcoal	yes	no	various
Panaulauca	4150	9650 ± 145	11,261-10,513	charcoal	yes	no	no
Quiqche	3600	9940 ± 200	12,087-10,706	charcoal	yes	no	no
Asana	3435	9820 ± 150	11,715-10,704	charcoal	yes	yes	no
Toquepala	2800	9490 ± 140	11,175-10,304	charcoal	yes	no	no
Hakenasa	4100	9980 ± 40	11,622-11,239	charcoal	yes	yes	no

Las Cuevas	4485	10,070 ± 30	11,715-11,314	charcoal	yes	no	no
Pampa el Muerto 15	3175	9510 ± 95	11,143-10,500	burned bone	yes	no	no
Quebrada Blanca	4500	9510 ± 70	11,083-10,512	charcoal	yes	no	no
Tuina 1	3160	9080 ± 130	10,554-9726	charcoal	yes	no	no
Tuina 5	3810	10,060 ± 70	11,830-11,259	charcoal	yes	yes	no
Chulqui 1A	3280	9590 ± 60	11,161-10,684	charcoal	yes	yes	no
Salar de Imilac 7	3020	9960 ± 50	11,623-11,216	charcoal	yes	yes	no
Salar de Punta Negra 1	2975	9230 ± 50	10,500-10,241	peat	no	no	not applicable
Salar de Punta Negra 17	2960	9260 ± 40	10,509-10,247	charcoal	yes	yes	no
Salar de Punta Negra 19	2960	9460 ± 50	11,062-10,502	charcoal	yes	yes	no
Salar de Punta Negra 20	2960	9480 ± 50	11,066-10,509	charcoal	yes	yes	no
Hornillos 2	4020	9710 ± 270	11,870-10,252	charcoal	yes	no	*Parastrephia spp., Baccharis incarum*
Huachichocana 3	3400	9620 ± 130	11,229-10,571	charcoal	yes	charcoal lenses (hearths?) in Layer E3	no
Alero Cuevas	4400	9880 ± 100	11,713-10,819	charcoal	yes	no	no
Quebrada Seca 3	4050	9410 ± 120	11,073-10,248	charcoal	yes	no	*Parastrephia* spp., *Baccharis incarum,* *Adesmia horrida*

Our review indicates that though evidence for fire at those high elevation sites is ubiquitous, little is known about the fuel used to produce the fires. If identifications were made, those rely on macrobotanical evidence.

Experimental combustion (**Objective 3**)

Through informed selection of various identified regionally available fuel sources, we chose three distinct fuels for the experimental combustion: *Polylepis rugulosa* (queñua), *Parastrephia* spp. (tola), and *Azorella compacta* (llareta or yareta). We

observe differences in combustion behaviour, burn duration, and residue formation among fuel types, indicating that fuel selection will influence the archaeological signature (*e.g*. charcoal and ash presence and morphology). Llareta showed the qualitatively "best" combustion characteristics.

Comparison to Cuncaicha (**Objective 3**)

We microscopically compare the ash of the three plant species to ash previously identified at Cuncaicha rock shelter in thin section. Llareta ash components (ash oxalate pseudomorphs) display a distinctive shape that we also identify in the deposit at Cuncaicha. Llareta presents the most likely primary fuel source identified at Cuncaicha, though charred organic remains (charcoal) of the other two species have also been identified macrobotanically at the site – though in very small quantities, contrasting the high amounts of charcoal produced by those species in the experimental fires.

Resource use and successful habitation (**Objective 3**)

While critical resources—including water, shelter, fuel, food, and lithic raw materials—have been documented at both Cuncaicha and Quebrada Jaguay-280, the degree of investigation varies considerably across sites and resource types. At QJ-280, zooarchaeological analyses by Reitz et al. (2016, 2017) have elucidated the significance of marine dietary resources, while Furlotte (2024) complements this work by demonstrating the contribution of plant resources to subsistence strategies and identifying taxa likely exploited as fuel. Provenance studies of lithic raw materials by Tanner (2001) and first insights by Sandweiss et al. (1998) reveal raw material procurement from multiple sources at varying distances from the site, indicating diverse patterns of landscape use.

Early work at Cuncaicha examined lithic materials and zooarchaeological remains, providing initial insights into dietary and raw material resources. (Rademaker et al., 2014, 2016), though detailed investigations are pending. The nature of fuel resources utilised at Cuncaicha had remained uncertain in previous research. The present study not only identifies the most probable fuel source employed at the site but also demonstrates the availability of numerous alternative fuel resources. These findings indicate substantial resource abundance and diversity within the Dry Puna ecosystem surrounding Cuncaicha.

Yet, a systematic comparative examination of the spatial distribution of critical resources relative to site-specific foraging radii remains to be undertaken and may elucidate aspects of site function and mobility organisation.

Archaeological Implications

With our study we argue that fire likely played an important adaptive role in high-elevation Andean settings, but the archaeological visibility of burning depends strongly on fuel source, combustion parameters, and post-depositional preservation. Without accounting for these factors, archaeologists may under-detect fire use in cold, extreme environments.

Our experimental–archaeological framework helps recalibrate how we interpret fire traces (or apparent absence thereof) in high-altitude contexts and emphasizes the need for microanalytical techniques to complement established methods.

Lastly, we highlight that the local high-elevation Puna is a place of relative resource richness and diversity, in regard to lithic raw materials, prey, and - as we have now shown - also fuel, creating a well-suitable habitat for hunter-gatherers.

Paper 3 - Microstratigraphy and site formation processes at Quebrada Jaguay 280 (Peru)

Title	**Microstratigraphy and site formation processes at Quebrada Jaguay 280 (Peru)**
First Author	Sarah A. Meinekat
Co-authors	Emily B.P. Milton, Daniela P. Osorio, Susan M. Mentzer, Christopher E. Miller, Daniel Sandweiss, Kurt Rademaker
DOI	10.1002/gea.70054
Journal	Geoarchaeology
Status	published

In this study, we examine the microstratigraphy and site formation at Quebrada Jaguay-280 from a micro-contextual and multi-methodological perspective. The combination of different micro-analytical techniques (micromorphology, μFTIR μXRF), which have not been applied at the site before, allows us to address questions of the site setting, deposition, and post-depositional processes. Further, we discuss the nature and formation of the previously described induration and evaluate the extent of

bioturbation at the site. Our approach integrates insights from the landscape scale down to the elemental level.

Geomorphology and Site Setting (**Objective 1**)

During the Terminal Pleistocene (~12 ka), the paleoshoreline was approximately eight km from the site (versus 2.5 km today). Before human occupation, the location was within an active alluvial fan system characterized by high-energy deposition. During occupation, the active channel had likely shifted away from the site, creating more stable conditions that favoured archaeological preservation. However, modern mining has severely disturbed the surrounding landscape, limiting broader geomorphological interpretations.

Induration (**Objective 1**)

One of our study's most significant finding concerns the indurated sediment. Rather than representing a specific occupation layer or surface, we find that the induration results from paedogenic salt formation—primarily halite (NaCl) and gypsum ($CaSO_4 \cdot 2H_2O$). µXRF mapping reveals that the impregnation doesn't correlate with specific microstratigraphic units but formed through post-depositional processes, such as coastal fog (*garúa*) depositing salts on the surface and subsequent percolation and translocation moving salts through the sediment. The induration is not recommended as a chronostratigraphic marker as it cuts across occupation layers and results from complex soil formation processes unrelated to specific human activities.

Taphonomy and Preservation (**Objective 1**)

We observe salt crystal formation significantly impacting the archaeological preservation. µXRF mapping shows halite and gypsum growing within cracks of shells, bones, and charcoal, causing in situ fragmentation. This process breaks and weathers faunal remains, impregnates charcoal, causing disintegration upon dissolution. Further, the extremely indurated sediment is complicate to excavate, impacting the archaeological work and causing (if work is continued) reduced artefact provenience resolution.

Bioturbation is also evident at QJ-280, including a large krotovina (animal burrow) that moved sediment through deposits. We highlight the risk that such features can

potentially mimicking anthropogenic features like postholes – that have previously been reported at the site.

Human Behaviour and Occupation (**Objective 2**)

Microstratigraphic analysis revealed spatial and temporal variation in site use.

We propose that Area 1 initially served as a peripheral refuse area with low-density, horizontally oriented, unburnt shell fragments (Balbo et al., 2010; Villagran, 2019; Villagran et al., 2011b).

Later periods show increased inclusion of anthropogenic components, mostly small, completely burned fragments of shell and fine charred organic matter and larger charcoal pieces, suggesting a shift toward living space or habitation area with maintenance and/ or reworking taking place (Aldeias et al., 2019; Aldeias & Bicho, 2016; Miller et al., 2010; Villagran et al., 2011b).

Eventually that deposit was cut and capped by a shell-supported deposit with interconnected shells, indicative of dumping or tossing into a midden, representing a fast-deposition event (Aldeias & Bicho, 2016; Duarte et al., 2019; Miller et al., 2010; Shillito et al., 2011; Villagran, 2019).

Any deposits above this level have been lost due to modern disturbance.

For Area 2, we suggest that it functioned first as a living space with evidence of fire maintenance (small, completely burned shell fragments and dispersed charcoal) and site cleaning, indicating maintenance practices (Aldeias et al., 2019; Aldeias & Bicho, 2016; Miller et al., 2010; Villagran et al., 2011b).

The site's use transitioned to refuse disposal in later periods, resulting in shell-dominated deposits that overlie earlier occupation layers, a pattern consistent with Area 1 (Aldeias & Bicho, 2016; Duarte et al., 2019; Miller et al., 2010; Shillito et al., 2011; Villagran, 2019).

Also in this area, any deposits above this level have been lost due to modern disturbance.

One notable observation is that, at first glance contrary to proposed early maritime adaptations and specialized fishing strategies during the site's initial occupation (Reitz et al., 2016, 2017; Sandweiss et al., 1998), the lowest microstratigraphic units -

representing the earliest deposits - contain minimal marine shell in our samples. While this pattern may reflect a diachronic change in shellfish exploitation, Villagran et al. (2011b) demonstrate a high lateral variability in shell distribution within a deposit that can explain the spatial heterogeneity.

With regard to occupation intensity, the microstratigraphic evidence is consistent with rapid depositional processes and/or punctuated, single-event accumulations rather than sustained occupations.

Archaeological Implications

Our study suggests that QJ-280 functioned as a repeatedly used, short-term camp within a broader mobility system rather than a permanent settlement. The combination of microcontextual analysis with landscape-scale observations thereby provides new perspectives on early coastal lifeways in western South America.

The research also has methodological implications for other hyperarid coastal sites across South America (Peru, Chile) where similar salt formation affects archaeological deposits and complicates archaeological excavation and interpretation. To better understand the paedogenic processes at the site, and the relationship in the formation of different salt minerals, we propose a landscape scale investigation of soluble salts and pedogenesis in the study region as a field for future research.

Our present study further shows that features previously interpreted as anthropogenic features may instead reflect bioturbation and require careful, microcontextual analysis focussed on samples from proposed features.

Chapter 5: Concluding Remarks and Future Directions

Fundamental questions had remained unresolved at Cuncaicha rock shelter and Quebrada Jaguay-280, including the contemporaneity of earliest occupation deposits, the degree of seasonality and occupation intensity during initial settlement, and adapted resource procurement.

The present dissertation addresses some of these gaps through multiple complementary approaches. The geoarchaeological investigations at both sites validate stratigraphic integrity, assess the degree of bioturbation, and evaluate its impact on depositional contexts. Additionally, otherwise invisible depositional components and post-depositional processes affecting site formation are revealed. Furthermore, this work advances our understanding of resource availability and exploitation by identifying fuel sources in the Puna.

The preservation contexts at these sites present both opportunities and analytical challenges. At Cuncaicha, the absence of microstratigraphic resolution limits interpretations of occupation intensity based on geoarchaeology alone. QJ-280's preserved microstratigraphy is consistent with seasonal occupation patterns. Yet the open-air configuration of QJ-280, where spatial expansion was readily available, contrasts fundamentally with the spatially constrained rock shelter environment at Cuncaicha, raising questions about the direct comparability of their depositional records. While it is essential to consider these differences, this dissertation also demonstrates the efficacy of a microcontextual, geoarchaeological approach across fundamentally different site contexts, revealing the analytical power regardless of environmental setting or depositional regime.

At Cuncaicha, integration of these geoarchaeological findings with future material culture studies—particularly analyses of lithic and faunal assemblages—will enhance interpretations of site use and occupation intensity at Cuncaicha. The fuel resource data contribute to broader questions of resource availability and exploitation in the Puna environment and should be synthesized with provenance studies of locally available resources, potentially revealing additional suitable micro-regions within the high-elevation Puna landscape.

At Quebrada Jaguay-280, the present results establish a foundation for subsequent geoarchaeological investigations, including detailed analysis of potential anthropogenic features in relation to documented bioturbation and paedogenic alterations, and potential application of a microfacies concept. Furthermore, this study provides the stratigraphic context necessary for future archaeological analyses and establishes a framework for developing a refined radiocarbon chronology. In addition, future integration of this work with the field notes from 2017 together with information from the 1990s yields a unique opportunity to tie together contextual information on an archaeological deposit through decades of archaeological fieldwork. This integration underscores a fundamental methodological principle: rigorous geoarchaeological inquiry necessarily originates from comprehensive field-based observation and meticulous stratigraphic recording.

The scope of inquiry must extend beyond the present sites to consider differential archaeological signatures and settlement processes across regions, with explicit attention to latitudinal patterns as outlined in the preceding review. Geoarchaeological research at Pachamachay and Panaulauca from previous fieldwork is particularly relevant in this context. Recent studies at Telarmachay (Le Neün et al., 2023), and the wider Junín region (Marsh & Rademaker, 2025; Rozas-Davila et al., 2023) have intensified interest in this area, and geoarchaeological samples from Pachamachay and Panaulauca will aid in contextualising these sites within regional settlement patterns.

Future investigations must continue this interdisciplinary integration, as well as combining detailed site-level analyses with regional-scale comparative frameworks with latitudinal variation to better comprehend the complexity and success of early human settlement of the Americas' most extreme environments.

References

Abbott, M. B., Wolfe, B. B., Wolfe, A. P., Seltzer, G. O., Aravena, R., Mark, B. G., Polissar, P. J., Rodbell, D. T., Rowe, H. D., & Vuille, M. (2003). Holocene paleohydrology and glacial history of the central Andes using multiproxy lake sediment studies. *Palaeogeography, Palaeoclimatology, Palaeoecology*, *194*(1), 123–138. https://doi.org/10.1016/S0031-0182(03)00274-8

Aldeias, V. (2017). Experimental Approaches to Archaeological Fire Features and Their Behavioral Relevance. *Current Anthropology*, *58*(16), 191–205. https://doi.org/10.1086/691210.

Aldeias, V., & Bicho, N. (2016). Embedded Behavior: Human Activities and the Construction of the Mesolithic Shellmound of Cabeço da Amoreira, Muge, Portugal. *Geoarchaeology*, *31*(6), 530–549. https://doi.org/10.1002/gea.21573

Aldeias, V., Dibble, H. L., Sandgathe, D., Goldberg, P., & McPherron, S. J. P. (2016). How heat alters underlying deposits and implications for archaeological fire features: A controlled experiment. *Journal of Archaeological Science*, *67*, 64–79. https://doi.org/10.1016/j.jas.2016.01.016

Aldeias, V., Gur-Arieh, S., Maria, R., Monteiro, P., & Cura, P. (2019). Shell we cook it? An experimental approach to the microarchaeological record of shellfish roasting. *Archaeological and Anthropological Sciences*, *11*(2), 389–407. https://doi.org/10.1007/s12520-016-0413-1

Aldenderfer, M. (1998). *Montane Foragers: Asana and the south-central Andean archaic*. University of Iowa Press.

Aldenderfer, M. (2006). Modelling plateau peoples: The early human use of the world's high plateaux. *World Archaeology*, *38*(3), 357–370. https://doi.org/10.1080/00438240600813285

Baker, P. A., & Fritz, S. C. (2015). Nature and causes of Quaternary climate variation of tropical South America. *Quaternary Science Reviews*, *124*, 31–47.

Baker, P. A., Seltzer, G. O., Fritz, S. C., Dunbar, R. B., Grove, M. J., Tapia, P. M., Cross, S. L., Rowe, H. D., & Broda, J. P. (2001). The History of South American Tropical Precipitation for the Past 25,000 Years. *Science*, *291*(5504), 640–643. https://doi.org/10.1126/science.291.5504.640

Balbo, A., Villagran, X. S., Madella, M., Vila, A., & Estevez, J. (2010). *An experimental approach for archeological soil micromorphology: Building a model for site taphonomy in coastal shell middens of the Beagle Channel (Argentina)*.

Banerjea, R. Y., Bell, M., Matthews, W., & Brown, A. (2015). Applications of micromorphology to understanding activity areas and site formation processes in experimental hut floors. *Archaeological and Anthropological Sciences*, *7*(1), 89–112. https://doi.org/10.1007/s12520-013-0160-5

Beresford-Jones, D., Pullen, A., Chauca, G., Cadwallader, L., García, M., Salvatierra, I., Whaley, O., Vásquez, V., Arce, S., Lane, K., & French, C. (2018). Refining the

Maritime Foundations of Andean Civilization: How Plant Fiber Technology Drove Social Complexity During the Preceramic Period. *Journal of Archaeological Method and Theory*, *25*(2), 393–425. https://doi.org/10.1007/s10816-017-9341-3

Berna, F. (2017). FTIR Microscopy. In *Archaeological Soil and Sediment Micromorphology* (pp. 411–415). John Wiley & Sons, Ltd. https://doi.org/10.1002/9781118941065.ch39

Berna, F., Goldberg, P., Horwitz, L. K., Brink, J., Holt, S., Bamford, M., & Chazan, M. (2012). Microstratigraphic evidence of in situ fire in the Acheulean strata of Wonderwerk Cave, Northern Cape province, South Africa. *Proc. Natl. Acad. Sci. U.S.A*, *109*(20). https://doi.org/10.1073/pnas.1117620109.

Betancourt, J. L., Latorre, C., Rech, J. A., Quade, J., & Rylander, K. A. (2000). A 22,000-Year Record of Monsoonal Precipitation from Northern Chile's Atacama Desert. *Science*, *289*(5484), 1542–1546. https://doi.org/10.1126/science.289.5484.1542

Bird, B. W., Abbott, M. B., Rodbell, D. T., & Vuille, M. (2011). Holocene tropical South American hydroclimate revealed from a decadally resolved lake sediment δ18O record. *Earth and Planetary Science Letters*, *310*(3), 192–202. https://doi.org/10.1016/j.epsl.2011.08.040

Bird, J. B., Hyslop, J., & Skinner, M. D. (1985). *The preceramic excavations at the Huaca Prieta, Chicama Valley, Peru. Anthropological papers of the AMNH ; v. 62, pt. 1*. http://hdl.handle.net/2246/241

Borrero, L. A. (2016). Ambiguity and Debates on the Early Peopling of South America. *PaleoAmerica*, *2*(1), 11–21. https://doi.org/10.1080/20555563.2015.1136498

Borrero, L. A., & Santoro, C. M. (2022). Metapopulation Processes in the Long-Term Colonization of the Andean Highlands in South America. *Journal of World Prehistory*, *35*(2), 135–162. https://doi.org/10.1007/s10963-022-09167-x

Bullock, P., Fedoroff, N., & Jongerius, A. (1985). *Handbook for soil thin section description*. Waine. https://research.wur.nl/en/publications/handbook-for-soil-thin-section-description

Buonasera, T., Herrera-Herrera, A. V., & Mallol, C. (2019). Experimentally Derived Sedimentary, Molecular, and Isotopic Characteristics of Bone-Fueled Hearths. *J Archaeol Method Theory*, *26*(4), 1327–1375. https://doi.org/10.1007/s10816-019-09411-3.

Bush, M. B., Hansen, B. C. S., Rodbell, D. T., Seltzer, G. O., Young, K. R., León, B., Abbott, M. B., Silman, M. R., & Gosling, W. D. (2005). A 17 000-year history of Andean climate and vegetation change from Laguna de Chochos, Peru. *Journal of Quaternary Science*, *20*(7–8), 703–714. https://doi.org/10.1002/jqs.983

Bustamante, M. G., Cruz, F. W., Vuille, M., Apaéstegui, J., Strikis, N., Panizo, G., Novello, F. V., Deininger, M., Sifeddine, A., Cheng, H., Moquet, J. S., Guyot, J. L., Santos, R. V., Segura, H., & Edwards, R. L. (2016). Holocene changes in monsoon

precipitation in the Andes of NE Peru based on δ18O speleothem records. *Quaternary Science Reviews*, *146*, 274–287. https://doi.org/10.1016/j.quascirev.2016.05.023

Canti, M. G. (2003). Aspects of the chemical and microscopic characteristics of plant ashes found in archaeological soils. *CATENA*, *54*(3), 339–361. https://doi.org/10.1016/S0341-8162(03)00127-9

Canti, M. G. (2025). Fire and its products: Recent developments in geoarchaeological microscopy and multi-disciplinary analysis. *Journal of Archaeological Science*, *179*, 106236. https://doi.org/10.1016/j.jas.2025.106236

Canti, M. G., & Brochier, J. É. (2017). Plant Ash. In *Archaeological Soil and Sediment Micromorphology* (pp. 147–154). John Wiley & Sons, Ltd. https://doi.org/10.1002/9781118941065.ch17

Capriles, J. M., Albarracin-Jordan, J., Lombardo, U., Osorio, D., Maley, B., Goldstein, S. T., Herrera, K. A., Glascock, M. D., Domic, A. I., Veit, H., & Santoro, C. M. (2016). High-altitude adaptation and late Pleistocene foraging in the Bolivian Andes. *Journal of Archaeological Science: Reports*, *6*, 463–474.

Cardich, A. (1964). *Lauricocha: Fundamentos para una Prehistoria de los Andes Centrales*. Centro Argentino de Estudios Prehistóricos, Buenos Aires.

Chala-Aldana, D., Bocherens, H., Miller, C., Moore, K., Hodgins, G., & Rademaker, K. (2018). Investigating mobility and highland occupation strategies during the Early Holocene at the Cuncaicha rock shelter through strontium and oxygen isotopes. *Journal of Archaeological Science: Reports*, *19*, 811–827. https://doi.org/10.1016/j.jasrep.2017.10.023

Chauchat, C. (1988). Early hunter-gatherers on the Peruvian coast. In R. W. Keatinge (Ed.), *Peruvian Prehistory: An Overview of Pre-Inca and Inca society*. Cambridge University Press.

Chazan, M. (2017). Toward a Long Prehistory of Fire. *Current Anthropology*, *58*(S16), 351–359. https://doi.org/10.1086/691988.

Cheng, H., Sinha, A., Cruz, F. W., Wang, X., Edwards, R. L., d'Horta, F. M., Ribas, C. C., Vuille, M., Stott, L. D., & Auler, A. S. (2013). Climate change patterns in Amazonia and biodiversity. *Nature Communications*, *4*(1), 1411. https://doi.org/10.1038/ncomms2415

Clark, J. D., & Harris, J. W. K. (1985). Fire and its roles in early hominid lifeways. *Afr Archaeol Rev*, *3*(1), 3–27. https://doi.org/10.1007/BF01117453.

Cornwall, I. W. (1953). Soil science and archaeology with illustrations from some British Bronze Age monuments. *Proceedings Prehistoric Society*, *2*, 129–147.

Costamagno, S., Théry-Parisot, I., & Guilbert, R. (2005). Taphonomic consequences of the use of bones as fuel.: Experimental data and archaeological applications. In *Biosphere to Lithosphere New studies in vertebrate taphonomy*.

Courty, M. A. (2001). Microfacies Analysis Assisting Archaeological Stratigraphy. In P. Goldberg, V. T. Holliday, & C. R. Ferring (Eds.), *Earth Sciences and Archaeology* (pp. 205–239). Springer US. https://doi.org/10.1007/978-1-4615-1183-0_8

Courty, M. A., Goldberg, P., & Macphail, R. (1989). Soils and micromorphology in archaeology. *Cambridge: Cambridge*.

Cross, S. L., Baker, P. A., Seltzer, G. O., Fritz, S. C., & Dunbar, R. B. (2000). A new estimate of the Holocene lowstand level of Lake Titicaca, central Andes, and implications for tropical palaeohydrology. *The Holocene*, *10*(1), 21–32. https://doi.org/10.1191/095968300671452546

Dalrymple, J. B. (1958). The Application of Soil Micromorphology to Fossil Soils and Other Deposits from Archaeological Sites. *Journal of Soil Science*, *9*(2), 199–209. https://doi.org/10.1111/j.1365-2389.1958.tb01911.x

deFrance, S. (2009). Quebrada Tacahuay and early maritime foundations on the far southern Peruvian coast: The 2001 field season. *Andean Civilization: A Tribute to Michael E. Moseley*, 55–73.

Dillehay, T. D., Bonavia, D., Jr, S. L. G., Pino, M., Vásquez, V., & Tham, T. R. (2012). A late pleistocene human presence at Huaca Prieta, Peru, and early Pacific Coastal adaptations. *Quaternary Research*, *77*(3), 418–423. https://doi.org/10.1016/j.yqres.2012.02.003

Dillehay, T. D., Goodbred, S., Pino, M., Vásquez Sánchez, V. F., Tham, T. R., Adovasio, J., Collins, M. B., Netherly, P. J., Hastorf, C. A., Chiou, K. L., Piperno, D., Rey, I., & Velchoff, N. (2017). Simple technologies and diverse food strategies of the Late Pleistocene and Early Holocene at Huaca Prieta, Coastal Peru. *Science Advances*, *3*(5), e1602778. https://doi.org/10.1126/sciadv.1602778

Dillehay, T. D., Rossen, J., Maggard, G., Stackelbeck, K., & Netherly, P. (2003). Localization and possible social aggregation in the Late Pleistocene and Early Holocene on the north coast of Perú. *Quaternary International*, *109–110*, 3–11. https://doi.org/10.1016/S1040-6182(02)00198-2

Dillon, M., Leiva González, S., Zapata, M., Lezama, P., & Quipuscoa Silvestre, V. (2011). Floristic checklist of the Peruvian Lomas Formations. *Arnaldoa*, *18*, 7–32.

Dillon, M., Nakazawa, M., & Leiva, S. (2003). *The Lomas formations of coastal Peru: Composition and biogeographic history*. *43*, 1–9.

Dinerstein, E., Olson, D., Joshi, A., Vynne, C., Burgess, N. D., Wikramanayake, E., Hahn, N., Palminteri, S., Hedao, P., Noss, R., Hansen, M., Locke, H., Ellis, E. C., Jones, B., Barber, C. V., Hayes, R., Kormos, C., Martin, V., Crist, E., … Saleem, M. (2017). An Ecoregion-Based Approach to Protecting Half the Terrestrial Realm. *BioScience*, *67*(6), 534–545. https://doi.org/10.1093/biosci/bix014

Duarte, C., Iriarte, E., Diniz, M., & Arias, P. (2019). The microstratigraphic record of human activities and formation processes at the Mesolithic shell midden of Poças de São Bento (Sado Valley, Portugal). *Archaeological and Anthropological Sciences*, *11*(2), 483–509. https://doi.org/10.1007/s12520-017-0519-0

Eggert, M. K. H. (2008). *Prähistorische Archäologie: Konzepte und Methoden* (4th ed.). utb GmbH. https://doi.org/10.36198/9783838536965

Ekdahl, E. J., Fritz, S. C., Baker, P. A., Rigsby, C. A., & Coley, K. (2008). Holocene multidecadal- to millennial-scale hydrologic variability on the South American Altiplano. *The Holocene*, *18*(6), 867–876. https://doi.org/10.1177/0959683608093524

Engel, F. (1957). Early Sites on the Peruvian Coast. *Southwestern Journal of Anthropology*, *13*(1), 54–68. https://doi.org/10.1086/soutjanth.13.1.3629157

Engel, F. (1970). Exploration of the Chilca Canyon, Peru. *Current Anthropology*, *11*, 55–58.

Eren, M., Durant, A., Neudorf, C., Haslam, M., Shipton, C., Bora, J., Korisettar, R., & Petraglia, M. (2010). Experimental examination of animal trampling effects on artifact movement in dry and water saturated substrates: A test case from South India. *Journal of Archaeological Science*, *37*(12). https://ora.ox.ac.uk/objects/uuid:9a61ec43-74a7-4980-b757-a658f142a421

Fitzpatrick, E. A. (1993). *Soil Microscopy and Micromorphology*. John Wiley & Sons Ltd.

Francken, M., Beier, J., Reyes-Centeno, H., Harvati, K., & Rademaker, K. (2018). *The human skeletal remains from the Cuncaicha rock shelter, Peru* (pp. 125–152).

Furlotte, B. A. (2024). *Hunting for the Gathering: Terminal Pleistocene and Early Holocene Plant Resource Exploitation at the Quebrada Jaguay (QJ-280) Site, Southern Coastal Peru*. https://hdl.handle.net/10388/15768

Goebel, T., Waters, M. R., & O'Rourke, D. H. (2008). The late Pleistocene dispersal of modern humans in the Americas. *Science (New York, N.Y.)*, *319*(5869), 1497–1502. https://doi.org/10.1126/science.1153569

Goldberg, P. (1979). Micromorphology of Pech-de-l'Azé II sediments. *Journal of Archaeological Science*, *6*(1), 17–47. https://doi.org/10.1016/0305-4403(79)90031-1

Goldberg, P., & Berna, F. (2010). Micromorphology and context. *Quaternary International*, *214*(1), 56–62. https://doi.org/10.1016/j.quaint.2009.10.023

Goldberg, P., & Macphail, R. I. (2006). *Practical and Theoretical Geoarchaeology* (1st ed.). Wiley. https://doi.org/10.1002/9781118688182

Goldberg, P., Miller, C. E., & Mentzer, S. M. (2017). Recognizing Fire in the Paleolithic Archaeological Record. *Current Anthropology*, *58*, 175–190.

Goldberg, P., Miller, C. E., Schiegl, S., Ligouis, B., Berna, F., Conard, N. J., & Wadley, L. (2009). Bedding, hearths, and site maintenance in the Middle Stone Age of Sibudu Cave, KwaZulu-Natal, South Africa. *Archaeological and Anthropological Sciences*, *1*(2), 95–122. https://doi.org/10.1007/s12520-009-0008-1

Goldberg, P., Nash, D. T., & Petraglia, M. D. (Eds.). (1993). *Formation Processes in Archaeological Context*. Prehistory Press,U.S.

Goldberg, P., Weiner, S., Bar-Yosef, O., Xu, Q., & Liu, J. (2001). Site formation processes at Zhoukoudian, China. *Journal of Human Evolution*, *41*(5), 483–530. https://doi.org/10.1006/jhev.2001.0498

Gruver, S. (2018). Occupational Seasonality and Paleoenvironmental Reconstruction at Quebrada Jaguay 280. *Graduate Research Theses & Dissertations*. https://huskiecommons.lib.niu.edu/allgraduate-thesesdissertations/7082

Haaland, M. M., Friesem, D. E., Miller, C. E., & Henshilwood, C. S. (2017). Heat-induced alteration of glauconitic minerals in the Middle Stone Age levels of Blombos Cave, South Africa: Implications for evaluating site structure and burning events. *Journal of Archaeological Science*, *86*, 81–100. https://doi.org/10.1016/j.jas.2017.06.008

Haaland, M. M., Miller, C. E., Unhammer, O. F., Reynard, J. P., Van Niekerk, K. L., Ligouis, B., Mentzer, S. M., & Henshilwood, C. S. (2021). Geoarchaeological investigation of occupation deposits in Blombos Cave in South Africa indicate changes in site use and settlement dynamics in the southern Cape during MIS 5b-4. *Quaternary Research*, *100*, 170–223. https://doi.org/10.1017/qua.2020.75

Haas, R., Stefanescu, I. C., Garcia-Putnam, A., Aldenderfer, M., Clementz, M. T., Murphy, M. S., Llave, C. V., & Watson, J. T. (2017). Humans permanently occupied the Andean highlands by at least 7 ka. *Royal Society Open Science*, *4*(6), 170331. https://doi.org/10.1098/rsos.170331

Haller von Hallerstein, S. (2017). *Multi-isotopic Paleo-diet Reconstruction of Hunter-gatherers in the Peruvian Puna* [Unpublished MSc thesis]. Institute for Archaeological Sciences, University of Tübingen.

Hillyer, R., Valencia, B. G., Bush, M. B., Silman, M. R., & Steinitz-Kannan, M. (2009). A 24,700-yr paleolimnological history from the Peruvian Andes. *Quaternary Research*, *71*(1), 71–82. https://doi.org/10.1016/j.yqres.2008.06.006

Jackson, D., & Méndez, C. (2005). Primeras ocupaciones humanas en la costa del semiárido de Chile: Patrón de asentamientos y subsistencia. *Actas Del XVI Congreso Nacional de Arqueología Chilena*, 493–502.

Jackson, D., Méndez, C., Seguel, R., Maldonado, A., & Easton, G. (2007). Initial Occupation of the Pacific Coast of Chile during Late Pleistocene Times. *Current Anthropology*, *48*. https://doi.org/10.1086/520965

Jackson, D., Seguel, R., Báez, P., & Prieto, X. (1999). Asentamientos y evidencias culturales del Complejo Cultural Huentelauquén en la comuna de Los Vilos, Provincia del Choapa. *Anales Del Museo de Historia Natural de Valparaíso*, *24*, 5–28.

Jones, K. B., Hodgins, G. W. L., & and Sandweiss, D. H. (2019). Radiocarbon Chronometry of Site QJ-280, Quebrada Jaguay, a Terminal Pleistocene to Early Holocene Fishing Site in Southern Peru. *The Journal of Island and Coastal Archaeology*, *14*(1), 82–100. https://doi.org/10.1080/15564894.2017.1338316

Karakostis, F. A., Reyes-Centeno, H., Franken, M., Hotz, G., Rademaker, K., & Harvati, K. (2021). Biocultural evidence of precise manual activities in an Early Holocene individual of the high-altitude Peruvian Andes. *American Journal of Physical Anthropology*, *174*(1), 35–48. https://doi.org/10.1002/ajpa.24160

Karkanas, P. (2007). Identification of lime plaster in prehistory using petrographic methods: A review and reconsideration of the data on the basis of experimental and case studies. *Geoarchaeology*, *22*(7), 775–796. https://doi.org/10.1002/gea.20186

Karkanas, P., Brown, K. S., Fisher, E. C., Jacobs, Z., & Marean, C. W. (2015). Interpreting human behavior from depositional rates and combustion features through the study of sedimentary microfacies at site Pinnacle Point 5-6, South Africa. *Journal of Human Evolution*, *85*, 1–21. https://doi.org/10.1016/j.jhevol.2015.04.006.

Karkanas, P., & Goldberg, P. (2018). *Reconstructing archaeological sites: Understanding the geoarchaeological matrix*. John Wiley & sons.

Karkanas, P., Shahack-Gross, R., Ayalon, A., Bar-Matthews, M., Barkai, R., Frumkin, A., Gopher, A., & Stiner, M. C. (2007). Evidence for habitual use of fire at the end of the Lower Paleolithic: Site-formation processes at Qesem Cave, Israel. *Journal of Human Evolution*, *53*(2), 197–212. https://doi.org/10.1016/j.jhevol.2007.04.002

Keefer, D. K., deFrance, S. D., Moseley, M. E., Richardson, J. B., Satterlee, D. R., & Day-Lewis, A. (1998). Early Maritime Economy and El Niño Events at Quebrada Tacahuay, Peru. *Science*, *281*(5384), 1833–1835. https://doi.org/10.1126/science.281.5384.1833

Keefer, D. K., Moseley, M. E., & deFrance, S. D. (2003). A 38 000-year record of floods and debris flows in the Ilo region of southern Peru and its relation to El Niño events and great earthquakes. *Palaeogeography, Palaeoclimatology, Palaeoecology*, *194*(1), 41–77. https://doi.org/10.1016/S0031-0182(03)00271-2

Kubiëna, W. L. (1938). *Micropedology*.

Kubiëna, W. L. (1956). *Zur Mikromorphologie, Systematik und Entwicklung der rezenten und fossilen Lößböden*. https://doi.org/10.23689/fidgeo-1230

Kubiëna, W. L. (1967). *Die mikromorphometrische Bodenanalyse.* Enke.

Kubiëna, W. L. (1970). *Micromorphological Features of Soil Geography*. Rutgers University Press.

Kuhn, S. L., & Stiner, M. C. (2019). Hearth and Home in the Middle Pleistocene. *Journal of Anthropological Research*, *75*(3), 305–327.

Lanning, E. P. (1967). *Peru Before the Incas*. Prentice-Hall.

Lavallée, D. (2000). *The first South Americans: The peopling of a continent from the earliest evidence to high culture*. University of Utah Press. https://hal.science/hal-01923430

Lavallée, D., Julien, M., Béarez, P., Bolaños, A., Carré, M., Chevalier, A., Delabarde, T., Fontugne, M., Rodríguez-Loredo, C., Klaric, L., Usselmann, P., & Vanhaeren, M. (2011). Quebrada de los burros: Los primeros pescadores del litoral pacífico en el

extremo sur peruano. *Chungará (Arica)*, *43*(especial), 333–351. https://doi.org/10.4067/S0717-73562011000300002

Le Neün, M., Dufour, E., Zazzo, A., Tombret, O., Thil, F., Wheeler, J. C., Cucchi, T., & Goepfert, N. (2023). Holocene occupation of the Andean highlands: A new radiocarbon chronology for the Telarmachay rockshelter (Central Andes, Peru). *Quaternary Science Reviews*, *312*, 108146. https://doi.org/10.1016/j.quascirev.2023.108146

Lebon, M., Reiche, I., Bahain, J.-J., Chadefaux, C., Moigne, A.-M., Fröhlich, F., Sémah, F., Schwarcz, H. P., & Falguères, C. (2010). New parameters for the characterization of diagenetic alterations and heat-induced changes of fossil bone mineral using Fourier transform infrared spectrometry. *Journal of Archaeological Science*, *37*(9), 2265–2276. https://doi.org/10.1016/j.jas.2010.03.024

Leierer, L., Carrancho Alonso, Á., Pérez, L., Herrejón Lagunilla, Á., Herrera-Herrera, A. V., Connolly, R., Jambrina-Enríquez, M., Hernández Gómez, C. M., Galván, B., & Mallol, C. (2020). It's getting hot in here – Microcontextual study of a potential pit hearth at the Middle Paleolithic site of El Salt, Spain. *Journal of Archaeological Science*, *123*, 105237. https://doi.org/10.1016/j.jas.2020.105237

Llagostera, A., Weisner, R., Castillo, G., Cervellino, M., & Costa-Junqueira, M. (2000). El Complejo Huentelauquén bajo una perspectiva macroespacial y multidisciplinaria. *Actas Del XIV Congreso Nacional de Arqueología Chilena*, *1*, 461–482.

López Mendoza, P., Loyola, R., Carrasco, C., Latorre, E., & Méndez, V. (2024). Human dynamics in the Southern Puna of Chile (25°-27°s) during the Late Holocene: Abandonment, re-occupation and diversification. *Frontiers in Environmental Archaeology*, *3*. https://doi.org/10.3389/fearc.2024.1423960

Loyola, R., Núñez, L., & Cartajena, I. (2019). What's it like out there? Landscape learning during the early peopling of the highlands of the south-central Atacama desert. *Quaternary International*, *533*, 7–24. https://doi.org/10.1016/j.quaint.2019.07.007

Lynch, T. F. (1971). Preceramic Transhumance in the Callejón de Huaylas, Peru. *American Antiquity*, *36*(2), 139–148. https://doi.org/10.2307/278667

Macphail, R. I., Cruise, G. M., Allen, M. J., Linderholm, J., & Reynolds, P. (2004). Archaeological soil and pollen analysis of experimental floor deposits; with special reference to Butser Ancient Farm, Hampshire, UK. *Journal of Archaeological Science*, *31*(2), 175–191. https://doi.org/10.1016/j.jas.2003.07.005

Macphail, R. I., & Goldberg, P. (2018). *Applied Soils and Micromorphology in Archaeology*. Cambridge University Press.

Maldonado, A., Betancourt, J. L., Latorre, C., & Villagran, C. (2005). Pollen analyses from a 50 000-yr rodent midden series in the southern Atacama Desert (25° 30′ S). *Journal of Quaternary Science*, *20*(5), 493–507. https://doi.org/10.1002/jqs.936

Mallol, C., Hernández, C. M., Cabanes, D., Machado, J., Sistiaga, A., Pérez, L., & Galván, B. (2013). Human actions performed on simple combustion structures: An experimental approach to the study of Middle Palaeolithic fire. *Quaternary International*, *315*, 3–15. https://doi.org/10.1016/j.quaint.2013.04.009

Mallol, C., Hernández, C. M., Cabanes, D., Sistiaga, A., Machado, J., Rodríguez, Á., Pérez, L., & Galván, B. (2013a). The black layer of Middle Palaeolithic combustion structures. *Interpretation and Archaeostratigraphic Implications. Journal of Archaeological Science*, *40*(5), 2515–2537. https://doi.org/10.1016/j.jas.2012.09.017.

Mallol, C., Mentzer, S. M., & Miller, C. E. (2017). Combustion Features. In C. Nicosia & G. Stoops (Eds.), *Archaeological soil and sediment micromorphology* (pp. 299–330). Wiley.

Marcazzan, D., & Meinekat, S. A. (2022). Creating qualitative datasets in geoarchaeology: An easy-applicable description template for archaeological thin section analysis using Stoops 2003. *MethodsX*, *9*, 101663. https://doi.org/10.1016/j.mex.2022.101663

Marcazzan, D., Miller, C. E., & Conard, N. J. (2022). Burning, dumping, and site use during the Middle and Upper Palaeolithic at Hohle Fels Cave, SW Germany. *Archaeol Anthropol Sci*, *14*(9), 1–26. https://doi.org/10.1007/s12520-022-01647-7.

Marcazzan, D., Miller, C. E., Ligouis, B., Duches, R., Conard, N. J., & Peresani, M. (2023). Middle and Upper Paleolithic occupations of Fumane Cave (Italy): A geoarchaeological investigation of the anthropogenic features. *Journal of Anthropological Sciences*, *100*, 1–26. https://doi.org/10.4436/JASS.10002.

Marsh, E. J., & Rademaker, K. (2025). Human–environment interactions in the Lake Junín basin: Fire, megafauna, deforestation, and domestication, from the peopling of the Andes to the Inca Empire. *Quaternary Science Reviews*, *351*, 109159. https://doi.org/10.1016/j.quascirev.2024.109159

Martinez Dyrzo, H., & Mentzer, S. M. (in prep.). *An Experimental Wood Ash Database: Physical Properties and Morphologies.*

McInnis, H. (1999). *Subsistence and maritime adaptations at Quebrada Jaguay, Camaná, Peru: A faunal analysis* [PhD Thesis, University of Maine]. https://scholar.google.com/scholar?cluster=8179533489966797093&hl=en&oi=scholarr

Meignen, L., Goldberg, P., & Bar-Yosef, O. (2007). The hearths at kebara cave and their role in site formation processes. In L. Meignen & O. Bar-Yosef (Eds.), *The Middle and Upper Paleolithic archaeology of the Kebara Cave, Mt Carmel, Israel.* American School of Prehistoric Research, Peabody Museum, Harvard University Press.

Meinekat, S. A., Miller, C. E., & Rademaker, K. (2021). A site formation model for Cuncaicha rock shelter: Depositional and postdepositional processes at the high-altitude keysite in the Peruvian Andes. *Geoarchaeology*, *37*, 304–331.

Meinekat, S. A., Milton, E. B. P., Furlotte, B., Zarrillo, S., & Rademaker, K. (2023). Fire as high-elevation cold adaptation: An evaluation of fuels and Terminal Pleistocene combustion in the Central Andes. *Quaternary Science Reviews*, *316*, 108244. https://doi.org/10.1016/j.quascirev.2023.108244

Meinekat, S. A., Milton, E. B. P., Osorio, D. P., Mentzer, S. M., Miller, C. E., Sandweiss, D. H., & Rademaker, K. (subm.). Microstratigraphy and site formation processes at Quebrada Jaguay 280 (Peru). *Geoarchaeology*.

Menéndez, L. P., Rademaker, K., & Harvati, K. (2019). Revisiting East–West Skull Patterns and the Role of Random Factors in South America: Cranial Reconstruction and Morphometric Analysis of the Facial Skeleton from Cuncaicha Rockshelter (Southern Peru). *PaleoAmerica*, *5*(4), 315–334. https://doi.org/10.1080/20555563.2019.1703167

Mentzer, S. M. (2009). Bone as a fuel source: The effects of initial fragment size distribution. In I. Théry-Parisot, S. Costamagno, A. Henry, & L. Oosterbeek (Eds.), *Gestion des combustibles au paléolithique et au mésolithique: Nouveaux outils, nouvelles interprétations*. Archaeopress.

Mentzer, S. M. (2012). Microarchaeological Approaches to the Identification and Interpretation of Combustion Features in Prehistoric Archaeological Sites. *Journal of Archaeological Method and Theory*, *21*, 616–668.

Mentzer, S. M. (2017). Micro XRF. In C. Nicosia & G. Stoops (Eds.), *Archaeological Soil and Sediment Micromorphology* (1st ed., pp. 431–440). Wiley. https://doi.org/10.1002/9781118941065.ch41

Mentzer, S. M. (2022). 15. Analysemethoden—FTIR. In *Geoarchäologie* (1st ed., pp. 331–333). Springer Spektrum.

Mentzer, S. M., & Quade, J. (2013). Compositional and Isotopic Analytical Methods in Archaeological Micromorphology. *Geoarchaeology*, *28*(1), 87–97. https://doi.org/10.1002/gea.21425

Miller, C. E. (2011). Deposits as Artifacts. *TÜVA Mitteilungen*, *12*, 91–107.

Miller, C. E., Conard, N. J., Goldberg, P., & Berna, F. (2010). Dumping, Sweeping and Trampling: Experimental Micromorphological Analysis of Anthropogenically Modified Combustion Features. *Palethnologie. Archéologie et Sciences Humaines*, *2*, Article 2. https://doi.org/10.4000/palethnologie.8197

Miller, C. E., Goldberg, P., & Berna, F. (2013). Geoarchaeological investigations at Diepkloof Rock Shelter, Western Cape, South Africa. *Journal of Archaeological Science*, *40*(9), 3432–3452. https://doi.org/10.1016/j.jas.2013.02.014

Miller, C. E., & Sievers, C. (2012). An experimental micromorphological investigation of bedding construction in the Middle Stone Age of Sibudu, South Africa. *Journal of Archaeological Science*, *39*(10), 3039–3051. https://doi.org/10.1016/j.jas.2012.02.007

Milton, E. B. P., Meinekat, S. A., Hallerstein, S. H. von, Osorio, D., Seabrook, M., Zuniga, E., Zuniga, E., Bocherens, H., Brown, S., Moore, K., Rademaker, K., & Drucker, D. (in prep.). *12,000 Years of Local Foraging in the High Andes* [In prep.].

Milton, E. B. P., Stansell, N. D., Bocherens, H., Brownlee, A., Chala-Aldana, D., & Rademaker, K. (2022). Examining surface water δ18O and δ2H values in the western Central Andes: A watershed moment for anthropological mobility studies. *Journal of Archaeological Science*, *146*, 105655. https://doi.org/10.1016/j.jas.2022.105655

Moreno, A., Santoro, C. M., & Latorre, C. (2009). Climate change and human occupation in the northernmost Chilean Altiplano over the last ca. 11 500 cal. A BP. *Journal of Quaternary Science*, *24*(4), 373–382.

Moseley, M. E. (1975). *The maritime foundations of Andean civilization*. https://ehrafarchaeology.yale.edu/document?id=se40-003

Murphree, W. C., & Aldeias, V. (2022). The evolution of pyrotechnology in the Upper Palaeolithic of Europe. *Archaeol Anthropol Sci*, *14*(10). https://doi.org/10.1007/s12520-022-01660-w.

Nakatsuka, N., Lazaridis, I., Barbieri, C., Skoglund, P., Rohland, N., Mallick, S., Posth, C., Harkins-Kinkaid, K., Ferry, M., Harney, É., Michel, M., Stewardson, K., Novak-Forst, J., Capriles, J. M., Durruty, M. A., Álvarez, K. A., Beresford-Jones, D., Burger, R., Cadwallader, L., … Fehren-Schmitz, L. (2020). A Paleogenomic Reconstruction of the Deep Population History of the Andes. *Cell*, *181*(5), 1131-1145.e21. https://doi.org/10.1016/j.cell.2020.04.015

Nicosia, C., & Stoops, G. (2017). *Archaeological soil and sediment micromorphology*. Wiley.

Núñez, L., & Santoro, C. M. (1988). Cazadores de la puna seca y salada del área centro-sur Andina (Norte de Chile). *Estudios Atacameños*, *9*, 11–60.

Nunnery, J. A., Fritz, S. C., Baker, P. A., & Salenbien, W. (2019). Lake-level variability in Salar de Coipasa, Bolivia during the past ~40,000 yr. *Quaternary Research*, *91*(2), 881–891. https://doi.org/10.1017/qua.2018.108

Osorio, D., Parodi, S., Milton, E., Meinekat, S., Moore, K., Huidobro, C., Steele, J., & Rademaker, K. (in prep.). *Dwelling in the Andean Sky: Lithic Technology at Cuncaicha Rockshelter during the Terminal Pleistocene (12,300-11,100 cal BP), Dry Puna of Peru* [In prep.].

Osorio, D., Steele, J., Sepúlveda, M., Gayo, E. M., Capriles, J. M., Herrera, K. A., Ugalde, P. C., Pol-Holz, R., Latorre, C., & Santoro, C. M. (2017). The Dry Puna as an ecological megapatch and the peopling of South America: Technology, mobility, and the development of a late Pleistocene/early Holocene Andean hunter-gatherer tradition in northern Chile. *Quaternary International*, *461*, 41–53.

Pfeiffer, M., Latorre, C., Santoro, C. M., Gayo, E. M., Rojas, R., Carrevedo, M. L., McRostie, V. B., Finstad, K. M., Heimsath, A., Jungers, M. C., De Pol-Holz, R., & Amundson, R. (2018). Chronology, stratigraphy and hydrological modelling of extensive wetlands and paleolakes in the hyperarid core of the Atacama Desert

during the late quaternary. *Quaternary Science Reviews*, *197*, 224–245. https://doi.org/10.1016/j.quascirev.2018.08.001

Piperno, D. R. (2011). The Origins of Plant Cultivation and Domestication in the New World Tropics: Patterns, Process, and New Developments. *Current Anthropology*, *52*(S4), S453–S470. https://doi.org/10.1086/659998

Pitblado, B. L., & Rademaker, K. (2024). The Earliest Peopling of the Rocky and Andes Mountains. In F. Carrer, M. Callanan, P. Della Casa, F. Fontana, S. Reinhold, & H. Saul (Eds.), *The Oxford Handbook of Mountain Archaeology* (p. 0). Oxford University Press. https://doi.org/10.1093/oxfordhb/9780197608005.013.36

Placzek, C., Quade, J., & Patchett, P. J. (2006). Geochronology and stratigraphy of late Pleistocene lake cycles on the southern Bolivian Altiplano: Implications for causes of tropical climate change. *GSA Bulletin*, *118*(5–6), 515–532. https://doi.org/10.1130/B25770.1

Politis, G. G., Gutiérrez, M. A., Rafuse, D. J., & Blasi, A. (2016). The Arrival of Homo sapiens into the Southern Cone at 14,000 Years Ago. *PLOS ONE*, *11*(9), e0162870. https://doi.org/10.1371/journal.pone.0162870

Pollard, A. M. (1999). Geoarchaeology: An introduction. *Geological Society, London, Special Publications*, *165*(1), 7–14. https://doi.org/10.1144/GSL.SP.1999.165.01.01

Posth, C., Nakatsuka, N., Lazaridis, I., Skoglund, P., Mallick, S., Lamnidis, T. C., Rohland, N., Nägele, K., Adamski, N., Bertolini, E., Broomandkhoshbacht, N., Cooper, A., Culleton, B. J., Ferraz, T., Ferry, M., Furtwängler, A., Haak, W., Harkins, K., Harper, T. K., … Reich, D. (2018). Reconstructing the Deep Population History of Central and South America. *Cell*, *175*(5), 1185-1197.e22. https://doi.org/10.1016/j.cell.2018.10.027

Pothier Bouchard, G., Mentzer, S. M., Riel-Salvatore, J., Hodgkins, J., Miller, C. E., Negrino, F., Wogelius, R., & Buckley, M. (2019). Portable FTIR for on-site screening of archaeological bone intended for ZooMS collagen fingerprint analysis. *Journal of Archaeological Science: Reports*, *26*, 101862. https://doi.org/10.1016/j.jasrep.2019.05.027

Prates, L., Politis, G. G., & Perez, S. I. (2020). Rapid radiation of humans in South America after the last glacial maximum: A radiocarbon-based study. *PLOS ONE*, *15*(7), e0236023. https://doi.org/10.1371/journal.pone.0236023

Prieto, G., & Sandweiss, D. H. (Eds.). (2020). *Maritime Communities of the Ancient Andes* (1st ed.). University Press of Florida. https://doi.org/10.2307/j.ctvwvr380

Pucéat, E., Reynard, B., & Lécuyer, C. (2004). Can crystallinity be used to determine the degree of chemical alteration of biogenic apatites? *Chemical Geology*, *205*(1), 83–97. https://doi.org/10.1016/j.chemgeo.2003.12.014

Pueyo, J. J., Sáez, A., Giralt, S., Valero-Garcés, B. L., Moreno, A., Bao, R., Schwalb, A., Herrera, C., Klosowska, B., & Taberner, C. (2011). Carbonate and organic matter sedimentation and isotopic signatures in Lake Chungará, Chilean Altiplano, during

the last 12.3 kyr. *Palaeogeography, Palaeoclimatology, Palaeoecology*, *307*(1), 339–355. https://doi.org/10.1016/j.palaeo.2011.05.036

Pulgar Vidal, J. (1987). Las ocho regiones naturales del Perú. *PEISA Lima*. https://journals.openedition.org/terrabrasilis/1027

Quade, J., Rech, J. A., Betancourt, J. L., Latorre, C., Quade, B., Rylander, K. A., & Fisher, T. (2008). Paleowetlands and regional climate change in the central Atacama Desert, northern chile. *Quaternary Research*, *69*(3), 343–360. https://doi.org/10.1016/j.yqres.2008.01.003

Rademaker, K. (2014). Late Ice-Age Human Settlement of the High-Altitude Peruvian Andes. *Mitteilungen Der Gesellschaft Für Urgeschichte*, *23*, 13–35.

Rademaker, K. (2024). Updated Peru archaeological radiocarbon database, 20,000–7000 14C BP. *Quaternary International*, *703*, 32–48. https://doi.org/10.1016/j.quaint.2024.01.012

Rademaker, K., Glascock, M. D., Reid, D. A., Zuñiga, E., & Bromley, G. R. M. (2022). Comprehensive mapping and compositional analysis of the Alca obsidian source, Peru. *Quaternary International*, *619*, 56–71. https://doi.org/10.1016/j.quaint.2021.11.029

Rademaker, K., Glascock, M., Kaiser, B., Gibson, D., Lux, D., & Yates, M. (2013). Multi-technique geochemical characterization of the Alca obsidian source, Peruvian Andes. *Geology*, *41*, 779–782. https://doi.org/10.1130/G34313.1

Rademaker, K., & Hodgins, G. (2018). *Exploring the chronology of occupations and burials at Cuncaicha rockshelter, Peru* (pp. 107–124).

Rademaker, K., Hodgins, G., Moore, K., Zarrillo, S., Miller, C., Bromley, G. R. M., Leach, P., Reid, D. A., Álvarez, W. Y., & Sandweiss, D. H. (2014). Paleoindian settlement of the high-altitude Peruvian Andes. *Science*, *346*, 466–469.

Rademaker, K., Hodgins, G., Moore, K., Zarrillo, S., Miller, C., Bromley, G. R. M., Leach, P., Reid, D., lvarez, W. Y., & Sandweiss, D. H. (2016). Cuncaicha Rockshelter, a Key Site for Understanding Colonization of the High Andes: Reply to Capriles et al. *Current Anthropology*, *57*(1), 101–103.

Rademaker, K., & Moore, K. (2019). Variation in the Occupation Intensity of Early Forager Sites of the Andean Puna. In A. K. Lemke (Ed.), *Foraging in the Past* (pp. 76–118). University Press of Colorado. https://doi.org/10.5876/9781607327745.c004

Ramirez, E., Hoffmann, G., Taupin, J. D., Francou, B., Ribstein, P., Caillon, N., Ferron, F. A., Landais, A., Petit, J. R., Pouyaud, B., Schotterer, U., Simoes, J. C., & Stievenard, M. (2003). A new Andean deep ice core from Nevado Illimani (6350 m), Bolivia. *Earth and Planetary Science Letters*, *212*(3), 337–350. https://doi.org/10.1016/S0012-821X(03)00240-1

Rapp, G. (Rip), & Hill, C. L. (2006). *Geoarchaeology: The Earth-Science Approach to Archaeological Interpretation*. Yale University Press. https://www.jstor.org/stable/j.ctt1cc2kd9

Reitz, E. J., McInnis, H. E., Sandweiss, D. H., & deFrance, S. D. (2016). Terminal Pleistocene and Early Holocene fishing strategies at Quebrada Jaguay and the Ring Site, southern Perú. *Journal of Archaeological Science: Reports*, *8*, 447–453. https://doi.org/10.1016/j.jasrep.2016.05.035

Reitz, E. J., McInnis, H. E., Sandweiss, D. H., & and deFrance, S. D. (2017). Variations in Human Adaptations During the Terminal Pleistocene and Early Holocene at Quebrada Jaguay (QJ-280) and the Ring Site, Southern Perú. *The Journal of Island and Coastal Archaeology*, *12*(2), 224–254. https://doi.org/10.1080/15564894.2016.1172381

Renfrew, C. (1976). Archaeology and the earth sciences. In *Geoarchaeology: Earth Science and the Past* (pp. 1–5).

Rentzel, P., Nicosia, C., Gebhardt, A., Brönnimann, D., Pümpin, C., & Ismail-Meyer, K. (2017). Trampling, Poaching and the Effect of Traffic. In *Archaeological Soil and Sediment Micromorphology* (pp. 281–297). John Wiley & Sons, Ltd. https://doi.org/10.1002/9781118941065.ch30

Richardson, J. B. (1981). Modeling the development of sedentary maritime economies on the coast of Peru: A preliminary statement. *Annals of the Carnegie Museum*, *50*, 139–150. https://doi.org/10.5962/p.214488

Rick, J. W. (Ed.). (1980). *Prehistoric hunters of the High Andes. Studies in archaeology*. Academic Pr.

Rigsby, C. A., Bradbury, J. P., Baker, P. A., Rollins, S. M., & Warren, M. R. (2005). Late Quaternary palaeolakes, rivers, and wetlands on the Bolivian Altiplano and their palaeoclimatic implications. *Journal of Quaternary Science*, *20*(7–8), 671–691. https://doi.org/10.1002/jqs.986

Rothwell, R. G. (1989). The Smear Slide Method. In R. G. Rothwell (Ed.), *Minerals and Mineraloids in Marine Sediments: An Optical Identification Guide* (pp. 21–24). Springer Netherlands. https://doi.org/10.1007/978-94-009-1133-8_2

Rozas-Davila, A., Rodbell, D. T., & Bush, M. B. (2023). Pleistocene megafaunal extinction in the grasslands of Junín-Peru. *Journal of Biogeography*, *50*(4), 755–766. https://doi.org/10.1111/jbi.14566

Sandgathe, D. M., & Berna, F. (2017). Fire and the Genus. *Current Anthropology*, *58*(S16), S165–S174. https://doi.org/10.1086/691424

Sandgathe, D. M., Dibble, H. L., Goldberg, P., McPherron, S. P., & Hodgkins, J. (2011). Timing of the appearance of habitual fire use. *Proceedings of the National Academy of Sciences 108(29), E298; Author Reply E299*. https://doi.org/10.1073/pnas.1106759108.

Sandgathe, D. M., Dibble, H. L., Goldberg, P., McPherron, S. P., Turq, A., Niven, L., & Hodgkins, J. (2011). On the Role of Fire in Neandertal Adaptations in Western Europe: Evidence from Pech de l'Azé and Roc de Marsal, France. *PaleoAnthropology*, 216–242.

Sandweiss, D. H. (2014). Early Coastal South America. In *The Cambridge World Prehistory* (pp. 1058–1074). Cambridge University Press. https://doi.org/10.1017/CHO9781139017831.071

Sandweiss, D. H., McInnis, H., Burger, R. L., Cano, A., Ojeda, B., Paredes, R., Sandweiss, M. del C., & Glascock, M. D. (1998). Quebrada Jaguay: Early South American Maritime Adaptations. *Science*, *281*(5384), 1830–1832. https://doi.org/10.1126/science.281.5384.1830

Sandweiss, D. H., & Rademaker, K. M. (2011). El poblamiento del sur peruano: Costa y sierra. *Boletín de Arqueología PUCP*, *15*, 275–293. https://doi.org/10.18800/boletindearqueologiapucp.201101.010

Sandweiss, D. H., Richardson III, J. B., Reitz, E. J., Hsu, J. T., & Feldman, R. A. (1989). Early maritime adaptations in the Andes: Preliminary studies at the Ring Site, Peru. *Ecology, Settlement, and History in the Osmore Drainage, Peru*, *545*, 35–84.

Santoro, C. M., Gayo, E. M., Capriles, J. M., Rivadeneira, M. M., Herrera, K. A., Mandakovic, V., Rallo, M., Rech, J. A., Cases, B., Briones, L., Olguín, L., Valenzuela, D., Borrero, L. A., Ugalde, P. C., Rothhammer, F., Latorre, C., & Szpak, P. (2019). From the Pacific to the Tropical Forests: Networks of Social Interaction in the Atacama Desert, Late in the Pleistocene. *Chungara Revista de Anropología Chilena*, *51*, 5–25.

Santoro, C. M., & Núñez, L. (1987). Hunters of the Dry Puna and the Salt Puna in Northern Chile. *Andean Past*, *1*, 57–109.

Schiappacasse, V., & Niemeyer, H. (1975). Apuntes para el estudio de la transhumancia en el valle de Camarones (provincia de Tarapacá, Chile). *Estudios atacameños*, *3*, 49–52. https://doi.org/10.22199/S07181043.1975.0003.00008

Schiegl, S., Goldberg, P., Pfretzschner, H.-U., & Conard, N. J. (2003). Paleolithic burnt bone horizons from the Swabian Jura: Distinguishing between in situ fireplaces and dumping areas. *Geoarchaeology*, *18*(5), 541–565. https://doi.org/10.1002/gea.10080

Schiffer, M. B. (1972). Archaeological Context and Systemic Context. *American Antiquity*, *37*(2), 156–165. https://doi.org/10.2307/278203

Schiffer, M. B. (1987). *Formation processes of the archaeological record* (1. ed). Univ. of New Mexico Pr.

Seltzer, G., Rodbell, D., & Burns, S. (2000). Isotopic evidence for late Quaternary climatic change in tropical South America. *Geology*, *28*(1), 35–38. https://doi.org/10.1130/0091-7613(2000)28<35:IEFLQC>2.0.CO;2

Shahack-Gross, R., & Ayalon, A. (2013). Stable carbon and oxygen isotopic compositions of wood ash: An experimental study with archaeological implications. *Journal of Archaeological Science*, *40*(1), 570–578. https://doi.org/10.1016/j.jas.2012.06.036

Shahack-Gross, R., Berna, F., Karkanas, P., Lemorini, C., Gopher, A., & Barkai, R. (2014). Evidence for the repeated use of a central hearth at Middle Pleistocene (300

ky ago) Qesem Cave, Israel. *Journal of Archaeological Science*, *44*, 12–21. https://doi.org/10.1016/j.jas.2013.11.015

Shillito, L.-M., Matthews, W., Almond, M. J., & Bull, I. D. (2011). The microstratigraphy of middens: Capturing daily routine in rubbish at Neolithic Catalhoyuk, Turkey. *Antiquity*, *85*(329), 1024–1038.

Shimelmitz, R., Kuhn, S. L., Jelinek, A. J., Ronen, A., Clark, A. E., & Weinstein-Evron, M. (2014). 'Fire at will': The emergence of habitual fire use 350,000 years ago. *Journal of Human Evolution*, *77*, 196–203. https://doi.org/10.1016/j.jhevol.2014.07.005.

Sorensen, A. (2017). On the relationship between climate and Neandertal fire use during the Last Glacial in south-west France. *Quaternary International*, *436*, 114–128. https://doi.org/10.1016/j.quaint.2016.10.003

Sorensen, A. (2019). The Uncertain Origins of Fire-Making by Humans: The State of the Art and Smouldering Questions. *Mitteilungen der Gesellschaft für Urgeschichte*, *28*, 11–50.

Stahlschmidt, M. C., Mallol, C., & Miller, C. E. (2020). Fire as an Artifact-Advances in Paleolithic Combustion Structure Studies: Introduction to the Special Issue. *J Paleo Arch*, *3*(4), 503–508. https://doi.org/10.1007/s41982-020-00074-1.

Stahlschmidt, M. C., Miller, C. E., Ligouis, B., Hambach, U., Goldberg, P., Berna, F., Richter, D., Urban, B., Serangeli, J., & Conard, N. J. (2015). On the evidence for human use and control of fire at Schöningen. *Journal of Human Evolution*, *89*, 181–201. https://doi.org/10.1016/j.jhevol.2015.04.004

Steele, J., & Politis, G. (2009). AMS 14C dating of early human occupation of southern South America. *Journal of Archaeological Science*, *36*(2), 419–429. https://doi.org/10.1016/j.jas.2008.09.024

Stein, J. K. (1987). Deposits for Archaeologists. In *Advances in Archaeological Method and Theory* (pp. 337–395). Elsevier. https://doi.org/10.1016/B978-0-12-003111-5.50009-9

Stein, J. K. (2001). A Review of Site Formation Processes and Their Relevance to Geoarchaeology. In P. Goldberg, V. T. Holliday, & C. R. Ferring (Eds.), *Earth Sciences and Archaeology* (pp. 37–51). Springer US. https://doi.org/10.1007/978-1-4615-1183-0_2

Stoops, G. (2021). *Guidelines for Analysis and Description of Soil and Regolith Thin Sections* (1st ed.). Wiley. https://doi.org/10.1002/9780891189763

Stoops, G., Mees, F., & Marcelino, V. (2010). *Interpretation of micromorphological features of soils and regoliths*. Elsevier.

Stothert, K. E. (1985). The Preceramic Las Vegas Culture of Coastal Ecuador. *American Antiquity*, *50*(3), 613–637. https://doi.org/10.2307/280325

Stothert, K. E., Piperno, D. R., & Andres, T. C. (2003). Terminal Pleistocene/Early Holocene human adaptation in coastal Ecuador: The Las Vegas evidence.

Quaternary International, *109–110*, 23–43. https://doi.org/10.1016/S1040-6182(02)00200-8

Tanner, B. R. (2001). *Lithic Analysis of Chipped Stone Artifacts Recovered From Quebrada Jaguay, Peru* [The University of Maine]. https://digitalcommons.library.umaine.edu/etd/667

Théry-Parisot, I. (2002). *The gathering of firewood during Palaeolithic time* (S. Thiébault, Ed.).

Théry-Parisot, I., Costamagno, S., Brugal, J.-P., Fosse, P., & Guilbert, R. (2005). *The use of bone as fuel during the Palaeolithic, experimental study of bone combustible properties. The zooarchaeology of fats, oils, milk and dairying*.

Thompson, L. G., Davis, M. E., Mosley-Thompson, E., Sowers, T. A., Henderson, K. A., Zagorodnov, V. S., Lin, P.-N., Mikhalenko, V. N., Campen, R. K., Bolzan, J. F., Cole-Dai, J., & Francou, B. (1998). A 25,000-Year Tropical Climate History from Bolivian Ice Cores. *Science*, *282*(5395), 1858–1864. https://doi.org/10.1126/science.282.5395.1858

Thompson, L. G., Mosley-Thompson, E., Davis, M. E., Lin, P.-N., Henderson, K. A., Cole-Dai, J., Bolzan, J. F., & Liu, K. -b. (1995). Late Glacial Stage and Holocene Tropical Ice Core Records from Huascarán, Peru. *Science*, *269*(5220), 46–50. https://doi.org/10.1126/science.269.5220.46

Toffolo, M. B. (2025). *Infrared Spectroscopy of Archaeological Sediments* (1st ed.). Cambridge University Press. https://doi.org/10.1017/9781009387590

Troll, C. (1958). *Las culturas superiores andinas y el medio geográfico*.

Troll, C. (1968). *The Cordilleras of the Tropical Americas: Aspects of Climatic, Phytogeographical and Agrarian Ecology*. Ferd. Dümmlers.

van Breukelen, M. R., Vonhof, H. B., Hellstrom, J. C., Wester, W. C. G., & Kroon, D. (2008). Fossil dripwater in stalagmites reveals Holocene temperature and rainfall variation in Amazonia. *Earth and Planetary Science Letters*, *275*(1), 54–60. https://doi.org/10.1016/j.epsl.2008.07.060

Villagran, X. S. (2019). The Shell Midden Conundrum: Comparative Micromorphology of Shell-Matrix Sites from South America. *Journal of Archaeological Method and Theory*, *26*(1), 344–395. https://doi.org/10.1007/s10816-018-9374-2

Villagran, X. S., Balbo, A. L., Madella, M., Vila, A., & Estevez, J. (2011a). Experimental micromorphology in Tierra del Fuego (Argentina): Building a reference collection for the study of shell middens in cold climates. *Journal of Archaeological Science*, *38*(3), 588–604. https://doi.org/10.1016/j.jas.2010.10.013

Villagran, X. S., Balbo, A. L., Madella, M., Vila, A., & Estevez, J. (2011b). Stratigraphic and spatial variability in shell middens: Microfacies identification at the ethnohistoric site Tunel VII (Tierra del Fuego, Argentina). *Archaeological and Anthropological Sciences*, *3*(4), 357–378. https://doi.org/10.1007/s12520-011-0074-z

Villagran, X. S., Strauss, A., Miller, C., Ligouis, B., & Oliveira, R. (2017). Buried in ashes: Site formation processes at Lapa do Santo rockshelter, east-central Brazil. *Journal of Archaeological Science*, *77*, 10–34. https://doi.org/10.1016/j.jas.2016.07.008

Vining, B. R., Steinman, B. A., Abbott, M. B., & Woods, A. (2019). Paleoclimatic and archaeological evidence from Lake Suches for highland Andean refugia during the arid middle-Holocene. *The Holocene*, *29*(2), 328–344. https://doi.org/10.1177/0959683618810405

Wadley, L., Sievers, C., Bamford, M., Goldberg, P., Berna, F., & Miller, C. (2011). Middle Stone Age bedding construction and settlement patterns at Sibudu, South Africa. *Science (New York, N.Y.)*, *334*(6061), 1388–1391. https://doi.org/10.1126/science.1213317

Waters, M. R. (2019). Late Pleistocene exploration and settlement of the Americas by modern humans. *Science*, *365*(6449), eaat5447. https://doi.org/10.1126/science.aat5447

Weiner, S. (2010). *Microarchaeology: Beyond the Visible Archaeological Record*. Cambridge University Press. https://doi.org/10.1017/CBO9780511811210

Weiner, S., Berna, F., Cohen-Ofri, I., Shahack-Gross, R., Albert, R., Karkanas, P., Meignen, L., & Bar-Yosef, O. (2007). Mineral Distributions in Kebara Cave. Diagenesis and its Effect on the Archaeological Record. In *American School of Prehistoric Research Bulletin 49* (pp. 131–146).

Yacobaccio, H. D. (2017). Peopling of the high Andes of northwestern Argentina. *Quaternary International*, *461*, 34–40. https://doi.org/10.1016/j.quaint.2017.01.006

Appendix I – Sample lists

Table 3: Sample list of geoarchaeological investigation at Quebrada Jaguay-280 in 2017. QJ: Quebrada Jaguay; A: Area; U: Unit; N: North, S: South, W: West; SW: Southwest; SE: Southeast; OS: Off-Site; ref: reference.

Sample number	Type	Location
QJ16-17-01	Block	QJ-16, U1
QJ16-17-02	Block	QJ-16, U2
QJ16-17-03	Block	QJ-16, U2
QJ-17-01	Block	QJ-280, Sector1, N wall
QJ-17-02	Block	QJ-280, Sector1, W wall
QJ-17-03	Block	QJ-280, Sector1, S wall
QJ-17-04	Block	QJ-280, Sector1, W wall
QJ-17-05	Block	QJ-280, Sector1, W wall
QJ-17-06	Block	QJ-280, Area2, U10, SE corner
QJ-ref-17-04	Block	QJ-280, OS, outcrop1
QJ-ref-17-08	Block	QJ-280, OS, outcrop2
QJ-ref-17-13	Block	QJ-280, OS, outcrop3
QJ-ref-17-15	Block	QJ-280, OS, outcrop3
QJ-17-15	Block	QJ-280, S1 west wall, U3B (Sandweiss)
QJ-17-16	Block	QJ-280, A1, U2 south wall/ U1 north wall
QJ-17-11	Block	QJ-280, A1, U2 south wall/ U1 north wall
QJ-17-12	Block	QJ-280, A1, U2, sw corner
QJ-17-13	Block	QJ-280, A1, U4
QJ-17-14	Block	Qj-280, A1, U4
QJ-17-15	Block	QJ-280, A2, west wall, U3b (sandweiss)
QJ-17-16	Block	QJ-280, A1, U1 north wall
QJ-17-17	Block	QJ-280, A2, U12, SW corner
QJ-17-18	Block	QJ-280, A2, U10
QJ16-17-01a	Bulk	QJ-16, U1
QJ16-17-01b	Bulk	QJ-16, U1
QJ16-17-01c	Bulk	QJ-16, U1
QJ16-17-01d	Bulk	QJ-16, U1
PC343-17-01	Bulk	Pampa Colorada
QJ16-17-02a	Bulk	QJ-16, U2
QJ16-17-02b	Bulk	QJ-16, U2
QJ16-17-02c	Bulk	QJ-16, U2
QJ16-17-03a	Bulk	QJ-16, U2
QJ-17-02a	Bulk	QJ-280, Sector1, W wall
QJ-17-02b	Bulk	QJ-280, Sector1, W wall
QJ-17-02c	Bulk	QJ-280, Sector1, W wall
QJ-17-02d	Bulk	QJ-280, Sector1, W wall
QJ-17-03a	Bulk	QJ-280, Sector1, S wall
QJ-17-03b	Bulk	QJ-280, Sector1, S wall
QJ-17-03c	Bulk	QJ-280, Sector1, S wall
QJ-17-03c.1	Bulk	QJ-280, Sector1, S wall
QJ-17-03d	Bulk	QJ-280, Sector1, S wall
QJ-17-03e	Bulk	QJ-280, Sector1, S wall
QJ-17-05a	Bulk	QJ-280, Sector1, W wall
QJ-17-05b	Bulk	QJ-280, Sector1, W wall
QJ-17-05c	Bulk	QJ-280, Sector1, W wall

QJ-17-05d	Bulk	QJ-280, Sector1, W wall
QJ-17-07	Bulk	QJ-280, Area2, U10, SE corner
QJ-17-08	Bulk	QJ-280, Area2, U10, SE corner
QJ-17-09	Bulk	QJ-280, Area2, U10, SE
QJ-17-10	Bulk	QJ-280, Area2, U10, SE
QJ-ref-17-01	Bulk	QJ-280. Sector1, N wall profile 1A
QJ-ref-17-02	Bulk	QJ-280, OS, outcrop1
QJ-ref-17-03	Bulk	QJ-280, OS, outcrop1
QJ-ref-17-04a	Bulk	QJ-280, OS, outcrop1
QJ-ref-17-05	Bulk	QJ-280, OS, outcrop1
QJ-ref-17-06	Bulk	QJ-280, OS, outcrop2
QJ-ref-17-07	Bulk	QJ-280, OS, outcrop2
QJ-ref-17-08a	Bulk	QJ-280, OS, outcrop2
QJ-ref-17-09	Bulk	QJ-280, OS, outcrop2
QJ-ref-17-10	Bulk	volcanic ash outcrop, OS
QJ-ref-17-11	Bulk	QJ-280, OS, outcrop3
QJ-ref-17-12	Bulk	QJ-280, OS, outcrop3
QJ-ref-17-13a	Bulk	QJ-280, OS, outcrop3
QJ-ref-17-14	Bulk	QJ-280, OS, outcrop3
QJ-ref-17-15a	Bulk	QJ-280, OS, outcrop3
QJ-ref-17-16	Bulk	QJ-280, OS, outcrop3
QJ-ref-17-17	Bulk	base of QJ-1
QJ-17-15a	Bulk	QJ-280, S1 west wall, U3B (Sandweiss)
QJ-17-15b	Bulk	QJ-280, S1 west wall, U3B (Sandweiss)
QJ-17-15c	Bulk	QJ-280, S1 west wall, U3B (Sandweiss)
QJ-17-15d	Bulk	QJ-280, S1 west wall, U3B (Sandweiss)
QJ-17-15e	Bulk	QJ-280, S1 west wall, U3B (Sandweiss)
QJ-17-15f	Bulk	QJ-280, S1 west wall, U3B (Sandweiss)
QJ-17-16a	Bulk	QJ-280, A1, U2 south wall/ U1 north wall
QJ-17-16b	Bulk	QJ-280, A1, U2 south wall/ U1 north wall
QJ-17-11a	Bulk	QJ-280, A1, U2 south wall/ U1 north wall
QJ-17-11b	Bulk	QJ-280, A1, U2 south wall/ U1 north wall
QJ-17-11c	Bulk	QJ-280, A1, U2 south wall/ U1 north wall
QJ-17-11d	Bulk	QJ-280, A1, U2 south wall/ U1 north wall
QJ-17-11e	Bulk	QJ-280, A1, U2 south wall/ U1 north wall
QJ-17-11f	Bulk	QJ-280, A1, U2 south wall/ U1 north wall
QJ16-ref-17-01	Plant	QJ-16, N slope

Table 4: Sample list from geoarchaeological investigation at Pachamachay in 2019. PAX: Pachamachay; U: Unit; N: North; W: West.

Sample number	Type	Location
PAX-19-1	Block	U10 Nwall
PAX-19-2	Block	U10 Nwall
PAX-19-3	Block	U10 Nwall
PAX-19-4	Block	U10 Nwall
PAX-19-5	Block	U10 Wwall
PAX-19-6	Block	U10 Wwall
PAX-19-1a	Bulk	U10 Nwall

PAX-19-1b	Bulk	U10 Nwall
PAX-19-2a	Bulk	U10 Nwall
PAX-19-2b	Bulk	U10 Nwall
PAX-19-2c	Bulk	U10 Nwall
PAX-19-3a	Bulk	U10 Nwall
PAX-19-3b	Bulk	U10 Nwall
PAX-19-4a	Bulk	U10 Nwall
PAX-19-4b	Bulk	U10 Nwall
PAX-19-4c	Bulk	U10 Nwall
PAX-19-4d	Bulk	U10 Nwall
PAX-19-5a	Bulk	U10 Wwall
PAX-19-5b	Bulk	U10 Wwall
PAX-19-5c	Bulk	U10 Wwall
PAX-19-5d	Bulk	U10 Wwall
PAX-19-6a	Bulk	U10 Wwall
PAX-19-6b	Bulk	U10 Wwall

Table 5: Sample list of geoarchaeological investigation at Panaulauca in 2019. PAN: Panaulauca; U: Unit; N: North.

Sample number	Type	Location
PAN-19-1	Block	natural profile along road, for reference
PAN-19-2	Block	U1 Nwall
PAN-19-3	Block	U1 Nwall
PAN-19-4	Block	U1 Nwall
PAN-19-5	Block	U1 Nwall
PAN-19-6	Block	U1 Nwall
PAN-19-7	Block	U1 Nwall
PAN-19-8	Block	U1 Nwall
PAN-19-9	Block	U1 Nwall
PAN-19-10	Block	U1 Nwall
PAN-19-11	Block	U1 Nwall
PAN-19-1a	Bulk	natural profile along road, for reference
PAN-19-1b	Bulk	natural profile along road, for reference
PAN-19-2a	Bulk	U1 Nwall
PAN-19-2b	Bulk	U1 Nwall
PAN-19-2c	Bulk	U1 Nwall
PAN-19-2d	Bulk	U1 Nwall
PAN-19-2e	Bulk	U1 Nwall
PAN-19-3a	Bulk	U1 Nwall
PAN-19-3b	Bulk	U1 Nwall
PAN-19-4a	Bulk	U1 Nwall
PAN-19-4b	Bulk	U1 Nwall
PAN-19-4c	Bulk	U1 Nwall
PAN-19-4d	Bulk	U1 Nwall
PAN-19-5a	Bulk	U1 Nwall
PAN-19-5b	Bulk	U1 Nwall
PAN-19-5c	Bulk	U1 Nwall

PAN-19-6a	Bulk	U1 Nwall
PAN-19-6b	Bulk	U1 Nwall
PAN-19-6c	Bulk	U1 Nwall
PAN-19-6d	Bulk	U1 Nwall
PAN-19-6e	Bulk	U1 Nwall
PAN-19-7a	Bulk	U1 Nwall
PAN-19-7b	Bulk	U1 Nwall
PAN-19-7c	Bulk	U1 Nwall
PAN-19-8a	Bulk	U1 Nwall
PAN-19-8b	Bulk	U1 Nwall
PAN-19-8c	Bulk	U1 Nwall
PAN-19-9a	Bulk	U1 Nwall
PAN-19-9b	Bulk	U1 Nwall
PAN-19-9c	Bulk	U1 Nwall
PAN-19-10a	Bulk	U1 Nwall
PAN-19-10b	Bulk	U1 Nwall
PAN-19-10c	Bulk	U1 Nwall
PAN-19-11a	Bulk	U1 Nwall
PAN-19-11b	Bulk	U1 Nwall

Table 6: Sample list of combustion experiment in Pucuncho in 2022.

Sample name	Type
Llareta ash	Bulk
Llareta charcoal	Bulk
Llareta-1	Smear Slide
Llareta-2	Smear Slide
Tola ash	Bulk
Tola charcoal	Bulk
Tola-1	Smear Slide
Tola-2	Smear Slide
Queñua ash	Bulk
Queñua charcoal	Bulk
Queñua -1	Smear Slide
Queñua -2	Smear Slide

Appendix II – Paper 1

Received: 3 November 2020 | Revised: 13 September 2021 | Accepted: 22 September 2021

DOI: 10.1002/gea.21889

RESEARCH ARTICLE

Geoarchaeology An International Journal WILEY

A site formation model for Cuncaicha rock shelter: Depositional and postdepositional processes at the high-altitude keysite in the Peruvian Andes

Sarah Ann Meinekat[1] | Christopher E. Miller[1,2,3] | Kurt Rademaker[4]

[1]Institute for Archaeological Sciences, University of Tübingen, Tübingen, Germany

[2]Senckenberg Centre for Human Evolution and Paleoenvironment, University of Tübingen, Tübingen, Germany

[3]SFF Centre for Early Sapiens Behaviour (SapienCE), University of Bergen, Bergen, Norway

[4]Department of Anthropology, Michigan State University, East Lansing, Michigan, USA

Correspondence
Sarah Ann Meinekat, Institute for Archaeological Sciences, University of Tübingen, Hölderlinstraße 12, 72074 Tübingen, Germany.
Email: sarah-ann.meinekat@uni-tuebingen.de

Funding information
Deutsche Forschungsgemeinschaft, Germany; National Science Foundation, United States

Abstract

We report results from geoarchaeological investigations at Cuncaicha rock shelter (4480 m above sea level) in the high Andes of southern Peru. Using field observations, geomorphological, micromorphological, micro-Fourier transform infrared spectroscopy, Bayesian modeling of radiocarbon ages, and archaeological data, we analyzed the entire stratigraphic sequence to determine depositional and postdepositional processes and agents to assess the impact of bioturbation and to correlate the deposits with regional paleoenvironmental information. The archaeological record is represented well on a microscale, and bioturbation has not destroyed the stratigraphic integrity. The Terminal Pleistocene sediments that contain the oldest archaeological material at the site, dating to ~12.3–11.1 ka, are especially well preserved and capped by a layer of tufa. Depositional changes from autochthonous carbonate precipitation during the Terminal Pleistocene toward allochthonous aeolian sedimentation in the Early Holocene reflect changing environmental and climatic conditions. Formation of a soil during the Late-Middle Holocene caused postdepositional alterations and likely correlates to variable environmental conditions. We use these results to formulate a site formation model for Cuncaicha rock shelter that integrates archaeological, chronological, and paleoenvironmental data.

KEYWORDS
Andes, Bayesian modeling, geoarchaeology, micromorphology, site formation processes, Terminal Pleistocene

1 | INTRODUCTION

The high Central Andes was one of the most extreme environments colonized by hunter-gatherers during the peopling of the Americas (Osorio et al., 2017; Rademaker & Moore, 2018). Excavations at the rock shelter site of Cuncaicha (4480 m above sea level [masl]) in the Pucuncho Basin of southern Peru have revealed evidence of an initial residential occupation during the Terminal Pleistocene 12.3–11.1 ka[1] (Rademaker & Hodgins, 2018; Rademaker et al., 2014, 2016). Glacial geologic data generated locally (Bromley et al., 2009, 2011) and

[1]All ages are reported as thousands of calibrated radiocarbon years before present (ka), using the SHCal20 calibration and the 95% calibrated ranges, rounded to the nearest 0.1 ka (Hogg et al., 2020).

Scientific editing by Sarah Sherwood.

paleoenvironmental records throughout the central Andes (e.g., Baker & Fritz, 2015; Blard et al., 2011; Moreno et al., 2009; Quade et al., 2008) indicate that high-elevation Andean environments 12,500 years ago and earlier were favorable for human settlement. Archaeological sites in the high Andes from Ecuador to Argentina show that early South Americans were already familiar with and successfully exploiting high-elevation resources and landscapes in the Terminal Pleistocene (Capriles et al., 2016; Jolie et al., 2011; Loyola et al., 2017, 2020; Nami & Stanford, 2016; Núñez et al., 2002; Rademaker et al., 2014; Santoro et al., 2019; Yacobaccio, 2017; Yataco Capcha & Nami, 2016). Together, these lines of environmental and archaeological evidence indicate remarkable adaptive abilities of late ice-age hunter-gatherers and suggest the possibility that an Andean megapatch formed a migration corridor through western South America (Osorio et al., 2017).

The key goals of this study are to develop a site formation model for Cuncaicha rock shelter, to assess the stratigraphic integrity of the site, and to assess the geochronological model proposed by Rademaker and Hodgins (2018). Bayesian modeling identifies distinct occupation phases, whereas the archaeological stratigraphy is continuous without apparent unconformities. Using a multimethodological geoarchaeological approach, we analyzed the formation history of the deposits in Cuncaicha rock shelter. A detailed analysis of the stratigraphic sequence identified the sedimentary components and depositional agents and allowed the construction of a site formation model.

The impact of bioturbation was examined, as this process can impact the archaeological record. Especially in the oldest deposits, it is important to investigate whether the anthropogenic material is in situ or has been translocated. Disturbance of sediment in Andean caves and rock shelters is known from many sites—oftentimes caused by modern-day use of the sites or looting activities (Engel, 1981; Lynch, 1980). Bioturbation is another important factor for such movements and has been documented in other Andean sites, such as Guitarrero Cave (Lynch, 1980). However, no targeted approach to study bioturbation specifically or site formation processes in general was applied at these sites.

Specific questions regarding Cuncaicha's formation during the Terminal Pleistocene and Mid-Holocene arose during excavation, which we have addressed in the study presented here. Additionally, we were able to not only establish the stratigraphic context of the earliest occupation but also investigate varying patterns of human occupation at Cuncaicha from the Terminal Pleistocene through the Holocene, and the relationship of the site to environmental change over time. The presence of paleoenvironmental signatures within the Cuncaicha deposits presents an opportunity to explore human–environment dynamics over thousands of years and to use this exceptional archaeological sequence as a unique source of paleoenvironmental information for the west Central Andes.

1.1 | Site setting

Cuncaicha rock shelter is situated in the Pucuncho Basin (4300–4600 masl) of southern Peru, which is located approximately 160 km northwest of the city of Arequipa by linear distance (Figure 1A). Three of the tallest summits in the region define the basin: Nevado Firura (5500 masl) to the north, Nevado Solimana (6095 masl) to the west, and Nevado Coropuna (6375 masl) to the south.

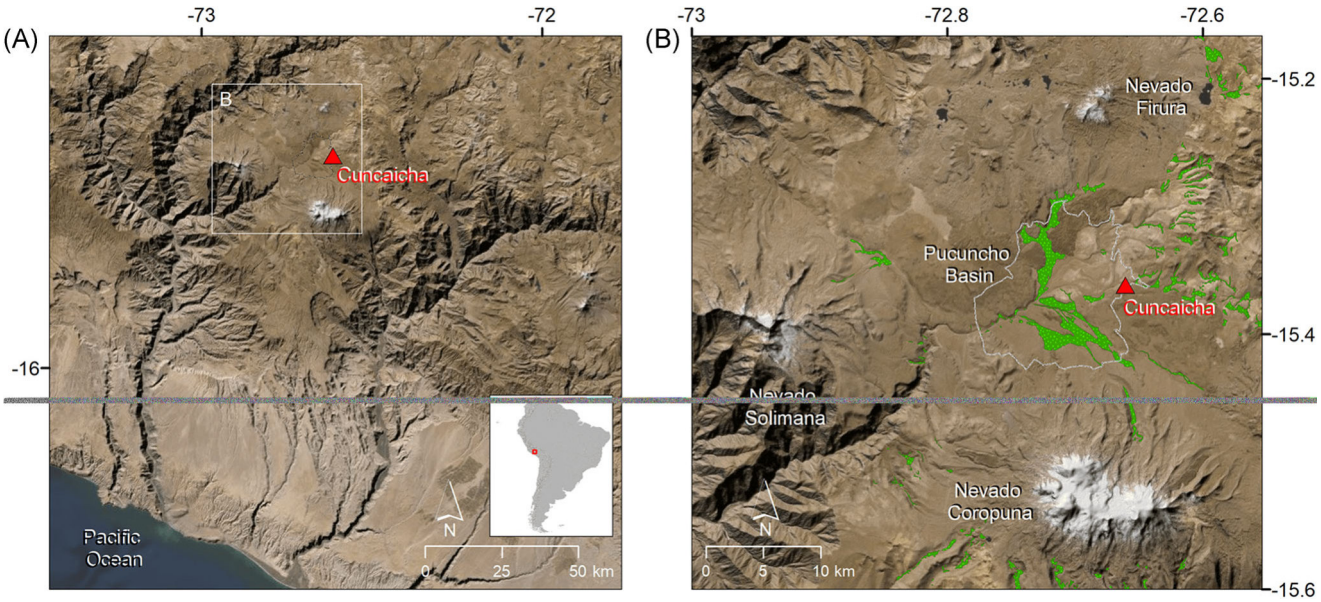

FIGURE 1 (A) Satellite image showing the location of Cuncaicha rock shelter in the Andes of southern Peru. (B) Detailed satellite image of project area. The white line defines the approximate limits of the Pucuncho Basin using the 4500 m topographic contour. Wetlands are digitized in green. Data sources: Satellite imagery (ESRI, Maxar, GeoEye, Earthstar Geographic, CNES/Airbus DS, USDA, USGS, AeroGRID, IGN, GIS User Community), Digital Elevation Model ALOS PALSAR 15-m (de Lima Moraes, 2018), Cotahuasi and Chuquibamba topographic quadrangles (Instituto Geográfico Nacional, 1990, 1995) [Color figure can be viewed at wileyonlinelibrary.com]

The Puncho Basin is located in the Dry Puna, an ecological zone of grasslands, shrub lands, lakes, and wetlands (Troll, 1968). It is characterized by a wet (January–March) and a dry (April–December) season. The overall climate is semiarid with low mean annual precipitation (600–800 mm), primarily driven by snow during the wet season (Dornbusch, 1998; Fick & Hijmans, 2017; Instituto Geográfico Nacional, 1990, 1995).

The basin was formed by successive periods of volcanic activity and contains ignimbrites of Miocene to Pliocene age overlain by Quaternary stratovolcanoes and andesitic lava flows of Pliocene to Holocene age (Figure 2) (Lajo Soto et al., 2001; Olchauski & Dávila, 1994; Thouret et al., 2002). Ignimbrites mapped in the basin are generally fine-grained and result in a gentle topography with little to no soil formation and sparse vegetation cover outside of wetlands. Aeolian deflation of some surfaces has created desert pavements. These volcanic deposits have been subject to glaciations of various extents, though ice limits from the Last Glacial Maximum and later remained well above the elevation of the basin and Cuncaicha rock shelter (Bromley et al., 2009, 2011; Rademaker et al., 2014; Úbeda et al., 2018). Glaciofluvial deposits mantle ignimbrites along stream courses and on outwash fans. Especially interesting for the early human settlement of the region, the Puncho Basin is located within the Alca obsidian source, and obsidian crops out in Pliocene-age Sencca/Arma Formation (Np-ar) ignimbrites exposed throughout the basin (Figure 2; Rademaker et al., 2013). Grasslands and wetland peat-bogs, that is *bofedales*, are extensive within the basin (Figure 1B) and serve as a habitat to camelid herds.

Cuncaicha rock shelter is located at the eastern margin of the Puncho Basin, where the Quebrada Cuncaicha perennial stream enters the basin from a west-draining valley. The rock shelter opens to the north, overlooking the eastern side of the Puncho Basin and Nevado Firura. A steep hillslope, covered by andesite slabs and boulders and the spiky *Stipa ichu* and *Opuntia* spp., leads down to the Sencca/Arma Formation alluvial fan surface, which is cut by Quebrada Cuncaicha (Figure 3). The fan is less steep than the slope leading up to the rock shelter. The alluvial fan has only little surface vegetation and is made up of ignimbrite and grus. Along the northern edge of the fan, the sediment shifts to the alluvial deposits of Quebrada Cuncaicha.

The rock shelter, formed by slab exfoliation processes at the northern edge of an andesite flow of the Pliocene Barroso Group (Olchauski & Dávila, 1994), is 14 m wide and shallow, with a maximum depth of 6 m from the drip line to the rear wall. Large slabs of collapsed shelter roof form a low berm at the present drip line and in front of the shelter, indicating that the shelter was larger previously. Glacially rounded andesite boulders found atop the shelter were likely deposited during the penultimate or earlier glacial period before formation of the rock shelter.

Inside the shelter, the walls show signs of weathering. Water may be observed seeping down with calcareous minerals precipitating, especially along the bedrock joints, though the rock shelter sediments are dry from the surface to the base of the sequence. We have observed these processes at other rock shelters in the area as well. Rodent dung is abundant on the modern surface of the shelter floor; there is no notable deposition of bat or bird guano. Today, while abandoned, the surface of the rock shelter is vegetated by grassy and weedy species. There is no evidence for modern-day use of the rock shelter as a campsite or animal corral, though the latter would not be expected, given the shelter's location near the top of a

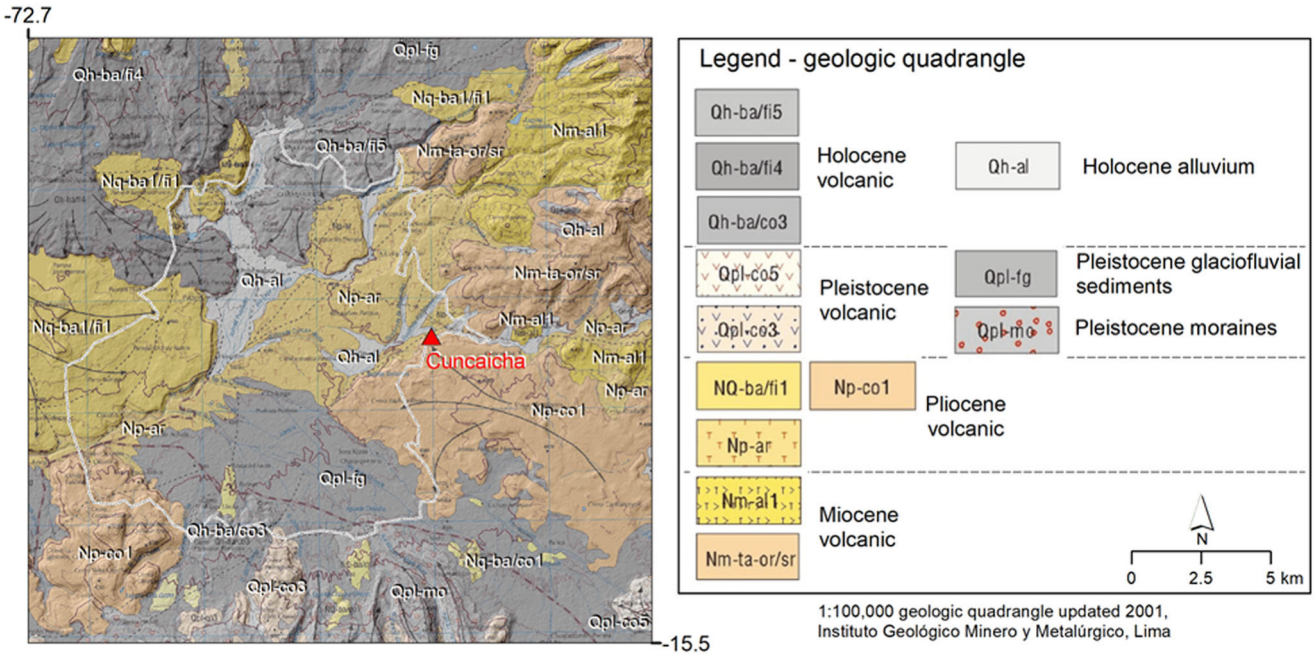

FIGURE 2 Geologic map of the project area. The legend shows major geologic formations. Data sources: Cotahuasi geologic quadrangle (Lajo Soto et al., 2001; Olchauski & Dávila, 1994), Digital Elevation Model ALOS PALSAR 15-m (de Lima Moraes, 2018) [Color figure can be viewed at wileyonlinelibrary.com]

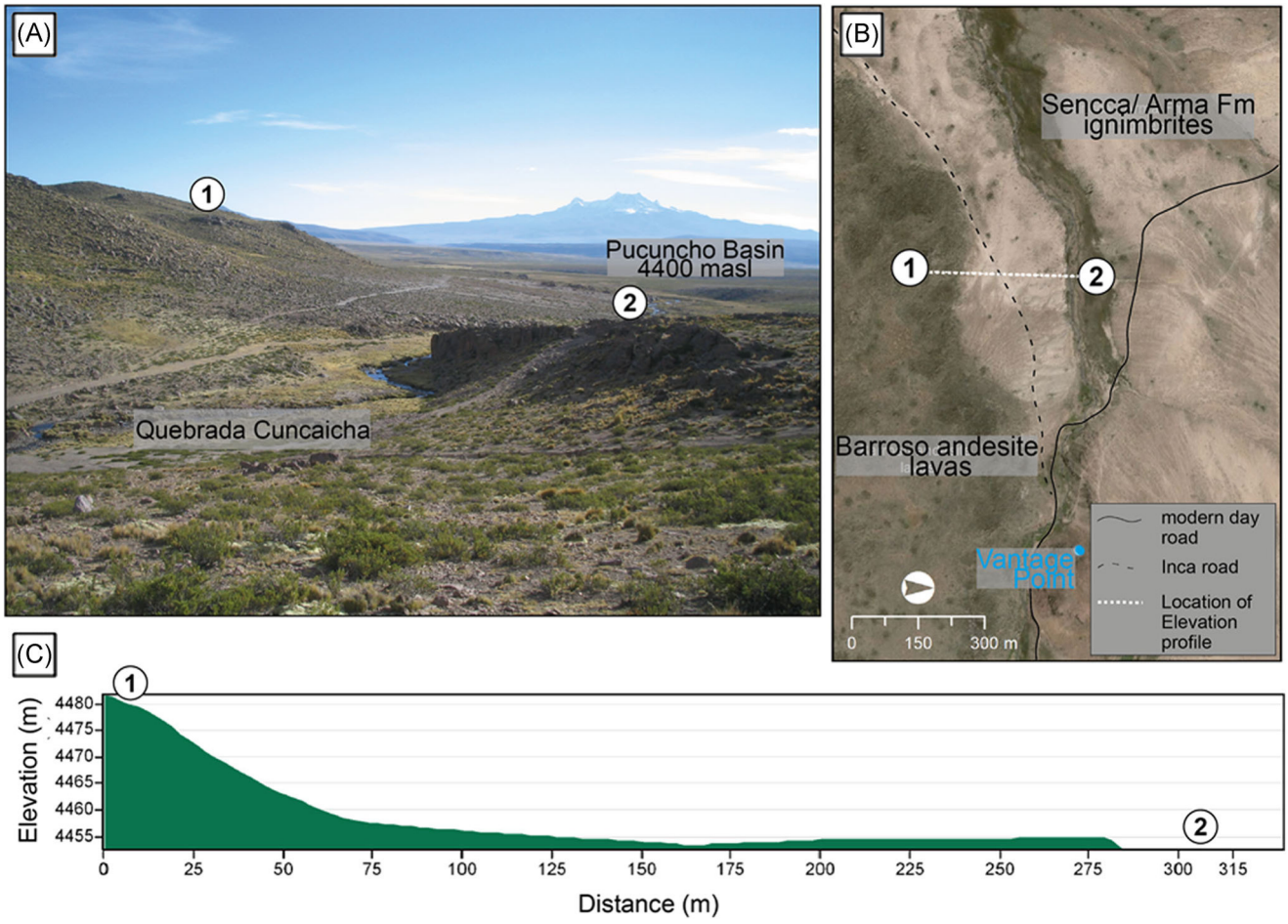

FIGURE 3 (A) Photo of Cuncaicha rock shelter (1) and the Pucuncho Basin, facing west. (2) The closest point of the Quebrada Cuncaicha to the rock shelter. In the background, Nevado Solimana (6095 masl), which constitutes the western border of the basin, is visible. (B) Satellite image of area with the location of (1) Cuncaicha rock shelter and (2) Quebrada Cuncaicha. The location of the elevation profile (C) is indicated, as well as the course of the modern road, and the pre-Columbian Inca road. The vantage point of the photograph (A) is shown. Note that on the satellite image, the increased vegetation along the quebrada is visible. Cuncaicha rock shelter is situated in a Barroso andesite lava formation. Sencca/Arma formation ignimbrites dominate the surface of the Pucuncho Basin in this area. East of the rock shelter, a weakly developed alluvial fan can be seen. On the northern side of the quebrada bed, gullies incise the slope surface and form small fans toward the river. (C) Elevation profile produced using ArcGIS 3D Analyst. Surface elevations are derived from corrected GPS and the total station survey of the project area [Color figure can be viewed at wileyonlinelibrary.com]

25-m hillslope ~300 m from Quebrada Cuncaicha and preferred pasturage (Figure 3). Dozens to hundreds of camelid corrals are found throughout the Pucuncho Basin, visible as round and rectangular dry-laid stone enclosures.

1.2 | Archaeological record at Cuncaicha

Cuncaicha rock shelter was excavated in 2010, 2012, 2014, and 2015. A combined total of 12.5 m^2 of excavations within the overhang uncovered a rich archaeological record of episodic occupations spanning from the Terminal Pleistocene through the Late Holocene. The excavation primarily focused inside of the rock shelter, where deposits were less affected by massive slabs of roof fall. Within the shelter, 17 excavation units were opened up over the four excavation seasons (Figure 4). Units 1–2 were excavated in 2010, Units 3–8 were excavated in 2012, Units 9–10 were excavated in 2014, and Units 9–13s and Units 19–21 were excavated in 2015 (Rademaker & Hodgins, 2018). The phased excavation allowed for different profiles to be studied for the geoarchaeological investigation and to be sampled for micromorphology. The main profiles that were sampled are located in Units 2, 9, 10, 11, 12, and 13. The cultural deposits in these units are up to 130 cm deep. The burials at Cuncaicha rock shelter were found in Units 9, 11/19, 13, and 13s. The pit features related to the burials are separated from the general discussion of the stratigraphic sequence.

Five archaeological strata (I–V) and an underlying sterile stratum (VI) were identified (Rademaker et al., 2014). However, most of the strata appear lithologically similar and consist largely of decimeter-thick, homogeneous layers without distinctive

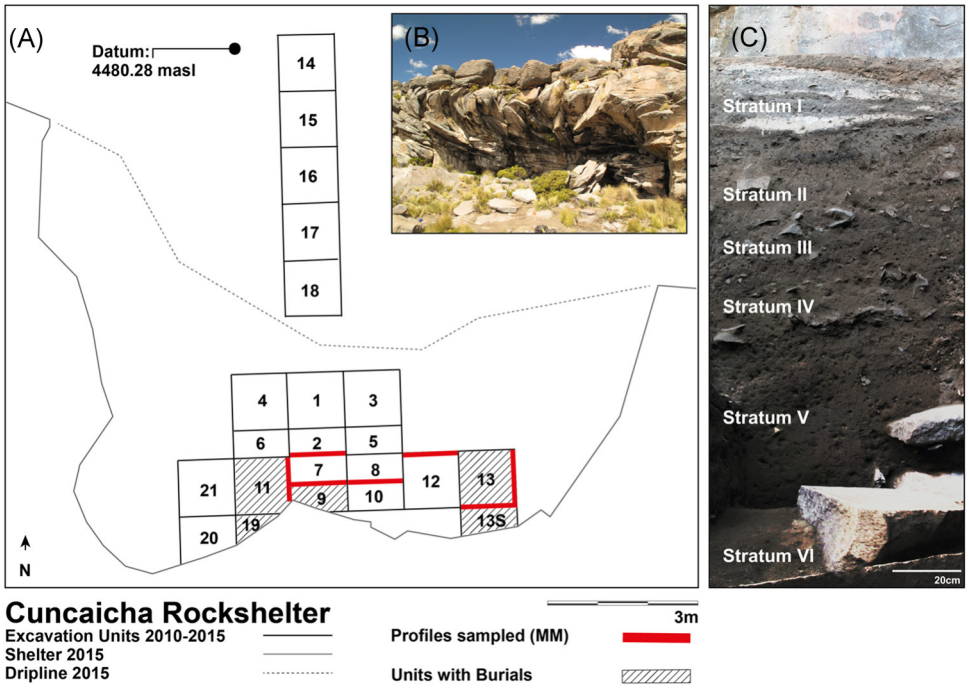

FIGURE 4 (A) Planview of Cuncaicha rock shelter with excavated units. Profiles sampled for micromorphology (MM) are highlighted in red. (B) Photograph of Cuncaicha rock shelter. Andesite slabs have deposited in front through ongoing slab exfoliation processes. On top, rounded glacial boulders are visible. (C) Profile photo showing deposits at Cuncaicha rock shelter, taken from the south wall in Unit 7. The deposits consist of 6-dm-thick strata that show subtle changes. In this photo, Stratum I shows the most significant features with distinctive ash lenses. For information on the field description of each stratum, including Munsell colors, the reader is referred to Table 3 [Color figure can be viewed at wileyonlinelibrary.com]

microstratigraphic units (Figure 4C). No sterile sediment layers are present between the archaeological strata. The sediment shows slight color differences as well as differences in the amount of coarse components, which led to the initial differentiation of the strata. Aside from color differences, a cemented mineral formation between Strata V and IV was used as a chronostratigraphic marker, and the presence of ash lenses and charcoal accumulations in the upper two strata allowed distinction from the lower strata. Thirty-eight accelerator mass spectrometry (AMS) radiocarbon ages were obtained on bone collagen from large herbivore bones in direct association with abundant anthropogenic artefacts (Table S1; Rademaker & Hodgins, 2018; Rademaker et al., 2014). The ages correspond with distinct episodes of occupation during the Terminal Pleistocene, Early Holocene, Late-Middle Holocene, and Late Holocene (Table 1). The relationship between ages and stratigraphy, which will be examined in detail in this paper, highlights several temporal and depositional hiatuses during which no natural or anthropogenic sediments have been detected.

Eleven more collagen AMS ages were obtained on human burials encountered during the 2014 and 2015 excavations (Table S1). Bayesian modeling indicates that site occupations and interment events did not overlap (Rademaker & Hodgins, 2018). Stable isotope analyses revealed that all people buried at Cuncaicha, including the most ancient three burials from the Early Holocene (~9.3–8.8, ~9.0–8.6, and ~8.5–8.4 ka), spent their formative years at high altitude (Chala-Aldana et al., 2018) and procured their diet from the highlands (Haller von Hallerstein, 2017).

Analysis of the rich archaeological record, first focusing on comparison of the lithic and faunal assemblages to those from other high-altitude Andean sites, hints at Cuncaicha being used as a residential base camp as early as the Terminal Pleistocene (Rademaker & Moore, 2018). Furthermore, preliminary analysis of the faunal assemblage has suggested that the site was occupied during the wet season at minimum (Moore, 2016). Ongoing analyses of Cuncaicha's material assemblages are focusing on the provenance of lithic raw materials, lithic technology and morphology, tool uses, and mobility indicators, plant and animal subsistence remains, domestic activities including food processing and combustion, use and manufacture of special objects, such as bone and shell beads and ochre, association of artefacts with individual burials, and cultural connections with related archaeological sites in other ecological zones. All of these analyses provide information on the function of Cuncaicha within larger settlement systems and the evolution of Andean biocultural adaptations. Geoarchaeological data are essential for contextualizing inferences made from material assemblage patterns and linking the site to its surrounding landscape.

TABLE 1 Bayesian modeled occupation spans in cal BP and intervening hiatuses in years using OxCal 4.4 (Bronk Ramsey, 2009) and SHCal20 (Hogg et al., 2020)

Component	Starting date (68.3%) cal BP	Ending date (68.3%) cal BP	Max span (68.3%) years	Starting date (95.4%) cal BP	Ending date (95.4%) cal BP	Max span (95.4%) years
LMH II		5440–5110	145		5455–4845	320
LMH I	5665–5490		80	5875–5330		185
EH-LMH hiatus			3665–3915			3420–4140
EH	9535–9340	9460–9290	90	9580–9300	9480–9210	210
TP-EH hiatus			1825–2490			1535–2530
TP II		11,830–11,350	150		11,840–11,060	350
TP I	12,045–11,840		215	12,275–11,780		435

Abbreviations: Amodel = 157.9; Amodel overall = 141.3; EH, Early Holocene; LMH, Late-Middle Holocene; TP, Terminal Pleistocene.

2 | METHODS

2.1 | Bayesian modeling of occupation chronology

We used Bayesian modeling of the Terminal Pleistocene, Early Holocene, and Late-Middle Holocene radiocarbon ages ($n = 35$) to examine occupation spans and the duration of hiatuses between occupation components. The Late Holocene portion of the sequence is not yet well dated, so it is omitted here.

Using OxCal 4.4 (Bronk Ramsey, 2009), AMS ages were structured within a stratigraphic model taking into account the excavated contexts providing dated samples. The structure of the model used occupation boundaries, phases (sets of unordered ages), and sequences (sets of ordered ages). Phases were defined as clusters of radiocarbon ages obtained from distinct strata. We experimented with various model structures to compare outputs. This sensitivity test revealed relatively low variance in outputs, suggesting that the results are reliable. Occupation spans calculated the maximum duration of distinct occupation components, and intervals calculated the duration of radiocarbon hiatuses between occupation components. Spans and intervals were calculated at the 68.3% and 95.4% probability ranges using the SHCal20 calibration (Hogg et al., 2020).

2.2 | Sediment micromorphology

The present study follows a multidisciplinary approach, combining different geoarchaeological methods. Studies like Ozán et al. (2019) at Baño Nuevo cave in Chilean Patagonia have shown this to be a promising approach to understand early South American sites in a broader context. The main geoarchaeological method used in this study is micromorphology, which is the study of oriented, intact sediment using indurated blocks and thin sections. The samples presented in this paper derive from 3 years of excavation at Cuncaicha rock shelter, in 2012, 2014, and 2015. During all field seasons, block samples for micromorphological studies were taken together with loose sediment samples. All samples were transferred to the University of Tübingen, Institute for Archaeological Sciences, Geoarchaeology Working Group, for processing and analysis. During the 2012, 2014, and 2015 field seasons, C. E. Miller and S. A. Meinekat collected block samples from the main profiles in the rock shelter, spanning the whole stratigraphic sequence—from the sterile basal layer, Stratum VI, to the most recent Holocene one, Stratum I. These micromorphological blocks are denoted with a prefix CUN-xx. The block samples were cut from the profiles or within the unit as monoliths using plaster bandages to preserve their integrity (Figure 5).

For processing, the samples were first dried in an oven at 50°C. After drying, the samples were indurated under vacuum in polyester resin, styrene, and methylethelketone peroxide (MEKP)-hardener. Once the blocks were hardened, they were sliced and subsampled for thin-section production using a diamond blade rock saw. The thin sections were produced by grinding the samples to 30 µm thickness. In total, 26 archaeological thin sections were produced and analyzed for this study, providing a complete coverage of the archaeological sequence (Tables 2 and S3). The thin sections were observed by the naked eye and under magnification using a Zeiss Axio Imager petrographic microscope with plane-polarized light (PPL), cross-polarized light (XPL), oblique incident light (OIL), and fluorescence (both blue light and ultraviolet). The analysis and description of the thin sections followed the terminology and protocols established by Stoops (2003) and Courty et al. (1989).

2.3 | Fourier transform infrared spectroscopy (FTIR)

While the main method used was micromorphology, we also integrate data obtained through FTIR and micro (µ-)FTIR analyses, to complement field and micromorphological analyses and to identify mineral components. FTIR analyses were conducted on sediment samples from the 2015 excavation using the Agilent Technologies Cary 660 FTIR spectrometer at the Geoarchaeology Laboratory at the University of Tübingen. Samples were ground using an agate mortar and pestle. The ground samples were analyzed with the FTIR spectrometer using an Attenuated Total Reflectance (ATR) crystal, with 32 co-added scans at 4 cm^{-1} resolution over a spectral range of 400–4000 cm^{-1}. The Essential FTIR and

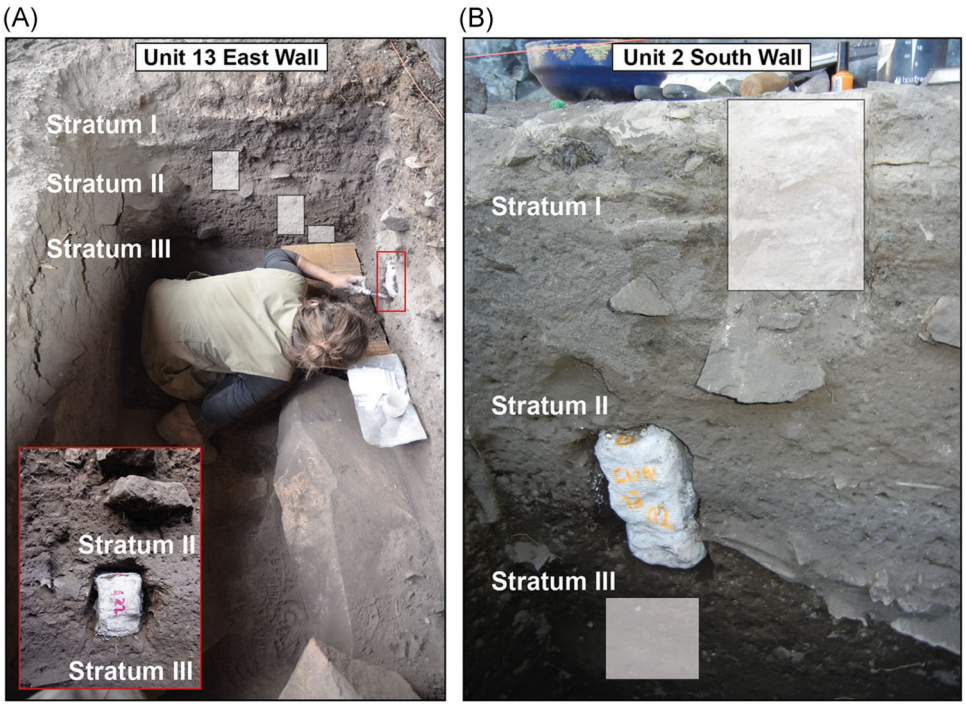

FIGURE 5 Sampling of profiles in Cuncaicha rock shelter for micromorphological block samples. The fine, dry, and very loose sediment with many large bedrock, lithic, and bone fragments impeded the use of Kubiena boxes for sampling. Block samples for thin-section production were taken by (1) photographically documenting the intact profile; (2) carving the sides of the block; (3) placing plaster bandages around the sediment block; (4) documenting the sample in profile with photographs, marking orientation, and labeling; (5) carefully breaking the sample from the profile; and (6) covering the backside of the sample with plaster bandages. (A) Sampling of CUN-15-122 by SAM in 2015. The inset (red box) shows the frontal photograph of the sample that is being taken in the photo. The sample was placed at the contact between Stratum II and Stratum III. White boxes show where samples CUN-15-125, CUN-15-126, and CUN-15-127 (left to right) were taken. (B) South profile of Unit 2 during the 2012 excavation with sample CUN-12-02 still in profile. White boxes show the position of samples CUN-12-01 (top) and CUN-12-03 (bottom) [Color figure can be viewed at wileyonlinelibrary.com]

Resolutions Pro software packages were used for mineralogical identification. Alongside this, μFTIR analyses were conducted on selected thin sections (CUN-12-09, CUN-15-14) to identify mineral compositions, possible products of postdepositional chemical alteration, and heating processes of components observed under the microscope, using the Agilent Technologies Cary 610 FTIR microscope, with 32 coadded scans at 4 cm^{-1} resolution between 4000 and 570 cm^{-1}. The data were collected as individual point measurements, with a sampling area of ~50–70 μm diameter. For interpretation of the obtained spectra, reference databases were used, mainly the databases generated by S. Weiner (http://www.weizmann.ac.il/kimmel-arch/infrared-spectra-library), the RRUFF project (www.RRUFF.info; Lafuente et al., 2015), and the mineral collection of Dr. S. Mentzer from the Geoarchaeology Working Group in Tübingen.

3 | RESULTS

3.1 | Bayesian modeling of occupation chronology

All except 1 of the 23 Terminal Pleistocene faunal ages were included in the model. The one omitted age is Beta-297423, an AMS measurement on non-ultra-filtered (UF) collagen. A split of this sample (AA94254) was dated at the Arizona AMS Lab using collagen ultrafiltration. A χ^2 test indicated that the two measurements are statistically different. The Arizona measurement on UF collagen is considered the more reliable, so it was retained for the model, and the Beta Analytic measurement was discarded. Three Terminal Pleistocene faunal specimens were split and dated at the Arizona AMS Lab using collagen UF and at the PaleoResearch Institute using XAD purification. χ^2 tests indicated statistical similarity for measurements generated by both labs on all three specimens (see Table S1), weighted means of the splits were calculated, and these were used in Bayesian models. Details of the Bayesian model structure and plots of modeled ages and components are provided in the Supporting Information.

We first attempted to group the 19 Terminal Pleistocene individual and weighted mean ages into a single occupation phase. However, this produced poor agreement and convergence indices, with flags on the oldest and youngest ages. Cuncaicha's Terminal Pleistocene occupation coincides with a segment of the SHCal20 radiocarbon calibration curve where calibrated ages are difficult to resolve. The ages cluster on two distinct plateau segments and an intervening slope (Figure S1). To explore the spread of the Terminal

TABLE 2 List of archaeological thin sections from Cuncaicha rock shelter with provenience information

Sample ID	Stratum	Component	Unit	Profile/feature
CUN-12-01A	1	LH	2	South
CUN-12-01B	1 → 2	LH	2	South
CUN-12-01C	2	LH	2	South
CUN-12-02A	2	LH	2	South
CUN-12-02B	2 → 3	LH → LMH	2	South
CUN-12-02C	3	LMH	2	South
CUN-12-03	3 → 4	LMH → EH	2	South
CUN-12-09	5 → 6	EH → TP	2	South
CUN-12-06A	5	TP	9	Feat. 12-04 (base)
CUN-12-06B	5	TP	9	Feat. 12-04 (base)
CUN-12-07	4	EH	9	Feat. 12-04 (top)
CUN-15-117	5	TP	9	North
CUN-14-01	5	TP	10	North
CUN-15-116	5	TP	10	North
CUN-12-08	5	TP	11	East
CUN-15-118	5	TP	11	East
CUN-15-14	4 → 5	EH → TP	12	Center of unit
CUN-15-120	5	TP	12	North
CUN-15-128	2 → 3	LH → LMH	12	North
CUN-15-122	2 → 3	LH → LMH	13	South
CUN-15-125A	2	LH	13	East
CUN-15-125B	2	LH	13	East
CUN-15-126A	2 → 3	LH → LMH	13	East
CUN-15-126B	3	LMH	13	East
CUN-15-127A	3	LMH	13	East
CUN-15-127B	3 → 4	LMH →EH	13	East

Abbreviations: EH, Early Holocene; LH, Late Holocene, LMH, Late-Middle Holocene; TP, Terminal Pleistocene.

Pleistocene ages, we modeled the ages as two contiguous early (TP I) and late (TP II) phases and then as two sequential phases. The contiguous-phase model inserts an additional "transition" boundary between an early group and late group of ages, assuming quasi-continuous occupation activity between the two distinct phases. The sequential-phase model inserts two internal boundary commands between groups of ages and allows for the possibility of two distinct, ordered occupation phases separated by a hiatus.

Comparison of these two-phase models showed highly consistent results, with the contiguous-phase model having a slightly better agreement index (Amodel = 158.9) than the sequential-phase model (Amodel = 152.5). No gap between modeled early and late Terminal Pleistocene phases is indicated (Figures 6 and S2), suggesting that the difficulty in modeling the Terminal Pleistocene occupation as a single phase is likely an artefact of the irregular SHCal20 calibration curve during this period of time. A statistically similar, continuous but time-transgressive accumulation of Terminal Pleistocene occupation evidence is supported by both models and consistent with original interpretations of unmodeled ages (Rademaker et al., 2014).

Considering the contiguous-phase model and both Terminal Pleistocene phases together, the Terminal Pleistocene occupation of Cuncaicha is constrained to a shorter maximum time period (785 years at the 95.4% confidence interval) (Table 1, Figure S3) than suggested by the calibrated age ranges of the individual faunal ages. Separating the Terminal Pleistocene occupation from the subsequent Early Holocene occupation, a hiatus of 1535–2530 years (95.4% range) or 1825–2490 years (68.3% range) is indicated—about two millennia.

The seven Early Holocene AMS ages were modeled as a single phase. The Early Holocene occupation spans a maximum of 210 years (95.4% range) or a maximum of 90 years (68.3% range). Whether the Early Holocene component lasted one or two centuries, it was much shorter than the preceding Terminal Pleistocene occupation. Following the end of the Early Holocene occupation, a hiatus of three to four millennia is indicated before the start of the Late-Middle Holocene occupation.

Modeling the six Late-Middle Holocene ages as a single phase did not produce good agreement or convergence indices. Rademaker

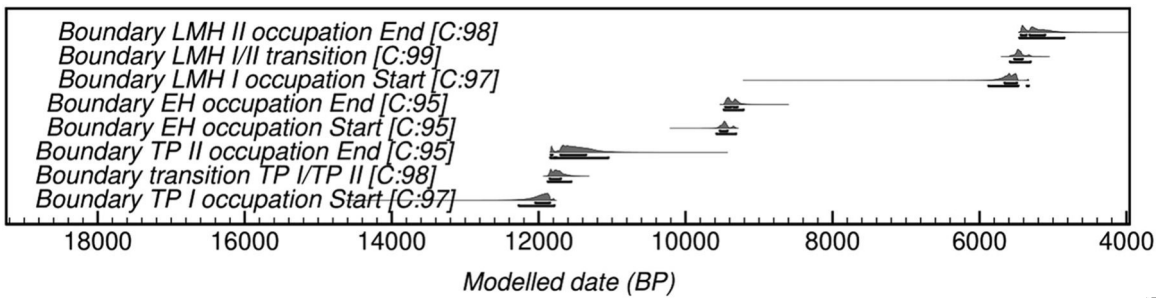

FIGURE 6 Bayesian model plot of boundaries, with two Terminal Pleistocene contiguous phases (TP I and TP II), a single Early Holocene phase, and two Late-Middle Holocene contiguous phases (LMH I and LMH II). No gaps are indicated either between TP I and TP II or between LMH I and LMH II. This suggests quasi-continuous but time-transgressive accumulation of occupation evidence in both periods. C, convergence indices

and Hodgins (2018) identified the likely reason for this issue, a lower than optimal dating density for this occupation component. The six Late-Middle Holocene ages form distinct early and late clusters of three ages each. Using a sequential two-phase model, the Late-Middle Holocene occupation spans a maximum of 505 years (95.4% range) or 225 years (68.3% range).

3.2 | Field observations and sediment micromorphology

Here, we provide a detailed description of the strata at Cuncaicha for the first time, combining field observations with those made under magnification. Table 3 provides specific remarks on the sedimentary components, noting whether they are geogenic, biogenic, or anthropogenic. The micromorphological analysis confirms that the sedimentary components are largely similar across the different strata; however, their frequency and occurrence in the different strata allow for further differentiation.

3.2.1 | Stratum VI

Stratum VI is the anthropogenically sterile sediment that pre-dates Stratum V at >12.3 ka. Micromorphology block CUN-12-09, collected from the south profile of Unit 2, captures the subtle transition from Stratum V to Stratum VI in the bottom left corner. In general, the Stratum VI sediment is of light brownish color and compact (Figure 7). Aside from the absence of anthropogenic material, the Stratum VI groundmass resembles the groundmass in the overlying Stratum V.

3.2.2 | Stratum V

Stratum V is associated with the earliest Terminal Pleistocene occupation at the site (~12.3–11.1 ka), with 23 ages from Units 1, 2, 7, 9, and 13s (Tables 1 and S1). Thin sections were produced from micromorphological block samples from Units 2 (CUN-12-09), 9 (CUN-12-06, CUN-15-116), 10 (CUN-14-01, CUN-15-117), 11 (CUN-12-08, CUN-15-118), and 12 (CUN-15-120) (see Tables S2 and S3). Generally, Stratum V sediment has fewer coarse inclusions than the overlying strata. Under the microscope, a further differentiation is possible (Figure 8). Stratum V sediment is quite homogeneous in the sheltered and undisturbed part of the rock shelter (Units 2, 11, 12). Stratum V is defined by a highly calcareous, compact groundmass with moderate inclusions of burned bone and bedrock fragments, as well as microdebitage. In contrast to the general findings from Stratum V based on samples from Units 2, 11, and 12, in the thin sections from pit feature 12-04 in Unit 9 (CUN-12-06, CUN-14-01), the microstructure is considerably more disintegrated and looser than Stratum V (Table S2). Furthermore, in the feature thin sections CUN-14-01 and CUN-12-06 A and B and CUN-15-116, sediment is decalcified.

Burning of bones as an indicator for anthropogenic activity has been tested with μFTIR analyses (Figure 9). Analyses were performed on bone fragments included in CUN-12-09, originating from the Strata V–VI contact in Unit 2. The μFTIR spectra from the bone fragments indicate that the bones have been burned, matching the spectra from the burned bone reference collections.

3.2.3 | Transition V–IV

At the transition from Stratum IV to Stratum V, a compact mineral layer was identified. One fragment of the mineral layer, deriving from the Unit 13 north wall, has been directly dated (see Section 4.2, Tables 1 and S1). Another fragment of this layer from Unit 12 was processed into a thin section (CUN-15-14) (Tables S2 and S3). Macroscopically, the layer appears to be cementing Terminal Pleistocene sediment. The overall structure shows biomorphic forms with some vegetal voids visible with the naked eye. Macroscopically, the layer appears to be tufa, a calcareous spring deposit forming under ambient wet conditions.

Microscopically, the overall appearance, the microstructure, and the voids resemble normal, calcareous tufa. Compositionally, however, alterations are visible. The sediment in the mineral layer appears to be cemented, and the matrix is completely composed of a concreted mineral formation. The mineral is beige in plane-polarized light (Figure 10B) and under cross-polarized light, the layer appears almost entirely isotropic, except for some inclusions of anisotropic mineral grains (mostly plagioclase from the bedrock). This suggests the presence of a phosphatic mineral instead of a calcareous one. The sediment directly below this layer in Unit 12 (CUN-15-120) is decalcified as well (Table S2).

We analyzed the layer in thin section (CUN-15-14) using fluorescence microscopy. Under blue light, the amorphous mineral is highly fluorescent (Figure 10B), supporting the identification of a phosphatic mineral phase. Adding UV light to the blue light, secondary mineral formations were additionally visible. We also conducted FTIR analysis on a loose sample from the Unit 12 north profile. The FTIR spectrum matches with apatite spectra from the reference spectral library (Figure 10A). Furthermore, μFTIR analyses were performed on the CUN-15-14 thin section. In the thin section, domains composed almost exclusively of the suspected apatite were selected, before collecting spectra on these points. The μFTIR spectrum also matches apatite spectra from the reference spectral library. All of these observations support the identification of the mineral layer at the Stratum V/IV contact as tufa that underwent diagenetic transformation into apatite.

3.2.4 | Stratum IV

Stratum IV dates to the Early Holocene (~9.6–9.2 ka) based on seven AMS ages from Units 1, 2, 7, and 13 (Tables 1 and S1). This stratum is laterally extensive, homogeneous, and about 30 cm thick.

TABLE 3 Results from the geoarchaeological samples and thin-section analyses per stratum

Stratum	Field observations	Macroscopic thin-section observations (see also Table S3)	Microscopic thin-section observations (see also Table S2)			Interpretation
			Geogenic	Biogenic	Anthropogenic	
VI (Figure 7)	Depth: >120–130 cm below surface Hand coring to 150 cm encountered coarse clastic material increasing with depth until refusal on bedrock slabs Munsell 10 YR 4/3 Brown compact sandy silt	Similar to Stratum V	Tufa-related carbonates Predominance of micritic carbonates with few coarse inclusions, i.e., andesite rockfall, results in homogeneous, compact groundmass interrupted by voids	Organic matter visible as amorphous organic fine material Some channels, probably by root or microfauna activity	None	Archaeologically sterile substratum
V (Figure 8)	Depth: ~80 to ~120–130 cm below surface ~40–50 cm thick, laterally extensive Munsell 10 YR 3/2-4/2 Very dark grayish brown to dark grayish brown silt	Fewer coarse inclusions than the overlying strata	Groundmass consists of micritic calcite, related to tufa formation Biomorphic tufa forms within a matrix of micritic tufa-related carbonates Some laminations with diatoms within the tufa-related carbonates High carbonate amount condenses the groundmass and leads to a compact microstructure Geogenic material other than carbonates, such as natural volcanic glass, is present but is less frequent than in the Holocene strata Autochthonous andesite fragments present, with only minor weathering processes	Amorphous organic fine material associated with micritic carbonate Some channels interrupt the groundmass and rework material locally, as seen in microgranular infillings Compared to Stratum VI, the groundmass is more microgranular	Ash-derived carbonates present Single ash oxalate pseudomorphs, articulated ash oxalate pseudomorphs Small amounts of charcoal present Lithic microdebitage of a variety of raw materials (red jasper, quartzite, obsidian) Bone fragments, most of which exhibit signs of heating	First human occupation in Terminal Pleistocene and tufa formation
Transition V–IV (Figure 10)	Depth: ~80 cm below surface ~5–10 cm thick, discontinuous Munsell 10 YR 3/2 dark brown and 10 YR 4/2 dark grayish brown	Mineral layer appears to be cementing Terminal Pleistocene sediment Coarse inclusions of possibly burnt bone and bedrock fragments Fine organic speckles frequent and increase	The sediment in the mineral layer appears to be cemented, and the matrix is completely composed of a concreted mineral formation Microcrystalline mineral formation is intermixed with typical silty groundmass			Phosphatized tufa layer

TABLE 3 (Continued)

Stratum	Field observations	Macroscopic thin-section observations (see also Table S3)	Microscopic thin-section observations (see also Table S2)			Interpretation
			Geogenic	Biogenic	Anthropogenic	
	mottled, compact, gravelly Mineral layer and concretions identified as tufa	toward the upper rim of the thin section Overall structure shows biomorphic forms with some voids				
IV (Figure 11A,B)	Depth: ~50 to ~80 cm below surface ~30-cm thick, laterally extensive Munsell 10 YR 3/2 Very dark grayish brown, homogeneous fine silt Resembles Stratum II	The gray color and coarse inclusions of bedrock fragments, bone, and charcoal are observable with the naked eye in thin section and are consistent in all of the thin sections from Stratum IV	Moderately calcareous groundmass, but a decrease in micritic carbonates compared to Stratum V Few tufa-related carbonates present Silt and fine sand-sized material prevalent, including plagioclase mineral grains, as well as common inclusion of natural volcanic glass Relatively unweathered andesite bedrock fragments common	Amount of biogenic, amorphous plant tissue is very low Aside from the microgranular microstructure, channels provide evidence for localized mixing of material by insects or roots	Sand-sized bone fragments are either calcined, or of brownish color, suggesting burning Bone fragments do not show signs of weathering Sand-sized charcoal fragments more common than humified organic matter Lithic microdebitage represented by sand-sized flakes of obsidian	Early Holocene occupation Increase of allochthonous silt-sized, aeolian particles reflects change in the depositional environment
III (Figure 11C–H)	Depth: ~30–40 to ~50 cm below surface Variably thick, 10–20 cm where present, not laterally extensive across the entire excavation area Munsell 10 YR 2/1-2/2 black to very dark brown homogeneous silty sand with high charcoal content	Not visible macroscopically in samples CUN-15-128 and CUN-15-122	Microstructure is microgranular, very open, and coarse fragments are completely unoriented Does not contain tufa-related carbonates Under crossed polarized light, the groundmass is generally noncalcareous However, secondary carbonate features are prominent Around voids, mostly channels, coatings, and hypocoatings of secondary calcite are present Silty cappings and coatings on the coarse fraction components are evident	Significant increase in amorphous plant material visible in plane-polarized light Humified, finely comminuted organic matter explains distinctive darker color Channels, some with infillings, some of which are crescent-shaped, are frequent	High bone fragment and charcoal content compared to the other strata Frequent sand-sized and larger gravel-sized bone fragments exhibit signs of heating. Bone fragments in thin sections appear to be larger than in the underlying strata, matching the field observations. Alongside heating processes, some bone fragments display signs of weathering Few to no ash oxalate pseudomorphs are present. In the thin sections from Unit 2, some single ash oxalate pseudomorphs are	Late-Middle Holocene occupation Formation of an A-horizon

(Continues)

TABLE 3 (Continued)

Stratum	Field observations	Macroscopic thin-section observations (see also Table S3)	Microscopic thin-section observations (see also Table S2)			Interpretation
			Geogenic	Biogenic	Anthropogenic	
			Bedrock fragments are present and show signs of weathering		included. In Units 12 and 13, ash oxalate crystals are completely absent Microdebitage of obsidian, microcrystalline volcanic rock, and jasper is prevalent Ochre is indicated in the thin section CUN-12-02C	
II (Figure 12)	Depth: ~15–25 to ~30–40 cm below surface 15 cm thick, observed across the entire excavation area Munsell 10 YR 3/2 Very dark grayish brown, homogeneous fine silt Ceramic sherds diagnostic to <4 ka in all units	Bedrock fragments, burnt bone, and charcoal Similar to Stratum IV	The fine fraction is mainly composed of silt-sized particles mixed with some clay and fine sand Natural volcanic glass shards and small fragments of pumice are included in the groundmass Carbonates are an important component. Primary carbonates more frequent than secondary carbonates. Formation of secondary carbonate features around channels, as coatings and hypocoatings Tufa-forming processes. Small tufa aggregates, either in situ or reworked throughout the excavation area. In Unit 13, there is an increase in tufa aggregates, some reworked Groundmass inside these aggregates is similar to the surrounding groundmass, indicating only localized reworking Further material mixing is evidenced by silt coatings of the coarse fraction	Microstructure is microgranular and rather loosely packed Further material mixing in Stratum II is evidenced by the presence of channels, some of which are infilled Biogenic components decrease significantly compared to the underlying Stratum III. Only some humified plant matter can be observed	Coarse components are dominated by small sand-sized bone fragments. Some bone fragments are larger, and most of them indicate heating processes Charcoal fragments Microdebitage of obsidian, red, and yellow jasper is frequent Ash-derived carbonates contribute to the groundmass. Many single or articulated round ash oxalate pseudomorphs	Late Holocene occupation Mixed signals indicate less unidirectional trends

TABLE 3 (Continued)

Stratum	Field observations	Macroscopic thin-section observations (see also Table S3)	Microscopic thin-section observations (see also Table S2)			Interpretation
			Geogenic	Biogenic	Anthropogenic	
I (Figure 13)	Depth: 0 to 15–25 cm below surface 15–25 cm thick and extensive throughout the excavated area Munsell 10 YR 6/1 black fine organic silt with high charcoal content, 10 YR 3/2 very dark grayish brown fine silt, 10 YR 8/1 white ash lenses <4 ka diagnostic ceramic in all units	Coarse inclusions mostly consist of burnt bone fragments and charcoal Bedrock fragments and ceramic sherds Combustion-related material displays typical repetitive sequencing of intact, stacked combustion features of rubefied sediment, charcoal, and ash layers Localized mixing of materials. Contacts between layers are undulating and not always sharp. Aggregates including different material than the surrounding groundmass are visible Channels cut through distinct layers, results in mixing of these layers	Allochthonous geogenic material less common than in the other strata and concentrated in specific layers, while other microlayers are almost purely anthropogenic, e.g. in ash layers Amount of geogenic sediment reduced by the prevalence of anthropogenic-derived materials, such as ashes Secondary carbonates present as coatings and hypocoatings around voids, as infillings in channels, or as impregnation in the groundmass, mostly sparitic, with higher birefringence Relative to primary carbonates, secondary carbonates are minor Formation of geogenic tufa In calcareous groundmass, formation of calcified plant tissue, resulting in tufa nodules. Some tufa-forming processes result in micritic layers of laminated tufa. No laterally extensive tufa layer is present Some reworked tufa fragments	Biogenic input limited to sporadic inclusions of uncarbonized plant tissue	Amount, size, and type of charcoal fragments varies between different microlayers Formation of ash oxalate pseudomorphs observed in charcoal. Some ash oxalate pseudomorphs still in articulation or in distinct ash layers Amount of carbonates in the groundmass decreases in the charcoal-rich layers and mostly concentrated on ash oxalate pseudomorphs	Late Holocene/Modern occupation Mixed signals indicate less unidirectional trends Stacked combustion layers resulting from multiple burning events

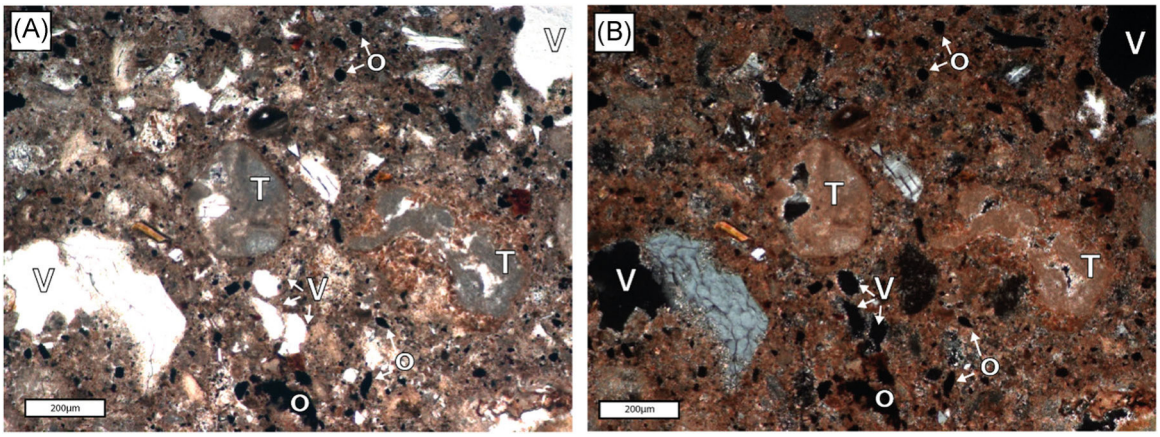

FIGURE 7 Photomicrographs of the archaeologically sterile Stratum VI, taken from CUN-12-09. (A) and (B) The typical massive groundmass of Stratum VI dominated by micritic carbonates in plane-polarized light (A) and cross-polarized light (B). The groundmass is interrupted by some voids (v), mostly vughs. Two tufa aggregates are visible (T). Tufa aggregates are composed of micritic calcite. Fine organic matter (o) is visible in the form of amorphous organic material. Note that there is more organic matter included [Color figure can be viewed at wileyonlinelibrary.com]

Thin sections containing Stratum IV sediment were produced from micromorphological block samples deriving from the south wall of Unit 2 (CUN-12-03), as well as from the top of the pit feature 12-04 from the north profile in Unit 9/10 (CUN-12-07) (Tables S2 and S3). Macroscopically, Stratum IV resembles Stratum II. Stratum IV contains carbonates, especially in the form of anthropogenically derived ashes, but in comparison to Stratum V, the amount of allochthonous silt-sized particles in relation to primary carbonates increased. Sediment from the top of pit feature 12-04 in Unit 9 is noncalcareous and shows increased weathering processes (Figure 11A,B).

3.2.5 | Stratum III

Stratum III dates to the Late-Middle Holocene (~5.9–4.8 ka) based on six ages from Units 2, 6, and 7 (Tables 1 and S1). Thin sections from Stratum III derive from micromorphology blocks in Units 12 and 13 (CUN-15-122, CUN-15-126, CUN-15-127, CUN-15-128), as well as from the south wall of Unit 2 (CUN-12-02, CUN-12-03) (Tables S2 and S3). Stratum III was not visible in the field in samples CUN-15-128 and CUN-15-122, but there is a clear transition from Stratum II to III visible under the microscope (Figure 12B). The most distinctive characteristic of this stratum is a homogeneous dark color and high bone fragment and charcoal content. Under the microscope, differences between Stratum III and the other strata are more readily visible. The microstructure in Stratum III is more granular, very open, and coarse fragments are completely unoriented; channels, some with infillings and some of which are crescent-shaped, are frequent (Figure 11C–H). Stratum III is also characterized by the presence of abundant, finely comminuted organic material and weathering of bone and andesite. The groundmass of Stratum III is noncalcareous, but shows prominent secondary carbonate features.

3.2.6 | Stratum II

Stratum II dates to the Late Holocene, based on one AMS age from Unit 2 (~2.1–1.9 ka) and ceramic sherds diagnostic to <4 ka in all units (Tables 1 and S1). Thin sections from Stratum II derive from block samples from the south wall of Unit 2 (CUN-12-02), Unit 12 (CUN-15-128), and Unit 13 (CUN-15-122, CUN-15-125) (Tables S2 and S3). Under the microscope, Stratum II shows some diagnostic characteristics, which can be observed in all of the thin sections deriving from this stratum. These include a rather uniform groundmass, characterized by small sand-sized bone fragments and moderate carbonate content, indicating frequent combustion activity as well as small-scale tufa formation, similar to Stratum I (Figure 12).

3.2.7 | Stratum I

Stratum I dates to the Late Holocene based on one AMS age from Unit 7 (0.8–0.6 ka), the presence of <4 ka diagnostic ceramic in all units, and occasional historic artifacts (Tables 1 and S1). In the field, it appeared less homogeneous than Stratum II, with stacked charcoal and ash lenses.

Three thin sections (CUN-12-01A, B, C) from Stratum I were produced out of block sample CUN-12-01 from the Unit 2 column (Tables S2 and S3). The different layers are defined by a change in the main components from ash-rich to charcoal-rich to rubefied sediment layers. The lowest thin section of Stratum I, CUN-12-01C, captures the transition to Stratum II. In the upper 2/3 of the thin section, the distinctive layering of sediment is evident (Figure 13). Combustion-related material displays the typical sequencing of intact combustion features of rubefied sediment, charcoal, and ash layers (Mentzer, 2014). This sequence is repetitive, displaying stacked combustion features resulting from multiple burning events.

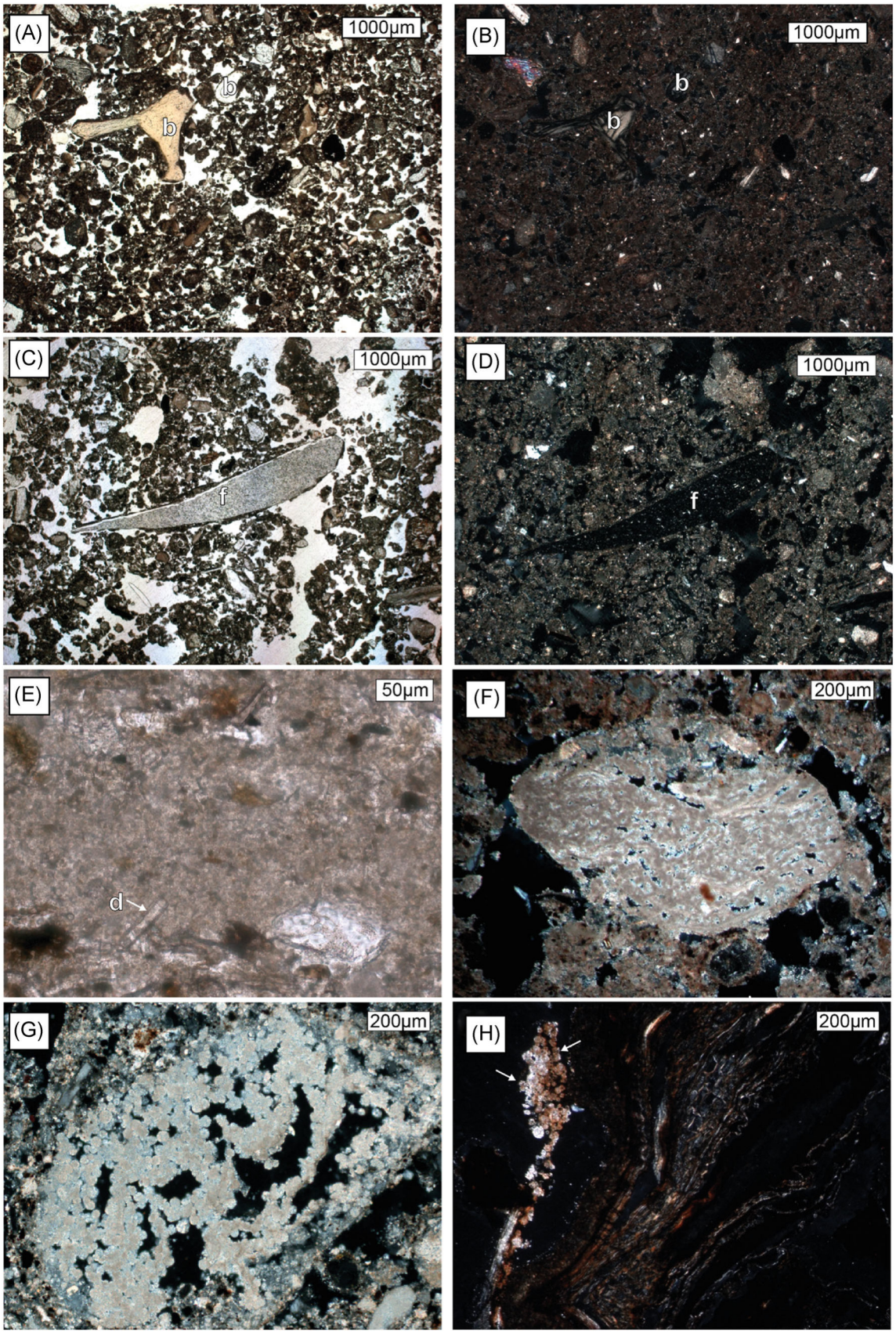

FIGURE 8 (See caption on next page)

4 | DISCUSSION

4.1 | Stratigraphic integrity and bioturbation

We used the results from the micromorphological investigation to assess the role of bioturbation at Cuncaicha. Potential causes of bioturbation can include krotovinas, microfaunal reworking and passages, pedogenesis, and trampling. Bioturbation can occur as a postdepositional or syndepositional process.

In thin section, many channels indicative of root activity and microfauna passage (Stoops, 2010) were identified. The infillings in some of these channels display a crescent-shaped microstructure, typical for bioturbation caused by soil microfauna. These features are in the range of millimeters to centimeters. In the most recent strata, such cuts by channels are best preserved. The prevalent microstructure in Cuncaicha rock shelter is microgranular. This microstructure can be caused by root and microfauna activity including small mammals such as rodents. Reworking of sediment in the active zone during occupation can also cause this structure (Stoops, 2010). This type of microstructure is most developed in Stratum III.

The bioturbation that we observe in thin section at Cuncaicha rock shelter most likely represents syndepositional mixing of sediments that can also be caused by human activity, including, for example trampling, on the surface during or shortly after the deposition of sediment. Even though almost all the sediment is reworked, the different strata are distinctive and well separated. The integrity of the stratigraphic sequence is best illustrated by very distinct contacts between different strata, as observed in thin section (Figure 12B). The bioturbation processes seem to be ubiquitous but localized in the sense that material is not transported over large distances. Suspected rodent burrows were also excavated separately from the intact matrix. Large-scale disturbances, such as burial-related pit features, are well defined and were separated from the matrix during excavation.

Geoarchaeological evidence for only centimeter-scale bioturbation fits with the assemblages of chronologically diagnostic ceramics and projectile points and the AMS chronology. Thirty AMS ages obtained from multiple areas of the site for the Terminal Pleistocene ($n = 23$) and Early Holocene ($n = 7$) components show no inversions.

4.2 | Terminal Pleistocene tufa formation

The oldest deposits at Cuncaicha that show signs of anthropogenic activity are from Terminal Pleistocene Stratum V. Stratum V is dominated by carbonates that are anthropogenically and geogenically derived. Anthropogenic-derived carbonates are from ashes, some of which are still articulated ash oxalate pseudomorphs. The geogenic-derived carbonates are related to tufa formation. Thin-section analyses illustrate that the Terminal Pleistocene deposits are defined by micritic carbonates, capped by the formation of a tufa layer at the transition to Stratum IV. The andesite bedrock is noncalcareous and so is the allochthonous geogenic sediment. Weathering products of the andesite bedrock are not carbonate-rich, but the included plagioclase provides a source of calcium. Calcium carbonate ($CaCO_3$) has been identified in Cuncaicha, mainly in the form of tufa deposits. Tufa is a calcium carbonate deposit that develops "under ambient temperature conditions by biomediation and/or physico-chemical processes associated with freshwater discharge" (Pedley et al., 2003, p. 23). Biomediation and related metabolic processes linked to microbial activity, including, for instance, biofilms, diatoms, and cyanobacteria, are an important source for calcium carbonate precipitation (Ford & Pedley, 1996; Goudie et al., 1993; Pedley et al., 2003; Riding, 2000). Diatoms are present in the deposits at Cuncaicha rock shelter in the Terminal Pleistocene sediment (Figure 8E).

The fabric of the resulting carbonates can vary to a great degree. Micrite and sparite are common (Ford & Pedley, 1996; Riding, 2000). Within thrombolytic tufa, forms can vary, but as seen in AlShuaibi et al. (2015), biomorph forms as observed in Cuncaicha are common. Tufa aggregates in Cuncaicha sediment are dominated by biomorph formations, as identified in thin sections of Strata I, II, and V, which is indicative of calcification of plants and related microorganisms. Micritic tufa-related carbonates within the groundmass are predominantly present in Stratum V but can also be found in Strata II and I. The geogenic carbonate formations in Stratum V decrease

FIGURE 8 Stratum V micrographs. Note the change to a more microgranular microstructure compared to Stratum VI, while some microlaminations are preserved (e.g., in E). (A) and (B) Overview of the microgranular, calcareous groundmass of Stratum V in plane-polarized light (PPL) (A) and cross-polarized light (XPL) (B). In the groundmass, fragments of bones are visible (b). The yellow color in PPL and gray brown color in XPL suggest low-temperature burning (~300°C) according to Villagrán et al. (2017). Mostly rounded bedrock fragments of the local andesite are included. (C) and (D) Microdebitage flake (f) of microcrystalline lithic raw material in PPL (C) and XPL (D) identified using the criteria by Angelucci (2017, 2010). In this stratum, obsidian, jasper, and quartzite micro-debitage could be identified in thin section. (E) Close-up of tufa-related micritic groundmass with microlaminations in which a diatom (d) is visible in PPL. (F) Tufa fragment (center) in calcareous groundmass. The tufa fragment itself is composed of micritic calcite, often with a cloudy, clotted appearance, with sparitic rims that microscopically display a biomorphic fabric reminiscent of the biological agents contributing to the formation of the tufa. (G) Ash oxalate pseudomorphs in Stratum V in XPL. Ash oxalate pseudomorphs are the result of burning of calcium oxalate crystals that are present in plants and upon combustion, they recrystallize as micritic calcite crystals holding the shape of the original oxalates that, in most species, is rhombic (Canti, 2003; Canti & Brochier, 2017; Mentzer, 2014). Note here the distinctive round shape of the micritic ash oxalate pseudomorphs. (H) Photomicrograph of experimentally burned *Azorella compacta* in XPL. Arrows point to the accumulation of round ash oxalate pseudomorphs. Experimental burning of local puna taxa show that different taxa show this distinctive shape of ash oxalate pseudomorphs, out of which *A. compacta* is most suitable for fuel [Color figure can be viewed at wileyonlinelibrary.com]

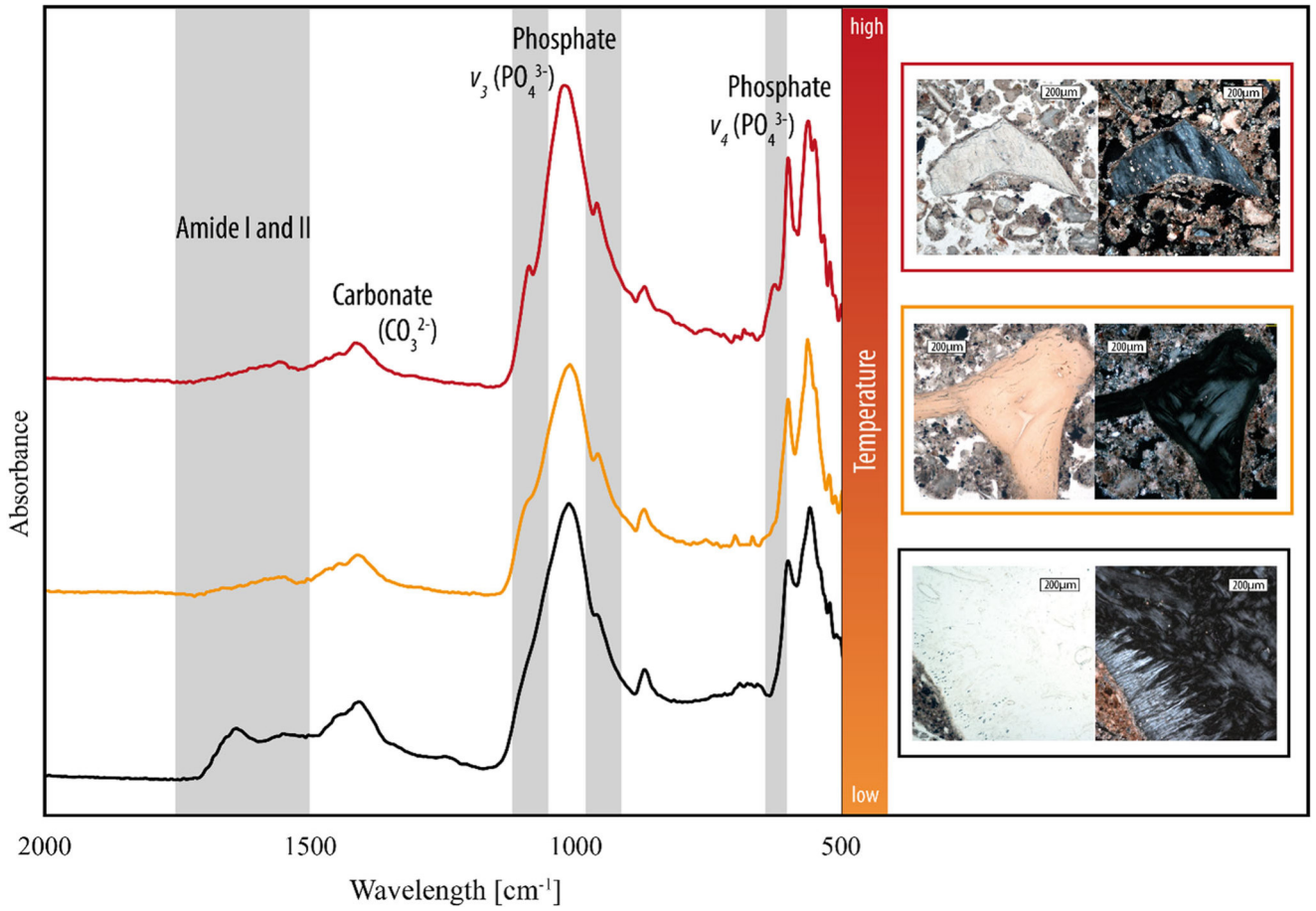

FIGURE 9 Zoom on the double bond and fingerprint region of absorbance µFTIR spectra of three bone fragments from the lowest Stratum V deposit from CUN-12-09 that have been burned to different degrees: not burned (black-bottom), burned at a low temperature (yellow-middle), and burned at a high temperature (red-top). Gray shading indicates the relevant peaks discussed here. To the right, photomicrographs of the analyzed bone fragments are shown. Colors of frames correspond to the colors of spectra. Description of spectra and photomicrographs after Ellingham et al. (2015) and Villagrán et al. (2017). The unburned bone (black) has collagen preserved as indicated by the amide peaks. There are no peaks present that indicate burning. There is no peak or shoulder at 1080 cm^{-1}; at 960 cm^{-1}, the spectrum shows a shoulder. There is no peak at 630 cm^{-1}. The photomicrographs show a translucent bone in plane-polarized light (PPL) and a bone that shows strong low-order interference colors in cross-polarized light (XPL). The low-temperature burned bone (yellow) displays a strong decrease in absorbance for the amide bonds. The unburned bone shows that the presence of collagen peaks is not a question of preservation; when unburned, preservation of collagen is good even in the lowest Stratum V. Hence, the absence of amide peaks in this context suggests that this is a result of burning. No peaks indicative of high-temperature burning (>600°C) are present, but at 1080 cm^{-1}, a shoulder starts to form and at 960 cm^{-1}, the shoulder developed into a peak. Therefore, the spectrum suggests low-temperature burning. This is supported by the photomicrographs that show a light brown-yellow bone fragment in PPL and weaker gray interference colors with a hint of brown (for this, see also Figure 8A,B) in XPL. This color scheme, together with the lack of high-temperature peaks, suggests that the bone was burned at approximately 200–300°C. The high-temperature burned bone (red) shows peaks indicative of burning >600°C. Also, here, no collagen peaks are present. At 1080 cm^{-1}, a well-expressed peak is visible. Additionally, a peak at 630 cm^{-1} appeared. In PPL, the photomicrograph shows a bone fragment that is not as translucent as the unburned bone but has a hint of light gray color and it looks distressed with many small fissures. In XPL, the bone fragment shows a moderate bluish gray interference color with a subtle cloudy appearance. The spectrum and the micrographs together suggest burning at >600°C. In general, these measurements further illustrate: (1) the exceptional bone and collagen preservation at the site in the Terminal Pleistocene deposits and (2) the side by side unburned bone and bone burned to different temperatures indicates once more that these are not in situ hearths [Color figure can be viewed at wileyonlinelibrary.com]

drastically with the shift to the Early Holocene Stratum IV. Evidence for tufa formation only appears again in the Late Holocene strata (I and II), but it is more limited than in the Terminal Pleistocene. The transition from the Terminal Pleistocene to the Early Holocene indicates a shift away from autochthonous carbonate formations toward the deposition of allochthonous aeolian material.

4.3 | Late-Middle Holocene pedogenesis

Stratum III was recognized by its distinctive features in the field, as well as under the microscope. The dark color is caused by an increased amount of finely comminuted humified organic matter as evidenced by the micromorphology results. But how did the plant

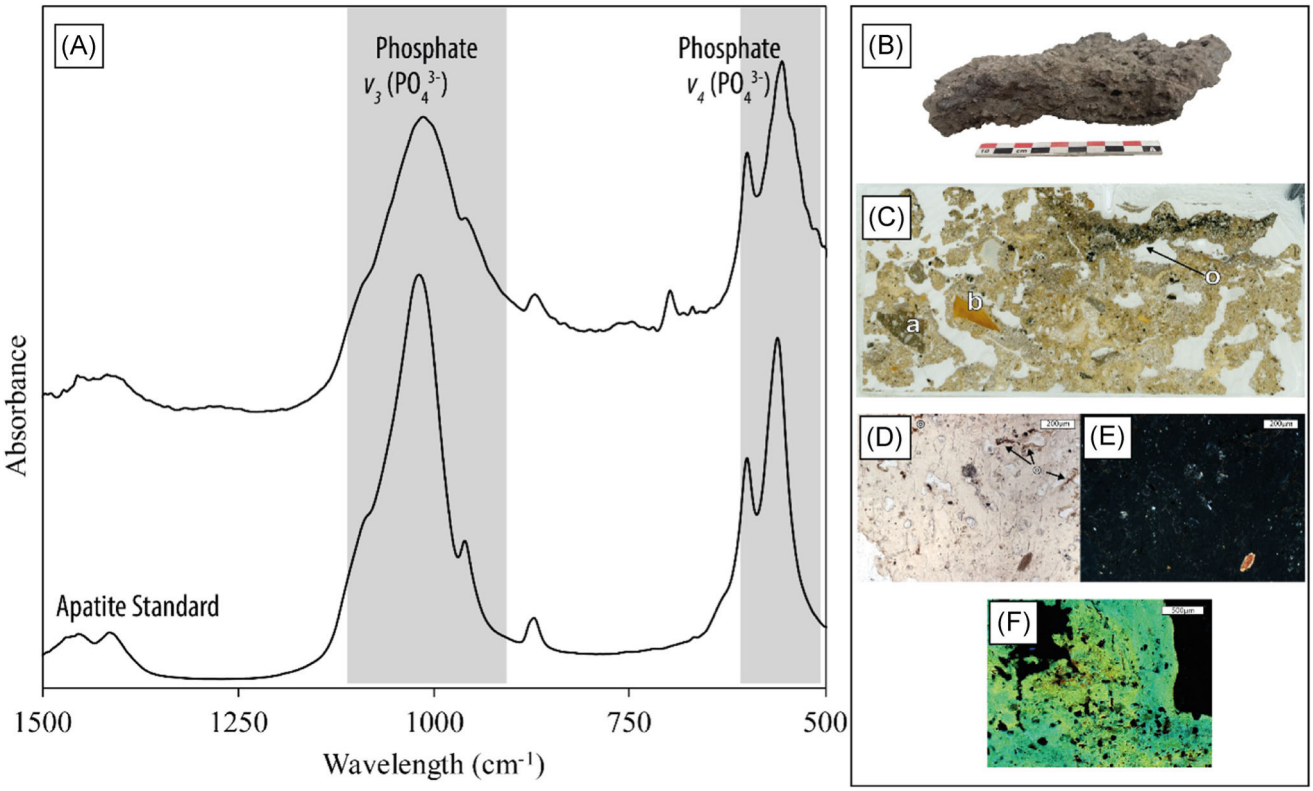

FIGURE 10 Mineral formation at the transition from Stratum V to Stratum IV. (A) Absorbance µFTIR spectrum of mineral in CUN-15-14 (top) together with the spectrum of apatite standard (bottom). (Apatite standard used in the Geoarchaeology Laboratory, University of Tübingen; apatite source: bone.) Zoom on fingerprint region. Note how the sample matches the apatite spectrum, especially the typical phosphate peaks (gray shading). (B) Fragment in the lab before processing. This fragment derives from Unit 13 and was used for the AMS dating. The piece processed into thin section derives from Unit 12. (C) Scan of the thin section CUN-15-14. The sample shows a beige groundmass that is a mix of silty material and coarse fragments of andesite bedrock (a) and bone (b) that is cemented by a mineral formation. Organic fine material is commonly included throughout the sample and accumulated on the upper rim (arrow, o). (D) and (E) Micrograph of CUN-15-14 in plane-polarized light (PPL) (D) and cross-polarized light (XPL) (E). Note the amorphous mineral with humified, amorphous organic fine material (o) that is beige in PPL and almost completely isotropic in XPL. (F) Micrograph from the same slide under blue light and UV light. The mineral shows autofluorescence. Many phosphate as well as some calcium carbonate minerals are fluorescent (Stoops, 2017). In the micrograph, different shades of fluorescence are visible, suggesting a secondary mineral formation [Color figure can be viewed at wileyonlinelibrary.com]

material get introduced to the site? Its presence, together with the decalcification processes, secondary carbonate features, intense bioturbation, an increase in weathering of bone, artefacts, and andesite bedrock eboullís (hinting at higher soil acidity), indicates the formation of a soil A-horizon in the sediment of Stratum III. This led to secondary carbonate features precipitated in voids that are indicative of pedogenesis and demonstrate downward percolation processes of water with carbonates in solution (Goldberg & Macphail, 2006). This process is still ongoing as indicated by similar formations in Strata II and I. Homogenization, weathering, humification, and calcium carbonate movement, all typical for the formation of a soil A-horizon (Goldberg & Macphail, 2006), are indicated. The pedogenesis in Stratum III contributes to the bioturbation processes in this stratum.

The decalcification goes deeper than the stratum in which organic material accumulated, partly decalcifying Stratum IV in some parts of the rock shelter and even reaching down to Stratum V, for example as seen in the thin section from the Unit 12 north wall (CUN-15-120). This is associated with a postdepositional process linked to increased soil acidity. Not only carbonates were dissolved but also all of the sedimentary components that react to acidity. A large in situ fragment of the tufa sampled from Unit 13 was dated at the Arizona AMS Laboratory (AA 107848) (Table S1). Two AMS measurements obtained are 4031 ± 28 BP (4.6–4.3 ka) and 4598 ± 23 BP (5.4–5.1 ka). These ages do not agree with the stratigraphic location of the tufa between Terminal Pleistocene Stratum V and Early Holocene Stratum IV. No large-scale turbation processes are present that could explain the young ages. However, considering that the tufa was recrystallized sometime after its original deposition, the AMS ages probably constrain the recrystallization process and not the original tufa formation. The age of original deposition of the tufa layer can be bracketed by underlying Terminal Pleistocene and overlying Early Holocene AMS ages, which suggest tufa formation during the radiocarbon hiatus between ~11.1 and 9.6 ka.

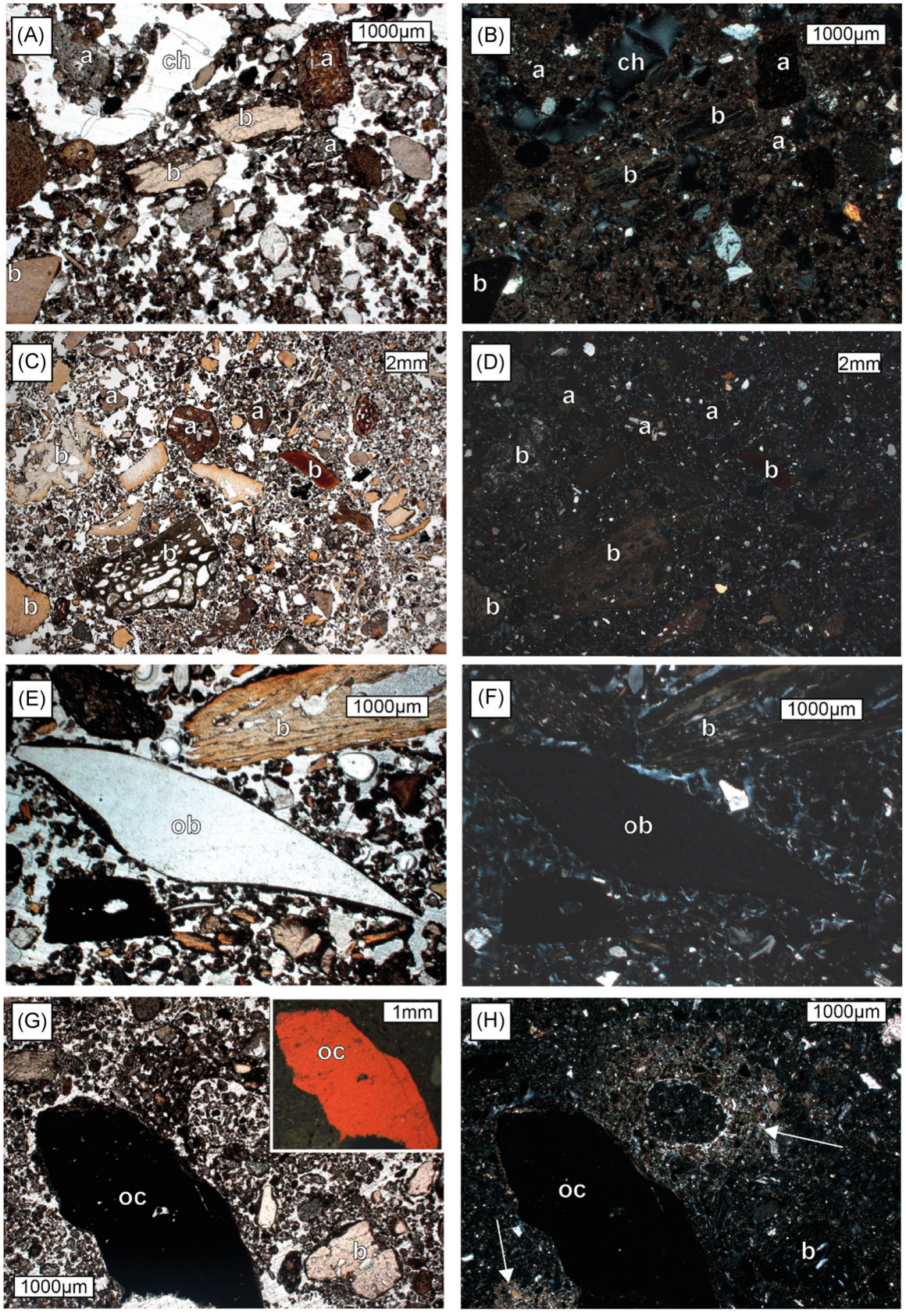

FIGURE 11 (See caption on next page)

4.4 | Site formation model and paleoenvironmental history

Beyond providing behavioral information on some of the Andes' first residents, the geoarchaeological record from Cuncaicha constitutes a unique and long-term archive of paleoenvironmental information from the Central Andes over the past ~12,000 years. Two important questions are when and why different formation and postdepositional processes commenced. By combining Bayesian modeling of AMS ages with the results from the geoarchaeological analyses, we are able to link the local paleoenvironmental and human occupational record from Cuncaicha with broader, regional trends in the climate of the high Andes.

4.4.1 | Terminal Pleistocene

Based on abundant glacial geologic data generated locally at Nevado Coropuna (Bromley et al., 2009, 2011; Úbeda et al., 2018) and throughout the central Andes (Bromley et al., 2016; Jomelli et al., 2014; Kelly et al., 2015; Rodbell & Seltzer, 2000; Stansell et al., 2015), Andean glaciers were retreating from their Antarctic Cold Reversal maxima after 13.2 ka, and the climate was warming well before the initial occupation of Cuncaicha at ~12.3 ka.

The initial formation of Stratum V began with human occupation of Cuncaicha rock shelter. Anthropogenic activity deposited ashes, charcoal, burned bone fragments, and lithic microdebitage, as indicated by micromorphological analysis of the sediments. This geoarchaeological evidence is fully consistent with insights from the Terminal Pleistocene "macro-scale" artifact, faunal, and paleobotanical assemblages. Together, these lines of evidence suggest combustion of local plants, such as *Azorella compacta* cushion plants and woody shrubs, extensive processing of hunted herbivores (Moore, 2016), food preparation, and the production, maintenance, use, and discard of lithic tools fashioned from a variety of local raw materials for various activities. Anthropogenic sediments accumulated for up to ~785 years, though the cumulative occupation span in the Terminal Pleistocene could have been briefer.

During the Terminal Pleistocene occupation, tufa also was forming in the rock shelter. Tufa as a spring deposit requires wet conditions to form. In fact, the most prominent tufa formations, that is in Strata VI, V, and in the tufa layer at the Stratum V/IV contact, coincide with the Central Andean Pluvial Event (CAPE) II. The CAPE was first identified in paleowetlands in the Salar de Punta Negra in the Chilean Atacama Desert, with CAPE I dating to 15.9–13.8 ka and CAPE II dating to 12.7–9.7 ka (Quade et al., 2008). Since their identification, numerous proxy records from the Chilean Atacama (Betancourt et al., 2000; Maldonado et al., 2005; Nester et al., 2007; Pfeiffer et al., 2018; Pueyo et al., 2011) have further confirmed the timing of these wet phases.

Well-developed paleohydrologic proxy records from Lake Titicaca (Baker & Fritz, 2015; Baker, Rigsby, et al., 2001; Baker, Seltzer, et al., 2001; Nunnery et al., 2019; Placzek et al., 2006; Sylvestre et al., 1999) at the same latitude as Cuncaicha also indicate that these two periods of greatly increased moisture were the most significant within the past 20,000 years. The Tauca and Coipasa highstands, dated, respectively, to 18.0–14.5 and 12.5–11.9 ka, are teleconnected with the northern hemisphere Heinrich Stadial 1 and Younger Dryas (Blard et al., 2011).

At Cuncaicha, the Terminal Pleistocene occupation was coeval with the CAPE II/Coipasa highstand period of increased moisture, which would have favored productivity of highland habitats such as the Pucuncho Basin. The culmination of this wet phase likely resulted in the formation of the tufa layer at the final occupation surface of Stratum V. The formation of the tufa might also be linked to the abandonment of the site, as it suggests a relatively stable surface. However, sporadic or seasonal visits of the site cannot be excluded based on the tufa formation alone.

4.4.2 | Early Holocene

A hiatus in occupation of Cuncaicha rock shelter is registered between ~11.1 and 9.6 ka, possibly a response to a severe arid climate phase. Ice cores (Ramirez et al., 2003; Thompson et al., 1995, 1998), speleothems (Bustamante et al., 2016; Cheng et al., 2013; Van Breukelen

FIGURE 11 Strata IV and III micrographs. (A) and (B) Stratum IV in plane-polarized light (PPL) (A) and cross-polarized light (XPL) (B) sediment in CUN-12-03. The groundmass is calcareous, but compared to Stratum V, a decrease in micritic carbonates in the groundmass can be observed. The coarse fraction here contains andesite bedrock fragments (a) and bone fragments (b). The microstructure is microgranular and quite open, interrupted by channels (ch), likely produced by microfauna activity. (C) and (D) Micrographs from Stratum III in PPL (C) and XPL (D) in CUN-15-127A. Note the increase in (burned) bone fragments (b) of medium to coarse sand size, the reworked microstructure and in XPL the absence of carbonates in the groundmass. (D) A completely decalcified groundmass with no birefringence. The birefringent particles are mostly plagioclase mineral grains. (E) and (F) Also come from Stratum III sediment in CUN-15-127A. Here, there is a prominent obsidian flake (ob) in the middle that is translucent in PPL (E) and opaque in XPL (F) that is coated by silt. Above the flake, a large bone fragment (b) is visible that show signs of weathering as also seen in some of the bones (b) in (C)/(D) and the bone fragment (b) in (G)/(H). Note that the groundmass is characterized by finely comminuted organic material and also in this micrograph, it is completely decalcified. (G) and (H) show Stratum III sediment in CUN-12-02B. Note here the inclusion of an ochre piece (oc). In (G), the inset of the same ochre piece under oblique incident light is shown. In XPL (H), secondary carbonate formation becomes apparent (arrows). Around a loose continuously infilled channel, a calcareous hypocoating formed, which is sparitic at the rim, and at the bottom, an impregnation of the groundmass with calcite is visible [Color figure can be viewed at wileyonlinelibrary.com]

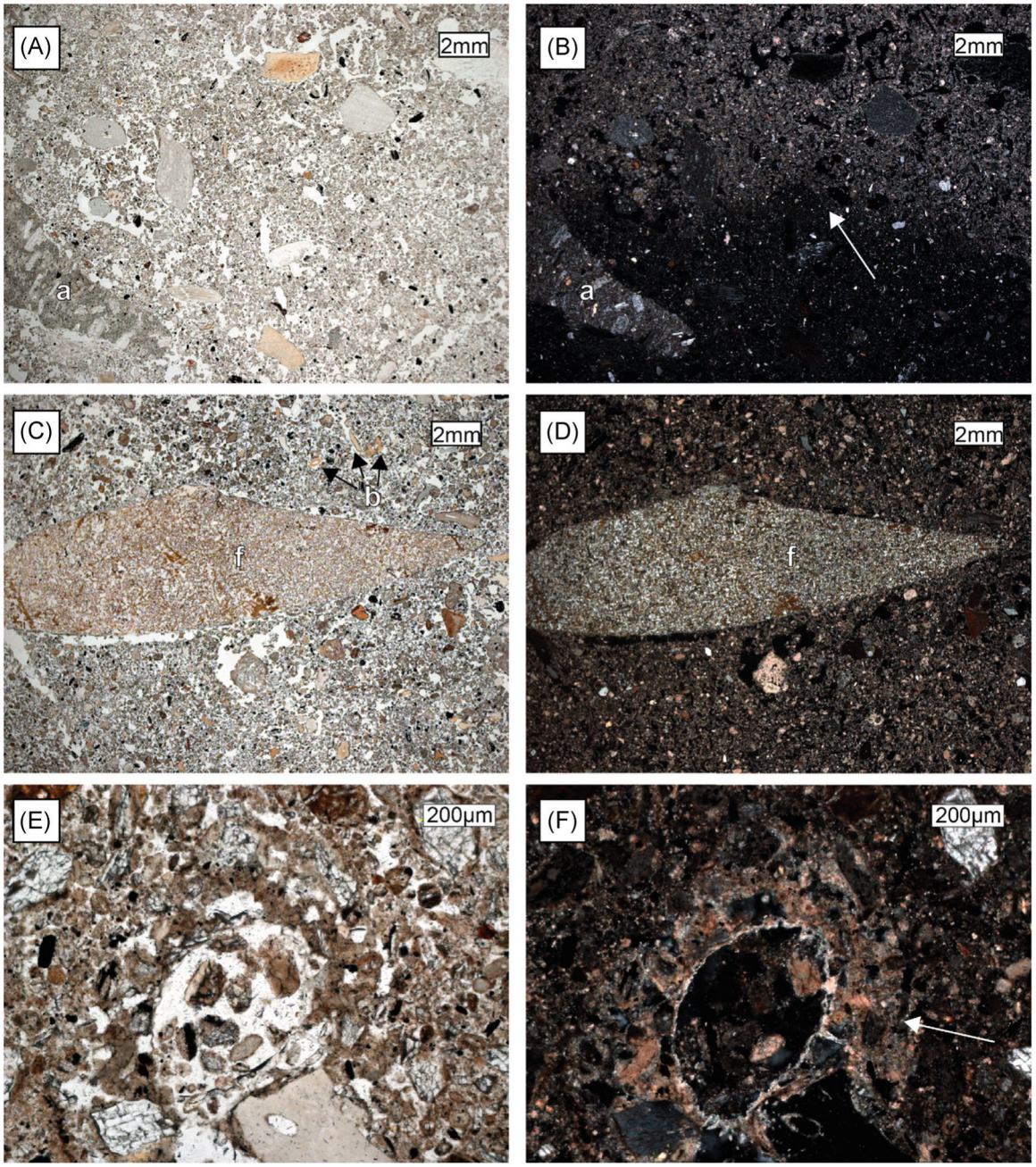

FIGURE 12 Stratum II micrographs. (A) and (B) The contact of Stratum III to Stratum II (arrow) in CUN-15-126A. The contact is defined by the transition of the calcareous, birefringent groundmass of Stratum II to a decalcified groundmass of Stratum III. A large andesite fragment (a) protrudes into Stratum III. (C) and (D) Typical Stratum III sediment in plane-polarized light (PPL) (C) and cross-polarized light (XPL) (D) in CUN-15-125B. In the middle of the photomicrographs, a microcrystalline flake of yellow jasper (f) is included. Note the loosely packed, microgranular microstructure. In the groundmass, many small, down to fine sand sized, bone fragments (e.g., b, arrows) are included. Under crossed polarizers, a moderately micritic groundmass is visible. Under higher resolution, it shows that part of the carbonates derives from ashes, a smaller fraction from some tufa forming. (E) and (F) A hypocoating of secondary carbonates with a sparitic rim (arrow) around a loose discontinuously infilled channel in PPL (E) and XPL (F) in CUN-12-02B surrounded by a moderately calcareous groundmass [Color figure can be viewed at wileyonlinelibrary.com]

et al., 2008), and lakes (Baker & Fritz, 2015; Bird et al., 2011; Bush et al., 2005; Cross et al., 2000; Ekdahl et al., 2008; Hillyer et al., 2009; Seltzer et al., 2000) from throughout the central Andes and western Amazonia indicate a major shift to drier climate during this interval. Together with the hiatus in the archaeological AMS chronology, this represents a chronological and depositional unconformity, suggesting a cessation in sedimentation and absence of human presence. Two possible scenarios during that time are (1) erosion, which implies the transport of sediment out of the site, or (2) stasis, where there was no accumulation or erosion, or where deposition and erosion

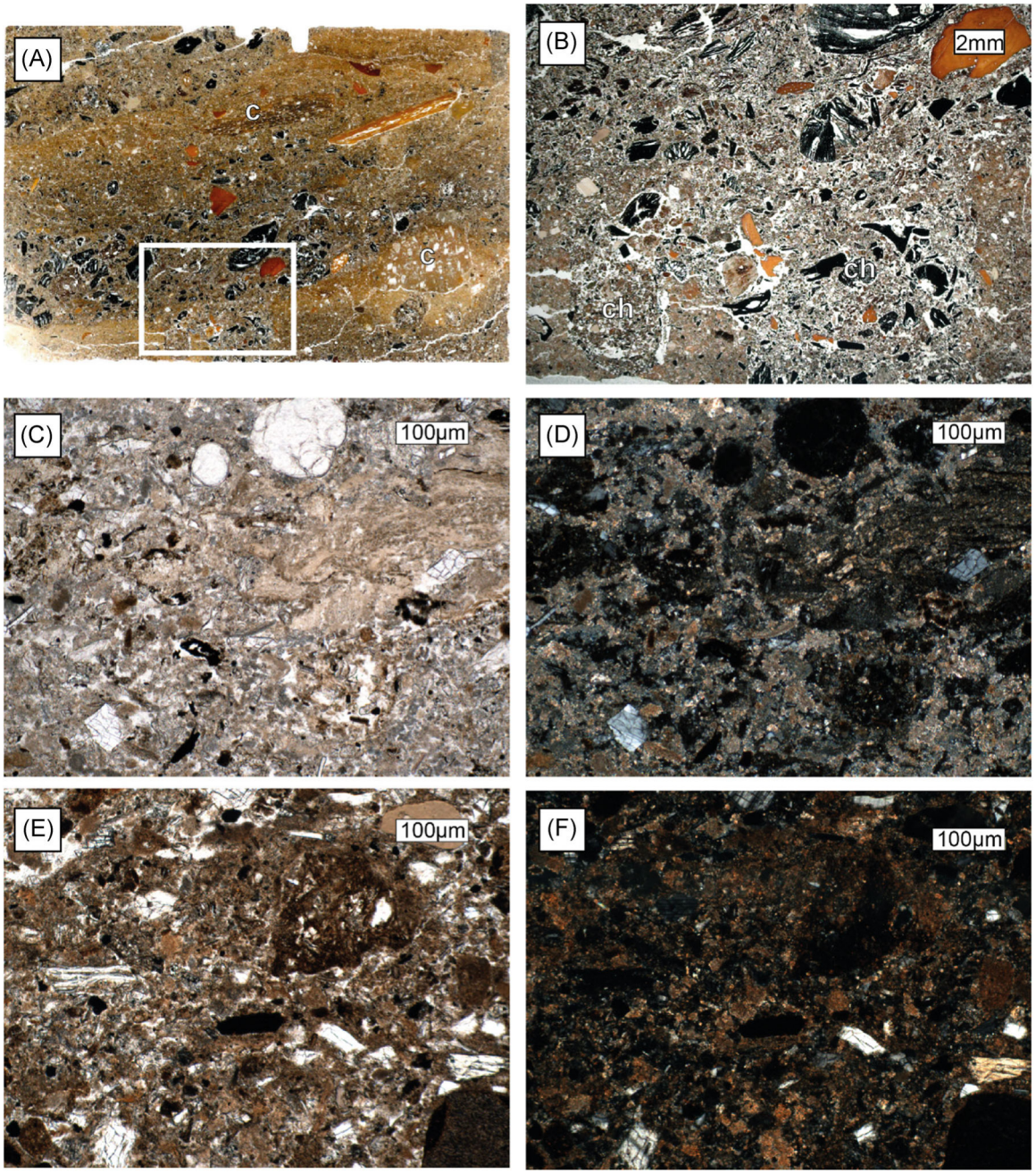

FIGURE 13 Stratum I scan and micrographs. (A) Scan of CUN-12-01B. Different microlayers are visible, with rubefied and charcoal-rich layers alternating in this thin section, suggesting the preservation of intact combustion features and multiple burning events (Mentzer, 2014) (see also SI2, CUN-12-01A to CUN-12-01C). For the coarse fraction, ceramic sherds (c) are included in this stratum, as well as charcoal and bone pieces. The white rectangle indicates the location of (B). (B) A micrograph in plane-polarized light (PPL) from the bottom of CUN-12-01B. Note how the layer of rubefied sediment has been interrupted in this location by two channels (ch). Compact, rubefied sediment with few coarse inclusions is cut into and filled with material from the upper, charcoal-rich layer with an open microstructure and completely unoriented coarse inclusions of charcoal and bone fragments. (C) and (D) are taken from an ash layer in CUN-12-01A in PPL (A) and cross-polarized light (XPL) (D). Micritic, round ash oxalate pseudomorphs are a main component of the groundmass in this layer. In the upper right corner of the thin section, laminated ashes are preserved that are phosphatic in parts. Charred organic matter is visible. (E) and (F) derive from a rubefied layer in CUN-12-1B and show the groundmass in PPL (E) and XPL (F). Note how there is a reddish color to the groundmass that is a result of oxidization of iron-containing components upon burning (see Mentzer, 2014) [Color figure can be viewed at wileyonlinelibrary.com]

were in equilibrium. Unfortunately, the geoarchaeological and micromorphological data do not provide clear evidence either way.

However, because the Titicaca record indicates much drier conditions after ~11.9 ka relative to the preceding millennium, any removal of rock shelter sediments through water action in the Early to Middle Holocene would be inconsistent with regional paleoclimate data. Although removal of fine sediments by wind (deflation) is a possibility, this removal would have left larger clasts, such as lithic and faunal remains,

present in sediments, and faunal remains deposited during the ~11.1–9.6 ka interval would have been detected by our dating program. Sedimentological stasis might therefore be the more likely scenario, underscoring the importance of anthropogenic sedimentation for accumulation in rock shelters in this region.

Occupation and anthropogenic sedimentation at Cuncaicha resumed beginning ~9.6 ka, coeval with a shift in geogenic sediment source. With a decline in tufa formation, aeolian sediments from outside the rock shelter became more frequent, consistent with a more arid Early Holocene climate. Anthropogenic material, such as ashes, charcoal, burned bone fragments, and lithic microdebitage seen in thin section, is more abundant compared to the Terminal Pleistocene deposits, consistent with relatively higher content of Cuncaicha's Early Holocene material assemblages recovered in excavation (Rademaker & Moore, 2018).

Following abandonment of the site by ~9.2 ka, at least three human burials were emplaced into Cuncaicha shelter along the rear wall. These were dated ~9.3–8.8, 9.0–8.6, and 8.5–8.4 ka. Bayesian modeling reveals that the lifetimes of these three individuals likely did not overlap (Rademaker & Hodgins, 2018). Thus, although Cuncaicha rock shelter was not used as a residence during this time, highlanders were likely living elsewhere on the plateau (Chala-Aldana et al., 2018; Haller von Hallerstein, 2017), and the shelter became a place to inter the dead.

4.4.3 | Early to Middle Holocene

Cuncaicha's Early to mid-Holocene occupation hiatus between ~9.2 and 5.9 ka corresponds to the generally driest period of the Holocene documented in many paleohydrologic records throughout the central Andes (Abbott et al., 2003; Baker, Rigsby, et al., 2001; Bush et al., 2005; Moreno et al., 2009; Pueyo et al., 2011; Rigsby et al., 2005; Seltzer et al., 2000; Thompson et al., 1998; Vining et al., 2019), though there is substantial variation in the timing of peak aridity among records. Perhaps under an arid climatic regime, the amount of freshwater in Quebrada Cuncaicha was insufficient to make Cuncaicha a feasible campsite. If so, hunter-gatherers would have moved to better watered locations in the Pucuncho Basin or beyond. This fits a pattern observed in the archaeological record of the Chilean Atacama, with consequent migration to more suitable eco-refuges (Grosjean et al., 1997; Núñez et al., 2002, 2013). Depositionally, the question remains—what happened at the site during this period of nonoccupation? Since there is no sterile deposit between the Early and Middle Holocene occupation layers, either the deposits were eroded away, or they were never deposited in the first place.

Beginning as early as 5.9 ka and lasting possibly until 4.8 ka, Cuncaicha was reoccupied and Stratum III accumulated. Geogenic material from the Pucuncho Basin, and especially anthropogenic material, mostly sand-sized burned bone fragments, combustion-related charcoal, microdebitage, and ochre, were deposited in Stratum III during the occupation of the site. The formation of a soil increased the amount of humified organic matter and initiated decalcification processes in the sediment. Soil formation may have started during the Late-Middle Holocene occupation, but as soil formation is usually tied to sedimentary stasis (Karkanas & Goldberg, 2018), a stronger development during the subsequent occupation hiatus is likely.

But why did a soil form during a possible period of stasis during the Late-Middle Holocene, when other, earlier periods of possible stasis show no evidence of soil formation? During the Late-Middle Holocene, increasing South American Summer Monsoon intensity raised lake levels in the Atacama and Central Andes after ~6 ka (Baker, Rigsby, et al., 2001; Fornace et al., 2014; Moreno et al., 2009; Pueyo et al., 2011), with different lakes and proxies variously registering this return to wetter conditions at ~5.5 ka (Ekdahl et al., 2008), at ~5 ka (Bird et al., 2011; Bustamante et al., 2016; Hillyer et al., 2009), at ~4.5 ka (Vining et al., 2019; Weide et al., 2017), at ~4 ka (Cross et al., 2000), and later (Abbott et al., 2003). This climatic shift can explain the formation of the soil A-horizon in Cuncaicha Stratum III that, just like the tufa, would have preferentially formed under wetter conditions. Whereas in the Terminal Pleistocene the sediment overlying bedrock was relatively thin, allowing tufa formation, by the time Stratum III had formed, a much thicker layer of organic-rich sediments had accumulated. This promoted percolation processes rather than the through-flow that caused the tufa layer to form at the Stratum V/IV contact. Phosphatization of the tufa layer at the Stratum V/IV contact was probably triggered by the soil formation processes and leaching of anthropogenic-rich deposits below the surface horizon. These processes likely began at least by 4.8 ka and likely continued beyond the end of the Late-Middle Holocene occupation.

4.4.4 | Late Holocene

Following another abandonment of the site by ~4.8 ka, at least two more burials were emplaced near the rear wall of Cuncaicha. An individual was placed as a seated burial in the southeast corner of the rock shelter at ~4.3–4.0 ka, followed by the interment of an individual in the southwest corner another millennium later (Rademaker & Hodgins, 2018).

Dating of the Late Holocene portion of the Cuncaicha sequence is incomplete, and it is unknown when reoccupation and deposition of Stratum II began. Moreover, based on the current density of dates for the Late Holocene strata, it is not possible to say whether occupation of Cuncaicha in the Late Holocene was relatively continuous (to the degree that radiocarbon dating can resolve it) or punctuated with hiatuses. Ongoing work on lithic and also ceramic typology may yield insights into this matter through a relative chronology. Aside from ceramics and lithics, the Late Holocene Stratum I contains stacked combustion features. The more distinctively expressed layers in this stratum may be a result of its relatively young age and better preservation.

In the Late Holocene strata postdating ~4.8 ka, we observe more mixed signals in the sediment at Cuncaicha. Less humified organic material became incorporated than in the preceding Late-Middle

Holocene, but it was more than in the Terminal Pleistocene and Early Holocene deposits. Some tufa formation was present but was very localized. Aeolian material remained a significant geogenic sediment source. These mixed signals match with the less unidirectional regional climatic trend in the Late Holocene. Especially the most recent two millennia, after 2 ka, are dominated by a somewhat higher degree of climatic variability documented in high-resolution lake and speleothem records (Bird et al., 2011; Bustamante et al., 2016; Hillyer et al., 2009; Kanner et al., 2013; Van Breukelen et al., 2008).

5 | CONCLUSIONS

This geoarchaeological work at Cuncaicha rock shelter provided new insights into the deposits at the site and clarified some open questions that arose during the field seasons and some that were raised by peers (e.g., Capriles et al., 2016; Rademaker et al., 2016).

In general, (bio)turbation in the deposits at Cuncaicha appears to have been ubiquitous, but small (cm) in scale in terms of translocation of sediment, which suggests that it occurred syndepositionally or shortly after accumulation. Large, whole-scale mixing between strata is not evident, as seen in the distinct contacts between strata, by the absence of inversions in the AMS dates, and by stratigraphically consistent distributions of diagnostic lithic and ceramic artifacts. Features indicating large-scale turbation, such as pit features and also krotovinas and burrows, could be readily identified in the field and were carefully separated from the matrix during excavation.

The deposits contain a significant amount of anthropogenic materials and combustion-derived residues, such as charcoal and burned bone, which are particularly abundant. The geoarchaeological evidence for extensive burning is also supported by analysis of the faunal and botanical assemblages. One of the most important anthropogenic contributions to the deposits are ashes, in the form of round oxalate pseudomorphs. This distinctive form was found in taxa local to the Pucuncho Basin, out of which *A. compacta* is most suitable as fuel. Hearths (sensu Mentzer, 2014) are not preserved, except for in the latest stratum, in which stacked combustion features were identified.

Bayesian modeling of an extensive radiocarbon chronology indicates that there are at least two occupational hiatuses at Cuncaicha. However, we find no evidence of sterile deposits at the site and we find no evidence for erosion. It is possible that any micromorphological evidence for erosion would have been erased by the small-scale bioturbation. However, it is also possible that during periods of nonoccupation, stasis was the prevailing condition. Although some periods of stasis have been identified geoarchaeologically at Cuncaicha, such as soil formation during the Late-Middle Holocene, other hypothesized periods of stasis do not provide any clear evidence.

Excavations at Cuncaicha show that apart from the deposition of Stratum VI, all other deposits contain evidence for human occupation. At the microscopic scale, we also see a close association of geogenic and anthropogenic materials, so that despite a significant presence of nonanthropogenic components in all strata (e.g., aeolian volcanic silt, tufa, rockspall), anthropogenic components (e.g., bone, charcoal, ash) are found throughout the sequence. Furthermore, we note that although there are apparent hiatuses in use of the site for occupation, several of these hiatuses are marked by periods when the site was used for interment of the dead. Use of the site for burial is not associated with deposition, but rather with the formation of burial pits, that is, negative features excavated into existing strata.

One possible explanation for the pattern of site use and sedimentation at Cuncaicha is that occupation was more frequent than suggested by the current radiocarbon stratigraphy. However, hypothetical subsequent erosive episodes—which did not leave behind any clear geoarchaeological signature—also must have removed any evidence for human presence, except for the burial pits. We find no evidence of concomitant use of the site for occupation and burial (Rademaker & Hodgins, 2018). Another possibility is that human occupation provides a type of trigger that shifts the depositional regime within the shelter from one of stasis toward one of net accumulation, so that nonanthropogenic sediments only build up when humans provide some input of sediment through combustion and waste disposal. Ultimately, the record at Cuncaicha does not allow us to resolve this issue. Despite the remaining ambiguity of the link between human occupation, sediment accumulation and apparent occupational and stratigraphic "gaps," our geoarchaeological study provides some useful observations that suggest that sediment accumulation and human occupation are closely linked at Cuncaicha.

Although anthropogenic components are ubiquitous at Cuncaicha, geogenic components are variable and likely serve as proxies for changing environmental conditions. Tufa, indicating moist conditions at the site, formed mostly during the Pleistocene as a result of groundwater seeping through the bedrock in the back of the shelter. The formation of a tufa crust capping the Terminal Pleistocene deposits may be a sign of stasis during the occupational hiatus postdating the Terminal Pleistocene occupation. The tufa was phosphatized at some point later in time, likely triggered by a wet phase during the Late-Middle Holocene. The variable formation of tufa at Cuncaicha, together with the transition to a more aeolian depositional regime during the Early Holocene, as well as the formation of a soil horizon during the Late-Middle Holocene, indicate that Cuncaicha rock shelter preserves a number of paleoenvironmental signatures that correspond with well-documented, regional climatic events, such as CAPE II/Coipasa highstand, an Early to Middle Holocene arid period, and a subsequent Late-Middle Holocene wet period. The integration of high-resolution AMS chronology and micromorphology at Cuncaicha reported here contributes a 12,000-year archive of human behavior and paleoenvironmental change from the Andes of southern Peru. This approach will be further developed at other Andean archaeological sites to study long-term human–environment dynamics.

ACKNOWLEDGMENTS

The authors would like to acknowledge the US National Science Foundation (NSF Grant BCS-1659015 to K. R.) for providing funding for this project. Additionally, we would like to thank Susan M. Mentzer for assistance with the (μ-)FTIR analyses and the Deutsche

Forschungsgemeinschaft (DFG) for funding the purchase of the FTIR (MI 1748/1-1). University of Arizona AMS Lab Director Gregory Hodgins provided helpful guidance on AMS dating and Bayesian modeling. Open access funding enabled and organized by Projekt DEAL.

CONFLICTS OF INTERESTS

The authors declare that there are no conflicts of interests.

ORCID

Sarah Ann Meinekat http://orcid.org/0000-0001-8474-3634

Kurt Rademaker http://orcid.org/0000-0001-5676-4884

REFERENCES

Abbott, M. B., Wolfe, B. B., Wolfe, A. P., Seltzer, G. O., Aravena, R., Mark, B. G., Polissar, P. J., Rodbell, D. T., Rowe, H. D., & Vuille, M. (2003). Holocene paleohydrology and glacial history of the central Andes using multiproxy lake sediment studies. *Palaeogeography, Palaeoclimatology, Palaeoecology*, *194*(1–3), 123–138. https://doi.org/10.1016/S0031-0182(03)00274-8

AlShuaibi, A. A., Khalaf, F. I., & Al-Zamel, A. (2015). Calcareous thrombolitic crust on Late Quaternary beachrocks in Kuwait, Arabian Gulf. *Arabian Journal of Geosciences*, *8*(11), 9721–9732. https://doi.org/10.1007/s12517-015-1869-5

Angelucci, D. E. (2010). The recognition and description of knapped lithic artifacts in thin section. *Geoarchaeology*, *25*(2), 220–232. https://doi.org/10.1002/gea.20303

Angelucci, D. E. (2017). Lithic artefacts. In C. Nicosia & G. Stoops (Eds.), *Archaeological soil and sediment micromorphology* (pp. 223–230). Wiley.

Baker, P. A., & Fritz, S. C. (2015). Nature and causes of Quaternary climate variation of tropical South America. *Quaternary Science Reviews*, *124*, 31–47. https://doi.org/10.1016/j.quascirev.2015.06.011

Baker, P. A., Rigsby, C. A., Seltzer, G. O., Fritz, S. C., Lowenstein, T. K., Bacher, N. P., & Veliz, C. (2001). Tropical climate changes at millennial and orbital timescales on the Bolivian altiplano. *Nature*, *409*(6821), 698–701. https://doi.org/10.1038/35055524

Baker, P. A., Seltzer, G. O., Fritz, S. C., Dunbar, R. B., Grove, M. J., Tapia, P. M., Cross, S. L., Rowe, H. D., & Broda, J. P. (2001). The history of South American tropical precipitation for the past 25,000 years. *Science*, *291*(5504), 640–643. https://doi.org/10.1126/science.291.5504.640

Betancourt, J. L., Latorre, C., Rech, J. A., Quade, J., & Rylander, K. A. (2000). A 22,000-year record of monsoonal precipitation from northern Chile's Atacama Desert. *Science*, *289*(5484), 1542–1546. https://doi.org/10.1126/science.289.5484.1542

Bird, B. W., Abbott, M. B., Vuille, M., Rodbell, D. T., Stansell, N. D., & Rosenmeier, M. F. (2011). A 2,300-year-long annually resolved record of the South American summer monsoon from the Peruvian Andes. *Proceedings of the National Academy of Sciences of the United States of America*, *108*(21), 8583–8588. https://doi.org/10.1073/pnas.1003719108

Blard, P.-H., Sylvestre, F., Tripati, A. K., Claude, C., Causse, C., Coudrain, A., Condom, T., Seidel, J. L., Vimeux, F., Moreau, C., Dumoulin, J. P., & Lavé, J. (2011). Lake highstands on the Altiplano (Tropical Andes) contemporaneous with Heinrich 1 and the Younger Dryas: New insights from ^{14}C, U–Th dating and $\delta^{18}O$ of carbonates. *Quaternary Science Reviews*, *30*(27-28), 3973–3989. https://doi.org/10.1016/j.quascirev.2011.11.001

Bromley, G. R. M., Hall, B. L., Schaefer, J. M., Winckler, G., Todd, C. E., & Rademaker, K. M. (2011). Glacier fluctuations in the southern Peruvian Andes during the late-glacial period, constrained with cosmogenic ^{3}He. *Journal of Quaternary Science*, *26*(1), 37–43. https://doi.org/10.1002/jqs.1424

Bromley, G. R. M., Schaefer, J. M., Hall, B. L., Rademaker, K. M., Putnam, A. E., Todd, C. E., Hegland, M., Winckler, G., Jackson, M. S., & Strand, P. D. (2016). A cosmogenic ^{10}Be chronology for the local last glacial maximum and termination in the Cordillera Oriental, southern Peruvian Andes: Implications for the tropical role in global climate. *Quaternary Science Reviews*, *148*, 54–67. https://doi.org/10.1016/j.quascirev.2016.07.010

Bromley, G. R. M., Schaefer, J. M., Winckler, G., Hall, B. L., Todd, C. E., & Rademaker, K. M. (2009). Relative timing of last glacial maximum and late-glacial events in the central tropical Andes. *Quaternary Science Reviews*, *28*(23-24), 2514–2526. https://doi.org/10.1016/j.quascirev.2009.05.012

Bronk Ramsey, C. (2009). Bayesian analysis of radiocarbon dates. *Radiocarbon*, *51*(1), 337–360.

Bush, M. B., Hansen, B. C. S., Rodbell, D. T., Seltzer, G. O., Young, K. R., León, B., Abbott, M. B., Silman, M. R., & Gosling, W. D. (2005). A 17 000-year history of Andean climate and vegetation change from Laguna de Chochos, Peru. *Journal of Quaternary Science*, *20*(7-8), 703–714. https://doi.org/10.1002/jqs.983

Bustamante, M. G., Cruz, F. W., Vuille, M., Apaéstegui, J., Strikis, N., Panizo, G., Novello, F. V., Deininger, M., Sifeddine, A., Cheng, H., Moquet, J. S., Guyot, J. L., Santos, R. V., Segura, H., & Edwards, R. L. (2016). Holocene changes in monsoon precipitation in the Andes of NE Peru based on $\delta^{18}O$ speleothem records. *Quaternary Science Reviews*, *146*, 274–287. https://doi.org/10.1016/j.quascirev.2016.05.023

Canti, M. G. (2003). Aspects of the chemical and microscopic characteristics of plant ashes found in archaeological soils. CATENA 54(3), 339-361. https://doi.org/10.1016/S0341-8162(03)00127-9

Canti, M. G., & Brochier, J. E. (2017). Plant Ash. In (Eds.) Nicosia, C. & Stoops, G., *Archaeological soil and sediment micromorphology* (pp. 147–154). Hoboken, NJ: Wiley.

Capriles, J. M., Santoro, C. M., & Dillehay, T. D. (2016). Harsh environments and the Terminal Pleistocene peopling of the Andean highlands. *Current Anthropology*, *57*(1), 99–100. https://doi.org/10.1086/684694

Chala-Aldana, D., Bocherens, H., Miller, C., Moore, K., Hodgins, G., & Rademaker, K. (2018). Investigating mobility and highland occupation strategies during the Early Holocene at the Cuncaicha rock shelter through strontium and oxygen isotopes. *Journal of Archaeological Science: Reports*, *19*, 811–827. https://doi.org/10.1016/j.jasrep.2017.10.023

Cheng, H., Sinha, A., Cruz, F. W., Wang, X., Edwards, R. L., d'Horta, F. M., Ribas, C. C., Vuille, M., Stott, L. D., & Auler, A. S. (2013). Climate change patterns in Amazonia and biodiversity. *Nature Communications*, *4*, 1411. https://doi.org/10.1038/ncomms2415

Courty, M. A., Goldberg, P., & Macphail, R. (1989). Soils and micromorphology in archaeology. Cambridge manuals in archaeology. Cambridge University Press.

Cross, S. L., Baker, P. A., Seltzer, G. O., Fritz, S. C., & Dunbar, R. B. (2000). A new estimate of the Holocene lowstand level of Lake Titicaca, central Andes, and implications for tropical palaeohydrology. *The Holocene*, *10*(1), 21–32. https://doi.org/10.1191/095968300671452546

Dornbusch, U. (1998). Current large-scale climatic conditions in southern Peru and their influence on snowline altitudes. *Erdkunde*, *52*(1), 41–54.

Ekdahl, E. J., Fritz, S. C., Baker, P. A., Rigsby, C. A., & Coley, K. (2008). Holocene multidecadal- to millennial-scale hydrologic variability on the South American altiplano. *The Holocene*, *18*(6), 867–876. https://doi.org/10.1177/0959683608093524

Ellingham, S. T. D., Thompson, T. J. U., Islam, M., & Taylor, G. (2015). Estimating temperature exposure of burnt bone—A methodological

review. *Science & Justice: Journal of the Forensic Science Society*, *55*(3), 181–188. https://doi.org/10.1016/j.scijus.2014.12.002

Engel, F.-A. (Ed.) (1981). *Papers of the Department of Anthropology, Hunter College of the City University of New York. Prehistoric Andean ecology: Man, settlement and environment in the Andes; [abstracts of the archives of the Center for Arid Studies "CIZA" of the National Agrarian University of Peru*. Humanities Press.

Fick, S. E., & Hijmans, R. J. (2017). WorldClim 2: New 1km spatial resolution climate surfaces for global land areas. *International Journal of Climatology*, *37*(12), 4302–4315.

Ford, T. D., & Pedley, H. M. (1996). A review of tufa and travertine deposits of the world. *Earth-Science Reviews*, *41*(3-4), 117–175. https://doi.org/10.1016/S0012-8252(96)00030-X

Fornace, K. L., Hughen, K. A., Shanahan, T. M., Fritz, S. C., Baker, P. A., & Sylva, S. P. (2014). A 60,000-year record of hydrologic variability in the Central Andes from the hydrogen isotopic composition of leaf waxes in Lake Titicaca sediments. *Earth and Planetary Science Letters*, *408*, 263–271. https://doi.org/10.1016/j.epsl.2014.10.024

Goldberg, P., & Macphail, R. I. (2006). *Practical and theoretical geoarchaeology*. Blackwell Publishing Ltd. https://doi.org/10.1002/9781118688182

Goudie, A. S., Viles, H. A., & Pentecost, A. (1993). The Late-Holocene tufa decline in Europe. *The Holocene*, *3*(2), 181–186. https://doi.org/10.1177/095968369300300211

Grosjean, M., Núñez, L., Cartajena, I., & Messerli, B. (1997). Mid-Holocene climate and culture change in the Atacama Desert, northern Chile. *Quaternary Research*, *48*(2), 239–246. https://doi.org/10.1006/qres.1997.1917

Haller von Hallerstein, S. (2017). *Multi-isotopic Paleo-diet Reconstruction of Hunter-gatherers in the Peruvian Puna* [Unpublished MSc thesis]. Institute for Archaeological Sciences, University of Tübingen.

Hillyer, R., Valencia, B. G., Bush, M. B., Silman, M. R., & Steinitz-Kannan, M. (2009). A 24,900-year paleolimnological history from the Peruvian Andes. *Quaternary Research*, *71*, 71–82.

Hogg, A. G., Heaton, T. J., Hua, Q., Palmer, J. G., Turney, C. S., Southon, J., Bayliss, A., Blackwell, P. G., Boswijk, G., Bronk Ramsey, C., Pearson, C., Petchey, F., Reimer, P., Reimer, R., & Wacker, L. (2020). SHCal20 southern hemisphere calibration, 0-55,000 years cal BP. *Radiocarbon*, *62*(4), 759–778.

Instituto Geografico Nacionales. (1990, 1995). *Cotahuasi, Peru 1:100,000 Cuadrángulo Topográfico y Chuquibamba, Peru 1:100,000*. Cuadrángulo Topográfico.

Jolie, E. A., Lynch, T. F., Geib, P. R., & Adovasio, J. M. (2011). Cordage, textiles, and the late Pleistocene peopling of the Andes. *Current Anthropology*, *52*(2), 285–296. https://doi.org/10.1086/659336

Jomelli, V., Favier, V., Vuille, M., Braucher, R., Martin, L., Blard, P.-H., Colose, C., Brunstein, D., He, F., Khodri, M., Bourlès, D. L., Leanni, L., Rinterknecht, V., Grancher, D., Francou, B., Ceballos, J. L., Fonseca, H., Liu, Z., & Otto-Bliesner, B. L. (2014). A major advance of tropical Andean glaciers during the Antarctic cold reversal. *Nature*, *513*(7517), 224–228. https://doi.org/10.1038/nature13546

Kanner, L. C., Burns, S. J., Cheng, H., Edwards, R. L., & Vuille, M. (2013). High-resolution variability of the South American summer monsoon over the last seven millennia: Insights from a speleothem record from the central Peruvian Andes. *Quaternary Science Reviews*, *75*, 1–10. https://doi.org/10.1016/j.quascirev.2013.05.008

Karkanas, P., & Goldberg, P. (2018). *Reconstructing archaeological sites*. Wiley. https://doi.org/10.1002/9781119016427

Kelly, M. A., Lowell, T. V., Applegate, P. J., Phillips, F. M., Schaefer, J. M., Smith, C. A., Kim, H., Leonard, K. C., & Hudson, A. M. (2015). A locally calibrated, late glacial ^{10}Be production rate from a low-latitude, high-altitude site in the Peruvian Andes. *Quaternary Geochronology*, *26*, 70–85. https://doi.org/10.1016/j.quageo.2013.10.007

Lafuente, B., Downs, R. T., Yang, H., & Stone, N. (2015). The power of databases: The RRUFF project. In T. Armbruster & R. M. Danisi (Eds.), *Highlights in mineralogical crystallography* (pp. 1–30). Walter de Gruyter GmbH. https://doi.org/10.1515/9783110417104-003

Lajo Soto, A., Díaz Rodríguez, J., & Barreda De La Cruz, M. A. (2001). Mapa Geológico del Cuadrángulo de Cotahuasi, *Escala 1:100,000*. Instituto Geológico Minero y Metalúrgico.

de Lima Moraes, A. G. (2018). ALOS PALSAR High Resolution Terrain corrected (APhrtc) DEM.

Loyola, R., Cartajena, I., Núñez, L., & López (2017). Moving into an arid landscape: Lithic technologies of the Pleistocene-Holocene transition in the high-altitude basins of Imilac and Punta Negra, Atacama Desert. *Quaternary International*, *473*, 206–224. https://doi.org/10.1016/j.quaint.2017.10.010

Loyola, R., Núñez, L., & Cartajena, I. (2020). Expanding the edge: The use of caves and rockshelters during the Late-Pleistocene human dispersal into the Central Atacama Highlands. *PaleoAmerica*, *5*(4), 349–363. https://doi.org/10.1080/20555563.2019.1697919

Lynch, T. F. (1980). *Guitarrero cave. Early man in the Andes*. Academic Press.

Maldonado, A., Betancourt, J. L., Latorre, C., & Villagran, C. (2005). Pollen analyses from a 50 000-yr rodent midden series in the southern Atacama Desert (25° 30′ S). *Journal of Quaternary Science*, *20*(5), 493–507. https://doi.org/10.1002/jqs.936

Mentzer, S. M. (2014). Microarchaeological approaches to the identification and interpretation of combustion features in prehistoric archaeological sites. *Journal of Archaeological Method and Theory*, *21*(3), 616–668. https://doi.org/10.1007/s10816-012-9163-2

Moore, K. (2016). *Report on the 2015 season of excavation and Cuncaicha, and the 2015 and 2016 study seasons of the zooarchaeological samples from the site* [Unpublished manuscript].

Moreno, P. I., François, J. P., Villa-Martínez, R. P., & Moy, C. M. (2009). Millennial-scale variability in southern hemisphere westerly wind activity over the last 5000 years in SW Patagonia. *Quaternary Science Reviews*, *28*(1-2), 25–38. https://doi.org/10.1016/j.quascirev.2008.10.009

Nami, H. G., & Stanford, D. J. (2016). Dating the peopling of northwestern South America: An AMS date from El Inga site, highland Ecuador. *PaleoAmerica*, *2*(1), 60–63. https://doi.org/10.1080/20555563.2016.1139793

Nester, P. L., Gayó, E., Latorre, C., Jordan, T. E., & Blanco, N. (2007). Perennial stream discharge in the hyperarid Atacama Desert of northern Chile during the latest Pleistocene. *Proceedings of the National Academy of Sciences of the United States of America*, *104*(50), 19724–19729. https://doi.org/10.1073/pnas.0705373104

Núñez, L., Cartajena, I., & Grosjean, M. (2013). Archaeological silence and ecorefuges: Arid events in the Puna of Atacama during the Middle Holocene. *Quaternary International*, *307*, 5–13. https://doi.org/10.1016/j.quaint.2013.04.028

Núñez, L., Grosjean, M., & Cartajena, I. (2002). Human occupations and climate change in the Puna de Atacama, Chile. (Reports). *Science*, *298*(5594), 821–825.

Nunnery, J. A., Fritz, S. C., Baker, P. A., & Salenbien, W. (2019). Lake-level variability in Salar de Coipasa, Bolivia during the past ~40,000 yr. *Quaternary Research*, *91*(2), 881–891. https://doi.org/10.1017/qua.2018.108

Olchauski, E., & Dávila, D. (1994). *Geología de los Cuadrángulos de Chuquibamba y Cotahuasi*. Boletín No. 50, Serie A: Carta Geológica Nacional. Instituto Geológico Minero y Metalúrgico, Lima.

Osorio, D., Steele, J., Sepúlveda, M., Gayo, E. M., Capriles, J. M., Herrera, K., Ugalde, P., De pol-Holz, R., Latorre, C., & Santoro, C. M. (2017). The Dry Puna as an ecological megapatch and the peopling of South America: Technology, mobility, and the development of a Late Pleistocene/Early Holocene Andean hunter-gatherer tradition in northern Chile. *Quaternary International*, *461*, 41–53. https://doi.org/10.1016/j.quaint.2017.07.010

Ozán, I. L., Méndez, C., Oriolo, S., Orgeira, M. J., Tripaldi, A., & Vásquez, C. A. (2019). Depositional and post-depositional processes in human-modified cave contexts of west-central Patagonia (southernmost South America). *Palaeogeography, Palaeoclimatology, Palaeoecology*, *532*, 109268. https://doi.org/10.1016/j.palaeo.2019.109268

Pedley, M., Martin, J. A. G., Delgado, S. O., & Garcia Del Cura, M. (2003). Sedimentology of Quaternary perched springline and paludal tufas: Criteria for recognition, with examples from Guadalajara Province, Spain. *Sedimentology*, *50*(1), 23–44. https://doi.org/10.1046/j.1365-3091.2003.00502.x

Pfeiffer, M., Latorre, C., Santoro, C. M., Gayo, E. M., Rojas, R., Carrevedo, M. L., McRostie, V. B., Finstad, K. M., Heimsath, A., Jungers, M. C., De Pol-Holz, R., & Amundson, R. (2018). Chronology, stratigraphy and hydrological modelling of extensive wetlands and paleolakes in the hyperarid core of the Atacama Desert during the late Quaternary. *Quaternary Science Reviews*, *197*, 224–245. https://doi.org/10.1016/j.quascirev.2018.08.001

Placzek, C., Quade, J., & Patchett, P. J. (2006). Geochronology and stratigraphy of late Pleistocene lake cycles on the southern Bolivian Altiplano: Implications for causes of tropical climate change. *Geological Society of America Bulletin*, *118*(5-6), 515–532. https://doi.org/10.1130/B25770.1

Pueyo, J. J., Sáez, A., Giralt, S., Valero-Garcés, B. L., Moreno, A., Bao, R., Schwalb, A., Herrera, C., Klosowska, B., & Taberner, C. (2011). Carbonate and organic matter sedimentation and isotopic signatures in Lake Chungará, Chilean Altiplano, during the last 12.3kyr. *Palaeogeography, Palaeoclimatology, Palaeoecology*, *307*(1-4), 339–355. https://doi.org/10.1016/j.palaeo.2011.05.036

Quade, J., Rech, J. A., Betancourt, J. L., Latorre, C., Quade, B., Rylander, K. A., & Fisher, T. (2008). Paleowetlands and regional climate change in the central Atacama Desert, northern Chile. *Quaternary Research*, *69*(03), 343–360. https://doi.org/10.1016/j.yqres.2008.01.003

Rademaker, K., Glascock, M., Kaiser, B., Gibson, D., Lux, D., & Yates, M. (2013). Multi-technique geochemical characterization of the Alca obsidian source, Peruvian Andes. *Geology*, *41*, 779–782. https://doi.org/10.1130/G34313.1

Rademaker, K., & Hodgins, G. (2018). Exploring the chronology of occupations and burials at Cuncaicha rockshelter, Peru. In K. Harvati, H. Reyes-Centeno, & G. Jäger (Eds.), *Words, bones, genes, tools: Vol. 1. New perspectives on the peopling of the Americas* (1st ed., pp. 107–124). Kerns Verlag.

Rademaker, K., Hodgins, G., Moore, K., Zarrillo, S., Miller, C., Bromley, G. R., Leach, P., Reid, D. A., Álvarez, W. Y., & Sandweiss, D. H. (2014). Paleoindian settlement of the high-altitude Peruvian Andes. *Science*, *346*(6208), 466–469. https://doi.org/10.1126/science.1258260

Rademaker, K., Hodgins, G., Moore, K., Zarrillo, S., Miller, C., Bromley, G. R. M., Leach, P., Reid, D., Álvarez, W. Y., & Sandweiss, D. H. (2016). Cuncaicha rockshelter, a key site for understanding colonization of the high Andes. *Current Anthropology*, *57*(1), 101–103. https://doi.org/10.1086/684826

Rademaker, K., & Moore, K. (2018). Variation in the occupation intensity of early forager sites of the Andean puna. In A. K. Lemke (Ed.), *Foraging in the past: Archaeological studies of Hunter-Gatherer diversity* (pp. 76–118). University Press of Colorado. https://doi.org/10.5876/9781607327745.c004

Ramirez, E., Hoffmann, G., Taupin, J. D., Francou, B., Ribstein, P., Caillon, N., Ferron, F. A., Landais, A., Petit, J. R., Pouyaud, B., Schotterer, U., Simoes, J. C., & Stievenard, M. (2003). A new Andean deep ice core from Nevado Illimani (6350 m), Bolivia. *Earth and Planetary Science Letters*, *212*(3), 337–350. https://doi.org/10.1016/S0012-821X(03)00240-1

Riding, R. (2000). Microbial carbonates: The geological record of calcified bacterial-algal mats and biofilms. *Sedimentology*, *47*, 179–214. https://doi.org/10.1046/j.1365-3091.2000.00003.x

Rigsby, C. A., Bradbury, J. P., Baker, P. A., Rollins, S. M., & Warren, M. R. (2005). Late Quaternary palaeolakes, rivers, and wetlands on the Bolivian Altiplano and their palaeoclimatic implications. *Journal of Quaternary Science*, *20*(7-8), 671–691. https://doi.org/10.1002/jqs.986

Rodbell, D. T., & Seltzer, G. O. (2000). Rapid ice margin fluctuations during the Younger Dryas in the tropical Andes. *Quaternary Research*, *54*(3), 328–338. https://doi.org/10.1006/qres.2000.2177

Santoro, C. M., Gayo, E. M., Capriles, J. M., Rivadeneira, M. M., Herrera, K. A., Mandakovic, V., Rallo, M., Rech, J. A., Cases, B., Briones, L., Olguín, L., Valenzuela, D., Borrero, L. A., Ugalde, P. C., Rothhammer, F., Latorre, C., & Szpak, P. (2019). From the Pacific to the tropical forests: Networks of social interaction in the Atacama Desert, late in the Pleistocene. *Chungará (Arica)*, *51*. (1), 5–25. https://doi.org/10.4067/S0717-73562019005000602

Seltzer, G., Rodbell, D., & Burns, S. (2000). Isotopic evidence for late Quaternary climatic change in tropical South America. *Geology*, *28*(1), 35. https://doi.org/10.1130/0091-7613(2000)282.0.CO;2

Stansell, N. D., Rodbell, D. T., Licciardi, J. M., Sedlak, C. M., Schweinsberg, A. D., Huss, E. G., Delgado, G. M., Zimmerman, S. H., & Finkel, R. C. (2015). Late Glacial and Holocene glacier fluctuations at Nevado Huaguruncho in the Eastern Cordillera of the Peruvian Andes. *Geology*, *43*(8), 747–750. https://doi.org/10.1130/G36735.1

Stoops, G. (2003). *Guidelines for analysis and description of soil and regolith thin sections*. Soil Science Society of America.

Stoops, G. (2010). *Interpretation of micromorphological features of soils and regoliths* (1st ed.). Elsevier. http://site.ebrary.com/lib/alltitles/docDetail.action?docID=10415276

Stoops, G. (2017). Fluorescence microscopy. In C. Nicosia & G. Stoops (Eds.), *Archaeological soil and sediment micromorphology* (pp. 393–398). Wiley.

Sylvestre, F., Servant, M., Servant-Vildary, S., Causse, C., Fournier, M., & Ybert, J.-P. (1999). Lake-level chronology on the southern Bolivian Altiplano (18°–23°S) during Late-Glacial time and the Early Holocene. *Quaternary Research*, *51*(1), 54–66. https://doi.org/10.1006/qres.1998.2017

Thompson, L. G., Davis, M. E., Mosley-Thompson, E., Sowers, T. A., Henderson, K. A., Zagorodnov, V. S., Lin, P., Mikhalenko, V. N., Campen, R. K., Bolzan, J. F., Cole-Dai, J., & Francou, B. (1998). A 25,000-year tropical climate history from Bolivian ice cores. *Science*, *282*(5395), 1858–1864. https://doi.org/10.1126/science.282.5395.1858

Thompson, L. G., Mosley-Thompson, E., Davis, M. E., Lin, P. N., Henderson, K. A., Cole-Dai, J., Bolzan, J. F., & Liu, K. B. (1995). Late Glacial stage and Holocene tropical ice core records from Huascaran, Peru. *Science*, *269*(5220), 46–50. https://doi.org/10.1126/science.269.5220.46

Thouret, J.-C. E., Juvigne, J., Mariño, M., Moscol, A., Legeley-Padovani, I., Loutsch, J., & Rivera, M. (2002). Late Pleistocene and Holocene tephro-stratigraphy and chronology in southern Peru. *Sociedad Geológica Del Perú*, *93*, 45–61.

Troll, C. (1968). *Geo-ecology of the mountainous regions of the tropical Americas: Geo-ecologia de las regiones montañosas de las americas tropicales*. UNESCO.

Úbeda, J., Bonshoms, M., Iparraguirre, J., Sáez, L., de la Fuente, R., Janssen, L., Concha, R., Vásquez, P., & Masías, P. (2018). Prospecting glacial ages and paleoclimatic reconstructions northeastward of Nevado Coropuna (16° S, 73° W, 6377m), arid tropical Andes. *Geosciences*, *8*(8), 307. https://doi.org/10.3390/geosciences8080307

Van Breukelen, M. R., Vonhof, H. B., Hellstrom, J. C., Wester, W. C. G., & Kroon, D. (2008). Fossil dripwater in stalagmites reveals Holocene temperature and rainfall variation in Amazonia. *Earth and Planetary Science Letters*, *275*(1), 54–60. https://doi.org/10.1016/j.epsl.2008.07.060

Villagrán, X. S., Huisman, D. J., Mentzer, S. M., Miller, C. E., & Jans, M. M. (2017). Bone and other skeletal tissues. In C. Nicosia, & G. Stoops (Eds.), *Archaeological soil and sediment micromorphology* (pp. 9–38). Wiley.

Vining, B. R., Steinman, B. A., Abbott, M. B., & Woods, A. (2019). Paleoclimatic and archaeological evidence from Lake Suches for highland Andean refugia during the arid Middle Holocene. *The Holocene*, *29*(2), 328–344. https://doi.org/10.1177/0959683618810405

Weide, D. M., Fritz, S. C., Hastorf, C. A., Bruno, M. C., Baker, P. A., Guedron, S., & Salenbien, W. (2017). A ~6000 yr diatom record of mid- to late Holocene fluctuations in the level of Lago Wiñaymarca, Lake Titicaca (Peru/Bolivia). *Quaternary Research*, *88*(2), 179–192. https://doi.org/10.1017/qua.2017.49

Yacobaccio, H. D. (2017). Peopling of the high Andes of northwestern Argentina. *Quaternary International*, *461*, 34–40. https://doi.org/10.1016/j.quaint.2017.01.006

Yataco Capcha, J., & Nami, H. G. (2016). A reevaluation of Paleoamerican artifacts from Jaywamachay rockshelter, Ayacucho Valley, Peru. *PaleoAmerica*, *2*(4), 368–372. https://doi.org/10.1080/20555563.2016.1199198

SUPPORTING INFORMATION

Additional supporting information may be found in the online version of the article at the publisher's website.

How to cite this article: Meinekat, S. A., Miller, C. E., & Rademaker, K. (2021). A site formation model for Cuncaicha rock shelter: Depositional and postdepositional processes at the high-altitude keysite in the Peruvian Andes. *Geoarchaeology*, 1–28. https://doi.org/10.1002/gea.21889

Appendix III – Paper 2

Quaternary Science Reviews 316 (2023) 108244

Contents lists available at ScienceDirect

Quaternary Science Reviews

journal homepage: www.elsevier.com/locate/quascirev

Fire as high-elevation cold adaptation: An evaluation of fuels and Terminal Pleistocene combustion in the Central Andes

Sarah A. Meinekat [a,*], Emily B.P. Milton [b,c], Brett Furlotte [d], Sonia Zarrillo [e,f], Kurt Rademaker [a,b,c]

[a] Institute for Archaeological Sciences, Department of Geosciences, University of Tübingen, Tübingen, Germany
[b] Department of Anthropology, Michigan State University, East Lansing, MI, USA
[c] Environmental Science and Policy Program, Michigan State University, East Lansing, MI, USA
[d] Department of Archaeology and Anthropology, University of Saskatchewan, Saskatoon, Saskatchewan, Canada
[e] Department of Anthropology, University of British Columbia, Vancouver, British Columbia, Canada
[f] Cotsen Institute of Archaeology, University of California, Los Angeles, Los Angeles, CA, USA

ARTICLE INFO

Handling Editor: Claudio Latorre

Keywords:
Experimental archaeology
Geoarchaeology
Combustion
Fuel selection
Andes
Late pleistocene
Hunter-gatherers

ABSTRACT

The use of fire constitutes an essential cultural adaptation to cold, and archaeological evidence for fire can be expected in high-latitude and high-elevation regions successfully inhabited by modern humans. At Cuncaicha rockshelter (4480 m above sea level, or masl) in the southern Peruvian Andes, evidence for fire is present from the earliest occupation, dating to the Terminal Pleistocene (~12,500–11,200 cal BP). Yet, the site contains relatively few identifiable carbonized macrobotanical remains useful for identifying plants employed as combustible fuel. Based on a comprehensive review of nearly 40 early Andean archaeological sites above 2500 masl, little is known about fuels used for combustion. To understand fuel selection strategies at Cuncaicha, we conducted a combustion field experiment, evaluating the three highland plant taxa most likely to have been used as combustible fuels: *Polylepis rugulosa* (queñua) tree branches, *Parastrephia* spp. (tola) woody shrubs, and *Azorella compacta* (yareta) cushion plants. Temperature measurements informed on the combustion characteristics and efficiency of each fuel. We then compared the experimentally-produced fire residues to the geoarchaeological evidence from Cuncaicha. The resinous cushion plant yareta, endemic to the high Andes, may have been the primary fuel used at Cuncaicha based on the experiment outcome and the geoarchaeological evidence. Due to its high-temperature and complete combustion, yareta leaves little to no macrobotanical evidence, thus its identification at other Andean sites may require a multi-methodological approach. Because the geographic range of this plant corresponds with most early archaeological sites in the high Andes, yareta may have been a key resource enabling early settlement throughout the region.

1. Adaptation to high-elevation cold environments: the dry puna of the central Andes

The peopling of the Americas represents one of the final, large-scale migratory expansions of humans across the globe. In the Terminal Pleistocene, the first peoples entering the American continents encountered an extraordinary range of diverse environments, from rugged coasts to vast plains and forests, to some of the world's highest-elevation landscapes (Dillehay, 2009; Meltzer and Holliday, 2010; Pitblado, 2017).

In western South America recent discoveries of early archaeological sites in remote landscapes traditionally considered marginal (Méndez et al., 2018) have prompted a re-evaluation of long-standing settlement models. Terminal Pleistocene sites have been documented in the now hyper-arid core of the Atacama Desert in northern Chile (Latorre et al., 2013; Santoro et al., 2019), the Arid Diagonal in Bolivia (Capriles et al., 2016), and the high-elevation Andes of southern Peru (Rademaker et al., 2014). These sites provide evidence for an array of effective adaptation strategies.

Archaeological sites from Peru, Bolivia, Chile, and Argentina dated to the Terminal Pleistocene and Early Holocene attest to widespread, early human use of the high Andes (Fig. 1). Sauer (1944), Cardich

* Corresponding author. Institute for Archaeological Sciences, Hölderlinstr.12, 72074, Tübingen, Germany.
E-mail address: sarah-ann.meinekat@uni-tuebingen.de (S.A. Meinekat).

https://doi.org/10.1016/j.quascirev.2023.108244
Received 9 March 2023; Received in revised form 24 July 2023; Accepted 27 July 2023

(1958), and Lynch (1983) proposed that initial entry into the Andes could have occurred via relatively low-elevation north-south oriented cordilleras and inter-montane valleys of Colombia, then migration south through the highlands. The earliest sites known throughout the Andean puna (high-elevation grassland ecoregion extending from Peru to Chile and Argentina) share many characteristics. This led Osorio et al. (2017) to propose that the puna constituted an ecological *megapatch*, facilitating rapid southward exploration and settlement.

Unlike alpine mountain and plateau environments in high and temperate latitudes, which have strong temperature seasonality, low-latitude tropical mountains and plateaus, such as the central Andes in Peru, are characterized by small seasonal fluctuations in temperature but pronounced diurnal temperature variation. This tropical pattern can involve diurnal temperature ranges of 10° (Ecuador) to ca. 49 °C (Chile)

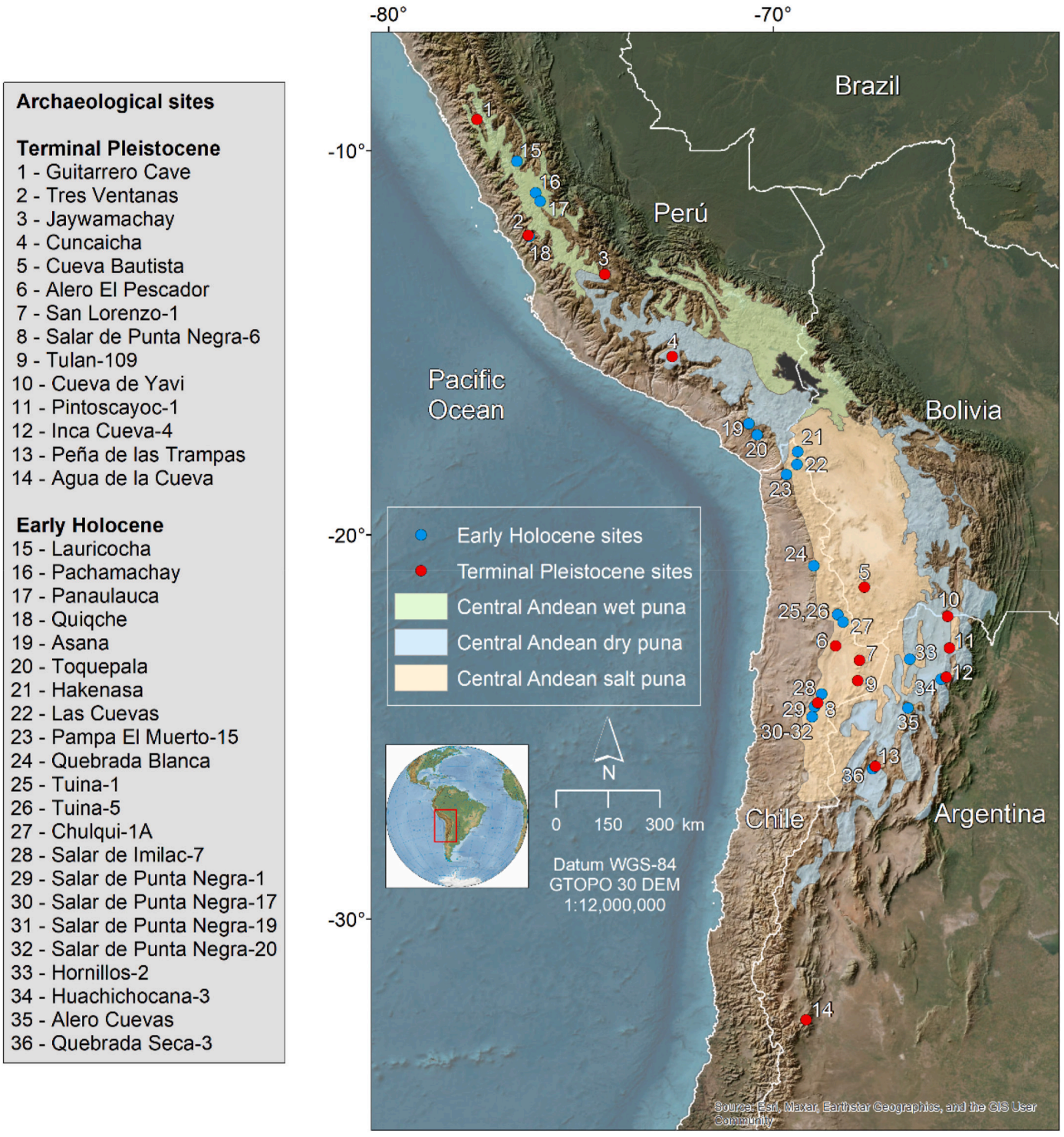

Fig. 1. Map of the central and southern Andes with all archaeological sites >2500 masl radiocarbon dated to the Terminal Pleistocene and first millennium of the Early Holocene. Chronological and combustion evidence for the archaeological sites including references is provided in Table 1. Further details are provided in the Supplemental Materials. Satellite image: ESRI, Maxar, Geoeye, Earthstar Geographics, Centro Nacional de Estudios Espaciales/Airbus Defence and Space, U.S. Department of Agriculture, AeroGRID, Instituto Geográfico Nacional del Perú, GIS User Community.

(Troll, 1968, p. 38), nights with temperatures below 0 °C throughout the year, and, though offset by warm days, low mean annual temperatures. For example, the cold nighttime temperatures at ca. 4500 masl in the Andes of southern Peru can reach below −10 °C, while during the day, temperatures above 10 °C are possible. These climatic features place important limits on biota and primary production.

The puna (3800–4800 masl) is the highest Andean landscape regularly inhabited by humans. Geomorphologically, the puna is defined as a highland plateau area where the peaks of volcanoes, some of which reach well over 6000 masl, present impressive landmarks on the horizon. Troll (1968) and Cabrera (1968) defined ecological sub-divisions for the puna - Wet, Dry, and Salt - in order of decreasing precipitation from north to south and from east to west (Fig. 1). This spatial pattern is determined by distance from the Atlantic source of Andean precipitation and the reach of the South American Summer Monsoon (Baker and Fritz, 2015). The dry puna is situated between 16° and 20°S and exhibits abundant perennial streams, wetlands, and lakes. Extensive grasslands, woody shrubs, limited groves of small trees, and cushion plants represent some of the plant life. Andean peat wetlands (*bofedales*) provide year-round freshwater, edible algae, and excellent habitat for wild camelids and birds (Squeo et al., 2006). The puna has higher herbivore density relative to all lower-elevation ecozones (Koford, 1957; Franklin, 1982).

However, above 2500 masl environmental parameters pose a unique set of adaptive conditions for the human body (Baker, 1978). Challenges to human physiology include cold temperatures, low humidity, high solar radiation, and hypoxia (Frisancho, 2013; Moore, 2017). While recent research has focused on understanding functional and genetic responses to altitude-induced hypoxia (Crawford et al., 2017; Eichstaedt et al., 2017; Jacovas et al., 2018; Brutsaert et al., 2019; Storz, 2021; Sharma et al., 2022), cold is a lesser-studied but critical biological stressor in high-elevation and high-latitude environments (Castellani and Young, 2016). Human adaptation to cold comprises both physiological and technological adjustments. Pertinent to understanding initial human exploration and settlement of cold environments is (1) the duration and severity of cold temperatures and precipitation, (2) the capacity to mitigate cold stress through technologies such as clothing, shelter, and use of fire, and (3) landscape characteristics such as shelter and resource availability.

In this paper we examine the adaptive role of fire for hunter-gatherers in the puna during the Terminal Pleistocene and Early Holocene. We review evidence for combustion in the early archaeological record focusing on Cuncaicha rock shelter, one of the highest-elevation Pleistocene sites known in the world. Building on previous geoarchaeological analyses, we present results from an experiment to evaluate the combustion characteristics of local puna fuels. Experimentally produced residues are then formally compared to archaeological evidence from Cuncaicha using a geoarchaeological approach. Finally, we discuss fuel selection and use at Cuncaicha and their implications for initial human dispersal and settlement in the high Andes.

1.2. Fire in the archaeological record – potentials and challenges

The evolution of fire (*e.g.,* Sorensen, 2019; Chazan, 2017; Sandgathe and Berna, 2017) presents a complex course of interactions between fire and the genus *Homo*. Consistent use of fire (MacDonald et al., 2021) dates back at least into the Middle Pleistocene, if not earlier (*e.g.,* Goldberg et al., 2017; Berna et al., 2012). Use of fire has been central (*e.g.,* Kuhn and Stiner, 2019; Binford, 1978) in human lifeways and reoccurred ever since (*e.g.,* Murphree and Aldeias, 2022; Clark et al., 2022; Sorensen, 2019; Sandgathe and Berna, 2017; Shimelmitz et al., 2014; Sandgathe et al., 2011a; Sandgathe et al., 2011b, Roebroeks and Villa, 2011).

Fire has been described as the "ultimate range expander" (Sorensen, 2019), especially regarding human dispersals into high latitudes and high elevations. Fire holds a unique adaptive role in mitigating cold because of its multifaceted technological and social uses (Clark and Harris, 1985). Beyond warmth, fire supports cooking, tool alterations, and waste disposal; it provides light, distance signaling, land management, and protection against animals (Clark and Harris, 1985). Fire also centers many social activities, including meal preparation and consumption, gathering for warmth, spiritual activities, storytelling, and cremation (Kuhn and Stiner, 2019). As such fire, and the fuel to create it, constitute critical resources for people (Binford, 1980).

Recently, archaeologists have advocated that fire remains should be considered as artifacts in their own right (Stahlschmidt et al., 2020). In the archaeological record, charcoal, heat-treated and heat-damaged artifacts, fire-cracked rock, materials and tools representative of fire starting, or thermal modifications all provide evidence of pyrotechnology (Bellomo, 1993). Evidence of pyrotechnology at the microscopic scale includes a variety of features and residues, which can provide valuable information on site formation, post-depositional processes, human behavior, and occupation intensity (*e.g.,* Karkanas, 2021; Mallol et al., 2017).

Identification and interpretation of combustion features pose specific challenges to the archaeologist and require careful analysis beyond field annotations (*e.g.,* Goldberg et al., 2017; Aldeias et al., 2016; Mentzer, 2012; Mallol et al., 2013). The differentiation between various combustion features, and hearth features especially, should be highlighted, as this forms the basis to any follow-up interpretations. A hearth feature is a specific contained primary combustion feature with evidence for in situ fire (Mentzer, 2017). Combustion feature is a more descriptive term that encompasses many different features related to burning (*e.g.,* but not exclusively: hearths, fumiers, conflagrations, fire installations, burning surfaces), and the term also includes contained secondary combustion features like rake-outs and dumps that can be difficult to distinguish from hearth features in the field (Mentzer, 2012, 2017; Mallol et al., 2017).

1.3. Early archaeological evidence for combustion and fuel use in the Andes

Table 1 lists all archaeological sites >2500 masl from the central and southern Andes radiocarbon dated to the Terminal Pleistocene (n = 14) and first millennium of the Early Holocene (n = 22), the material dated at each site, whether combustion features were documented, and the identification of fuel taxa. Thirty-four sites have ages on charcoal, and one site is dated with burned bone. These dated plant and animal materials are arguably burned due to anthropogenic activity, thus nearly all early Andean sites >2500 masl have evidence of anthropogenic combustion. The ubiquity of combustion evidence is unsurprising, given the need to mitigate cold nighttime temperatures and other potential social and subsistence benefits of congregating around a hearth (Kuhn and Stiner, 2019). The latter is suggested by the presence of subsistence remains in all, or nearly all, of the sites considered in Table 1.

Combustion features are documented in six of 14 Terminal Pleistocene components (42.8%) and nine of 22 Early Holocene components (40.9%). In most cases, these are described as discrete charcoal lenses or "floors," or charcoal and ash concentrations, sometimes accompanied by burned animal bones, lithics, or sediment (Table 1).

The earliest features described as hearths are reported from Cueva Bautista in Bolivia (Capriles et al., 2016) and Agua de la Cueva in northwest Argentina (García et al., 1999). These sites were extensively excavated to expose potential activity areas. Cueva Bautista has nine Terminal Pleistocene radiocarbon ages on dispersed charcoal (n = 5) and faunal bone collagen (n = 4) from Layers O and P (Capriles et al., 2016). Ages from basal Level P are significantly older than those from Level O. The oldest age from Level P is 10,917 ± 69 BP (13.0-12.7 ka[1]).

[1] ka = thousands of calibrated years ago using complete 95% ranges, obtained with the SHCal20 calibration curve (Hogg et al., 2020).

Table 1
Archaeological sites >2500 masl from the central and southern Andes radiocarbon dated to the Terminal Pleistocene (TP) and first radiocarbon millennium of the Early Holocene (EH).

# in Fig. 1	Site	Country	Elevation (masl)	Ecoregion	^{14}C BP	SHCal20 95% cal BP	Dated material	Combustion	TP/EH combustion features/description	Fuel ID	References
Terminal Pleistocene sites											
1	Guitarrero Cave	Peru	2580	Sechura desert	10,240 ± 45	12,013–11,648	cordage, wood artifacts, charcoal	yes	no	no	Lynch, 1980; Jolie et al., (2011)
2	Tres Ventanas	Peru	3810	wet puna	10,030 ± 170	12,432–10,879	Charcoal	yes	no	no	Engel (1970)
3	Jaywamachay	Peru	3350	Peruvian yungas	10,280 ± 170	12,600–11,319	Charcoal	yes	Hearth and charcoal floor at base of Stratum J3	no	Garcia Cook, 1981
4	Cuncaicha	Peru	4480	dry puna	10,380 ± 100	12,603–11,786	ultrafiltered bone collagen; charcoal	yes	no	present study	Rademaker et al., (2014)
5	Cueva Bautista	Bolivia	3935	salt puna	*10,917 ± 69	12,972–12,729	dispersed charcoal. bone collagen	yes	two shallow hearths in Zone O	no	Capriles et al., (2016)
6	Alero El Pescador	Chile	3300	salt puna	10,310 ± 130	12,606–11,349	charcoal	yes	yes	no	DeSouza (2004)
7	San Lorenzo 1	Chile	2950	salt puna	*10,400 ± 130	12,683–11,728	charcoal	yes	no	no	Núñez (1983)
8	Salar de Punta Negra 6	Chile	2975	salt puna	10,260 ± 60	12,432–11,638	charcoal	yes	no	no	Grosjean et al., (2005)
9	Tulan 109	Chile	2950	salt puna	*10,590 ± 150	12,751–11,953	charcoal	yes	no	no	Núñez et al., 2002, 2005
10	Cueva de Yavi	Argentina	3430	dry puna	*10,450 ± 55	12,598–12,019	charcoal	yes	no	no	Kulemeyer et al., (1999)
11	Pintoscayoc 1	Argentina	3780	dry puna	*10,720 ± 150	12,969–12,090	charcoal	yes	no	no	Hernández Llosas, 2000
12	Inca Cueva 4	Argentina	3650	dry puna	*10,620 ± 140	12,760–11,999	uncarbonized *Hypsocharis* sp. leaves	yes	hearths in Layer 2	*Polylepis* sp.	Aschero (1984); Aschero and Podesta (1986); Aschero (2010)
13	Peña de las Trampas	Argentina	3580	dry puna	10,190 ± 190	12,142–11,289	charcoal	yes	yes	no	Martínez, 2012
14	Agua de la Cueva	Argentina	2905	southern Andean steppe	*10,950 ± 90	13,070–12,736	charcoal	yes	hearths in Subunit 2 b	no	García et al., 1999
# in Fig. 1	Site	Country	Elevation (masl)	Ecoregion	^{14}C BP	SHCal20 95% cal BP	Dated material	Combustion	TP/EH combustion features/description	Fuel ID	References
Early Holocene sites											
15	Lauricocha (L-2)	Peru	3930	wet puna	9525 ± 260	11,629-9975	charcoal mixed with burned and unburned bone	yes	no	no	Cardich (1964)
16	Pachamachay	Peru	4300	wet puna	9010 ± 285	11,066-9429	charcoal	yes	no	various	Rick (1980); Pearsall (1980)
17	Panaulauca	Peru	4150	wet puna	9650 ± 145	11,261–10,513	charcoal	yes	no	no	Rick and Moore (1999)
18	Quiqche	Peru	3600	wet puna	9940 ± 200	12,087–10,706	charcoal	yes	no	no	Engel and Genoves, 1969; Engel, 1970
19	Asana	Peru	3435	Sechura desert	9820 ± 150	11,715–10,704	charcoal	yes	yes	no	Aldenderfer (1998)
20	Toquepala	Peru	2800	Sechura desert	9490 ± 140	11,175–10,304	charcoal	yes	no	no	Ravines 1964, 1967a, 1972
21	Hakenasa	Chile	4100	salt puna	9980 ± 40	11,622–11,239	charcoal	yes	yes	no	Moreno et al., (2009)
22	Las Cuevas	Chile	4485	salt puna	10,070 ± 30	11,715–11,314	charcoal	yes	no	no	Santoro and Chacama Rodríguez, 1984
23	Pampa el Muerto 15	Chile	3175	salt puna	9510 ± 95	11,143–10,500	burned bone	yes	no	no	Osorio et al., (2016)

(*continued on next page*)

Table 1 (*continued*)

# in Fig. 1	Site	Country	Elevation (masl)	Ecoregion	^{14}C BP	SHCal20 95% cal BP	Dated material	Combustion	TP/EH combustion features/description	Fuel ID	References
24	Quebrada Blanca	Chile	4500	salt puna	9510 ± 70	11,083–10,512	charcoal	yes	no	no	Grosjean et al., (2007)
25	Tuina 1	Chile	3160	salt puna	9080 ± 130	10,554-9726	charcoal	yes	no	no	Núñez et al., 2005
26	Tuina 5	Chile	3810	salt puna	10,060 ± 70	11,830–11,259	charcoal	yes	yes	no	Núñez et al., 2005
27	Chulqui 1 A	Chile	3280	salt puna	9590 ± 60	11,161–10,684	charcoal	yes	yes	no	Sinclaire A. 1985
28	Salar de Imilac 7	Chile	3020	salt puna	9960 ± 50	11,623–11,216	charcoal	yes	yes	no	Cartajena et al., (2014)
29	Salar de Punta Negra 1	Chile	2975	salt puna	9230 ± 50	10,500–10,241	Peat	no	no	not applicable	Grosjean et al., (2005), deSouza et al., 2021
30	Salar de Punta Negra 17	Chile	2960	salt puna	9260 ± 40	10,509–10,247	charcoal	yes	yes	no	deSouza et al., 2021
31	Salar de Punta Negra 19	Chile	2960	salt puna	9460 ± 50	11,062–10,502	charcoal	yes	yes	no	Cartajena et al., (2014)
32	Salar de Punta Negra 20	Chile	2960	salt puna	9480 ± 50	11,066–10,509	charcoal	yes	yes	no	Cartajena et al., (2014)
33	Hornillos 2	Argentina	4020	dry puna	9710 ± 270	11,870–10,252	charcoal	yes	no	*Parastrephia* spp., *Baccharis incarum*	Yacobaccio et al., (2014)
34	Huachichocana 3	Argentina	3400	dry puna	9620 ± 130	11,229–10,571	charcoal	yes	charcoal lenses (hearths?) in Layer E3	no	Aguerre et al., (1975); Fernández Distel, 1986
35	Alero Cuevas	Argentina	4400	dry puna	9880 ± 100	11,713–10,819	charcoal	yes	no	no	López and Restifo, 2017
36	Quebrada Seca 3	Argentina	4050	dry puna	9410 ± 120	11,073–10,248	charcoal	yes	no	*Parastrephia* spp., *Baccharis incarum, Adesmia horrida*	Rodríguez, 2000; Pintar (2008)

All ages calibrated using Calib 8.1.0 (Stuiver and Reimer, 2020) and the SHCal20 calibration (Hogg et al., 2020). The entire 95% calibrated ranges are reported. TP-Terminal Pleistocene, EH-Early Holocene. * indicates singular, unreplicated age.

Level O includes two hearth features, directly dated with unidentified charcoal to 10,336 ± 63 BP (12.5–11.8 ka) and 10,412 ± 60 BP (12.6–12.0 ka), and 10,433 ± 67 BP (12.6–12.0 ka). The three hearth ages are statistically indistinguishable and provide a pooled mean age of 10,393 ± 36 BP (12.5–12.0 ka). Given the possibility of old wood and non-human introduction of some of the dated faunal remains, the dated hearths may provide the most reliable age for initial human use of Cueva Bautista.

Subunit 2 b in Agua de la Cueva has five radiocarbon ages on charcoal spanning from 9210 ± 70 BP (10.6–10.2 ka) to 10,350 ± 220 BP (12.7–11.3 ka). A sixth age much older than the others, 10,950 ± 90 BP (13.1–12.7 ka), came from the base of the 2 b stratum (García et al., 1999). Hearths were identified based on thin, lens-shaped charcoal concentrations within the 2 b stratum, associated with lithics and burned animal bones. García (2010) also notes banding within the 2 b sediment, interpreted as the result of thermal alteration by hearths that were cleaned and no longer preserved.

Four other Terminal Pleistocene sites have features described as hearths - Jaywamachay in southern Peru (García Cook, 1982), Alero El Pescador in northern Chile (DeSouza, 2004), and Inca Cueva-4 and Peña de las Trampas in northwest Argentina (Aschero and Podestá, 1986; Martínez, 2012). Calibrated ages for all three sites are ~12.6–11.3 ka (Table 1). Importantly, most early Andean sites do not have preserved hearths, similar to the situation among contemporary sites in North America (Surovell and Waguespack, 2007). However, a lack of preserved hearths does not equate with ephemeral occupation evidence, as some of the most intense Andean occupations – as suggested by artifact, faunal, and paleobotanical material amounts – are also some of the ones lacking intact hearth features. Conversely, some of the sites with preserved hearths contain relatively few cultural materials (Rademaker and Moore, 2018). Intense, repeated longer-term occupations (in contrast to brief, short-term site visits) of relatively small interior spaces may work against the preservation of early combustion and other features (Rick, 1980; for a broader perspective, also see Miller et al., 2013; Karkanas et al., 2015).

Plant taxa used as fuel were securely identified at only four of 36 early Andean sites (~11%). These include Pachamachay in the wet puna of central Peru and Inca Cueva-4, Hornillos-2, and Quebrada Seca-3 in the dry puna of northwest Argentina (Table 1, Fig. 1).

In Early Holocene flotation samples (Levels 28 and below) from Pachamachay (4310 masl), Pearsall (1980) identified carbonized fragments of woody shrubs *Margyricarpus strictus* (Rosaceae), *Chuquiraga huamanpinta/Ribes* (Compositae/Saxifragaceae), *Proustia pungens* (Compositae), and *Polylepis* spp. (Rosaceae) trees, all located on the puna above 4000 masl, as well as *Dodonaea viscosa* (L.) *Jacq*. (Sapindaceae) from high valleys below the puna zone. These contexts have a single radiocarbon age on unidentified charcoal, 9010 ± 280 BP, (11,066–9429 cal BP). Some carbonized camelid dung also was found in early levels, though it is unclear whether the dung was used as fuel or deposited by animals and burned inadvertently.

Inca Cueva-4 (3650 masl) is located in a grove of *Polylepis tomentella* trees (*queñua*). Extensive excavation exposed a variety of features in Layer 2, including two small hearths, nearby uncarbonized queñua trunks, and uncarbonized queñua bark in a separate midden feature (Aschero, 1984). A single radiocarbon age of 9230 ± 70 BP (10.6–10.2 ka) was obtained on unidentified charcoal from one of the hearths. Aschero and Podestá (1986) reported three additional radiocarbon ages for Layer 2, including a singular, unreplicated Terminal Pleistocene age of 10,620 ± 40 BP (12.7–12.5 ka) on uncarbonized *Hypsocharis* spp. leaves and stems.

Formal anthracological analyses were carried out at the Early Holocene site Hornillos-2 (4020 masl). The oldest radiocarbon age of 9710 ± 270 BP (11.9–11.3 ka) comes from the basal Level 6 d, though the analyzed Early Holocene carbonized botanical sample came from Layer 6a, higher up in the stratigraphic sequence. Two radiocarbon ages of 9590 ± 50 BP (11.1–10.7 ka) on uncarbonized wood and 9150 ± 50 BP (10.5–10.2 ka) on charcoal from the immediately overlying Level 6 provide an approximate age for the analyzed anthracological sample. Charcoal identified as *Parastrephia*, and *Baccharis incarum* indicate a reliance on resinous shrubs as combustion fuel (Yacobaccio et al., 2014).

Rodríguez (2000) carried out detailed paleoethnobotanical and anthracological analyses at Quebrada Seca-3 (4050 masl). From a context dated to 9410 ± 120 BP (11.1–10.2 ka), three identified taxa included *Parastrephia* spp., *Baccharis incarum*, and *Adesmia horrida*. These resinous shrubs are ranked among the best fuel sources by modern indigenous pastoralists in the region according to ethnographic interviews, and woody shrubs are the only source of firewood available in the salt puna ecoregion (Rodríguez, 2000).

1.4. Combustion evidence from the dry puna: Cuncaicha rock shelter

Cuncaicha rock shelter (4480 masl) in the dry puna ecoregion of southern Peru contains occupations dating to the Terminal Pleistocene (12.5–11.2 ka), Early Holocene (9.6–9.2 ka), Late-Middle Holocene (5.9–4.8 ka), and Late Holocene (<2.1 ka) (Rademaker et al., 2014; Meinekat et al., 2021).

Evidence for combustion is present throughout the occupation sequence (Meinekat et al., 2021). Intact combustion features are only observed in the Late Holocene strata and composed of superimposed lenses of charcoal-rich, ash-rich, and some rubified layers, resulting in stacked combustion features (Mentzer, 2012). In the other strata, the combustion features have been reworked, probably by a mix of anthropogenic and natural processes. Yet all strata contain various lines of evidence for fire use in the rock shelter.

Evidence of fire in the Terminal Pleistocene component (12.5–11.2 ka) includes highly abundant thermally altered and calcined herbivore bone, heat damaged and altered lithics, carbonized macrobotanical remains, and fire-cracked rock. A micro-analysis using micromorphology and (μ)FTIR provided further evidence of fire throughout all time periods, based on the identification of plant ashes and presence of the macro-evidence reflected on the micro-scale, such as burned bones (Meinekat et al., 2021).

The Cuncaicha sediments contain ash oxalate pseudomorphs, the heat-altered derivatives of calcium oxalates that are especially present in woody species such as trees and shrubs but not common in grasses (Canti and Brochier, 2017). Therefore, the presence of such ash components hints at some use of woody plant fuels as fuel by the Cuncaicha occupants.

Despite anthropogenic ash content, there are relatively few carbonized plant macro-remains in the rockshelter sediments. Table S1 summarizes the identifiable wood macrobotanical remains recovered via water flotation from a sample of Terminal Pleistocene (3.0 m^2) and Early Holocene (2.5 m^2) contexts excavated within the shelter. Two taxa were identified in both components. *Parastrephia* spp. is ubiquitous in all contexts, and *Polylepis rugulosa* is in most contexts, with 50% ubiquity for both the Terminal Pleistocene and Early Holocene contexts. *Parastrephia* shrubs (which we refer to generally as tola) are found in the immediate vicinity of Cuncaicha, whereas the closest modern *Polylepis* tree (queñua) groves are 30 km southwest of the site, occurring below 4200 masl (Fig. 2).

Macrobotanical remains of both taxa are present in the Cuncaicha sediments in small amounts, though, in comparison, the weights and densities of *Parastrephia* are greater than *Polylepis* in both components. *Parastrephia* density does not generally exceed 0.5 g/L of sediment, and *Polylepis* density does not exceed 0.03 g/L. While carbonized woody macroremains are ubiquitous in the site's early deposits, clearly indicating that anthropogenic combustion took place in both the Terminal Pleistocene and Early Holocene, the small amounts of carbonized macroremains are inconsistent with the use of either taxon as a primary combustion fuel. Although only a small number of samples were analyzed, densities of the wood charcoal and species used do not appear to change in the subsequent Middle and Late Holocene occupation

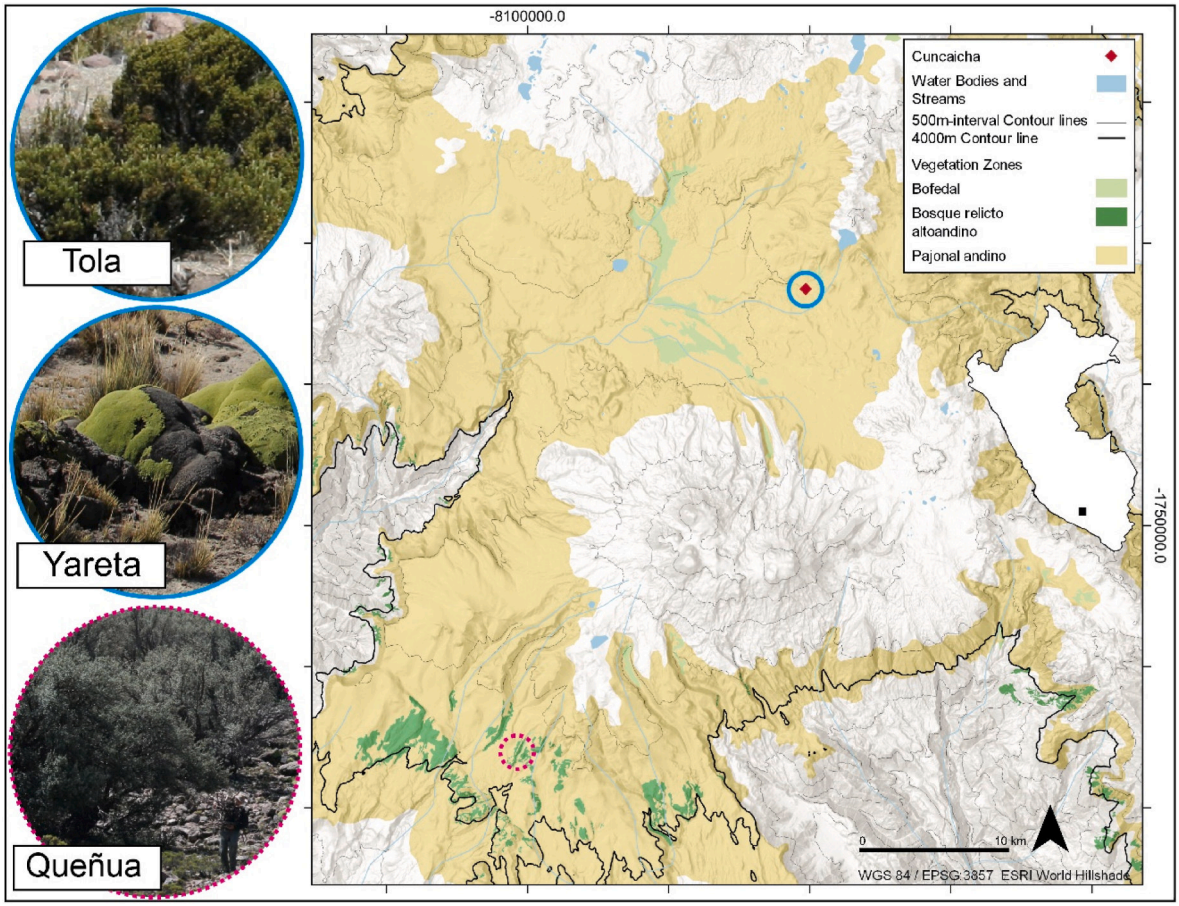

Fig. 2. Map of the study area showing Cuncaicha archaeological site and where the experiment was conducted. The map shows the vegetation zones that are habitat to the fuel species used for the experiment. The high Andean relict forest (*i.e., bosque relicto alto andino*) is habitat to queñua (*Polylepis* spp.), whereas yareta (*Azorella compacta*) and tola (*Parastrephia* spp.) are mostly found in the high Andean grasslands (*i.e., pajonal alto andino*). The *Bofedal* is high-elevation peatland. Circles indicate where the fuel was collected: Yareta and tola were collected next to Cuncaicha, Queñua was collected south-west of Nevado Coropuna. Ecosystem data obtained from Ministerio Ministerio del Ambiente, 2015, Ministerio del Ambiente, 2018.

components, indicating that taphonomic factors are not likely a factor for the paucity of wood charcoal in the Terminal Pleistocene and Early Holocene components.

Site cleaning does not explain the relative absence of macrobotanical remains, because these same flotation samples yielded substantial quantities of lithic microdebitage, faunal bone fragments, and other micro-artifacts, such as ochre, which also would have been removed if cleaning had taken place. Because geoarchaeological analyses securely identified anthropogenic ash content in the site sediments, some unidentified site formation process must explain the relative absence of carbonized woody macro-remains preserved in Cuncaicha's early sediments. A microcontextual approach and additional lines of evidence are therefore required to identify the most likely fuel(s) used by the inhabitants of Cuncaicha.

1.5. *Fuel selection strategies and previous experimental work in the Andes*

Any burned remains at an archaeological site are linked to both fire and fuel. Therefore, the question of fuel selection is essential to interpreting the archaeological record. Fuel selection strategies depend on the environmental conditions, but fuel selection is also influenced by the people who inhabit the site, group size, site function, occupation duration, and the purpose of the fire (Théry-Parisot et al., 2010; Théry-Parisot, 2002a). Studies of combustion features and fuel selection show how the selected fuel influences the archaeological remains, the site formation, and how it ultimately links to past human behavior, occupation intensity, and mobility (*e.g.,* Marcazzan et al., 2023, 2022; Tomé et al., 2022; Caruso Fermé and Civalero, 2019; Théry-Parisot, 2002a, 2002b).

Two theoretical approaches may support a test of fuel selection strategies: The *Principle of Least Effort (*PLE*)* and *Optimal Foraging Theory (OFT)*. As proposed by Joly et al. (2017) and Théry-Parisot et al. (2010), the former would predict fuels will occur in proportion to their frequency in the immediate site environment– with deviations indicating preferential decision making. In the case of the latter scenario, OFT might be considered.

Optimal Foraging Theory would favor those fuels that maximize net energy gain. To determine the optimal solution among a set of alternative candidates, one must consider the benefits of each fuel relative to the costs of procurement (Kelly, 2013; Bettinger et al., 2015). Optimal Foraging Theory is most often applied in subsistence studies; therefore, a fuel-focused study requires special considerations of fuel qualities. Although we cannot know which attributes would have been preferable to humans during the Terminal Pleistocene (Théry-Parisot et al., 2010), it is possible to examine fuel efficiency using an experimental approach. Important aspects of fuel efficiency include energy or time invested in transport, processing, fire making and maintenance, as well as combustion qualities including high temperature and long burn duration. Many experimental studies have focused on combustion practices and fuel selection during the Paleolithic (Aldeias, 2017 and references therein). Also in the Andes, there have been previous experimental, ethnographic, and archaeological studies focused on the identification of fuel and fuel selection strategies, with a regional emphasis on Argentina and Chile, and methodological emphasis on anthracological analyses.

Joly et al. (2017) conducted a combustion experiment in the Pampa del Tamarugal in northern Chile, performed anthracological analyses, and compared the results to the anthracological record of the Terminal Pleistocene archaeological site Quebrada de Maní 12 (1240 masl). The experiment identified available woody plant fuel resources, recorded the combustible qualities of the tested fuels (temperature and burn duration), and tested the results against the PLE. They conclude that the anthracological evidence does not support PLE, but that *Schinus molle* trees and *Myrica pavonis* shrubs were actively selected as fuel and as tinder, respectively.

Aguirre (2020) compiled ethnographic data on 16 woody plant species available in the region of Antofagasta de la Sierra, Catamarca, Argentina. This study highlights the variability and richness of fuel resources in the area and the potential of diachronic and technological changes of fuel selection. Aguirre and Rodríguez (2013) conducted a combustion experiment in the same region. Based on bibliographic and ethnobotanical research, they evaluated eight woody plant species, building experimental hearths at a locality of 3600 masl, recording temperature and time as well as starting/resulting weight (wood/-charcoal), and performing subsequent anthracological analyses. They observed that combustion of the three "best" species (based on ethnography and experiment), *Parastrephia lucida, Ephedra breana* and *Fabiana bryoides*, results in a relatively minor anthracological signal in the experimental setting, as well as in local archaeological sites.

Rodríguez et al. (2022) aimed to understand combustion practices at the Late Holocene Punta de la Peña 9 site by applying the results from Aguirre and Rodríguez (2013) and not only identifying 13 species that were used, but also calculating how much fuel was needed to create the combustion structure, taking the interpretation beyond fuel selection towards fire management practices.

Another case study from Antofagasta de la Sierra comes from Escola et al. (2013). They conducted anthracological studies at the Late Holocene archaeological site Alero sin Cabeza, using previous experimental anthracology studies by Rodríguez (1999, 2000, 2004a, 2004b) and Aguirre (2007, 2012). They identified local plant taxa, conducted sampling for anthracological analyses during the excavation (noting the lack of preserved combustion structures and hearth features), and identified the charcoal from the site. They carefully evaluated the combustion qualities and benefits of identified taxa against the presence in their samples, taking into account considerations from OFT and PLE. Further, they interpreted their results regarding seasonality and resource pressure through (over)use, which impacts fuel selection.

Among others, Joly (2008) conducted an experiment with three plant species, *Adesmia* spp., *Fabiana densa*, and *Parastrephia lepidophylla*, local to the Puna de Jujuy, Argentina. They evaluated the fuel quality regarding temperature and especially burn duration in relation to amount of invested fuel. *Adesmia* spp. and *Parastrephia* sp. showed better characteristics than *Fabiana densa*. Joly et al. (2009) combined ethnographic and archaeological study in the same region. They analyzed the anthracological record of Hornillos 2, an Early to Late Holocene archaeological site at 4020 masl. Ethnographic information on fuel was obtained from families in the village of Susques, resulting in a list of 19 plant species that were rated for combustion quality. Ethnographically, *Parastrephia* spp. was the preferred fuel. The anthracological analysis of archaeological charcoal from Hornillos 2 showed that *Parastrephia* spp and *Baccharis* spp. are the predominant taxa, with some other taxa like *Adesmia* sp. and *Fabiana* spp. also represented. They noted some diachronic changes as well as variation between different areas in which fuels were selected. However, *Parastrephia* spp. is represented consistently in the archaeological record and mentioned most frequently in the ethnographic record, highlighting its role as local fuel.

Caruso Fermé and Théry-Parisot (2011) conducted a combustion experiment with woody plant species local to the Patagonian Andean Forest, recording maximum temperature, combustion duration, flame duration, and amount of residues, with special focus on charcoal characteristics. Caruso Fermé (2012), Caruso Fermé and Théry-Parisot (2020), and Caruso Fermé and Civalero (2019) conducted various anthracological studies in Patagonia, Argentina, at the archaeological sites of Cerro Pintado, Paredón Lanfré, Orejas de Burro, Cerro Casa de Piedra 5, and Cerro Casa de Piedra 7. They studied the locally available plant fuels and compared them against the taxa represented in the archaeological records, and they also approached the question of fuel acquisition and transport.

These previous studies highlight the importance of identifying and testing local fuel resources around archaeological sites. A thorough understanding of resource diversity and richness in the study area requires field observations, ethnographic information, or both. Further, as the combustion of various fuels may result in different residue classes and preservation may affect residues differentially, various analytical methods can provide multi-level insights into site combustion behaviors. While most previous studies have focused on the anthracological record, the archaeological deposits at Cuncaicha and some sites in Argentina (Aguirre and Rodríguez, 2013) may require different approaches due to the relatively small amount of charcoal. Finally, interpretations of these analyses may benefit from either PLE or OFT, as both concepts point to optimal solutions.

1.6. Fuel selection for the combustion experiment

To understand fuel selection at Cuncaicha, we must evaluate resource availability, diversity, and richness in the Pucuncho Basin. Besides woody plant species, other potential types of fuel in the dry puna include dung, animal bones, and *Distichia muscoides* peat in bofedales. After reviewing the different fuel types and ethnographic and archaeological literature reporting their use for combustion, we will discuss our selection of three fuel types for our experiment.

1.6.1. Plants

The local dry puna habitat surrounding Cuncaicha contains many potential plant fuel sources, including *Stipa ichu* grasses, numerous small herbs and forbs, woody *Parastrephia* spp., *Tetraglochin cristata*, and *Baccharis* spp. shrubs, low-growing *Opuntia* spp. cacti, and cushion plants such as *Azorella compacta* and *Distichia muscoides* in respective terrestrial and wetland moor habitats. Occurring below 4200 masl, some 30 km southwest of Cuncaicha, are the only trees on the high-elevation plateau – small groves of *Polylepis rugulosa* trees.

Use of queñua wood is reported for the Awatimarka village inhabitants in Moquegua, southeast of our study area (Kuznar, 1995). *Polylepis* spp. was also used at Chinchero, an agricultural community located near Cuzco between 3000 and 5000 masl (Franquemont et al., 1990). At Panaulauca and Pachamachay, Pearsall (1980, 1988) identified Umbelliferae seeds in Late Holocene levels containing ceramics and hypothesized the use of yareta for on-site firing of pottery. *Azorella compacta* does not grow in the Junín department, where both Pachamachay and Panaulauca are located. In this case, the common name yareta is referring to the local *Azorella diapensiodes*, a low polster, mat forming plant.

While grasses have been suggested as a potential fuel in other locations (Lavallée et al., 1995; Pearsall, 1988), ichu is not considered for this study because it is not likely to be the most efficient fuel for the region. Furthermore, the presence of ash oxalate pseudomorphs in the Cuncaicha sediments does not suggest grassy species, but rather hints at the use of woody plant species.

1.6.2. Dung

Dung has been proposed as an important fuel in settings lacking trees, such as cold steppe and tundra environments (Rhode et al., 2003). In the Andes small dung pellets from wild and domesticated camelids could constitute a potential fuel source (Pearsall, 1980, 1988). Ethnographic studies of indigenous Andeans have contributed insights into the traditional use of plants as combustive fuel. Winterhalder et al. (1974) studied the Nuñoa pastoralist community in the department of Puno.

Despite the presence of *Polylepis* groves as high as 4250 masl near Nuñoa and the acknowledgment that the wood provided a good fire, most inhabitants preferred to use readily available cattle or llama dung because of the greater effort required to access the limited groves of *Polylepis*, far from households. Formal comparison of energetic efficiency among the possible fuels indicated a higher heat value (kcal/kg of fuel) for queñua wood relative to sheep, cattle, and llama dung. However, when dung was gathered from corrals adjacent to houses, a low collection cost (in kcal/kg) resulted in a higher energetic efficiency (kcal heat obtained/kcal energy expended in gathering) of dung relative to queñua wood.

Use of camelid dung as fuel was reported in Paratía in Puno (Flores Ochoa, 1968), Hualcán in Cuzco (Stein, 1961), and Awatimarka in Moquegua (Kuznar, 1995). At Chinchero, the inhabitants relied on guinea pig droppings as the primary traditional cooking fuel, along with *Polylepis* spp. (Franquemont et al., 1990). Local herders near Cuncaicha do not use dung as a primary fuel source. Furthermore, if dung pellets were used as fuel, we would expect burned dung pellets to be a notable component in the archaeobotanical record of the site, as described by Pearsall (1980, 1988) for Pachamachay and Panaulauca. However, we do not observe burned dung pellets in the archaeological deposit at Cuncaicha. Hence, we did not select dung for our experimental combustion.

1.6.3. Bone

Evidence for bone fuel comes from various regions, often where plant fuel is limited due to cold temperatures (Buonasera et al., 2019; Miller, 2015) such as Arctic environments (Vanlandeghem et al., 2020; Villagran et al., 2013). Various studies show that using bone as a fuel additive has a positive effect on the burn duration and fuel consumption (Mentzer, 2009; Théry-Parisot et al., 2005; Costamagno et al., 2005; Théry-Parisot, 2002b). From the broader study area for example, Joly (2008) and Joly (2009) mention the presence of burned bones. Today, bones are not used as fuel in the study area. However, bones burned to varying degrees are common in the Terminal Pleistocene and later deposits of Cuncaicha and in other early archaeological sites of the Andean puna, such as Hakenasa in northern Chile (LeFebvre (2004).

1.6.4. Peat

Pearsall (1988) suggests the use of *Distichia muscoides* polsters for combustion in the Late Holocene. Further, Flannery (1989) reports that at five puna communities located between 4200 and 4500 masl in Ayacucho, herders cut and dried blocks of *Distichia muscoides* peat to use as fuel. There are no documented instances of peat used for fuel in our study region, nor evidence from the deposits of Cuncaicha.

1.6.5. The chosen fuels

After reviewing the available local fuel resources, ethnographic literature, observations of local pastoralists (Fig. S1), personal experience camping on the plateau and making campfires, and previous macrobotanical and geoarchaeological insights, we selected the three most likely plateau fuels for our experiment: local *Azorella compacta* cushion plants (yareta), local woody *Parastrephia* spp. shrubs (tola), and non-local *Polylepis rugulosa* tree branches (queñua).

Queñua is found in all puna ecozones, between 9° and 32°S and can grow above 3500 masl (Gareca et al., 2010). In Peru, queñua trees are especially found in the ecosystem of the high Andean relic forest though they may also occur in the grasslands of the wet puna (*i.e., pajonal de puna húmeda*) (Ministerio del Ambiente, 2015, 2018). It is an evergreen tree species that grows along rocky slopes and streams (see Fig. 2). Based on extensive botanical survey of the Peruvian highlands, Mendoza and Cano (2011) documented three *Polylepis* species in the department of Arequipa (where the study area is located), with an upper elevation limit of 4600 masl. However, locally, Kuentz et al. (2007) identified pollen of *Polylepis rugulosa* only up to 4250 masl west of Nevado Coropuna. This upper elevation limit is consistent with large-scale paleoecological studies by Gosling et al. (2009) and with our field observations of the highest *Polylepis* groves at ~4250 masl in the study region. *Polylepis* is used for fuel due to its high resin content that allows it to burn easily under wet-season conditions (MacBride, 1936:29), but medicinal uses also have been reported (Bussmann et al., 2016; Ardiles et al., 2018).

Tola is a resinous shrub that can grow up to 2 m high. In Peru it is typical for the ecosystems of the Andean scrublands (*i.e., matorral andino*) and the grasslands of the dry puna (*i.e., pajonal de puna seca*), though it can also occur in the high Andean relic forest (Ministerio Ministerio del Ambiente, 2015; Ministerio del Ambiente, 2018) (see Fig. 2). It is used for fuel due to its high resin content that allows it to burn easily under wet season conditions (MacBride, 1936:29), but also medicinal uses have been reported (Bussmann et al., 2016; Ardiles et al., 2018).

Yareta is documented in the dry and salt puna ecoregions and can grow at elevations between 3800 and 5200 masl. In Peru, it is not only typical for the dry puna but is also found in the periglacial zone (*i.e., zona periglaciar*) (Pugnaire et al., 2020; Ministerio del Ambiente, 2015, 2018). Yareta is a slow-growing cushion plant that grows on north slopes in arid and cold climates in volcanic landscapes and can reach thousands of years of age[2] (Pugnaire et al., 2020; Kleier et al., 2015; Kleier and Rundel, 2004; Ralph, 1978). The cushion itself is made up of a central root system with a resinous parachute-like branch system of stems and leaves forming a hard canopy that can grow extensively, up to 20 m, where size classes depend on the elevation (Pugnaire et al., 2020; Kleier et al., 2015) (see also Fig. 2). Use of yareta as fuel has been reported, but it is also used for its medicinal properties (Hodge, 1946, 1960).

How comparable is today's vegetation distribution relative to the Terminal Pleistocene and Early Holocene? Lake and wetland sediment cores from the dry puna of northern Chile and southern Peru, including a site just 30 km southwest of Cuncaicha, contain *Apiaceae* (*Azorella*), *Asteraceae* (including shrubs *Parastrephia, Baccharis, Chuquiraga, Senecio*) and Rosaceae (*Polylepis*) pollen throughout their sequences, to >13,000 years ago (Baied and Wheeler, 1993; Kuentz et al., 2012). A synthesis of pollen and charcoal records from Ecuador and Peru indicates that patchy *Polylepis* woodlands have been distributed in the Andes from 2° to 18° S over at least the past 20,000 years (Valencia et al., 2018). Longer pollen records from the Huiñaimarca sub-basin of Lake Titicaca contain *Apiaceae* pollen (*Azorella*) over at least the past 60,000 years (Gosling et al., 2009). *Apiaceae*, *Asteraceae*, and *Polylepis* were all present 136,000 years ago (Marine Oxygen Isotope Stage 5e) in a Lake Titicaca core (Hanselman et al., 2005). All three of these plant types have likely been present in the Andean puna throughout the Quaternary. Yet, the occurrence of *Polylepis* trees and *Azorella compacta* cushion plants may have been reduced or eliminated in some areas of the Andes due to overharvesting in the Late Holocene (Gosling et al., 2009).

2. Methods

2.1. Fuel collection and experiment setup

On January 19th, 2022, we collected queñua, yareta and tola from three distinct locations on the plateau (Fig. 2). To compare the time invested collecting and quantity gathered among the three fuel types, we standardized the estimated volume of fuel per person-hour of gathering time.

For all three fuels, we collected only dead vegetation from the ground and only what was needed for the experiment. We selected the driest material possible, though some of the queñua and especially the

[2] Therefore, considering the age of the plants and that only dead parts of the plants are suitable as fuel, we should be aware of a potential old-wood effect if carbonized yareta was used to date an archaeological site, though Harpel et al. (2021) also highlight the potential of dating yareta and using it as a geochronological resource.

yareta were somewhat damp from recent rain and snow. However, early wet-season conditions did not greatly impact the ignition or maintenance of the fires. We transported the fuels to the experiment site on the north terrace of Quebrada Cuncaicha, a perennial stream ~300 m north of Cuncaicha rock shelter.

Currently the nearest *Polylepis* groves are found on the plateau ~30 km southwest of Cuncaicha. At a grove along the Chuquibamba-Cotahuasi highway, we collected dead branches from the ground in a 75-m radius around the field vehicle for ~15 min each or 45 person-minutes. Queñua branches and twigs of 5–10 cm diameter are lightweight, with papery, exfoliating bark and few leaves. This collection yielded approximately 0.33 m^3 of fuel.

Azorella compacta is widespread on the high-elevation volcanic plateau between the Majes and Ocoña rivers. These plants are especially numerous covering the Barroso Formation andesite lava flows that form the hillslopes surrounding the Pucuncho Basin, including the landform containing Cuncaicha rock shelter. One person collected dead cushions of yareta from the hillside just east of Cuncaicha shelter for ~20 min. Dead, gray-brown portions of the yareta mounds are easily identified relative to the vibrant green living cushions. The driest blocks are harvested from cushions growing against large rocks, and the dead cushions are easily dislodged from the substrate or from the living portion of the plant. Collection involves harvesting relatively few but large fragments, each of which can be split into multiple, smaller cone-shaped portions. Blocks composing a volume of ca. 0.25 m^3 were carried back to the experiment site.

Parastrephia spp. shrubs are widespread in the Pucuncho Basin and especially abundant along river terraces. Dead tola branches and roots are easily recognized by a white-gray color relative to the living brown stems and branches. Two people collected dried tola from the terrace adjacent to the experiment site for ~45 min. Collection involves harvesting small, twisted fragments of dead tola from many different plants. During the experiment, we ran out of fuel, and two people collected additional tola branches for ~15 min. We collected an estimated total volume of approximately 0.2 m^3.

Because burned bones are one of the main indicators of anthropogenic fire at Cuncaicha, we chose to add fresh bones to our experimental fires to produce residues. For bone material we collected a llama (*Lama glama*) carcass along the road on the west side of the Pucuncho Basin. This sample was relatively fresh, with green bone and some dried soft tissue and fur preserved. We selected a tibia and a femur. A second camelid carcass was collected approximately 25 m upstream from the experiment site. It was of similar state as the first specimen, but with less soft tissue. The last bone sample included two single dried and sun-bleached bones, a humerus and a radius, collected within 20 m of the experiment site. We dismembered the carcasses by hand to add limb bones to the fires during combustion.

In the Pucuncho Basin prevailing afternoon winds are from the west. We constructed a north-south rock wall to act as a windbreak and built the fires on the east, leeward side of the wall. West-east stone partitions separated the fires (Fig. 3). Queñua and tola fires were built against the rock windshield using a lean-to or pyramid construction. Following the

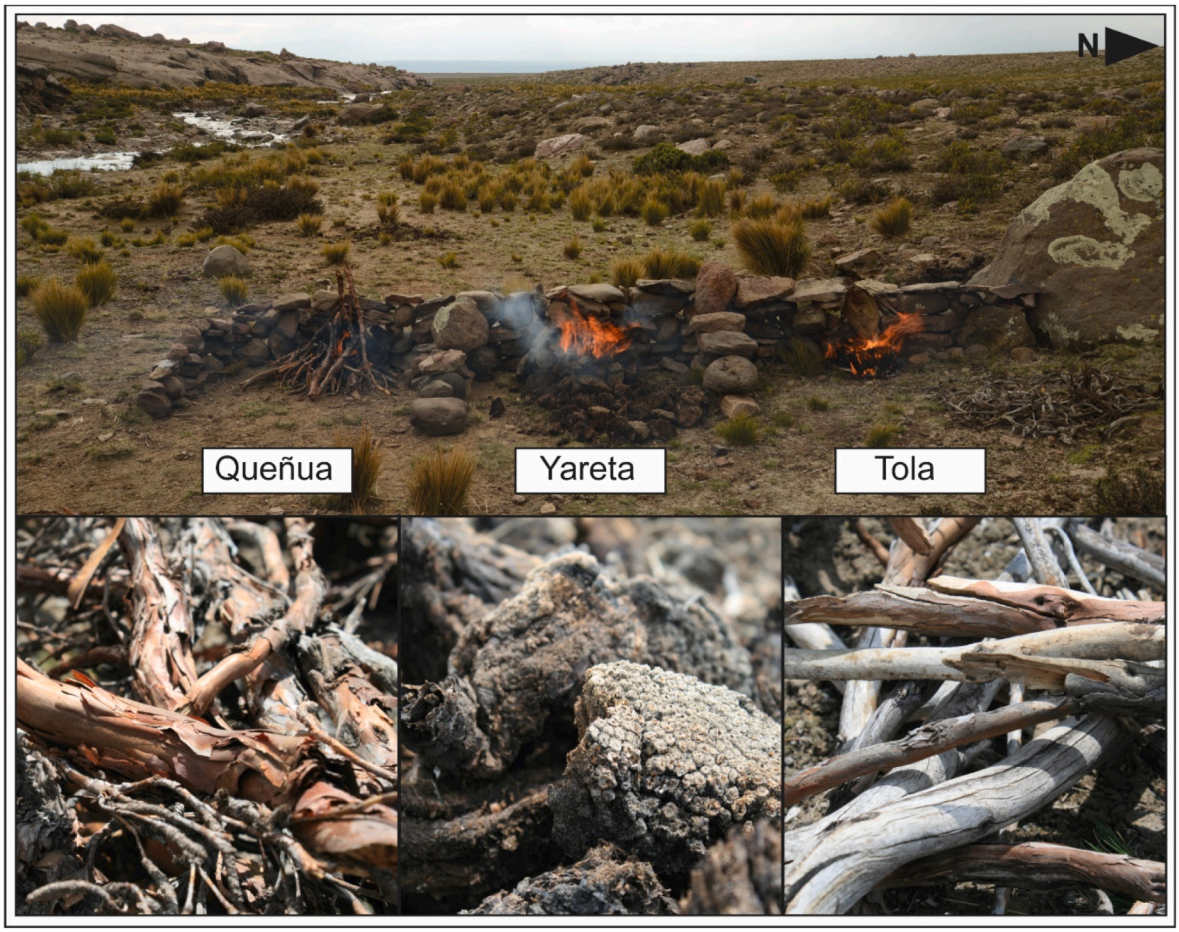

Fig. 3. Gathered fuel and set-up of experimental fires. Top: A rock dry wall was built as a windbreak with dividers between the three different fires adjacent to the riverbed of the Cuncaicha stream. Fires, left to right: queñua, yareta, tola. Bottom: Close-up photographs of the three fuels (Left to right: queñua, yareta, tola). Note the characteristics of each fuel: Queñua has long branches that are covered in paper-like, thin sheets of bark. Yareta fuel pile is comprised of dead chunks of the densely packed stems of the compact cushion mounds. Tola has short, woody branches that stem from the bottom part of the plant.

method used by local herders, the yareta fire was constructed as a beehive-shaped chamber using ~25 cone-shaped pieces of 10–20 cm, with the pointed ends of the cones toward the center. This structure effectively places the smallest, driest, and most resinous interior portions of the cushions near the central ignition point. The outer portions of the cushions can then progressively release water vapor during the burn. The fires were ignited sequentially in 10-min intervals to keep environmental conditions consistent among burns. Fires were started in sequential order from south to north, beginning with queñua (1), then yareta (2), and finally, tola (3). Ignition for all three fires used a small wad of dry paper and a match, then small twigs of tola for kindling. The queñua and tola fires required only a single ignition.

2.2. Combustion and temperature measurement

Throughout the experimental burn, temperature measurements for each fire were taken at regular intervals using an Omega® OS768-LS non-contact infrared thermometer (100°C–1800 °C range, accuracy ±2% of measured value) with a standard emissivity setting of 0.95. We did not use the thermocouple extension due to the difficult field situation and setup. Potential device measurement biases are equal for all three fires. Temperature readings were collected by holding the pyrometer approximately 50 cm from the fire and aiming the device between the base and center of the fire for 15 s until consistent readings were returned. Minimum, maximum, and average temperatures were recorded.

The first measurement for each fire was taken approximately 5 min after the fire was started. We then collected recurrent measurements on each fire every 10 min for the duration of the burn. Throughout the experiment, we maintained each fire at its original size by adding fresh fuel or modifying the fire structure to encourage the complete consumption of all fuel. Fires were sustained for approximately 90 min, after which fires were allowed to burn out. Two final temperature measurements on each fire were taken: (1) 5 min after the flames extinguished, and (2) 30 min following the final-flame measurement.

Although we used the added bone to provide a secondary temperature estimate (Ellingham et al., 2015; Stiner et al., 1995), and to create a reference collection, bones are also another potential fuel source, and their addition impacts the burning process (*e.g.,* Mentzer, 2009; Théry-Parisot et al., 2005). Therefore, we kept bone additions similar in all three fires. We added one sun-bleached and three freshly disarticulated camelid long bones to the coals in each fire approximately 30 min after ignition, when fires were well established. These bones were repositioned within the coals only during fire maintenance, and left within the coals to cool overnight.

2.3. Residue collection

The day following combustion, we returned to the experiment site and collected the different fire residues (charcoal, bones, and ashes) for further analyses. Both the queñua and tola fires were cold, but the yareta fire had retained hot coals, about 20 h after the final temperature measurements were taken the previous day. We raked out the fire contents to allow the remaining materials to cool before collection. We separated ashes and charcoal to estimate the relative amounts produced by the different fires. Ash samples, representative charcoal pieces, and all bone pieces were collected from all three fires. Every bone fragment (Figs. S2a–c) was macroscopically examined to provide a rough estimate of burning temperature and calcination stage, according to Stiner et al. (1995) and Ellingham et al. (2015).

2.4. Laboratory: Ash smear slides

The ash samples were transferred to the Geoarchaeology Laboratory of the Geoarchaeology Working Group at the Institute for Archaeological Sciences, Department of Geosciences at the University of Tübingen. A small amount of the samples was processed into smear slides. For smear slide production, 2–4 drops of Entellan® were placed on a slide using a glass pipette before adding 1–2 mg of sample with a scoop. The sample was dispersed with the Entellan® and then covered with a cover slide. After drying, the slides were analyzed using a Zeiss Axiometer petrographic microscope using 10x, 20x, and 40x magnification under plane-polarized and crossed-polarized light. Two slides were produced of each fire sample.

3. Results

3.1. Gathering time for fuels

Gathering yareta for one person-hour will result in the largest fuel volume (0.75 m^3), followed by queñua (0.44 m^3), and tola (0.20 m^3). These are rough estimates, but they allow us to rank the three fuels in terms of their gathering time, which we compare to fuel performance evaluated experimentally in the next section. The gathering time estimates do not include any time of transport that would be involved in transferring *Polylepis* wood from distant groves to Cuncaicha. Transport time for yareta and tola to the experiment site is negligible.

3.2. Temperature and duration of fires

We compare the combustion process among the fuels using a series of temperature measurements (Fig. 4, Table S2). The queñua and tola fires reached temperatures of over 700 °C 10 min after starting the fires. Yareta did not produce a temperature of over 700 °C until 20 min after ignition. This is explained by the dampness of the fuel, as the fire faltered and had to be restarted approximately 10 min after the original ignition.

Temperatures over 800 °C were measured after 40 min in the yareta fire and after 60 min in the queñua and tola fires. The maximum temperatures measured in the yareta fire were 895.2 °C and 887.6 °C, recorded after 80 and 90 min, respectively. The tola fire reached a similar temperature (882.3 °C) after 70 min. The queñua fire reached its maximum temperature of 853.1 °C at the 60-min mark.

While actively fed, all fires maintained temperatures between 650 °C and 900 °C. Declines in temperature were recorded directly after fuel additions, followed by increases in temperature. The yareta fire maintained the most consistent temperature throughout the burn.

Ninety minutes after ignition, we stopped adding fuel to the fires. Temperature measurements were 843.0 °C in the queñua fire, 887.6 °C in the yareta fire, and 857.3 °C in the tola fire. The most distinctive differences among the taxa were observed after the cessation of fuel addition.

For queñua, the open flame extinguished 20 min after we stopped adding fuel, at which time we recorded 802.6 °C. Five minutes later we opened the fire and took a measurement of 631.9 °C on exposed coals. Thirty minutes later we took the final queñua fire measurement of 443.5 °C, a decrease of 188° (30%) from fuel cessation.

Following the 90-min mark the yareta fire maintained flames for another 70 min. During this period, the temperature fluctuated between ca. 670 °C and 800 °C. We took a measurement of 673.9 °C just before the open flames extinguished completely. Five minutes after the final flames we measured 611.3 °C on open coals. We recorded a final temperature measurement of 521.1 °C 30 min later. Yareta presented the smallest temperature decrease (90 °C, or 15%) among the fuels for this time interval.

In the tola fire, the open flame disappeared almost immediately after fuel cessation. We exposed the coals and took a temperature measurement of 713.9 °C 5 min after flames disappeared. Thirty minutes later we took the final measurement of 523.1 °C. Tola presented the most rapid temperature decrease (191 °C, or 27%) in just 30 min, as shown in Fig. 4.

We returned to the experiment site 20 h later. The yareta fire residues were still smoldering with hot live coals. The other two fires were extinguished but slightly warm to the touch.

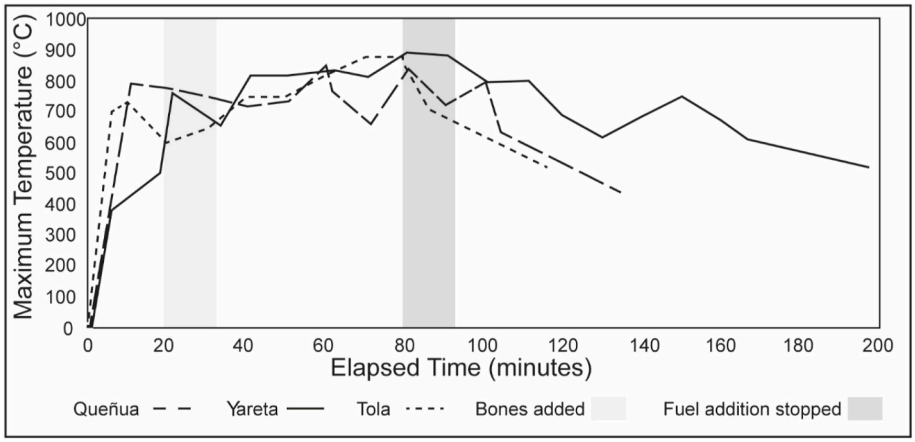

Fig. 4. Graph showing burning time-temperature curves of the three fires with times of bone addition and cessation of fuel addition indicated.

3.3. Analysis of fire residues

Burned bone, charcoal, and ashes were the main fire residues observed and sampled. The state of the bones yields information pertaining to burn temperatures. Charred organic matter and ashes on the other hand are directly linked to the fuel type and the combustion characteristics.

3.3.1. Burned bones

Macroscopically, the bones added to the fires all appear similar and were fragmented through the combustion process (Fig. 5, Figs. S2a–c). Fig. 5 shows the fires at the stage where bones were added, the unburned bones, as well as a bone example for each burning state. Because of fire maintenance, the fragments within each fire were mixed. Some fragmentation and the resulting difference in the number of bone pieces between fires must be attributed to breakage post-recovery due to transport. The burned bones from the three fires all exhibit similar burning and calcination stages. This is fully consistent with the >700 °C temperatures measured on all three fires.

3.3.2. Carbonized organic matter

The carbonized organic matter constitutes the remains of incomplete combustion. The three fuels exhibit large differences in the amount produced through the combustion of the fuels, shown in Fig. 6. Of the three fires, queñua produced by far the largest amount of charcoal, mostly elongated wood chunks, indicating incomplete combustion. This residue is consistent with the rapid decrease in temperature we observed after we stopped adding fuel. The yareta fire left behind the least charred organic matter of the three fuels. The few charred pieces were either very fragile fragments of the compacted top of the branches of the cushion plant (Fig. 6, top) or more woody pieces from the lower, twisted stem part of the cushion (Fig. 6, bottom). The extremely sparse charcoal that we encountered after burning the yareta indicates almost complete combustion of this fuel. Burning tola produced many pieces of carbonized organic matter. The carbonized pieces mostly consist of either twisted or elongated pieces of wood charcoal.

3.3.3. Ashes

The ash constitutes the remains of complete combustion and therefore loss of (almost) all organic matter. In general, the ashes contain a mix of components that, besides some leftover organic tissue and charcoal, may include siliceous aggregates, phytoliths, starch, amorphous sintered ashes, and ash oxalate pseudomorphs (*i.e.,* woody-plant derived ashes or calcium carbonate polycrystals) (Martinez Dyrzo and Mentzer, in prep; Canti, 2003). Out of these components, phytoliths and pseudomorphs are the most distinctive, though not identifiable to species level. In fact, ashes produced by the three fuels do exhibit differences which become apparent under the microscope, shown in Figs. 7–9.

Ash production is a process of recrystallization of different minerals (mainly calcium oxalates [whewellite/weddellite] - calcium oxide - calcium carbonate) included in the plant material (Canti and Brochier, 2017; Canti, 2003). The recrystallization process is influenced by time. As we are looking at very fresh, experimentally produced ashes that were analyzed within a month of combustion and not exposed to fresh air for long, recarbonization with atmospheric CO_2 is not always completed (Canti and Brochier, 2017). That means, in all three samples, we are observing some original oxalate crystals (*e.g.,* by exposure to low temperatures only), some micritic (*i.e.,* microcrystalline calcium carbonate) polycrystals that directly recrystallized into calcium carbonates and hold the shape the original oxalates (*i.e.,* ash oxalate pseudomorphs), and some mixed stages (mainly calcium oxide) in the process of recrystallization (Canti and Brochier, 2017; Canti, 2003). These different minerals are observable in the varying crystallinity, as well as in differences of the birefringence and interference colors with high birefringence in the original oxalates, and lower birefringence in the pseudomorphs. This might pose a difference to the comparison with archaeological material that had time to completely undergo recrystallization (and other, subsequent post-depositional processes), though the habit, shape, and general type of component are well comparable.

In describing the ashes, we will follow the description points from the "Woody-plant derived ashes grain mount database" (online soon) of the University of Tübingen, Institute for Archaeological Sciences, and the Senckenberg Center for Human Evolution and Paleoenvironment (Martinez Dyrzo and Mentzer, in prep).

Under the microscope we could identify a mix of different ash components, with two distinctive components of queñua ash (Fig. 7). The first is calcareous ash oxalate pseudomorphs that appear similar in size, depending on shape between 5 × 5 μm and 5 × 10 μm. They exhibit a cuboid or cubic ash habit. Some of the ash oxalate pseudomorphs are still articulated and visible as clusters in anatomical position. There are some clusters of random orientation. Some of the ash oxalate pseudomorphs seem to be calcium oxide, and are therefore not pseudomorphs *sensu stricto*, but rather appear to be the original calcium oxalates. Others have undergone recrystallization into micrite and are actual pseudomorphs. Some amorphous sintered ashes are also included in the queñua ash. The second distinctive feature in the queñua ash is phytoliths that are also often still articulated in anatomical connection. The phytoliths are mostly irregular, elongated, or blocky in shape. Some organic material is included, mostly as elongated fragment of charcoal, some amorphous organic tissue is also present.

The yareta ash also exhibits some distinctive characteristics (Fig. 8). Yareta burned almost completely down to ash. Some ashes were still holding the original shape of the cushion plant stems the next day (Fig. S3). This indicates that even after we abandoned the experiment

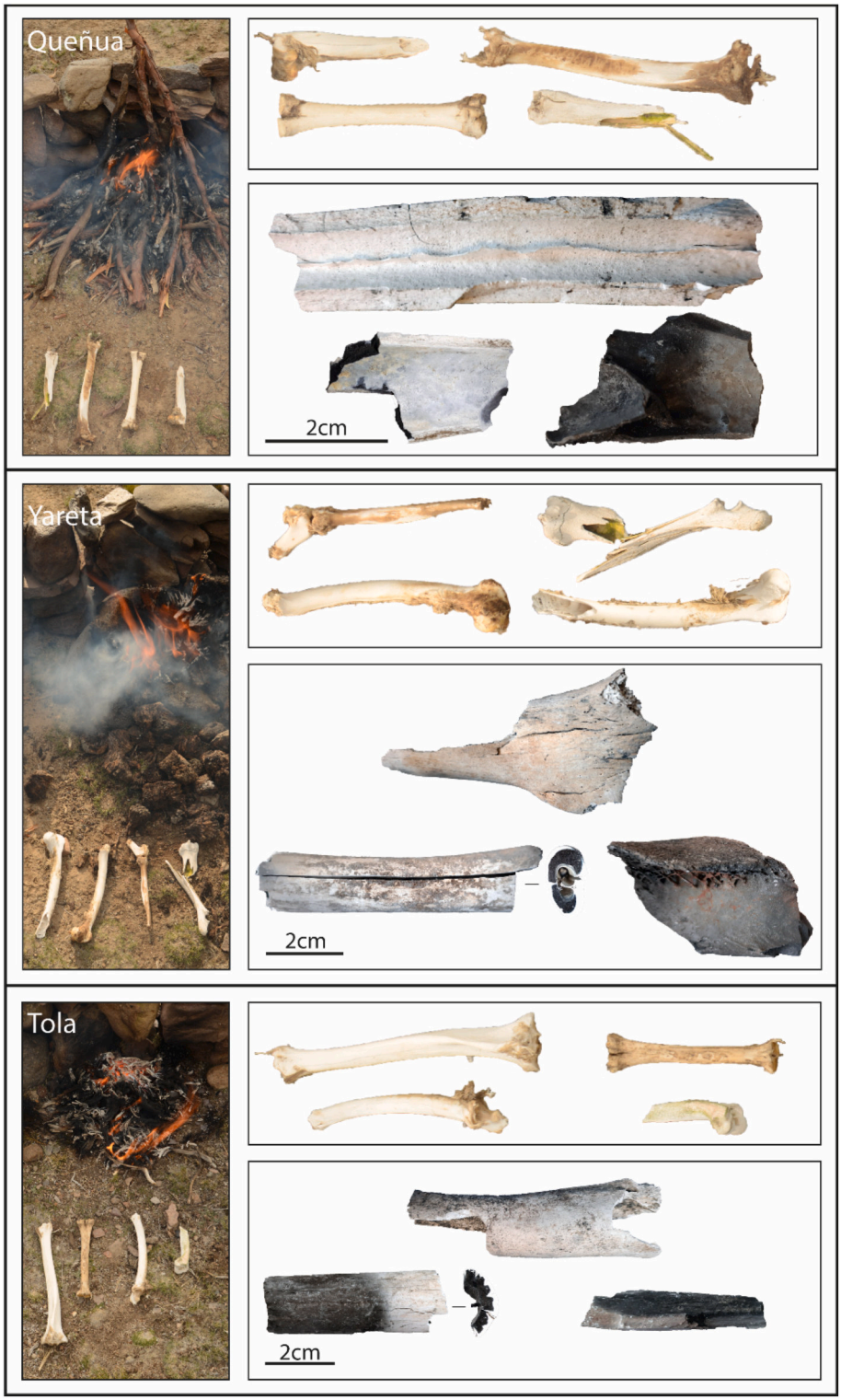

Fig. 5. Camelid bones added to the three fires. For each fuel: Left: Unburned bones in front of the respective fires. Three fresh bones and one dried and sun-bleached bone were added to each fire. Right top: Close-up of unburned bones. Right bottom: Close-up of one exemplary bone of each burning stage category (top: fully calcined, left bottom: partially calcined, right bottom: carbonized). Codes after Stiner et al. (1995, Table 3), temperature estimates after Ellingham et al. (2015, Table 2). For overview of all bone pieces recovered from the fires, see Figs. S2a–c.

site, the remaining fuel continued to combust. The ash composition of yareta is somewhat diverse, with different components. Under the microscope we saw that yareta ash, too, contains ash oxalate pseudomorphs. In contrast to the queñua pseudomorphs, yareta ash oxalate pseudomorphs are round or spherical and are micritic. The size of the pseudomorphs varies greatly in diameter (ca. 10–30 μm). There are also other spherulites that display an extinction cross and are not completely micritic. Some druse-like formations that appear rounded with an uneven rim and are bigger than the spherical oxalate pseudomorphs are present and either micritic or as oxalate. We observe little organic tissue and some amorphous sintered ashes. The amorphous sintered ashes sometimes display a range of typical brownish tones to slightly blueish hues in XPL. We did not encounter phytoliths.

The tola ash has a mixed composition with some calcareous formations, organic matter, single mineral grains, and some phytoliths (Fig. 9). Very few ash oxalate pseudomorphs were observed and they are not distinctive in shape. We encountered a calcareous cluster of pseudomorph-like micritic formations (340 × 180 mm) that held cell

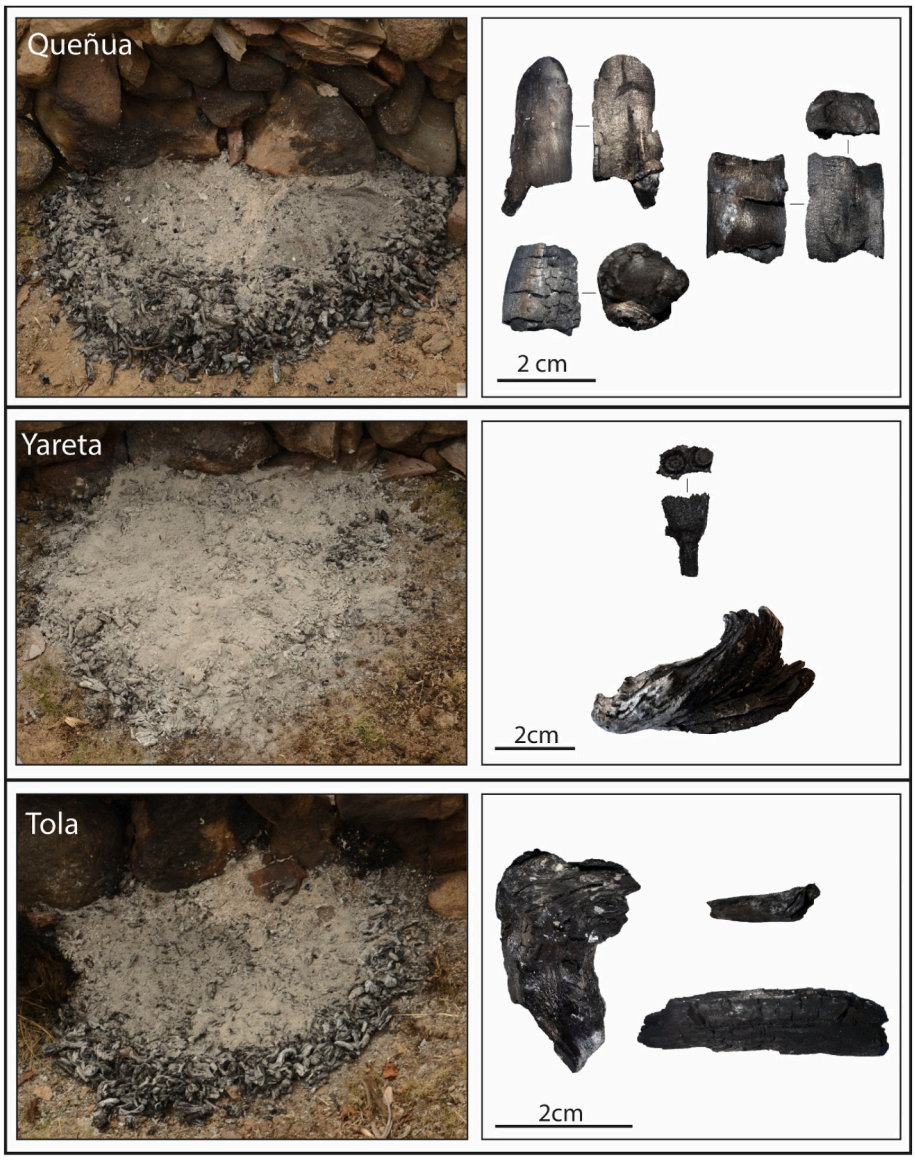

Fig. 6. Left: Fires after extinction with charcoal and ashes roughly separated by raking charcoal to the outside border of the fires. Note the relatively large amount and size of charcoal produced by the queñua fire, intermediate amount and size of charcoal produced in the tola fire, and relatively small amount and size of carbonized remains produced in the yareta fire. Right: Exemplary pieces of carbonized remains of each fuel.

skeleton position. The single pseudomorph habit is difficult to observe, it appears to be rather rhombic or cuboid (10 × 10 μm). In general, the tola ash samples are only moderately calcareous, though we observe frequent amorphous sintered ashes that display a brownish color. No large multi-cell phytolith clusters were encountered in the smear slides. Single cell phytoliths of varying shapes are observable in the tola ash. Some organic matter is still visible and mixed with the ash matrix. It is mostly fibrous charcoal or rather amorphous organic tissue.

4. Discussion

4.1. Evaluation of the experimental results

We will evaluate the different fuels regarding the aforementioned concepts, the Principle of Least Effort (PLE) and Optimal Foraging Theory (OFT). Fuel selection according to PLE would result in presence of immediately available, easy to collect fuel species. Prevalence of a specific fuel in favor of its efficiency and combustion qualities, would suggest fuel selection based on OFT.

4.1.1. Procurement effort

In terms of required gathering time, yareta is the most efficient fuel. A large volume of yareta can be harvested and processed quickly; further, transport costs are minimal because yareta is abundant in the immediate vicinity of the site. While tola shrubs are also close to Cuncaicha, they require a substantially greater time investment to gather because of the small size and dispersed distribution of the plant. As immediately available fuel resources, both yareta and tola could be gathered by any member of a co-residential group. In terms of procurement and transport costs, queñua requires the most investment. A large volume can be harvested quickly, but the closest extant groves are a ~60 km roundtrip walk from/to Cuncaicha. Therefore, gathering queñua would be much costlier with respect to time and energy than the local fuel alternatives.

It is unknown whether the ~4250 masl maximum elevation for *Polylepis* was the same in the Terminal Pleistocene and Early Holocene. If *Polylepis* groves had a more extensive distribution and occurred closer to the site, during the wetter Terminal Pleistocene, the transport cost for queñua wood could have been substantially lower. However, we assert it

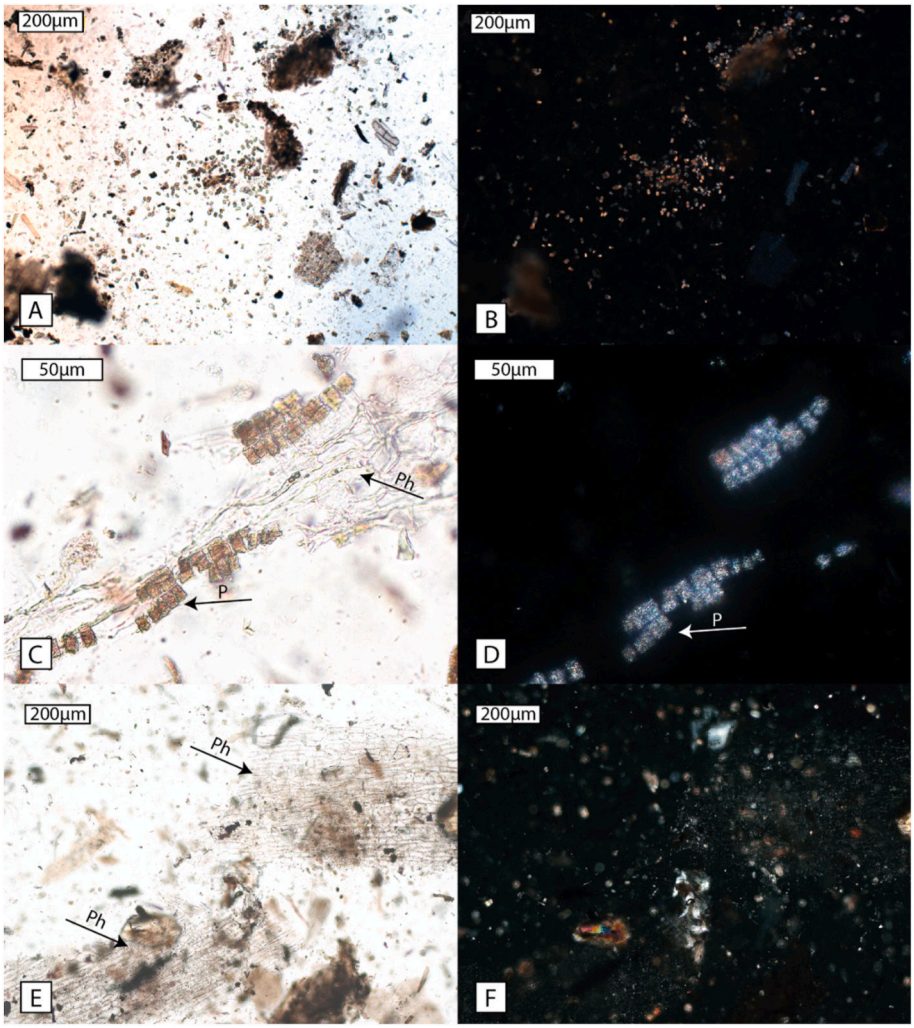

Fig. 7. Photomicrographs of queñua ash. A and B: Non-articulated, randomly oriented ash oxalate pseudomorphs after calcium oxalate crystals that are in varying stages of recrystallization in plane-polarized light (PPL) (A) and cross-polarized light (XPL) (B) displaying a cubic or cuboid habit. C and D: Close-up of cubic ash oxalate pseudomorphs [P] articulated aligned along the cell skeleton in PPL (C) and XPL (D). In PPL, articulated phytoliths [Ph] are visible, which become opaque in XPL. In XPL, the ash oxalate pseudomorphs are visible; here they do not seem to have undergone recrystallization into micrite but are closer to the original calcium oxalate crystals, as indicated by the high birefringence, first order interference colors, and larger crystal size. E and F: The phytoliths are irregular, mostly elongated, or blocky, and articulated along the cell skeleton [Ph]. They are visible in PPL (E) and invisible in XPL due to the silica composition (F).

was not used as a primary fuel source as experimental studies revealed queñua wood does not combust as completely as tola, and relatively small densities of queñua wood were recovered from the archaeological flotation.

4.1.2. Combustion quality

All fuels achieved temperatures exceeding 700 °C, so burning any of them in modest-sized fires could produce the fully calcined herbivore bone present in Cuncaicha's occupation components. The resinous tola and yareta (Hodge, 1946, 1960), reached slightly higher maximum temperatures (~900 °C) than queñua (max temp 853.1 °C). Increasing the fuel quantity and burn duration may have produced hotter temperatures. The goal of our experiment was not to find the maximum possible temperature, but the maximum temperature produced and sustained by a modest-sized campfire.

While we did not record fire temperatures continuously overnight, both queñua and tola last only a few hours. On the other hand, a relatively small yareta fire produced substantial heat and was still too hot to touch 20 h following the extinction of the flames. Once coals are established, a yareta fire will burn unattended for many hours. This fuel characteristic would provide clear benefits to foragers camping overnight and conducting various tasks around the camp during the daytime. Multiple authors report that dry yareta produces at least half the heat of an equal weight of bituminous coal (Perry Vega, 1946; Hodge, 1960; Marshall, 1971, p.276; Ralph, 1978; Wickens, 1995).

Given the ease of collection, high performance per yield, and proximity and abundance of yareta to Cuncaicha, we propose this taxon is the optimal choice for combustion out of the three fuels evaluated. According to PLE we would expect representation of yareta as well, together with tola. It is very likely that fuels were combined to produce fires. According to local practice and our own experience, a yareta beehive-shaped fire structure is best started with tola kindling and an even finer organic substance as tinder. We used paper, though ichu grass may have served this function in the past. While the experimental foraging and fire experiment data suggest which fuels would be optimally used for combustion at Cuncaicha, they do not tell us which fuels actually were used in the past. For this, we compare the experimentally produced fire residues to the archaeological remains from Cuncaicha.

4.2. Fuel at Cuncaicha – parallels between archaeological evidence and experimental results

4.2.1. Burned bones

Ethnoarchaeological studies show that common cooking practices do not visually alter or calcine bone, whereas repetitive burning of bones, for example by surface burning linked to site maintenance activities (Moore, 2016), can produce visual alterations and calcination (Moore et al., 2010). Looking at the use of bones as fuel, other studies (Stiner et al., 1995) indicate that bones directly introduced to fire as fuel will likely carbonize completely or calcine, whereas bone that was only subjected indirectly to fire will carbonize partially (see also Mentzer, 2009). In line with those observations, the bones added directly to the

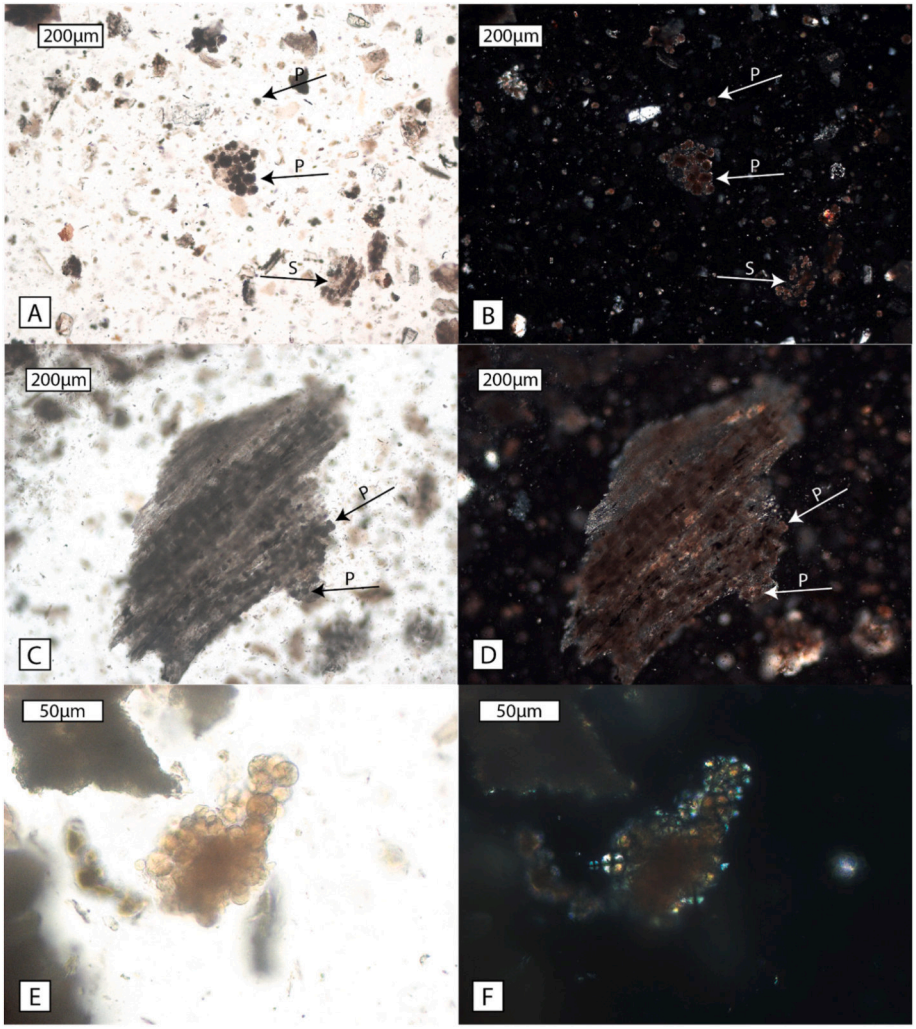

Fig. 8. Photomicrographs of yareta ash. Overall ash composition with distinctive round shaped ash oxalate pseudomorphs [P] in plane-polarized light (PPL) (A) and cross-polarized light (XPL) (B). Spherulitic aggregates [S] were also visible. C and D: Microcrystalline calcium carbonate ash oxalate pseudomorphs that are aligned along the cell skeleton in PPL (C) and XPL (D). Also here, the distinctive round shape of the single pseudomorphs is visible. E and F: Close-up of spherulites. In PPL (E) rounded shapes of varying sizes of a light brown color are visible. In XPL (F) a higher birefringence, and first order interference colors in combination with the typical extinction cross are visible.

experimental fires became fully carbonized or calcined. We can hypothesize that if bone was regularly used as fuel at Cuncaicha, we would predominantly encounter fully carbonized or calcined bone at the site. In a preliminary analysis of faunal remains of Cuncaicha, 4.4% of the Terminal Pleistocene bone fragments by weight are calcined, 11.4% are fully charred, 0.8% are partially charred or heat-altered, and 83.5% are not visibly thermally altered (Moore, 2016). Based on these observations, we conclude that bone was not the primary fuel source at Cuncaicha.

4.2.2. *Carbonized organic matter*

The most significant difference among the carbonized botanical remains from each experimental fire was the amount of the carbonized material. Queñua as well as tola produced relatively large amounts of wood charcoal fragments, whereas yareta left very few carbonized remains. Therefore, we would expect to find similarly larger quantities of queñua or tola charcoal if either was a primary fuel source. These observations are consistent with the archaeobotanical results based on sediment flotation, which yielded very few carbonized macroremains of wood or woody taxa in all occupation components (Table S1). Based on our experimental results, the small amounts of tola and queñua charcoal in the archaeological site sediments are inconsistent with use of either as a primary fuel. Tola macroremains are present in all early contexts, but they occur in such small amounts (<4 g per occupation component) that tola could not have served as the single primary combustion fuel. The extremely small amount of carbonized queñua macroremains (<0.2 g per occupation component) is consistent with a distant location of queñua groves from Cuncaicha and high transport cost making it a relatively less attractive fuel resource. The carbonized queñua macroremains that are present may be the result of inadvertent or purposeful burning of wooden tools or crafts.

4.2.3. *Ashes*

The ash oxalate pseudomorphs are the most distinctive ash components identifiable with the methods we applied. Ashes were previously identified in the archaeological strata in Cuncaicha, including the Terminal Pleistocene (Meinekat et al., 2021). The ash oxalate pseudomorphs in the Cuncaicha sediments exhibit a distinctive spherical shape (Fig. 10). Looking specifically at the Pleistocene sediments at Cuncaicha, we observe ash oxalate pseudomorphs as clusters of many, as well as single ash oxalate pseudomorphs. All of these pseudomorphs display a spherical habit. Because of the generally calcareous groundmass in the Pleistocene sediments, clusters of many pseudomorphs are easier to recognize than single pseudomorphs, though we also identified some single pseudomorphs in the calcareous groundmass (Fig. 10).

Out of the experimentally produced ashes, only ash oxalate pseudomorphs of yareta are similar in shape to the ash oxalate pseudomorphs in the archaeological sediments (Fig. 10). The combustion of queñua resulted in cubic and cuboid ash oxalate pseudomorphs dissimilar to those in the archaeological sediments. Although only a small sample of the Cuncaicha sediment has been analyzed, we would expect at least some cuboid ash oxalate pseudomorphs between the round

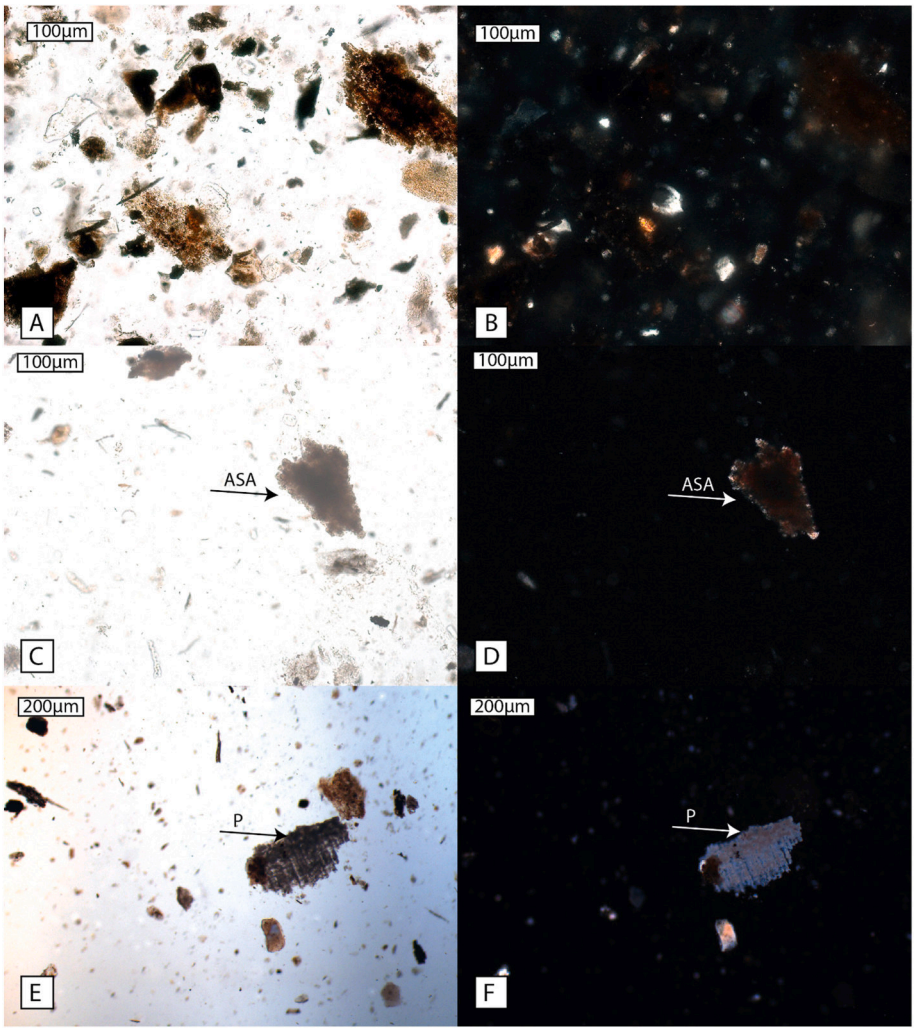

Fig. 9. A and B: Photomicrographs of tola ash. Overall ash composition in plane-polarized light (A) and cross-polarized light (B) with some amorphous organic material, elongated pieces of charcoal, and mineral grains. C and D: Photomicrographs in PPL (C) and XPL (D) that show amorphous sintered ashes [ASA]. E and F: Photomicrographs of micritic cluster of articulated pseudomorphs [P] in PPL (E) and XPL (F).

pseudomorphs if mainly queñua was used for combustion. The experimental tola ash is rather generic, with very few, non-spherical pseudomorphs. It is very possible that tola ash is present at Cuncaicha rock shelter, but given the absence of highly diagnostic morphologic features, tola is impossible to identify with present methods. Here, the above-mentioned archaeobotanical record gives insights.

Out of the three fuel sources that we evaluated, only the experimentally-produced yareta ash matches the morphology of the ashes in Cuncaicha sediments. However, this cannot be considered unequivocal evidence for the combustion of yareta at Cuncaicha. Ash oxalate pseudomorphs cannot be used independently to identify a fuel, as pseudomorphs are not taxon-specific. Previous attempts to link ash pseudomorph morphologies to specific fuel species in other regions have been unsuccessful (Aldeias, 2017; Canti and Brochier, 2017). An unpublished controlled combustion experiment in 2016 by the first author indicates that the ash oxalate pseudomorphs of *Opuntia* spp. cacti from adjacent to the site are similar to the round ash oxalate pseudomorphs identified in the Cuncaicha sediments (Fig. 10). However, *Opuntia* spp. is unlikely to have been used as fuel at Cuncaicha because of its poor combustion characteristics. Unlike some large cacti found at lower elevations, such as *Trichocereus* sp., that are known to make efficient fuel when dead and dried, the local *Opuntia* spp. is a non-woody cactus with small and juicy cladodes, growing close to the ground (Fig. 10).

4.3. Implications for early human settlement of the high Andes

Considering experimental and archaeological lines of evidence, the most parsimonious explanation for fuel use at Cuncaicha is that the Terminal Pleistocene and Early Holocene residents used locally available and highly combustible yareta as the main fuel to produce and maintain fires and tola as kindling.

These fires would have served multiple functions – for cooking, light, and warmth. Maintaining regular fires in Cuncaicha would have created a suitable micro-climate within the rock shelter, with the enclosing rock surfaces of the shelter retaining and radiating heat, providing a substantial advantage over alternative exposed, open-air locations. Regular fires in Cuncaicha would center social interactions among the group, concentrating activities within a protected and ultimately more comfortable setting.

The three tested plants' geographic ranges overlap in the Andean dry and salt puna ecoregions, and all three co-occur in the study area between 3800 and 4200 masl. Above 4200 both tola and yareta co-occur up to 4800 masl, with only yareta found up to 5200 masl (Kuentz et al., 2007). There is no area of the plateau containing archaeological sites, at least in the study region, where at least two of these combustible plant taxa are not available.

An important consideration for the Terminal Pleistocene habitation of the high-elevation puna is the availability of multiple fuels. Resource

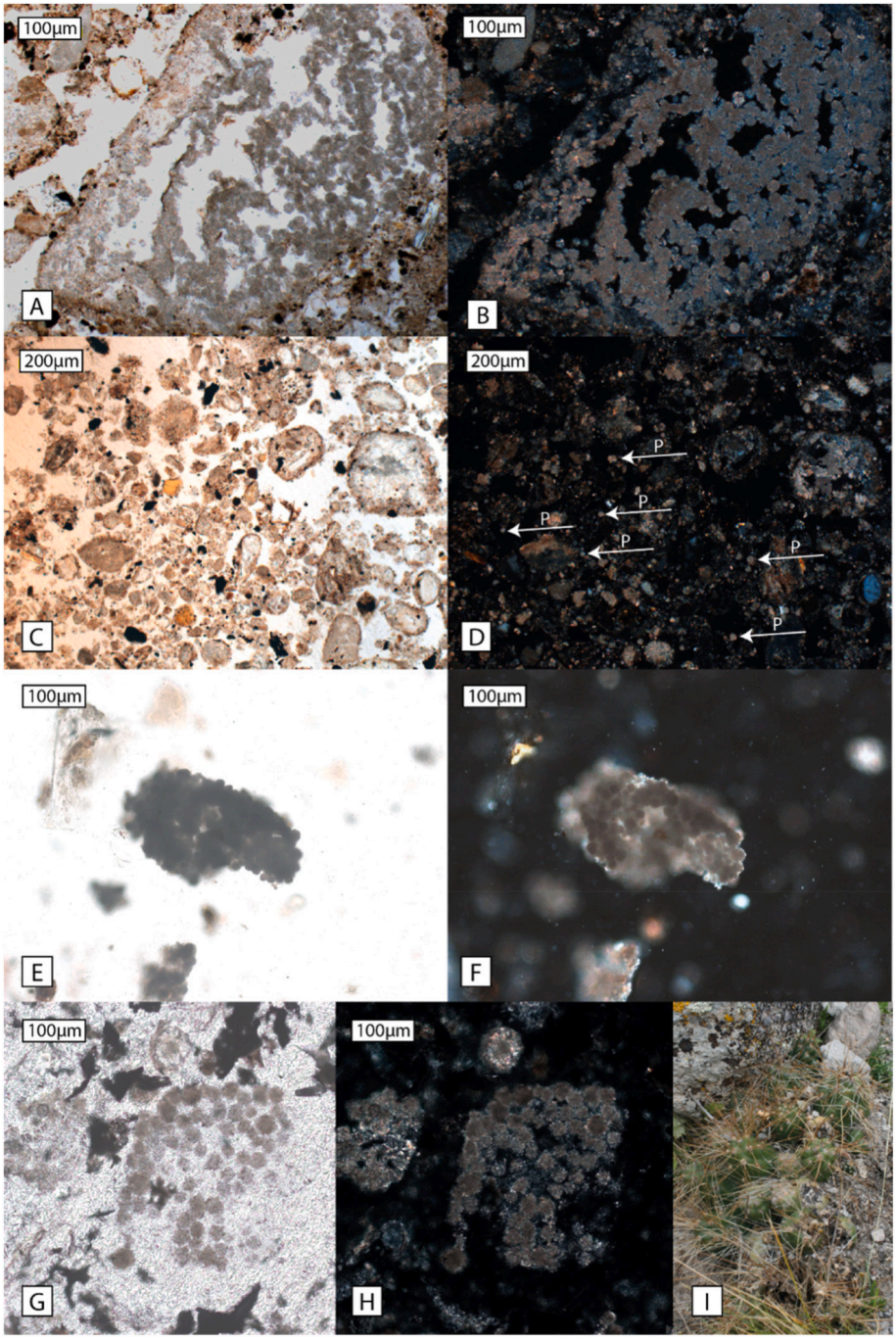

Fig. 10. A and B: Photomicrographs of ash oxalate pseudomorphs from the Terminal Pleistocene component at Cuncaicha rock shelter (sample CUN-12-09), with distinctive spherical habit, in PPL (A) and in XPL (B). C and D: Another example of spherical ash oxalates pseudomorphs from the Terminal Pleistocene components from Cuncaicha rock shelter (sample CUN-15-118) in PPL (C) and XPL (D) but here as single pseudomorphs [P] in the groundmass. For context information of samples CUN-12-09 and CUN-15-118 the reader is referred to Meinekat et al. (2021): Table 2 and Table S2. E and F: Spherical ash oxalate pseudomorphs in yareta ash from the present experiment in PPL (E) and XPL (F). G and H: Experimentally (unpublished experiment by first author, 2016) produced ash of *Opuntia* spp. in PPL (E) and XPL (F) that exhibits a spherical ash habit, too. (I) Photograph of *Opuntia* spp. growing close to the site.

diversity, abundance, and richness have important implications for landscape use. Even though based on the experiment yareta presents the most likely fuel used at Cuncaicha, there are suitable alternatives, such as tola and queñua, in the same ecoregion that could have been used for different purposes and depending on their availability. Though our experiment focused on three well-known plant species, the use of further notable alternatives (*e.g.,* dung, peat, ichu, bones) have been documented in the central Andes in later periods.

The range of *Azorella compacta* throughout the dry and salt puna ecoregions of southern Peru, western Bolivia, northern Chile, and northwest Argentina (Mathias and Constance, 1962; Martinez, 1993; Wickens, 1995) also contains the highest concentration of Terminal Pleistocene and Early Holocene archaeological sites in western South America (Fig. 1). Given this geographic correspondence, use of yareta as combustible fuel at other early Andean puna sites is expected and should be tested. Yet yareta has not been identified in any Andean puna site. Cuncaicha presents the most secure evidence to date for the early archaeological use of yareta as combustion fuel. Further paleoethnobotanical and geoarchaeological study of other early Andean sites should reveal whether use of yareta for combustion was part of a broadly applied adaptive strategy or presents a specialized behavior in the study area.

5. Conclusions

Archaeological evidence for fuel selection during the early occupation phases of the Andean puna is scarce, though the harvesting of woody material from locally available *Polylepis* spp. trees and

Parastrephia spp. shrubs has been suggested (Pearsall, 1980; Aschero and Podestá, 1986; Rodríguez et al., 2000; Pintar, 2008; Yacobaccio et al., 2014). Based solely on macrobotanical evidence from Cuncaicha rock shelter, it was unclear which fuels the first inhabitants used. To understand early combustion at Cuncaicha rock shelter, we identified possible fuels for evaluation in a formal combustion experiment and to generate residues for comparison with the archaeological sediments. All three fuels tested produced hot fires that can calcine bone and alter lithics. Yareta represents the optimal fuel based on local availability and abundance, high yield per foraging time, and high-performing combustion characteristics. When compared to the archaeological evidence at Cuncaicha, yareta ashes, with their distinctive round ash oxalate pseudomorphs, match the ashes in Terminal Pleistocene and Early Holocene sediments.

The experiment emphasizes the importance of multiple lines of evidence. If the interpretations of fuel use at Cuncaicha were based only on the anthracological record, yareta would go undetected because its complete combustion leaves no or almost no carbonized residues. This is the likely explanation for the absence of carbonized yareta remains in the sediments at Cuncaicha, despite an extensive program of fine screening and sediment flotation. In other Andean puna archaeological sites, yareta may act as a "ghost fuel," leaving behind material residues that have previously gone undetected by commonly employed archaeological recovery methods, including screening and water flotation to recover organic macroremains. A micro-contextual approach is probably required to detect the combustion products of yareta.

The suggested use of yareta as a primary fuel by the Terminal Pleistocene and Early Holocene occupants of Cuncaicha implies considerable knowledge about high Andean plant resources by 12.5–12.0 ka. Moreover, it bears noting that use of yareta as combustible fuel in the Terminal Pleistocene, as well as today, suggests that this resource has been used by Andean people for over 12,000 years. Availability of this key resource throughout the dry and salt puna ecoregions supports the hypothesis of the puna as a megapatch (Osorio et al., 2017), an area of similar resources that facilitated human dispersals through the central Andes. With abundant and critical resources such as herds of camelids, deer, rodents, and birds, high-quality and diverse lithic raw materials, natural shelters, and highly combustible wood and woody fuels, the central Andean puna presents an excellent habitat for hunter-gatherers. While the Pucuncho Basin area may be exceptional in its combination and abundance of those resources, similar studies in other areas of the Andean puna will be needed to characterize overall resource availability and human adaptive strategies. Understanding the role of the puna in the settlement of South America will require more studies focused on the potential for resources to support effective cultural adaptations to high elevation, and cold in particular, such as fire, shelter, and clothing.

Author contributions

SAM: Conceptualization, Methodology, Formal analysis, Investigation, Writing – original draft, Writing – review & editing, Visualization; EBPM: Conceptualization, Methodology, Investigation, Writing – original draft, Writing – review & editing; BF: Data provision, Writing – review & editing; SZ: Data provision, Writing – review & editing; KR: Conceptualization, Methodology, Investigation, Writing – original draft, Writing – review & editing, Funding acquisition

Declaration of competing interest

The authors declare that they have no known competing financial interests or personal relationships that could have appeared to influence the work reported in this paper.

Data availability

Data available in Supplementary Material

Acknowledgements

Excavations at Cuncaicha providing archaeological samples were authorized by the Peruvian Ministry of Culture (Resoluciones Directorales 849–2010, 569–2012. 343–2014, and 353–2015). The National Science Foundation (Grant BCS-1659015) and support from Michigan State University (Rademaker) funded the experimental fieldwork. A portion of the macrobotanical analysis was conducted while Zarrillo was a Postdoctoral Fellow at the Cotsen Institute of Archaeology, UCLA. We are grateful to the local communities in the Pucuncho Basin, and the Zuñiga family in particular, for sharing information pertaining to present-day fuel use in the Andes. We thank Katherine Moore for sharing her report on the zooarchaeological record from Cuncaicha with us. We thank Christopher Miller, Katherine Moore, Erica Cooper, and Diana Marcazzan for valuable comments and advice on the combustion experiment design and on earlier drafts of this paper. Two anonymous reviewers provided helpful comments that improved the manuscript.

Appendix A. Supplementary data

Supplementary data to this article can be found online at https://doi.org/10.1016/j.quascirev.2023.108244.

References

Aguerre, A.M., Fernández Distel, A.A., Aschero, C.A., 1975. Comentarios sobre nuevas fechas en la cronología arqueológica precerámica de la provincia de Jujuy, vol. 9. Relaciones de la Sociedad Argentina de Antropología, Buenos Aires, pp. 211–214.

Aguirre, M.G., 2007. Arqueobotánica del sitio Peñas Chicas 1.3, Antofagasta de la Sierra (Catamarca, Argentina). In: Marconetto, B., Babot, M.P., Oliszewski, N. (Eds.), Paleoetnobotánica del Cono Sur: Estudios de Casos y Propuestas Metodológicas. Museo de Antropología FF y H. Universidad Nacional de Córdoba, Córdoba, pp. 179–195.

Aguirre, M.G., 2012. Recursos Vegetales: Uso, Consumo y Producción en la puna Meridional Argentina (5000-1500 AP). Tesis para optar al Grado Académico de Doctor en Ciencias Naturales y Museo. Universidad Nacional de La Plata.

Aguirre, M.G., 2020. Combustibles leñosos empleados en la localidad de Antofagasta de la Sierra (Catamarca, Argentina). Bol. Soc. Argent. Bot. 55 (2), 311–325. https://doi.org/10.31055/1851.2372.v55.n2.26419.

Aguirre, M.G., Rodríguez, M.F., 2013. Experimentación con especies leñosas de la puna meridional de Argentina. Aportes a los estudios antracológicos. Comechingonia. Rev. Arqueol. 17 (2), 255–274. https://doi.org/10.37603/2250.7728.v17.n2.18200.

Aldeias, V., 2017. Experimental approaches to archaeological fire features and their behavioral relevance. Curr. Anthropol. 58 (16), 191–205. https://doi.org/10.1086/691210.

Aldeias, V., Dibble, H., Sandgathe, D., Goldberg, P., McPherron, S., 2016. How heat alters underlying deposits and implications for archaeological fire features: a controlled experiment. J. Archaeol. Sci. 67, 64–79. https://doi.org/10.1016/j.jas.2016.01.016.

Aldenderfer, M.S., 1998. Montane Foragers Asana and the South-Central Andean Archaic. University of Iowa Press, Iowa City.

Ardiles, A., Barrientos, R., Simirgiotis, M.J., Bórquez, J., Sepúlveda, B., Areche, C., 2018. Gastroprotective activity of Parastrephia quadrangularis (meyen), Cabrera from the Atacama Desert. Molecules 23 (9), 2361. https://doi.org/10.3390/molecules23092361.

Aschero, C.A., 1984. El sitio ICC-4: un asentamiento precerámico en la quebrada de Inca Cueva (Jujuy, Argentina). Estud. Atacameños 7, 53–60. https://doi.org/10.22199/S07181043.1984.0007.00006.

Aschero, C.A., 2010. Arqueologías de puna y Patagonia centro-meridional: comentarios generales y aporte al estudio de los cazadores-puneños en los proyectos dirigidos desde el IAM (1991-2009). In: Arenas, P., Aschero, C., Taboada, C. (Eds.), Rastros el Camino: Trayectos a los 80 Años del IAM-UNT. Editorial de la Universidad Nacional de Tucumán, pp. 257–293.

Aschero, C.A., Podestá, M.M., 1986. El arte rupestre en asentamientos precerámicos de la puna Argentina. Runa, Archivo para las Ciencias del Hombre 16. https://doi.org/10.34096/runa.v16i0.4389.

Baied, C., Wheeler, J.C., 1993. Evolution of high Andean puna ecosystems - environment, climate, and culture change over the last 12,000 years in the central Andes. Mt. Res. Dev. 13 (2), 145–156. https://doi.org/10.2307/3673632.

Baker, P.T., 1978. The Biology of High-Altitude Peoples. Cambridge University Press, Cambridge.

Baker, P.A., Fritz, S.C., 2015. Nature and causes of Quaternary climate variation of tropical South America. Quat. Sci. Rev. 124, 31–47. https://doi.org/10.1016/j.quascirev.2015.06.011.

Bellomo, R.V., 1993. A methodological approach for identifying archaeological evidence of fire resulting from human activities. J. Archaeol. Sci. 20 (5), 525–553. https://doi.org/10.1006/jasc.1993.1033.
Berna, F., Goldberg, P., Horwitz, L.K., Brink, J., Holt, S., Bamford, M., Chazan, M., 2012. Microstratigraphic evidence of in situ fire in the acheulean strata of wonderwerk cave, northern cape province, South Africa. Proc. Natl. Acad. Sci. U.S.A. 109 (20), E1215–E1220. https://doi.org/10.1073/pnas.1117620109.
Bettinger, R.L., Garvey, R., Tushingham, S., 2015. Hunter-gatherers: Archaeological and Evolutionary Theory, second ed. Springer, Boston, MA. https://doi.org/10.1007/978-1-4899-7581-2.
Binford, L.R., 1978. Dimensional analysis of behavior and site structure: learning from an Eskimo hunting stand. Am. Antiq. 43 (3), 330–361. https://doi.org/10.2307/279390.
Binford, L.R., 1980. Willow smoke and dogs' tails: hunter-gatherer settlement systems and archaeological site formation. Am. Antiq. 45, 4–20. https://doi.org/10.2307/279653.
Brutsaert, T.D., Kiyamu, M., Elias Revollendo, G., Isherwood, J.L., Lee, F.S., Rivera-Ch, M., Leon-Velarde, F., Ghosh, S., Bigham, A.W., 2019. Association of EGLN1 gene with high aerobic capacity of Peruvian Quechua at high altitude. Proc. Natl. Acad. Sci. U.S.A. 116 (48), 24006–24011. https://doi.org/10.1073/pnas.1906171116.
Buonasera, T., Herrera-Herrera, A.V., Mallol, C., 2019. Experimentally derived sedimentary, molecular, and isotopic characteristics of bone-fueled hearths. J. Archaeol. Method Theor 26 (4), 1327–1375. https://doi.org/10.1007/s10816-019-09411-3.
Bussmann, R.W., Paniagua Zambrana, N.Y., Moya Huanca, L.A., Hart, R., 2016. Changing markets - medicinal plants in the markets of La paz and el alto, Bolivia. J. Ethnopharmacol. 193, 76–95. https://doi.org/10.1016/j.jep.2016.07.074.
Cabrera, A.L., 1968. Ecología vegetal de la puna. In: Troll, C. (Ed.), Geo-Ecology of the Mountainous Regions of the Tropical Americas, vol. 9. Colloquium Geographicum, Bonn, Germany, pp. 91–116.
Canti, M.G., 2003. Aspects of the chemical and microscopic characteristics of plant ashes found in archaeological soils. Catena 54 (3), 339–361. https://doi.org/10.1016/S0341-8162(03)00127-9.
Canti, M.G., Brochier, J.E., 2017. Plant ash. In: Nicosia, C., Stoops, G. (Eds.), Archaeological Soil and Sediment Micromorphology. Wiley, Hoboken, NJ, pp. 147–154.
Capriles, J.M., Albarracin-Jordan, J., Lombardo, U., Osorio, D., Maley, B., Goldstein, S.T., Herrera, K.A., Glascock, M.D., Domic, A.I., Veit, H., Santoro, C.M., 2016. High-altitude adaptation and late Pleistocene foraging in the Bolivian Andes. J. Archaeol. Sci.: Report 6, 463–474. https://doi.org/10.1016/j.jasrep.2016.03.006.
Cardich, A., 1958. Los Yacimientos de Lauricocha; Nuevas Interpretaciones de la Prehistoria Peruana. Centro Argentino de Estudios Prehistóricos, Buenos Aires.
Cardich, A., 1964. Lauricocha: Fundamentos para una Prehistoria de los Andes Centrales. Centro Argentino de Estudios Prehistóricos, Buenos Aires.
Cartajena, I., Loyola, R., Núñez, L., Faúndez, E., 2014. Problemas y perspectivas en la interpretación del registro espacial de Punta Negra Imilac. In: Falabella, F., Sanhueza, L., Cornejo, L., Correa, I. (Eds.), Distribución Espacial en Sociedades no Aldeanas: Del Registro Arqueológico a la Interpretación Social, vol. 4. Serie Monográfica de la Sociedad Chilena de Arqueología, Santiago, pp. 143–162.
Caruso Fermé, L., 2012. Modalidades de Adquisición y Uso del Material Leñoso entre Grupos Cazadores-Recolectores Patagónicos (Argentina): Métodos y Técnicas de Estudios del Material Leñoso Arqueológico. Tesis para optar al Grado Académico de Doctor en Ciencias Naturales. Universitat Autònoma de Barcelona, España.
Caruso Fermé, L., Civalero, M.T., 2019. Fuel management in high mobility groups in Patagonia (Argentina) during the Holocene: anthracological evidences of the sites Cerro Casa de Piedra 5 and Cerro Casa de Piedra 7. Holocene 29 (7), 1134–1144. https://doi.org/10.1177/0959683619838044.
Caruso Fermé, L., Théry-Parisot, I., 2011. Experimentation and Combustion Properties of Patagonian Andean Forest (Argentina), vol. 11. Papeles del Laboratorio de Arqueología de Valencia-Extra, Saguntum, pp. 39–40.
Caruso Fermé, L., Théry-Parisot, I., 2020. Fuel management in Patagonian hunter-gatherer groups: evaluating the diameter of carbonized and non-carbonized wood from Cerro Casa de Piedra 7 site (Argentina). J. Archaeol. Sci.: Report 32, 102378. https://doi.org/10.1016/j.jasrep.2020.102378.
Castellani, J.W., Young, A.J., 2016. Human physiological responses to cold exposure: acute responses and acclimatization to prolonged exposure. Auton. Neurosci. 196, 63–74. https://doi.org/10.1016/j.autneu.2016.02.009.
Chazan, M., 2017. Toward a long prehistory of fire. Curr. Anthropol. 58 (16), 351–359. https://doi.org/10.1086/691988.
Clark, J.D., Harris, J.W.K., 1985. Fire and its roles in early hominid lifeways. Afr. Archaeol. Rev. 3 (1), 3–27. https://doi.org/10.1007/BF01117453.
Clark, A.E., Ranlett, S., Stiner, M.C., 2022. Domestic spaces as crucibles of Paleolithic culture: an archaeological perspective. J. Hum. Evol. 172, 103266 https://doi.org/10.1016/j.jhevol.2022.103266.
Costamagno, S., Théry-Parisot, I., Guilbert, R., 2005. Taphonomic consequences of the use of bones as fuel. Experimental data and archaeological applications. In: O'Connor, T. (Ed.), Biosphere to Lithosphere New Studies in Vertebrate Taphonomy. Oxbow Books, Oxford, pp. 51–62.
Crawford, J.E., Amaru, R., Song, J., Julian, C.G., Racimo, F., Cheng, J.Y., Guo, X., Yao, J., Ambale-Venkatesh, B., Lima, J.A., Rotter, J.I., Stehlik, J., Moore, L.G., Prchal, J.T., Nielsen, R., 2017. Natural selection on genes related to cardiovascular health in high-altitude adapted Andeans. Am. J. Hum. Genet. 101, 752–767. https://doi.org/10.1016/j.ajhg.2017.09.023.
deSouza, P.H., 2004. Cazadores recolectores del Arcaico Temprano y Medio en la cuenca superior del río Loa: sitios, conjuntos líticos y sistemas de asentamientos. Estud. Atacameños 27, 7–43. https://doi.org/10.4067/S0718-10432004002700002.
deSouza, P.H., Cartajena, I., Riquelme, R., Maldonado, A., Porras, M.E., Santander, B., Núñez, L., Díaz, L., 2021. Late pleistocene–early Holocene human settlement and environmental dynamics in the southern Atacama Desert highlands (24.0°S–24.5°S, northern Chile). Geoarchaeology 37, 13–31. https://doi.org/10.1002/gea.21849.
Dillehay, T.D., 2009. Probing deeper into first American studies. Proc. Natl. Acad. Sci. U.S.A. 106, 971–978. https://doi.org/10.1073/pnas.0808424106.
Eichstaedt, C.A., Pagani, L., Antao, T., Inchley, C.E., Cardona, A., Mörseburg, A., Clemente, F.J., Sluckin, T.J., Metspalu, E., Mitt, M., Mägi, R., Hudjashov, G., Metspalu, M., Mormina, M., Jacobs, G.S., Kivisild, T., 2017. Evidence of early-stage selection on EPAS1 and GPR126 genes in Andean high-altitude populations. Sci. Rep. 7, 13042 https://doi.org/10.1038/s41598-017-13382-4.
Ellingham, S.T.D., Thompson, T.J.U., Islam, M., Taylor, G., 2015. Estimating temperature exposure of burnt bone - a methodological review. Science & Justice Journal of the Forensic Science Society 55 (3), 181–188. https://doi.org/10.1016/j.scijus.2014.12.002.
Engel, F., 1970. Exploration of the chilca canyon, Peru. Curr. Anthropol. 11, 55–58. https://doi.org/10.1086/201093.
Engel, F., Genoves, S., 1969. On early man in the Americas. Curr. Anthropol. 10, 225.
Escola, P., Aguirre, M.G., Hocsman, S., 2013. La gestión de recursos leñosos por cazadores-recolectores transicionales en los sectores intermedios de Antofagasta de la Sierra (Catamarca, Argentina): el caso de alero sin cabeza. Rev. Chil. Antropol. 27. https://revistadeantropologia.uchile.cl/index.php/RCA/article/view/27359.
Fernández Distel, A.A., 1986. Las cuevas de Huachichocana, su posición dentro del precerámico con agricultura incipiente del noroeste argentino, vol. 8. Beiträge zur Allgemeinen und Vergleichenden Archäologie, Bonn, pp. 353–430.
Flannery, K.V., 1989. The Flocks of the Wamani: A Study of Llama Herders on the Punas of Ayacucho, Peru. Left Coast Press, Walnut Creek, Calif.
Flores Ochoa, J.A., 1968. Pastoralists of the Andes: the Alpaca Herders of Paratía. Institute for the Study of Human Issues, Philadelphia.
Franklin, W.L., 1982. Biology, ecology, and relationship to man of the South American camelids. In: Mares, M.A., Genoways, H.H. (Eds.), Mammalian Biology in South America, Special Publication Series, vol. 6. Pymatuning Laboratory of Ecology, University of Pittsburgh, pp. 457–489.
Franquemont, C., Franquemont, E., Davis, W., Plowman, T., King, S.R., Sperling, C.R., Niezgoda, C., 1990. The ethnobotany of Chinchero, an Andean community in southern Peru. Fieldiana Bot. 24, 1–66. https://doi.org/10.5962/bhl.title.2559.
Frisancho, A.R., 2013. Developmental functional adaptation to high altitude: review. Am. J. Hum. Biol. 25, 151–168. https://doi.org/10.1002/ajhb.22367.
García, A., 2010. La ocupación temprana de la vertiente oriental de los Andes centrales argentinos: el Alero Agua de la Cueva. Arqueología Rosarina Hoy 2, 7–34.
García Cook, A., 1982. The stratigraphy of Jaywamachay, Ac335. In: MacNeish, R., García Cook, A., Lumbreras, L. (Eds.), Prehistory of the Ayacucho Basin, Peru. University of Michigan Press, Ann Arbor, MI, pp. 57–79.
García, A., Zárate, M., Paez, M.M., 1999. The Pleistocene/Holocene transition and human occupation in the Central Andes of Argentina: Agua de la Cueva locality. Quat. Int. 53–54, 43–52. https://doi.org/10.1016/S1040-6182(98)00006-8.
Gareca, E.E., Hermy, M., Fjeldså, J., Honnay, O., 2010. *Polylepis* woodland remnants as biodiversity islands in the Bolivian high Andes. Biodivers. Conserv. 19, 3327–3346. https://doi.org/10.1007/s10531-010-9895-9.
Goldberg, P., Miller, C.E., Mentzer, S.M., 2017. Recognizing fire in the Paleolithic archaeological record. Curr. Anthropol. 58, 175–190. https://doi.org/10.1086/692729.
Gosling, W.D., Hanselman, J.A., Knox, C., Valencia, B.G., Bush, M.B., 2009. Long-term drivers of change in *Polylepis* woodland distribution in the central Andes. J. Veg. Sci. 20 (6), 1041–1052. https://doi.org/10.1111/j.1654-1103.2009.01102.x.
Grosjean, M., Núñez, L., Cartajena, I., 2005. Palaeoindian occupation of the Atacama Desert, northern Chile. J. Quat. Sci. 20, 643–653. https://doi.org/10.1002/jqs.969.
Grosjean, M., Santoro, C.M., Thompson, L.G., Núñez, L., Standen, V., 2007. Mid-Holocene climate and culture change in the south central Andes. In: Anderson, D.G., Maasch, K.A., Sandweiss, D.H. (Eds.), Climate Change and Cultural Dynamics: A Global Perspective on Mid-holocene Transitions. Elsevier, pp. 51–115. https://doi.org/10.1016/B978-012088390-5.50008-X.
Hanselman, J.A., Gosling, W.D., Paduano, G.M., Bush, M.B., 2005. Contrasting pollen histories of MIS 5e and the Holocene from Lake Titicaca (Bolivia/Peru). J. Quat. Sci. 20 (7–8), 663–670. https://doi.org/10.1002/jqs.979.
Harpel, C.J., Kleier, C., Aguilar, R., 2021. *Azorella compacta*'s long-term growth rate, longevity, and potential for dating geomorphological and archaeological features in the arid southern Peruvian Andes. J. Arid Environ. 188, 104470 https://doi.org/10.1016/j.jaridenv.2021.104470.
Hernández Llosas, M.I., 2000. Quebradas altas de Humahuaca a través del tiempo: el caso Pintoscayoc. Estudios Sociales del NOA 2, 167–224.
Hodge, W.H., 1946. Cushion plants of the Peruvian puna. J. N. Y. Bot. Gard. 47, 133–141.
Hodge, W.H., 1960. Yareta—fuel umbellifer of the andean puna. Econ. Bot. 14 (2), 113–118. https://doi.org/10.1007/BF02860013.
Hogg, A.G., Heaton, T.J., Hua, Q., Palmer, J.G., Turney, C.S.M., Southon, J., Bayliss, A., Blackwell, P.G., Boswijk, G., Bronk Ramsey, C., Pearson, C., Petchey, F., Reimer, P., Reimer, R., Wacker, L., 2020. SHCal20 southern hemisphere calibration, 0–55,000 years cal BP. Radiocarbon 62 (4), 759–778. https://doi.org/10.1017/RDC.2020.59.
Jacovas, V.C., Couto-Silva, C.M., Nunes, K., Lemes, R.B., de Oliveira, M.Z., Salzano, F.M., Bortolini, M.C., Hünemeier, T., 2018. Selection scan reveals three new loci related to high altitude adaptation in native Andeans. Sci. Rep. 8, 12733 https://doi.org/10.1038/s41598-018-31100-6.
Jolie, E.A., Lynch, T.F., Geib, P.R., Adovasio, J.M., 2011. Cordage, textiles, and the late Pleistocene peopling of the Andes. Curr. Anthropol. 52, 285–296. https://doi.org/10.1086/659336.

Joly, D.R., 2008. Étude de la Gestion du Combustible Osseux et Végétal dans les Stratégies Adaptatives des Chasseurs-Cueilleurs et des Groupes Agro-Pastoraux d'Argentine durant l'Holocène, vol. 1. Doctoral dissertation, Department of Science de la Matière, University of Rennes, Rennes, France.
Joly, D., March, R.J., Marguerie, D., Yacobaccio, H.D., 2009. Gestion des combustibles dans la province de Jujuy (puna, Argentine) depuis l'Holocène ancien: croisement des résultats ethnologiques et anthracologiques. In: Théry-Parisot, I., Costamagno, S., Henry, A., Oosterbeek, L. (Eds.), Gestion des Combustibles au Paléolithique et au Mésolithique: Nouveaux Outils, Nouvelles Interprétations, vol. 13. BAR International Series, pp. 39–52.
Joly, D., Santoro, C.M., Gayo, E.M., Ugalde, P.C., March, R.J., Carmona, R., Marguerie, D., Latorre, C., 2017. Late Pleistocene fuel management and human colonization of the Atacama Desert, northern Chile. Lat. Am. Antiq. 28 (1), 144–160. https://doi.org/10.1017/laq.2016.8.
Karkanas, P., 2021. All about wood ash: long term fire experiments reveal unknown aspects of the formation and preservation of ash with critical implications on the emergence and use of fire in the past. J. Archaeol. Sci. 135, 105476 https://doi.org/10.1016/j.jas.2021.105476.
Karkanas, P., Brown, K.S., Fisher, E.C., Jacobs, Z., Marean, C.W., 2015. Interpreting human behavior from depositional rates and combustion features through the study of sedimentary microfacies at site Pinnacle Point 5-6, South Africa. J. Hum. Evol. 85, 1–21. https://doi.org/10.1016/j.jhevol.2015.04.006.
Kelly, R.L., 2013. The Lifeways of Hunter-gatherers: the Foraging Spectrum. Cambridge University Press, Cambridge.
Kleier, C., Rundel, P.W., 2004. Microsite requirements, population structure and growth of the cushion plant *Azorella compacta* in the tropical Chilean Andes. Austral Ecol. 29, 461–470. https://doi.org/10.1111/j.1442-9993.2004.01386.x.
Kleier, C., Trenary, T., Graham, E.A., Stenzel, W., Rundel, P.W., 2015. Size class structure, growth rates, and orientation of the central Andean cushion *Azorella compacta*. PeerJ 3, e843. https://doi.org/10.7717/peerj.843.
Koford, C.B., 1957. The vicuña and the puna. Ecol. Monogr. 27 (2), 153–219.
Kuentz, A., Mera, A.G. de, Ledru, M.-P., Thouret, J.-C., 2007. Phytogeographical data and modern pollen rain of the puna belt in southern Peru (Nevado Coropuna, western Cordillera). J. Biogeogr. 34 (10), 1762–1776. https://doi.org/10.1111/j.1365-2699.2007.01728.x.
Kuentz, A., Ledru, M.-P., Thouret, J.-C., 2012. Environmental changes in the highlands of the western Andean Cordillera, southern Peru, during the Holocene. Holocene 22 (11), 1215–1226. https://doi.org/10.1177/0959683611409772.
Kuhn, S.L., Stiner, M.C., 2019. Hearth and home in the Middle Pleistocene. J. Anthropol. Res. 75 (3), 305–327. https://doi.org/10.1086/704145.
Kulemeyer, J.A., Lupo, L.C., Kulemeyer, J.J., Laguna, L.R., 1999. Desarrollo paleoecológico durante las ocupaciones humanas del precerámico del norte de la puna Argentina. In: Schäbitz, F., Leibricht, H. (Eds.), Beiträge zur Quartären Landschaftsentwicklung Südamerikas. Festschrift zum 65. Geburtstag von Professor Dr. Karsten Garleff, vol. 19. Bamberger Geographische Schriften, pp. 233–255.
Kuznar, L., 1995. Awatimarka: the Ethnoarchaeology of an Andean Herding Community. Harcourt Brace College Publishers, Fort Worth, TX.
Latorre, C., Santoro, C.M., Ugalde, P.C., Gayo, E.M., Osorio, D., Salas-Egaña, C., De Pol-Holz, R., Joly, D., Rech, J.A., 2013. Late Pleistocene human occupation of the hyperarid core in the Atacama Desert, northern Chile. Quat. Sci. Rev. 77, 19–30. https://doi.org/10.1016/j.quascirev.2013.06.008.
Lavallée, D., Julien, M., Wheeler, J., Karlin, C., 1995. Telarmachay: Cazadores y Pastores Prehistóricos de los Andes, vols. 1–2. Instituto Francés de Estudios Andinos, Lima.
LeFebvre, R.P., 2004. Hakenasa: the Archaeology of a Rock Shelter in the Altiplano of Northern Chile. PhD dissertation. Rutgers The State University of New Jersey PhD dissertation.
López, G.E.J., Restifo, F., 2017. El sitio Alero Cuevas, Puna de Salta, Argentina: secuencia de cambio en artefactos líticos y resolución cronológica macroregional durante el Holoceno temprano y medio. Chungará, Revista de Antropología Chilena 49 (1), 49–63. https://doi.org/10.4067/S0717-73562017005000005.
Lynch, T.F., 1980. Guitarrero Cave: Early Man in the Andes. Academic Press, New York.
Lynch, T.F., 1983. The paleo-Indians. In: Jennings, J.D. (Ed.), Ancient South Americans. Freeman and Co., San Francisco, California, pp. 87–132.
MacBride, J.F., 1936. Flora of Peru. In: Dahlgren, B.E. (Ed.), Botanical Series, Field Museum of Natural History, Chicago, vol. 13, 1.
MacDonald, K., Scherjon, F., van Veen, E., Vaesen, K., Roebroeks, W., 2021. Middle Pleistocene fire use: the first signal of widespread cultural diffusion in human evolution. Proc. Natl. Acad. Sci. U.S.A. 118 (31), e2101108118 https://doi.org/10.1073/pnas.2101108118.
Mallol, C., Hernández, C.M., Cabanes, D., Sistiaga, A., Machado, J., Rodríguez, Á., Pérez, L., Galván, B., 2013. The black layer of Middle Palaeolithic combustion structures. Interpretation and archaeostratigraphic implications. J. Archaeol. Sci. 40 (5), 2515–2537. https://doi.org/10.1016/j.jas.2012.09.017.
Mallol, C., Mentzer, S.M., Miller, C.E., 2017. Combustion features. In: Nicosia, C., Stoops, G. (Eds.), Archaeological Soil and Sediment Micromorphology. Wiley, Hoboken, NJ, pp. 299–330.
Marcazzan, D., Miller, C.E., Conard, N.J., 2022. Burning, dumping, and site use during the Middle and upper palaeolithic at hohle fels cave, SW Germany. Archaeological and Anthropological Science 14, 178. https://doi.org/10.1007/s12520-022-01647-7.
Marcazzan, D., Miller, C.E., Ligouis, B., Duches, R., Conard, N.J., Peresani, M., 2023. Middle and Upper Paleolithic occupations of Fumane Cave (Italy): a geoarchaeological investigation of the anthropogenic features. Journal of Anthropological Sciences 101. https://doi.org/10.4436/JASS.10002.
Marshall, A. (Ed.), 1971. The South American Handbook, 47th Annual Edition. Trade & Travel.
Martinez, S., 1993. Relaciones fenéticas entre las especies del genero *Azorella* (Apiaceae, Hydrocotyloideae). Darwiniana 32 (1/4), 159–170. http://www.jstor.org/stable/23222964.
Martínez, J.G., 2012. Evidence of early human burials in the southern Argentinian puna. In: Miotti, L., Salemme, M., Flegenheimer, N., Goebel, T. (Eds.), Southbound: Late Pleistocene Peopling of Latin America, Center for Study of First Americans. Texas A&M University, College Station, pp. 75–78.
Martinez Dyrzo, H., Mentzer, S., in prep. An Experimental Wood Ash Database: Physical Properties and Morphologies.
Mathias, M.E., Constance, L., 1962. Umbelliferae, flora of Peru, Part 5A. Publications of the field museum of natural history. Botany Series 13 (1), 3–97. https://doi.org/10.5962/bhl.title.2295.
Meinekat, S.A., Miller, C.E., Rademaker, K., 2021. A site formation model for Cuncaicha rock shelter: depositional and postdepositional processes at the high-altitude keysite in the Peruvian Andes. Geoarchaeology 37, 304–331. https://doi.org/10.1002/gea.21889.
Meltzer, D.J., Holliday, V.T., 2010. Would North American Paleoindians have noticed the Younger Dryas age climate changes? J. World PreHistory 23, 1–41. https://doi.org/10.1007/s10963-009-9032-4.
Méndez, C., Nuevo Delaunay, A., Reyes, O., Ozán, I.L., Belmar, C., López, P., 2018. The initial peopling of central western Patagonia (southernmost South America): late Pleistocene through Holocene site context and archaeological assemblages from Cueva de la Vieja site. Quat. Int. 473, 261–277. https://doi.org/10.1016/j.quaint.2017.07.014.
Mendoza, W., Cano, A., 2011. Diversidad del género *Polylepis* (Rosaceae, Sanguisorbeae) en los Andes peruanos. Rev. Peru. Biol. 18 (2), 197–200. https://doi.org/10.15381/rpb.v18i2.228.
Mentzer, S.M., 2009. Bone as a fuel source: the effects of initial fragment size distribution. In: Théry-Parisot, I., Costamagno, S., Henry, A., Oosterbeek, L. (Eds.), Gestion des Combustibles au Paléolithique et au Mésolithique: Nouveaux Outils, Nouvelles Interprétations, vol. 13. BAR International Series, pp. 53–64.
Mentzer, S.M., 2012. Microarchaeological approaches to the identification and interpretation of combustion features in prehistoric archaeological sites. J. Archaeol. Method Theor 21, 616–668. https://doi.org/10.1007/s10816-012-9163-2.
Mentzer, S.M., 2017. Hearths and combustion features. In: Gilbert, A. (Ed.), Encyclopedia of Geoarchaeology. Springer, Dordrecht, pp. 411–424. https://doi.org/10.1007/978-1-4020-4409-0_133.
Miller, C.E., 2015. A Tale of Two Swabian Caves: Geoarchaeological Investigations at Hohle Fels and Geißenklösterle. Tübingen Publications in Prehistory, Kerns, Tübingen.
Miller, C.E., Goldberg, P., Berna, F., 2013. Geoarchaeological investigations at diepkloof rock shelter, western cape, South Africa. J. Archaeol. Sci. 40 (9), 3432–3452. https://doi.org/10.1016/j.jas.2013.02.014.
Ministerio del Ambiente, 2015. Mapa Nacional de Cobertura Vegetal Memoria Descriptiva. Reporte del Ministerio del Ambiente, Lima, Perú. https://repositoriodigital.minam.gob.pe/handle/123456789/178.
Ministerio del Ambiente, 2018. Definiciones Conceptuales de los Ecosistemas del Perú. Reporte del Ministerio del Ambiente, Lima, Perú. https://repositoriodigital.minam.gob.pe/handle/123456789/1082.
Moore, K., 2016. Report on the 2015 Season of Excavation and Cuncaicha and the 2015 and 2016 Study Seasons of the Zooarchaeological Samples from the Site (Unpublished manuscript).
Moore, L.G., 2017. Human genetic adaptation to high altitudes: current status and future prospects. Quat. Int. 461, 4–13. https://doi.org/10.1016/j.quaint.2016.09.045.
Moore, K., Bruno, M., Capriles, J.M., Hastorf, C., 2010. Integrated contextual approaches to understanding past activities using plant and animal remains from Kala Uyuni, Lake Titicaca, Bolivia. In: VanDerwarker, A.M., Peres, T.M. (Eds.), Integrating Zooarchaeology and Paleoethnobotany: A Consideration of Issues, Methods, and Cases. Springer New York, New York, NY, pp. 173–203. https://doi.org/10.1007/978-1-4419-0935-0_8.
Moreno, A., Santoro, C.M., Latorre, C., 2009. Climate change and human occupation in the northernmost Chilean altiplano over the last ca. 11 500 cal. a BP. J. Quat. Sci. 24 (4), 373–382. https://doi.org/10.1002/jqs.1240.
Murphree, W.C., Aldeias, V., 2022. The evolution of pyrotechnology in the upper palaeolithic of europe. Archaeological and Anthropological Science 14 (10), 202. https://doi.org/10.1007/s12520-022-01660-w.
Núñez, L., 1983. Paleoindian and Archaic cultural periods in the arid and semiarid regions of northern Chile. Adv. World Archaeol. 2, 161–203.
Núñez, L., Grosjean, M., Cartajena, I., 2002. Human occupations and climate change in the Puna de Atacama, Chile. Science 298, 821–824. https://doi.org/10.1126/science.1076449.
Núñez, L., Grosjean, M., Cartajena, I., 2005. Ocupaciones Humanas y Paleoambientes en la Puna de Atacama. Instituto de Investigaciones Arqueológicas y Museo, Universidad Católica del Norte. Taraxacum, San Pedro de Atacama.
Osorio, D., Sepúlveda, M., Castillo, C., Corvalán, 2016. Análisis lítico y funcionalidad de sitio de los aleros de la precordillera de Arica (centro-sur andino) durante el período Arcaico (ca. 10.000-3700 años AP). Intersecc. Antropol. 17, 17–90.
Osorio, D., Steele, J., Sepúlveda, M., Gayo, E.M., Capriles, J.M., Herrera, K.A., Ugalde, P.C., De Pol-Holz, R., Latorre, C., Santoro, C.M., 2017. The dry puna as an ecological megapatch and the peopling of South America: technology, mobility, and the development of a late Pleistocene/early Holocene Andean hunter-gatherer tradition in northern Chile. Quat. Int. 461, 41–53. https://doi.org/10.1016/j.quaint.2017.07.010.
Pearsall, D.M., 1980. Pachamachay ethnobotanical report: plant utilization at a hunting base camp. In: Rick, J.W. (Ed.), Prehistoric Hunters of the High Andes. Academic Press, New York, London, Toronto, pp. 191–231.

Pearsall, D., 1988. Interpreting the meaning of macroremain abundance: the impact of source and context. In: Hastorf, C.A., Popper, V.S. (Eds.), Current Paleoethnobotany: Analytical Methods and Cultural Interpretations of Archaeological Plant Remain. University of Chicago Press, Chicago, pp. 97–118.
Perry Vega, E., 1946. Laretta compacta. La Farmacia Chilena 20 (4), 111–116.
Pintar, E., 2008. High altitude deserts: hunter-gatherers from the salt puna, northwest Argentina. International Journal of South American Archaeology 2, 47–55.
Pitblado, B.L., 2017. The role of the rocky mountains in the peopling of north America. Quat. Int. 461, 54–79. https://doi.org/10.1016/j.quaint.2017.07.009.
Pugnaire, F.I., Morillo, J.A., Armas, C., Rodriguez-Echeverria, S., Gaxiola, A., 2020. *Azorella compacta*: survival champions in extreme, high-elevation environments. Ecosphere 11 (2), e3031. https://doi.org/10.1002/ecs2.3031.
Rademaker, K., Moore, K., 2018. Variation in the occupation intensity of early forager sites of the Andean puna. Implications for settlement and adaptation. In: Lemke, A. (Ed.), Foraging in the Past: Archaeological Studies of Hunter-Gatherer Diversity. University Press of Colorado, pp. 76–118. https://doi.org/10.5876/9781607327745.c004.
Rademaker, K., Hodgins, G., Moore, K., Zarrillo, S., Miller, C., Bromley, G.R.M., Leach, P., Reid, D.A., Álvarez, W.Y., Sandweiss, D.H., 2014. Paleoindian settlement of the high-altitude Peruvian Andes. Science 346, 466–469. https://doi.org/10.1126/science.1258260.
Ralph, C.P., 1978. Observations on Azorella compacta (Umbelliferae), a tropical Andean cushion plant. Biotropica 10 (1), 62. https://doi.org/10.2307/2388107.
Ravines, R., 1972. Secuencia y cambios en los artefactos líticos del sur del Perú. Rev. Museo Nac. Museo Nac. 38, 133–184.
Ravines Sánchez, R.H., 1964. Fechas radiocarbónicas para la cueva no. 1 de Toquepala (Tal-1). Boletín del Museo Nacional de Antropología y Arqueología 1 (2), 2. Lima.
Rhode, D., Madsen, D.B., Brantingham, P.J., Goebel, T., 2003. Human occupation in the Beringian ''Mammoth-Steppe": starved for fuel, or dung-burner's paradise. Curr. Res. Pleistocene 20, 68–70.
Prehistoric hunters of the high Andes. In: Rick, J.W. (Ed.), 1980. Studies in Archaeology. Academic Press, New York, London, Toronto.
Rick, J.W., Moore, K.M., 1999. El preceramico de la Puna de Junín: el punto de vista desde Panaulauca. Boletín de Arqueología PUCP 3, 263–296.
Rodríguez, M.F., 1999. Plant species at an archaeological site of the southern Argentina puna (families: poaceae, Asteraceae, fabaceae and solanaceae). J. Ethnobiol. 19 (2), 228–247.
Rodríguez, M.F., 2000. Woody plant species used during the archaic period in the southern Argentine puna. Archaeobotany of quebrada seca 3. J. Archaeol. Sci. 27 (4), 341–361. https://doi.org/10.1006/jasc.1999.0515.
Rodríguez, M.F., 2004a. Cambios en el uso de los recursos vegetales durante los distintos momentos del Holoceno en la puna meridional Argentina. Chungará, Revista de Antropología Chilena 36, 403–413. https://doi.org/10.4067/S0717-73562004000300042.
Rodríguez, M.F., 2004b. Woody plant resources in the Southern Argentine puna: Punta de la Peña 9 archaeological site. J. Archaeol. Sci. 31 (10), 1361–1372. https://doi.org/10.1016/j.jas.2004.02.014.
Rodríguez, M.d.R., Aguirre, M.G., Babot, P., 2022. Firewood, architecture for fire and society. Agro-pastoralist atmospheres in the Argentine puna (South Central Andes, ca. 1500 B.P.). J. Archaeol. Sci.: Report 46, 103672. https://doi.org/10.1016/j.jasrep.2022.103672.
Roebroeks, W., Villa, P., 2011. On the earliest evidence for habitual use of fire in Europe. Proc. Natl. Acad. Sci. U.S.A. 108 (13), 5209–5214. https://doi.org/10.1073/pnas.1018116108.
Sandgathe, D.M., Berna, F., 2017. Fire and the genus *Homo*. Curr. Anthropol. 58, 165–174. https://doi.org/10.1086/691424.
Sandgathe, D.M., Dibble, H.L., Goldberg, P., McPherron, S.P., Hodgkins, J., 2011a. Timing of the appearance of habitual fire use. Proc. Natl. Acad. Sci. USA 108 (29), E298. https://doi.org/10.1073/pnas.1106759108 author reply E299.
Sandgathe, D.M., Dibble, H.L., Goldberg, P., McPherron, S.P., Turq, A., Niven, L., Hodgkins, J., 2011b. On the role of fire in Neandertal adaptations in western Europe: evidence from Pech de l'Azé and Roc de Marsal, France. PaleoAnthropology 216–242. https://doi.org/10.4207/PA.2011.ART54.
Santoro, C., Chacama Rodríguez, J., 1984. Secuencia de asentamientos precerámicos del extremo norte de Chile. Estud. Atacameños 7, 85–103. https://doi.org/10.22199/S07181043.1984.0007.0000.
Santoro, C.M., Gayo, E.M., Capriles, J.M., Rivadeneira, M.M., Herrera, K.A., Mandakovic, V., Rallo, M., Rech, J.A., Cases, B., Briones, L., Olguín, L., Valenzuela, D., Borrero, L.A., Ugalde, P.C., Rothhammer, F., Latorre, C., Szpak, P., 2019. From the Pacific to the tropical forests: networks of social interaction in the Atacama Desert, late in the Pleistocene. Chungará, Revista de Antropología Chilena 51, 5–25. https://doi.org/10.4067/S0717-73562019005000602.
Sauer, C.A., 1944. A geographic sketch of early man in America. Geogr. Rev. 34, 529–573. https://doi.org/10.2307/210028.
Sharma, V., Varshney, R., Sethy, N.K., 2022. Human adaptation to high altitude: a review of convergence between genomic and proteomic signatures. Hum. Genom. 16, 21. https://doi.org/10.1186/s40246-022-00395-y.
Shimelmitz, R., Kuhn, S.L., Jelinek, A.J., Ronen, A., Clark, A.E., Weinstein-Evron, M., 2014. 'Fire at will': the emergence of habitual fire use 350,000 years ago. J. Hum. Evol. 77, 196–203. https://doi.org/10.1016/j.jhevol.2014.07.005.
Sinclaire, A.C., 1985. Dos fechas radiocarbónicas del alero Chulqui, rio Toconce: noticia y comentario. Chungará, Revista de Antropología Chilena 14, 71–79.
Sorensen, A., 2019. The uncertain origins of fire-making by humans: the state of the art and smouldering questions. Mitteilungen der Gesellschaft für Urgeschichte 28, 11–50.
Squeo, F.A., Warner, B.G., Aravena, R., Espinoza, D., 2006. Bofedales: high altitude peatlands of the central Andes. Rev. Chil. Hist. Nat. 79, 245–255. https://doi.org/10.4067/S0716-078X2006000200010.
Stahlschmidt, M.C., Mallol, C., Miller, C.E., 2020. Fire as an artifact—advances in Paleolithic combustion structure studies: introduction to the special issue. Journal of Paleolithic Archaeology 3 (4), 503–508. https://doi.org/10.1007/s41982-020-00074-1.
Stein, W.W., 1961. Hualcan: Life in the Highlands of Peru. Cornell University Press, Ithaca, N.Y.
Stiner, M.C., Kuhn, S.L., Weiner, S., Bar-Yosef, O., 1995. Differential burning, recrystallization, and fragmentation of archaeological bone. J. Archaeol. Sci. 22 (2), 223–237. https://doi.org/10.1006/jasc.1995.0024.
Storz, J.F., 2021. High-altitude adaptation: mechanistic insights from integrated genomics and physiology. Mol. Biol. Evol. 38 (7), 2677–2691. https://doi.org/10.1093/molbev/msab064.
Stuiver, M., Reimer, P.J., 2020. Calib Radiocarbon Calibration Program Rev 8.1.0.
Surovell, T.A., Waguespack, N.M., 2007. Folsom hearth-centered use of space at barger gulch, locality B. In: Brunswig, R.H., Pitblado, B.L. (Eds.), Frontiers in Colorado Paleoindian Archaeology: from the Dent Site to the Rocky Mountains. University Press of Colorado, Boulder, pp. 219–259.
Théry-Parisot, I., 2002a. The gathering of firewood during Palaeolithic time. In: Thiébault, S. (Ed.), Charcoal Analysis, Methodological Approaches, Palaeoecological Results and Wood Uses. Proceedings of the Second International Meeting of Anthracology, Paris, vol. 1063. BAR International Series, pp. 243–250.
Théry-Parisot, I., 2002b. Fuel management (bone and wood) during the lower aurignacian in the pataud rock shelter (lower palaeolithic, les eyzies de Tayac, dordogne, France). Contribution of experimentation. J. Archaeol. Sci. 29 (12), 1415–1421. https://doi.org/10.1006/jasc.2001.0781.
Théry-Parisot, I., Costamagno, S., Brugal, J.-P., Fosse, P., Guilbert, R., 2005. The use of bone as fuel during the Palaeolithic, experimental study of bone combustible properties. In: Mulville, J., Outram, A.K. (Eds.), The Zooarchaeology of Fats, Oils, Milk and Dairying. Proceedings of the 9th Conference of the. International Council of Archaeozoology, Durham, pp. 50–59.
Théry-Parisot, I., Chabal, L., Chrzavzez, J., 2010. Anthracology and taphonomy, from wood gathering to charcoal analysis. A review of the taphonomic processes modifying charcoal assemblages, in archaeological contexts. Palaeogeogr. Palaeoclimatol. Palaeoecol. 291 (1–2), 142–153. https://doi.org/10.1016/j.palaeo.2009.09.016.
Tomé, L., Jambrina-Enríquez, M., Égüez, N., Herrera-Herrera, A.V., Davara, J., Marrero Salas, E., La Arnay de Rosa, M., Mallol, C., 2022. Fuel sources, natural vegetation and subsistence at a high-altitude aboriginal settlement in Tenerife, Canary Islands: microcontextual geoarchaeological data from Roques de García Rockshelter. Archaeological and Anthropological Science 14 (10). https://doi.org/10.1007/s12520-022-01661-9.
Troll, C., 1968. The cordilleras of the tropical Americas: aspects of climatic, phytogeographical and agrarian ecology. In: Troll, C. (Ed.), Geo-Ecology of the Mountainous Regions of the Tropical Americas, vol. 9. Colloquium Geographicum, Bonn, Germany, pp. 15–56.
Valencia, B.G., Bush, M.B., Coe, A.L., Orren, E., Gosling, W.D., 2018. *Polylepis* woodland dynamics during the last 20,000 years. J. Biogeogr. 45 (5), 1019–1030. https://doi.org/10.1111/jbi.13209.
Vanlandeghem, M., Desachy, B., Buonasera, T., Norman, L., Théry-Parisot, I., Carré, A., Petit, C., Elliott, M., Alix, C., 2020. Ancient arctic pyro-technologies: experimental fires to document the impact of animal origin fuels on wood combustion. J. Archaeol. Sci.: Report 33, 102414. https://doi.org/10.1016/j.jasrep.2020.102414.
Villagran, X.S., Schaefer, C.E.G.R., Ligouis, B., 2013. Living in the cold: Geoarchaeology of sealing sites from byers peninsula (livingston island, Antarctica). Quat. Int. 315, 184–199. https://doi.org/10.1016/j.quaint.2013.07.001.
Wickens, G.E., 1995. Llareta (Azorella compacta, Umbelliferae): a review. Econ. Bot. 49 (2), 207–212. http://www.jstor.org/stable/4255718.
Winterhalder, B., Larsen, R., Thomas, R.B., 1974. Dung as an essential resource in a highland Peruvian community. Hum. Ecol. 2 (2), 89–104. https://doi.org/10.1007/BF01558115.
Yacobaccio, H.D., Paz Catá, M., Morales, M.R., Joly, D., Solá, P., Cáceres, M., Oxman, B. I., Samec, C.T., 2014. Ocupaciones humanas tempranas en la puna de Atacama: el alero Hornillos 2, Susques (Jujuy). In: Escola, P.S., Hocsman, S. (Eds.), Artefactos Líticos, Movilidad y Funcionalidad de Sitios: Problemas y Perspectivas, vol. 2628. BAR International Series, pp. 1–10.

Appendix IV – Paper 3

Geoarchaeology

WILEY

Geoarchaeology An International Journal

RESEARCH ARTICLE OPEN ACCESS

Microstratigraphy and Site Formation Processes at Quebrada Jaguay 280 (Peru)

Sarah A. Meinekat[1] | Emily B. P. Milton[2] | Daniela P. Osorio[3] | Susan M. Mentzer[1,4] | Christopher E. Miller[1,4,5] | Daniel H. Sandweiss[6] | Kurt Rademaker[7]

[1]Department of Geosciences, Institute for Archaeological Sciences, University of Tübingen, Tübingen, Germany | [2]Department of Anthropology, National Museum of Natural History, Smithsonian Institution, USA | [3]Sociedad Chilena de Arqueología, Santiago, Chile | [4]Senckenberg Centre for Human Evolution and Palaeoenvironment, University of Tübingen, Tübingen, Germany | [5]SFF Centre for Early Sapiens Behaviour (SapienCE), University of Bergen, Bergen, Norway | [6]Anthropology Department and the Climate Change Institute, University of Maine, Orono, Maine, USA | [7]Department of Anthropology, Center for the Study of First Americans, Texas A&M University, College Station, Texas, USA

Correspondence: Sarah A. Meinekat (sarah-ann.meinekat@uni-tuebingen.de)

Received: 30 November 2025 | **Revised:** 28 February 2026 | **Accepted:** 10 March 2026

Scientific Editor: Justin Holcomb

Funding: National Science Foundation, Grant/Award Number: BCS-1659015

Keywords: μXRF | Early Holocene | Late Pleistocene | micromorphology | shell midden | South America

ABSTRACT

This study presents a microanalytical, geoarchaeological study of Quebrada Jaguay (QJ)-280, a Terminal Pleistocene–Holocene coastal site in southern Peru. Combining micromorphology, μXRF and μFTIR, we develop a site formation model that also reassesses site use and forager behaviour. Micro-contextual data provide new insights into sedimentation, taphonomy and human activity, revealing short-term, seasonal occupations with evidence of spatial shifts in site function and maintenance. Geomorphological observations indicate that the site, originally part of an active alluvial fan, became more stable during times of human occupation. Preservation, however, is compromised by several post-depositional processes. We observe bioturbation, as well as diagenesis of the faunal and botanical remains by mineral formations, highlighted by the combined contextual application of micromorphology and μXRF mapping. A notable stratigraphic feature, the 'indurated layer', is shown to result from salt action. The salt formation is a product of the setting on the arid coast and pedogenic processes, challenging its use as a chronological marker in the areas preserved for our study. Lastly, our findings suggest QJ-280 functioned as a repeatedly used, short-term camp within a broader mobility system, contributing new perspectives to early coastal lifeways in western South America.

1 | Introduction

On the Pacific coast of South America, various sites indicate that coastal landscapes played an important role for hunter–gatherer–fisher societies during the early occupation of the continent. Archaeological evidence dates to the Terminal Pleistocene (> 11.7 ka)—including, for example, sites in Ecuador (Stothert 1985), Peru (Chauchat 2006; Dillehay et al. 2003, 2012; Keefer et al. 1998; Maggard 2010; Sandweiss et al. 1998; Stackelbeck 2008) and Chile (Jackson et al. 2007; Llagostera et al. 2000; Salazar et al. 2013, 2018) (Figure 1). While these mostly site-level investigations have provided a wealth of information on adaptations to the coast, information is lacking on landscape-scale patterns of mobility, settlement and inter-site connections. Further, Rademaker (2024) shows that radiocarbon chronologies along the Pacific coast may require careful re-evaluation due to methodological issues. Therefore, we carried out new excavations of Quebrada-Jaguay 280 in 2017. Specific aims were to improve the site chronology,

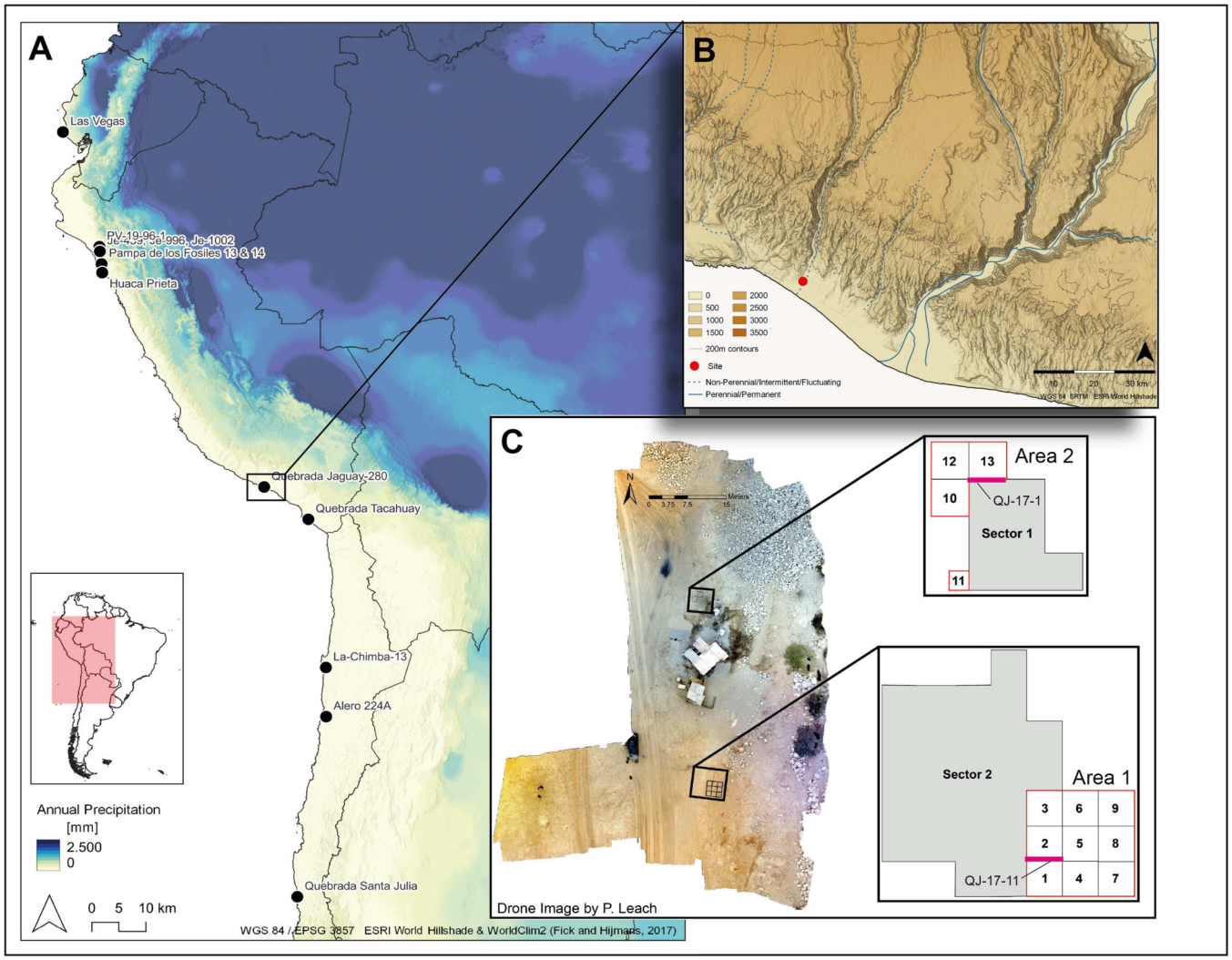

FIGURE 1 | (A) Map of South America with mean annual precipitation (Fick and Hijmans 2017) and Terminal Pleistocene coastal sites along the Pacific coast of South America and location of Quebrada Jaguay 280. (B) Zoom on site locality with elevation and river systems (perennial and non-perennial). (C) Drone imagery of site (courtesy of P. Leach) used for relocation and documentation of the site and location of excavation areas. Sector I (1990s/Sandweiss excavation) with Area 2 excavation units (10–13) (2017 excavation). Sector II (1990s/Sandweiss excavation) with Area 2 excavation units (1–9) (2017 excavation).

investigate occupation seasonality and understand site formation processes.

1.1 | Quebrada Jaguay 280: State of the Art and Previous Excavations

Quebrada Jaguay 280 (QJ-280), named after the adjacent stream, is a Terminal Pleistocene–Early Holocene archaeological site in southern Peru. It is renowned for contributing to our understanding of early marine resource subsistence strategies and for evidence of connections with the Andean highlands during the initial phase of occupation (Sandweiss 2008; Sandweiss et al. 1998; Sandweiss and Rademaker 2011).

The proposed maritime adaptation at QJ-280 is based on the absence of terrestrial faunal remains and abundance of preserved marine resources (McInnis 1999; Sandweiss et al. 1998), which include surf clams (*Mesodesma donacium*), crab, and cool-water fishes, especially the drum fish lornas and corvinas (*Sciaena deliciosa* and *Cilus gilberti*) (Reitz et al. 2016, 2017). The faunal data analysed by Reitz et al. (2016, 2017) suggest specialized fishing strategies from the earliest occupations of the site.

Non-coastal materials demonstrate a connection to interior and higher-elevation zones from the Terminal Pleistocene (Sandweiss et al. 1998; Sandweiss and Rademaker 2011). Such artefacts in the Pleistocene deposits include Alca-1, Alca-4 and Alca 5 obsidian, a highland-sourced raw material (Rademaker et al. 2013, 2022), and *Opuntia* sp. seeds (prickly pear cactus), which grows at higher elevations (> 2000 m) (Sandweiss and Rademaker 2011). The connection to interior and highland resources makes QJ-280 a unique case study for investigating settlement systems and inter-landscape connections.

Sandweiss et al. (1998) hypothesized the site was occupied seasonally during the Terminal Pleistocene and Early Holocene phases, based on water availability in the adjacent *quebrada* (Spanish for gorge/ravine) during the wet season, late in the austral summer. This proposal is supported by an isotopic study

of the *Mesodesma donacium* shells from these phases, which further constrain the annual occupation periods to February and March (Gruver 2018).

1.1.1 | *Excavations at QJ-280*

QJ-280 was first tested and dated in 1970 by Frédéric Engel, who acquired a single Pleistocene charcoal age of 10,200 ± 140 BP (12.5–11.3 ka,[1] 95% range), Dan Sandweiss excavated the site extensively in 1996 and 1999 (Engel 1981; Sandweiss et al. 1998).

1.1.1.1 | *1990s Excavations*

Excavations at QJ-280 in the 1990s encompassed four sectors (Sector I, II, III, IV), with two main excavated areas: Sector I and Sector II (Sandweiss et al. 1998; Tanner 2001) (Figure 1). Sandweiss et al. (1999, see also Tanner 2001) reported that Sector I consisted largely of shell midden deposits overlying and filling a circular semi-subterranean Early Holocene house structure, which contained additional features. The Early Holocene deposits cut through a pre-existing Terminal Pleistocene midden (Sandweiss et al. 1999; Tanner 2001). Sector II is described as a shell midden with pit features and postholes, possibly relating to a rectangular structure of Terminal Pleistocene age (Sandweiss 2014).

Sandweiss et al. (1998) report three chronological components based on conventional radiocarbon ages (Terminal Pleistocene (13–11 ka), Early Holocene I (10.6–10 ka) and Early Holocene II (~8.7–8.2 ka). Jones et al. (2019) identified a Middle Holocene component in the shell midden filling the Early Holocene structure in Sector I.

After the 1990s excavations, the Terminal Pleistocene component was divided into two separate phases based on the presence of an indurated layer that was encountered during the fieldwork (Andrus et al. 2000). The induration has been used as a chronostratigraphic marker for archaeological interpretations (Reitz et al. 2016, 2017; Tanner 2001). In previous publications, the Terminal Pleistocene occupation phases were labelled *Below-Induration* or *Pre-Induration*, and *Above-Induration* or *Post-Induration* (Reitz et al. 2016, 2017; Tanner 2001).

1.1.1.2 | *2017 Excavations*

In 2017, our team located and imaged the previously excavated sectors using ground-penetrating radar (GPR), GSSI Utility Scanner, and drone imagery from a DJI Phantom 3 Professional Quadcopter with an integrated GPS and camera with 3-axis stabilization gimbal (Figure 1). After successfully locating the Sandweiss sectors, we exposed old profiles by removing the backfill. New excavations targeted 13 new units, adjacent to the 1990s sectors, with Area 1 (Units 1–9) southeast of Sector II and Area 2 (Units 11–13) west of Sector I (Units 10–13) (Figure 1). Excavations were conducted in 1–5 cm levels, following stratigraphic changes; then sediment was dry screened (5 mm) and sieved (1 mm) before sorting and cataloguing artefacts. Suspected disturbances (e.g., krotovinas) and anthropogenic features were plotted using a total station, then excavated and processed separately from matrix sediment.

During the excavation, we encountered sediment that corresponds to the previously described 'induration'. Observation of the induration in profile showed that it was undulating and locally discontinuous, and at times extended vertically. The indurated sediment was present in both areas and was so compact that normal excavation techniques could not be applied.

1.2 | Research Questions and Objectives

Former interpretations of site function at QJ-280, including the domestic use of space and the presence of structures, are based on the stratigraphic and sedimentary observations of the 1990s fieldwork and subsequent analyses of the archaeological faunal, floral and lithic assemblages (Reitz et al. 2016, 2017; Sandweiss 2008; Sandweiss et al. 1998; Tanner 2001). However, an in-depth study of site formation processes at QJ-280 remained to be conducted.

This study provides the stratigraphic sequence and formation history of QJ-280 through a high-resolution geoarchaeological analysis of the deposits at the site. The sediment matrix yields information that is valuable for the interpretation of archaeological finds and features.

Methods involve a micro-contextual approach, which combines micromorphology, micro-X-ray fluorescence (μXRF) and micro-Fourier Transform Infrared Spectroscopy (μFTIR) to understand the (micro-) stratigraphy, site formation and post-depositional processes at QJ-280.

In particular, we focus on two specific block samples. The samples represent Areas 1 and 2 and span the complete (preserved) stratigraphic sequence. We address questions of overall site setting and formation—from the micro- to the (paleo)landscape scale:

- What was the site setting during the earliest phase of occupation?
- What sedimentary components, depositional agents, and diachronic changes and/or spatial differences are apparent in the deposit?
- What post-depositional processes affect the archaeological deposit and findings therein—such as bioturbation or diagenesis?
- What human behaviours and indicators of site use can be identified from the deposit?

Further questions arose during the excavations, as the induration complicated the excavation process and challenged the recovery of artefacts. Additional geoarchaeological questions developed in response to the induration include the following:

- What are the formation processes of the induration?
- Did transformation or translocation processes affect the induration?
- Can the induration provide a chronostratigraphic marker?

2 | Study Area and Paleoclimate

2.1 | Study Area

QJ-280 is located in southern Peru, approximately 20 km north of the town of Camaná, on the hyperarid coast.

The site is located in the northernmost extent of the hyperarid Atacama Desert, as defined by Houston (2006) from 15° to 30° South (Figures 1 and 2). The modern-day hyperarid climate of the region––in short––is a product of the rainshadow effect of the Andes and the steep temperature inversion (1000 masl) caused by the cold Peru–Chile current system (Garreaud et al. 2009; Houston 2006; Houston and Hartley 2003; Rech et al. 2006). Precipitation is low (< 100 mm annually) and seasonally variable and mostly related to El Niño-Southern Oscillation (ENSO) events (Garreaud et al. 2009; Houston 2006).

The ecosystem is characterized by the general lack of freshwater, though ephemeral streams and coastal fogs, that is, *garuá* (Chile: *camanchaca*), are active seasonally. The ephemeral stream is active for a few weeks during the austral summer (February–March) (Sandweiss et al. 1998). The closest perennial freshwater streams are found in the Colca (approximately 15 km distance) and Cotahuasi (approximately 27 km distance) drainages (Figures 2 and 3).

During the austral winter (July–September), the coastal fogs create the resource-rich lomas vegetation between 300 and 1000 m above sea level (masl) (Beresford-Jones et al. 2015; Dillon et al. 2003, 2011). Today, the vegetation cover in this region is low and a hyperarid, coastal desert (*desierto costero*) ecosystem prevails (Ministerio del Ambiente MINAM 2018).

Geologically, QJ-280 is situated on the narrow coastal plain of the Andean forearc region (Figure 2) (Armijo et al. 2015; Thouret et al. 2007). Different pre-Cenozoic formations crop out in the broader study area, especially plutonic rocks such as granite (Acosta et al. 2010 2010a, 2010b; Alván et al. 2015) (Figure 3). Cenozoic extrusive material, such as Sencca and Huaylilla ignimbrites, is found from the western Cordillera towards the piedmont (Acosta et al. 2010 2010a, 2010b; Thouret et al. 2007) (Figure 4). The Cenozoic Camaná formation is exposed from the Coastal Cordillera to the shore (Figure 3). This is a complex, at times discontinuous, sequence of deltaic materials from various geological sources within the Coastal and Western Cordilleras (Alván et al. 2015; Alván and von Eynatten 2014; Rüegg 1952).

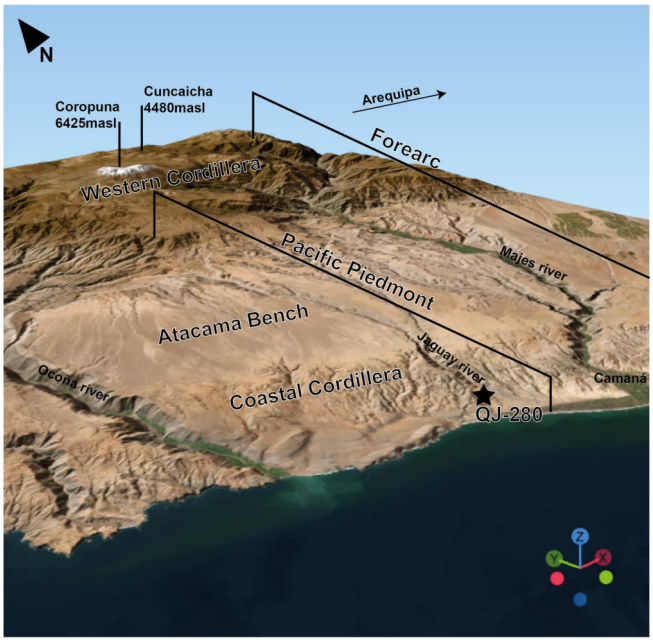

FIGURE 2 | Cutout 3-D display (ESRI World Imagery, retrieved 2024) of main units of Andean orogen in the broader study region, Ocoña to Majes, coast (QJ-280) to highland (Cuncaicha rock shelter) after Armijo et al. (2015).

The archaeological site is located where the quebrada channel emerges from the Coastal Cordillera into the coastal plain, creating an alluvial fan (Blair and McPherson 2009). The Quebrada Jaguay terminates in the Pacific, today about 2.5 km downstream from the site. It is directly bordered by Camaná formation bedrock, with batholith granite outcrops upstream (Figure 3). Especially in hyperarid regions, coastal alluvial fans demonstrate a complex, and at times poorly understood, interaction between climate, geology, resulting morphodynamics, and post-depositional processes at the landscape scale (Walk et al. 2020, 2022). These processes influence the preservation of the archaeological site and require consideration at the site scale.

2.2 | Paleoclimate

Various proxy records from the Atacama have consistently corroborated the timing of wet phases during the initial occupation of the region (Betancourt et al. 2000; Maldonado et al. 2005; Nester et al. 2007; Pfeiffer et al. 2018; Pueyo et al. 2011; Quade et al. 2008). The Central Andean Pluvial Event II (CAPE II) is a regional wet phase during the Terminal Pleistocene, dated between 12.7 and 9.7 ka, that was first identified within paleowetlands situated in the Salar de Punta Negra of Northern Chile (Quade et al. 2008). The Early Holocene period witnessed a warming trend in the Central Andes (Palacios et al. 2020). Throughout this period, evidence from lakes, ice cores, and speleothems across the central Andes and western Amazonia suggests a significant transition towards a drier climate relative to the Terminal Pleistocene CAPE II wet phase (Baker and Fritz 2015; Bird et al. 2011; Bush et al. 2005; Bustamante et al. 2016; Cheng et al. 2013; Cross et al. 2000; Ekdahl et al. 2008; Hillyer et al. 2009; Ramirez et al. 2003; Seltzer et al. 2000; Thompson et al. 1995, 1998; van Breukelen et al. 2008). The onset of the driest period within the Holocene, as documented in numerous paleohydrologic records across the central Andes occurs after 8.2 ka—in the Mid Holocene (Abbott et al. 2003; Baker et al. 2001; Bush et al. 2005; Moreno et al. 2009; Pueyo et al. 2011; Rigsby et al. 2005; Seltzer et al. 2000; Thompson 1998; Vining et al. 2019). However, there exists considerable variability in the timing of peak aridity among these records.

On the coast, changes in the sea surface temperature (SST) and ENSO are the main drivers for climatic shifts and patterns (Baker and Fritz 2015; Garreaud et al. 2009; Liebmann and Mechoso 2011). Reduced SST results in intensified *garúa* (i.e., marine fogs). *Garúa* plays a significant role in shaping geomorphic processes in the Atacama Desert. Besides contributing to intense salt weathering of exposed rocks, the humidity and salinity associated with these fogs also promote the cementation of loose sediments, as noted in several studies (e.g., Abele 1990; Cosentino et al. 2015; de Haas et al. 2014; Goudie et al. 2002; Hartley et al. 2005; Rech et al. 2003; Viles and Goudie 2007).

Further, the Holocene is a period during which we observe climatic variation at the coast that is related to ENSO variability. For the coast south of Lima, Carré et al. (2005, 2014, 2021) show that during the Early Holocene climate was relatively more humid with reduced SSTs and stronger ENSO activity compared

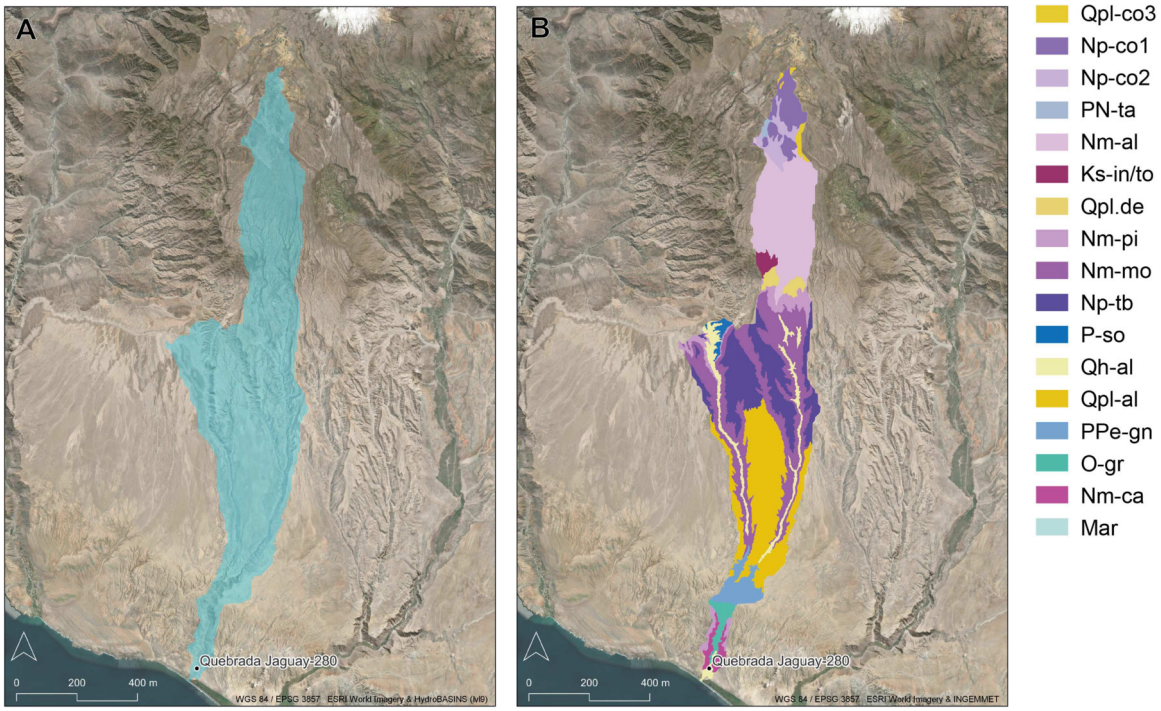

FIGURE 3 | (A) Jaguay watershed (Milton et al. 2022) based on HydroBASINS (Level 9) that corresponds to the catchment area of the coastal alluvial fan. (B) Geology within the catchment area (Acosta et al. 2010b). Qpl-co3—Barroso Group, Coropuna volcano stratum; Np-co1—Coropuna volcano 1; Np-co2—Coropuna volcano 2; PN-ta—Tacaza Group; Nm-al—Alpabamba Formation; Ks-in/to—Incahuasi-Tonalite Super-Unit; Qpl-de—Landslide deposit; Nm-pi—Pisco Formation; Nm-mo—Moquegua Formation; Np-tb—Barroso Group - Coropuna Tuffs; P-so—Sotillo Formation; Qh-al—Alluvial deposits - Poorly sorted gravels and sands in lime-sand matrix; Qpl-al—Alluvial deposit; PPe-gn—Basal Complex of the Coast (facies of gneiss/granules of Mollendo-Camana); O-gr—Atico-Camana granite batholith; Nm-ca—Caudalosa Formation; Mar—Sea.

to the subsequent Middle Holocene with drier climate and reduced ENSO activity. The Middle Holocene exhibited less frequent extreme weather events, reduced rainfall, and more pronounced aridity in the region (Carré et al. 2005, 2014). The modern-day ENSO regime was established around 3–4.5 ka (Carré et al. 2014).

These changes in the paleoclimate have implications for the archaeological record; for example, the pronounced Middle Holocene aridity has been proposed to trigger human migration to more suitable eco-refuges (Grosjean et al. 1997; Núñez et al. 2002, 2013).

3 | Methods

In this paper, we focus on two specific block samples, QJ-17-11 and QJ-17-01, that span the complete stratigraphic sequence in Area 1 and Area 2, respectively, to address questions of the overall site setting and formation. On a micro-scale, we integrate micromorphology, μXRF, and μFTIR for a micro-contextual approach to the study of site formation at QJ and combine these insights with macroscopic, landscape-scale observations.

3.1 | Micromorphology

Intact sediment block samples were collected at the site by cutting vertically oriented block samples from the profiles or unit surfaces as monoliths. Blocks were prepared using plaster bandages. All micromorphological blocks were denoted with a prefix QJ-17-xx, and the top and base of each block were measured in 3D space with a Nikon Nivo Total Station, allowing for a correlation between thin section and organic samples providing AMS ages.

The two block samples were processed into a total of five thin sections, QJ-17-01A/B/C and QJ-17-11A/B, in the University of Tübingen, Department of Geosciences, Geoarchaeology Laboratory and the Terrascope Laboratory in Troyes, France. The samples were dried in an oven at a low (40°C) temperature to avoid destruction of organic matter and mineral neoformations (e.g., of gypsum). After drying, the samples were impregnated using a mixture of methylethylketone peroxide (MEKP) hardener, styrene, and polyester resin, then sawn, mounted on slides, and ground to 30 μm thickness. The resulting thin sections were documented using a high-resolution Nikon film scanner in transmitted light mode as well as in cross-polarized light using two polarizing sheets (Haaland et al. 2019). The thin sections were then analysed according to standard procedures, using a Zeiss stereomicroscope and a Zeiss Axio Imager petrographic microscope, as well as Motic petrographic microscopes with plane-polarized (PPL), cross-polarized (XPL) light, following the descriptive terminology provided by Stoops (2021; 2003), Bullock et al. (1985), Courty et al. (1989), and interpretations based on Nicosia and Stoops (2017) and Stoops et al. (2010). Thin section descriptions were documented using the description template by Marcazzan and Meinekat (2022).

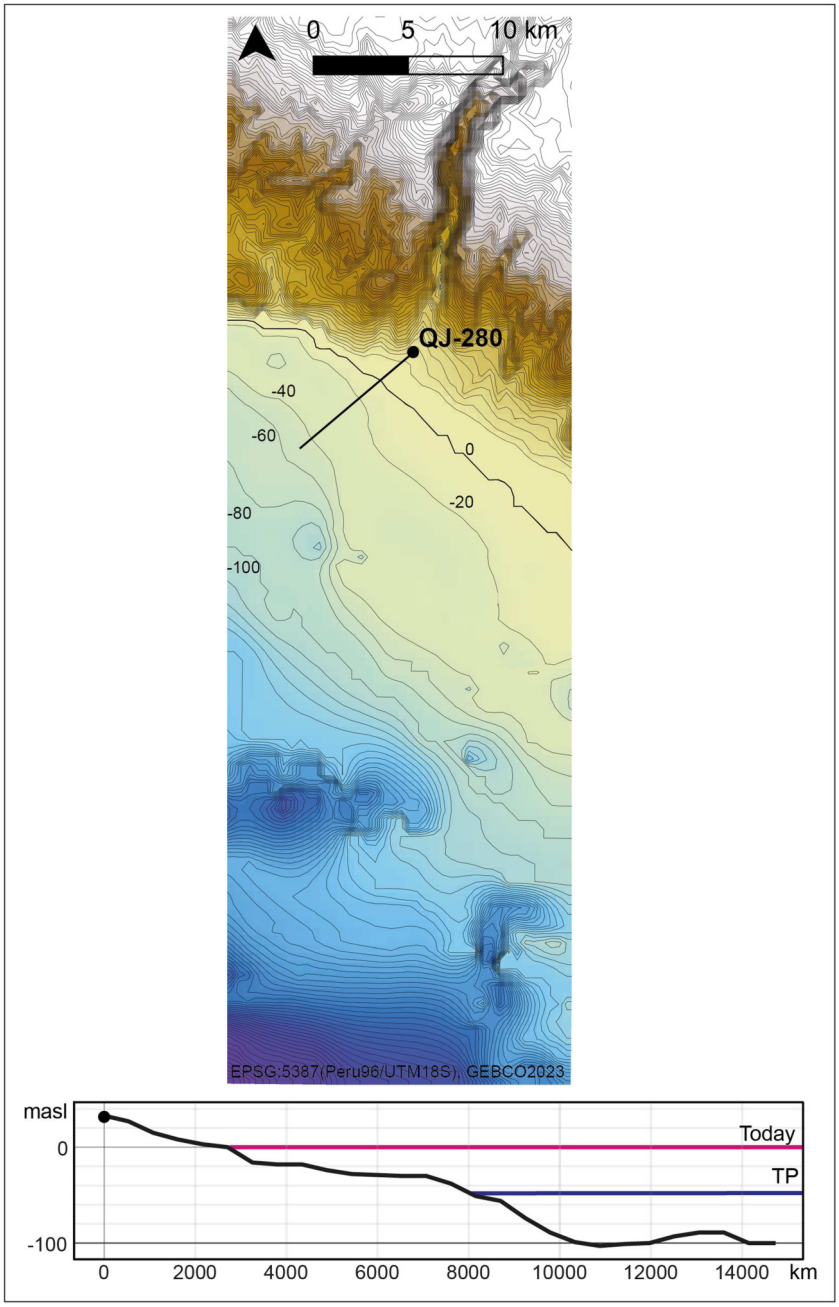

FIGURE 4 | Topographic and bathymetric map and cross-cut section from QJ-280 to Terminal Pleistocene paleoshoreline according to Lambeck et al. (2014).

3.2 | μFTIR

Most minerals were identified using their optical properties. To securely identify some of the minerals observed under the microscope, we conducted μFTIR analyses on the thin sections. This method allows us to detect elements, such as hydrogen and oxygen, that are too light to distinguish by XRF analyses (Mentzer 2017). The Agilent Technologies Cary 610 FTIR microscope in reflectance mode was utilized to collect the data, with 64 co-added scans at a resolution of 2 cm^{-1} within the spectral range of 4000 to 400 cm^{-1}. The data acquisition involved individual point measurements, each covering an approximate rectangular sampling area of variable dimension but typically allowing for the analysis of coarse to fine sand-sized objects or materials. Subsequent interpretation of the acquired spectra relied on reference databases, primarily an in-house reflectance database of the mineral collection curated by Dr. S. Mentzer at the Geoarchaeology Working Group in Tübingen.

3.3 | μXRF

In addition to micromorphology and μFTIR analyses, we performed complementary micro-contextual (Goldberg and Berna 2010; Mallol and Mentzer 2017) analyses to better understand depositional and post-depositional processes, as well as to visualize microstratigraphic fabrics, following techniques employed by Morrissey et al. (2023) and Wurz et al. (2022). The μXRF analyses are complementary to

micromorphology for components that are not visible using thin sections, and to FTIR analyses for minerals that cannot be documented using FTIR because of their bond characteristics or absorption outside of the spectral range. For this, we conducted micro-X-ray fluorescence spectroscopy (μXRF) analyses for elemental identification and mapping. The analyses were performed in the Microanalytic Laboratory of the Geoarchaeology Working Group, University of Tübingen using the Bruker M4 Tornado micro-XRF. We used all five thin sections for μXRF basic elemental identification. The thin sections were scanned under full vacuum with both detectors, a maximum tube voltage of 50 kV and a current of 600 μA. Overview scans of entire thin sections were produced with 50 μm pixel spacing and 25 ms dwell time per pixel. Detailed scans of selected areas had a 30 μm pixel spacing. For data processing, we used the Bruker M4 Tornado Software for elemental selection, deconvolution, and scaling adjustments. For visualization of specific mineral and material components, we processed selected μXRF data using a vector-based graphics software (Adobe Illustrator) to extract specific minerals (or find groups) based on pixel colour from the μXRF maps. For data selection, we divided the elements into those mainly derived from the geogenic component and those that can aid in the visualization of anthropogenic and post-depositional materials. In this second category, we focus on the elements sulphur (S), sodium (Na), chlorine (Cl), phosphorus (P), and calcium (Ca). These include minerals, especially halite (NaCl), that are difficult to identify using optical petrography. Therefore, combining μXRF and micromorphology data allows us to visualize information that otherwise is invisible. Table 1 summarizes the main elements of interest and their relationship to different sedimentary components. The combination of one or two different elements into composite maps using the Bruker M4 Tornado Software then allows for visual representation of a specific (micro-) find group.

To give an example, calcium will highlight different components. Here, these indicate mainly shell and gypsum pedofeatures. However, selecting calcium together with sulphur allows us to visualize both materials, but also to differentiate between the two components. Gypsum will be visualized as a mix of the colours chosen for the selected elements, while shell will be visible as only the colour chosen for calcium.

3.4 | Radiocarbon Dating

Following the 2017 fieldwork, the site chronology was improved using accelerator mass spectrometry (AMS) ages of short-lived carbonized macrobotanical remains, taken proximally to the micromorphological samples. All botanical samples were piece-plotted in situ, and short-lived remains were identified by Brett Furlotte. The samples were processed in the University of Arizona AMS Laboratory by Gregory Hodgins and reported by Furlotte (2024). Both micromorphological block samples reported in this paper include anthropogenic deposits dated from approximately 11.9–11.2 ka.

3.5 | A Macro-Perspective: Paleoshoreline Reconstruction

Londono et al. (2024) present reconstructed paleolandscape data on the archaeological sites of Quebrada de los Burros, Quebrada Tacahuay, the Ring Site, K4, and Quebrada Miraflores, which are located on the southern Peruvian coast, circa 200 km south of Quebrada Jaguay. Following their approach, we used published past sea-level data by Lambeck et al. (2014) and the GEBCO_2023 Gridded Bathymetry dataset with a 15 arc second spatial resolution (GEBCO Bathymetric Compilation Group 2023) to display the paleoshorelines during the initial occupation at Quebrada Jaguay 280.

4 | Results

4.1 | Macro-Level: Paleoshorelines, Geomorphology, and Field Observations

4.1.1 | *Paleoshorelines*

Today, the site is located about 2.5 km from the shoreline; however, during the Terminal Pleistocene (at ~12 ka), about 5.5 km more land surface was exposed, demonstrating that the paleoshoreline would have been approximately 8 km from the site (Figure 4).

TABLE 1 | Element key to mineral and feature/component.

Element	Mineral or rock	Site feature/component
Sulphur (S)	Gypsum ($CaSO_4 \cdot 2H_2O$)	Gypsum pedofeatures
Sodium (Na)	Halite (NaCl)	Salt impregnation
Chlorine (Cl)	Halite (NaCl)	Salt impregnation
Phosphorus (P)	Hydroxyapatite ($Ca_5[OH\|(PO_4)_3]$)	Bone
Calcium (Ca)	Hydroxyapatite ($Ca_5[OH\|(PO_4)_3]$)	Bone
	Gypsum ($CaSO_4 \cdot 2H_2O$)	Gypsum pedofeatures
	Calcite ($CaCO_3$)	Shell
	Aragonite ($CaCO_3$)	Shell
Aluminium (Al)	Various rock-forming minerals/rocks (e.g., granite)	Geogenic components
Iron (Fe)	Various rock-forming minerals/rocks (e.g., granite)	Geogenic components
Silica (Si)	Various rock-forming minerals/rocks (e.g., granite)	Geogenic components
Potassium (K)	Various rock-forming minerals/rocks (e.g., granite)	Geogenic components

4.1.2 | *Geomorphology*

On the modern-day surface of the coastal alluvial fan the complexity of the archaeological site setting is highlighted: In proximity to the archaeological site, besides alluvial and debris flow deposits, we observed dune formation (aeolian processes), thin duricrust developments (precipitation–evaporation processes in hyper-arid settings), as well as volcanic ash deposits (extrusive volcanic deposition) (Figure 5). However, little is known about the actual processes and morphostratigraphy of the coastal alluvial fan and their effect on the archaeological site.

Figure 6 demonstrates that the modern-day surface is almost completely overprinted by recent mining activities. Conclusions about the geomorphological setting are highly impaired and only allow for very broad and general observations. The catchment area of the fan includes the Jaguay watershed (Lehner and Grill 2013; Milton et al. 2022) (Figure 3). Two drainage systems merge into the main feeder channel about 13.5 km north of the site (Figures 4 and 7). The catchment therefore includes material from several formations—a wide range of volcanic, plutonic, and sedimentary sources (Figure 3).

QJ-280 is located about 1 km from the fan apex (Figure 7). Statements about the natural course of the incised channel today are not possible, as the deepest incision is part of the mining area (Figure 6). Besides (dirt) roads, we also observed tyre tracks that are not part of actual roads and document unorganized, unrestricted driving across the fan surface. Extensive quarrying, some shallow, some deeper, on the fan surface is observable. The area of the active depositional lobe is used for irrigation agriculture (Figure 7).

4.1.3 | *Field Observations*

Generally, the archaeological site is composed of an upper sandy unit containing the archaeological deposits, situated atop a clast-supported lower unit of boulders and gravels. The gravel unit is a mix of mostly well-rounded intrusive and extrusive volcanic rocks reflecting the diverse geology of the region as well as the alluvial setting, which is dominated by

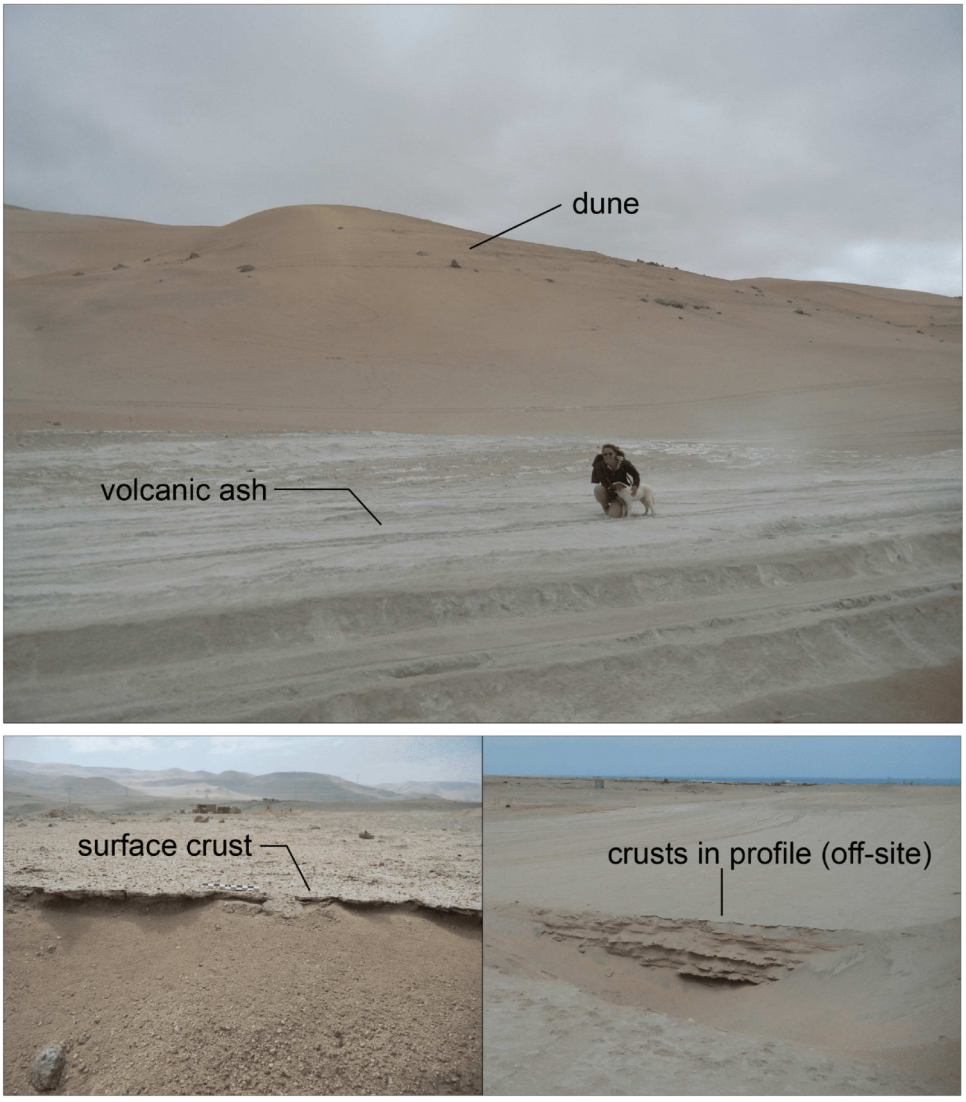

FIGURE 5 | Field photographs of the modern-day landscape surrounding the site, showing a variety of landforms and features, like dune and volcanic ash deposits, as well as the formation of thin surface crusts, as well as buried crusts in profiles off-site. Further, tyre tracks are visible on the surface. Photographs by S.A. Meinekat and C.E. Miller.

FIGURE 6 | Comparison of Sector I/Area 2 between field photos from 1999 (courtesy of D. Sandweiss) and 2017 (photograph by K. Rademaker). Notice the impact of gravel and sand mining in proximity to the archaeological site, severely altering the landscape.

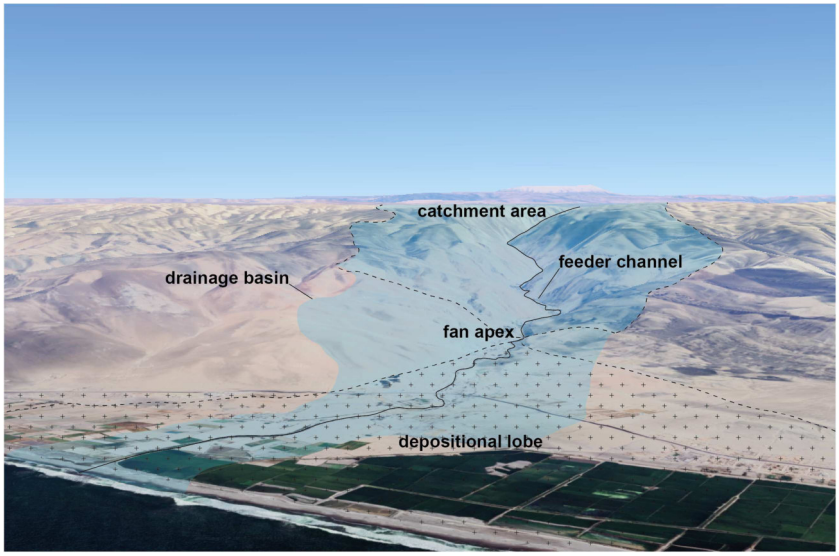

FIGURE 7 | Coastal alluvial fan morphology according to Blair and McPherson (2009) applied to the study area (GoogleEarth). Cross-hatched area overprinted by modern-day road/settlement/agriculture/mining.

debris-flow with expected material transport from the catchment area.

4.1.3.1 | *Area 2/Sector I*

A photomosaic of the north wall of Area 2/Sector I (Figure 8A), from which sample QJ-17-1 was taken, documents a sedimentary sequence characterized by pronounced textural variability and irregular stratigraphic boundaries. The lowermost unit consists of a basal deposit of well-rounded, coarse gravel to cobble-sized clasts, displaying poor sorting and a strongly undulating upper boundary, forming an uneven substrate. This unit is overlain by a sand-dominated deposit.

In the eastern part of the profile, a distinct volcanic ash (tephra) layer is present. This unit is laterally discontinuous and exhibits at least two erosional incisions, producing sharp, concave boundaries. These cuts are subsequently infilled by sand, indicating episodes of reworking and redeposition. Overlying both the ash and sand infill is a further deposit of very coarse, well-rounded gravel, which is laterally restricted and does not extend across the full west–east profile, suggesting localized high-energy depositional conditions.

The first unit containing archaeological material occurs above this gravel layer. In the western portion of the profile, it is expressed as a decimetre-thick, greyish, sand-dominated

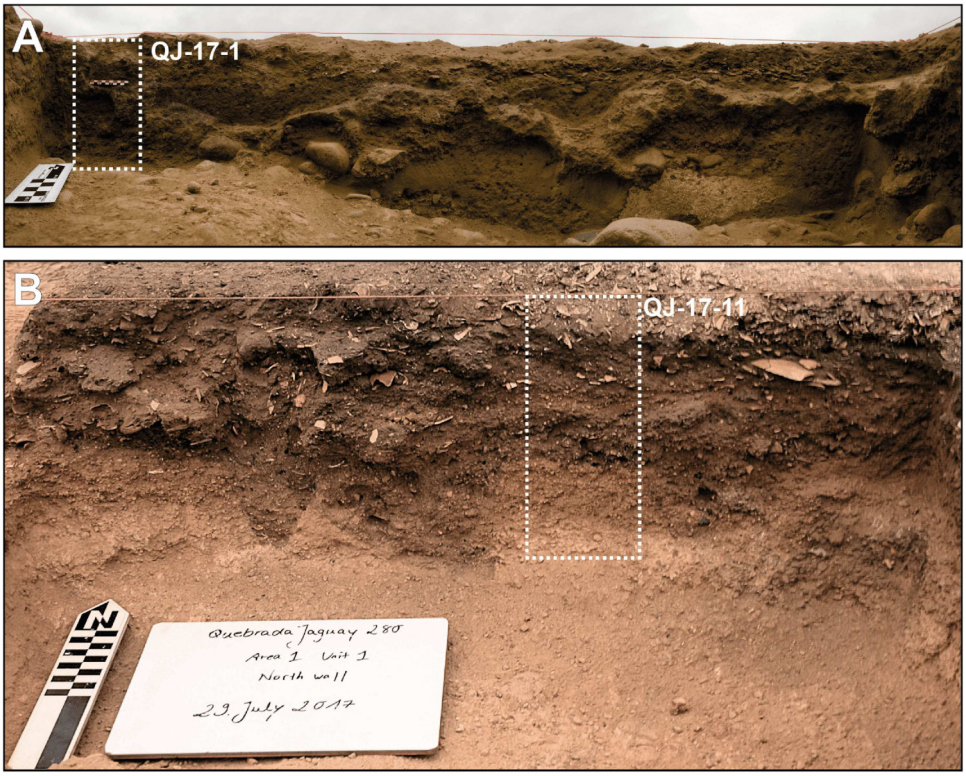

FIGURE 8 | (A) Photomosaic of Sector I north wall/Area 2, Unit 13 south wall with location of block sample QJ-17-1 (white dashed box). (B) Photograph of Area 1 Unit 1 north wall/Unit 2 south wall with location of block sample QJ-17-11 (white dashed box).

horizon with dispersed charcoal and shell fragments. The darker colouration likely reflects an increased organic content. Laterally, towards the east, this stratigraphic level contains isolated, large charcoal fragments, but the sediment matrix becomes coarser, consisting of a heterogeneous mix of sand and gravel with sparse anthropogenic inclusions in the overlying decimetre-thick deposit.

In the western half of the profile, the greyish archaeological horizon thins laterally, pinches out, and assumes a lenticular geometry with a relatively planar upper boundary. This unit is truncated by a small, pit-shaped feature, characterized by a sharp, irregular cut, indicating post-depositional disturbance. The entire sequence is capped by a shell-rich deposit within a sandy matrix, with shell frequency increasing upward. Although shell content is somewhat higher in the eastern half, the unit shows an overall vertical trend towards greater bioclastic concentration.

The uppermost surface consists of a loose, poorly consolidated sandy deposit exhibiting evidence of disturbance. Throughout the profile, sediment interpretation is complicated by zones of indurated material forming a highly undulating fabric, which locally obscures primary stratigraphic boundaries and biases the visual impression of unit continuity (Figure 8A).

4.1.3.2 | *Area 1/Sector II*

In Area 1, sample QJ-17-11 derives from the north wall profile of Unit 1 (Figure 8B). In the field, this profile exposed a sequence of archaeological horizons, with features and suspected biogenic disturbance structures (krotovinas). The lowermost unit consists of a yellowish, gravelly sand with a silty–sandy matrix and sparse gravel-sized clasts, indicating moderate to poor sorting. Unlike the basal deposits in Area 2, this unit lacks abundant coarse fluvial pebbles, suggesting a lower-energy depositional context.

Archaeological occupation horizons are readily distinguished by a darker colour, increased anthropogenic inclusions, and textural contrast, most notably the presence of shell material. The earliest archaeological horizon exhibits multiple cut features penetrating into the underlying sterile substratum, forming sharp, irregular lower boundaries. Overlying occupation layers consist of centimetre-thick, laterally continuous but slightly undulating horizons, composed of sand to silty sand with variable concentrations of shell and charcoal. These units display gradational to clear boundaries.

Localized zones of sediment induration were also observed within this profile; however, cementation is less pervasive and less intense than in Area 2, a difference reflected in the weaker structural coherence of the sediment and the greater ease of monolith sampling. The indurated material occurs discontinuously and does not form a fully cemented horizon in this profile.

To facilitate recovery of macro-artefacts from the indurated sediment fragments, the samples were soaked in water, following Andrus et al. (2000), who demonstrated that the cementing agent responsible for induration in comparable contexts consists predominantly of highly soluble halite. While this treatment enabled the recovery of lithic artefacts—albeit with reduced provenience resolution—it resulted in secondary

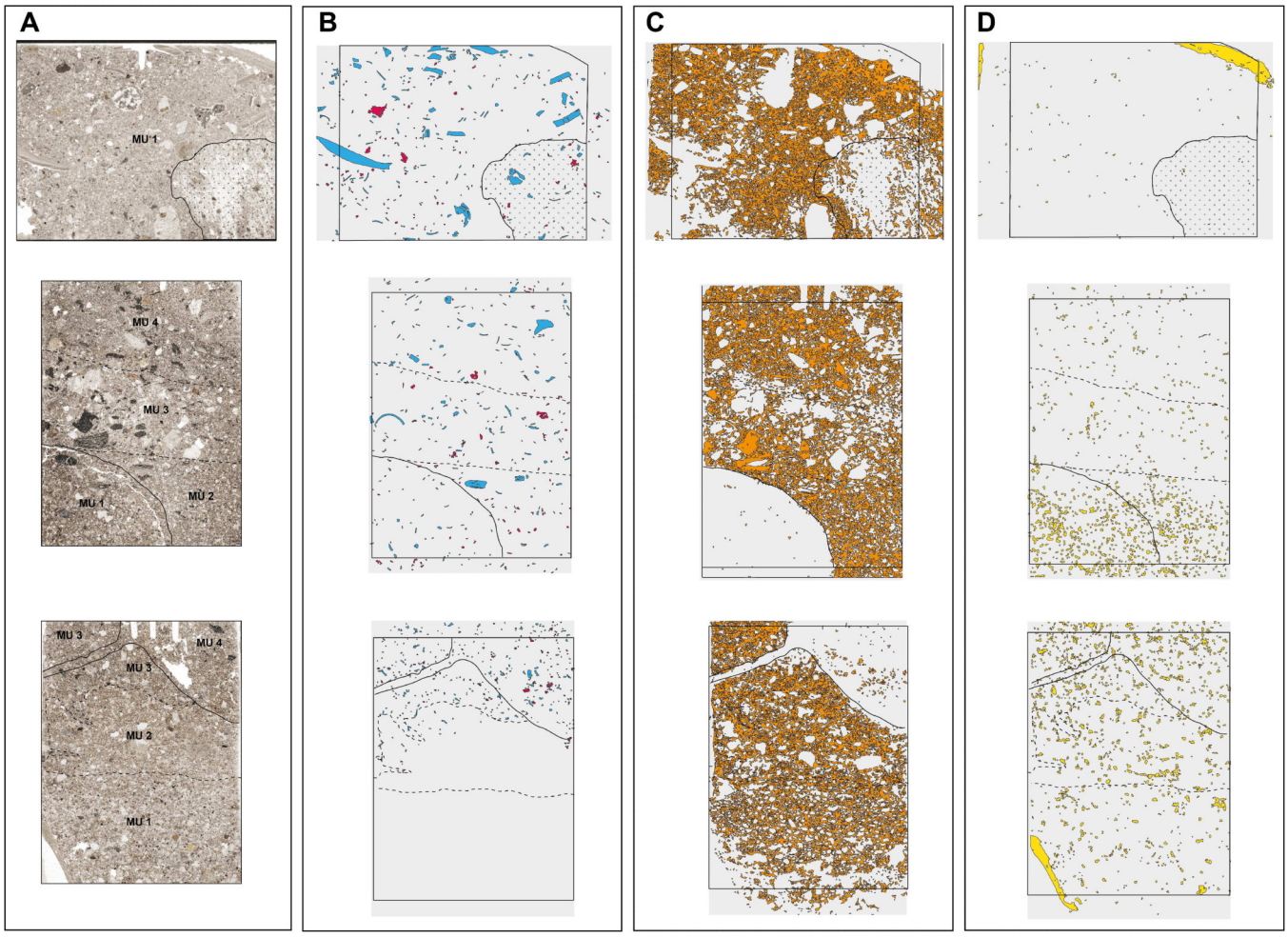

FIGURE 9 | Thin section scans and μXRF component maps of QJ-17-1, bottom to top QJ-17-1A, QJ-17-1B, QJ-17-1C. (A) Scans with micro-units. (B) Shell (blue) and bone (pink) distribution. (C) Halite (orange) distribution. (D) gypsum (yellow) distribution. In the bottom left of QJ-17-1C, a high gypsum accumulation is visible in the XRF map, but that is related to the plaster bandage used for sampling that is included in this thin section. The highest gypsum content in QJ-17-1A is related to part of the plaster bandage used for taking the block sample, which is included at the top of this thin section. In QJ-17-1A, we see a fabrication error on the lower right (and also a bit on the lower left) affecting the elemental distribution (as sample has been ground away), which is why we separated that area from analysis and interpretation.

fragmentation and partial disintegration of more fragile components, particularly charcoal and bone, indicating post-excavation alteration induced by dissolution processes.

4.2 | Microstratigraphy

The micromorphological analyses of five thin sections from QJ-280 led to the distinction of 14 microstratigraphic units (MU) within the five thin sections that are shown in Figures 9 and 10 and summarized in Table 2. Furthermore, we ran μXRF scans on and created elemental maps of all analysed thin sections that we processed to visualize the spatial distribution and abundance of gypsum, halite, bone, and shell content (Figures 9 and 10; Supporting Information S1: SM1).

We used μFTIR analyses to complement μXRF and micromorphological observations. The main goal was to differentiate between anhydrite ($CaSO_4$) and gypsum ($CaSO_4{\cdot}2H_2O$), as this, by the presence or absence of water, hints at distinct formation processes and conditions. Analyses on the thin sections suggest that the mineral formations at QJ are mainly gypsum, as suggested by the presence of H_2O peaks in the 3500–3200 cm^{-1} (O–H stretching) and 1750–1500 cm^{-1} (O–H bending) ranges (Figure 11).

4.2.1 | *Micromorphology Block QJ-17-1*

4.2.1.1 | *Thin Section QJ-17-1C*

In this, and the following thin section results, we describe the MUs from bottom (oldest) to top (youngest) for each thin section.

This thin section covers the deepest deposits in Area 2, Unit 12 south wall (equivalent to Sandweiss' Sector 1, Unit 2B north wall). The thin section covers the transition from a coarse, sandy, archaeologically sterile base layer to the first occupation deposit via gradual fining towards more loamy material.

The first, and lowest, MU (MU1, Figure 12A) is comprised of a coarse sandy component with a single-grain to intergrain microstructure and a mostly undifferentiated b-fabric. Coarse sandy rock fragments dominate this MU with very little silt and clay. No anthropogenic material is included. In the thin section,

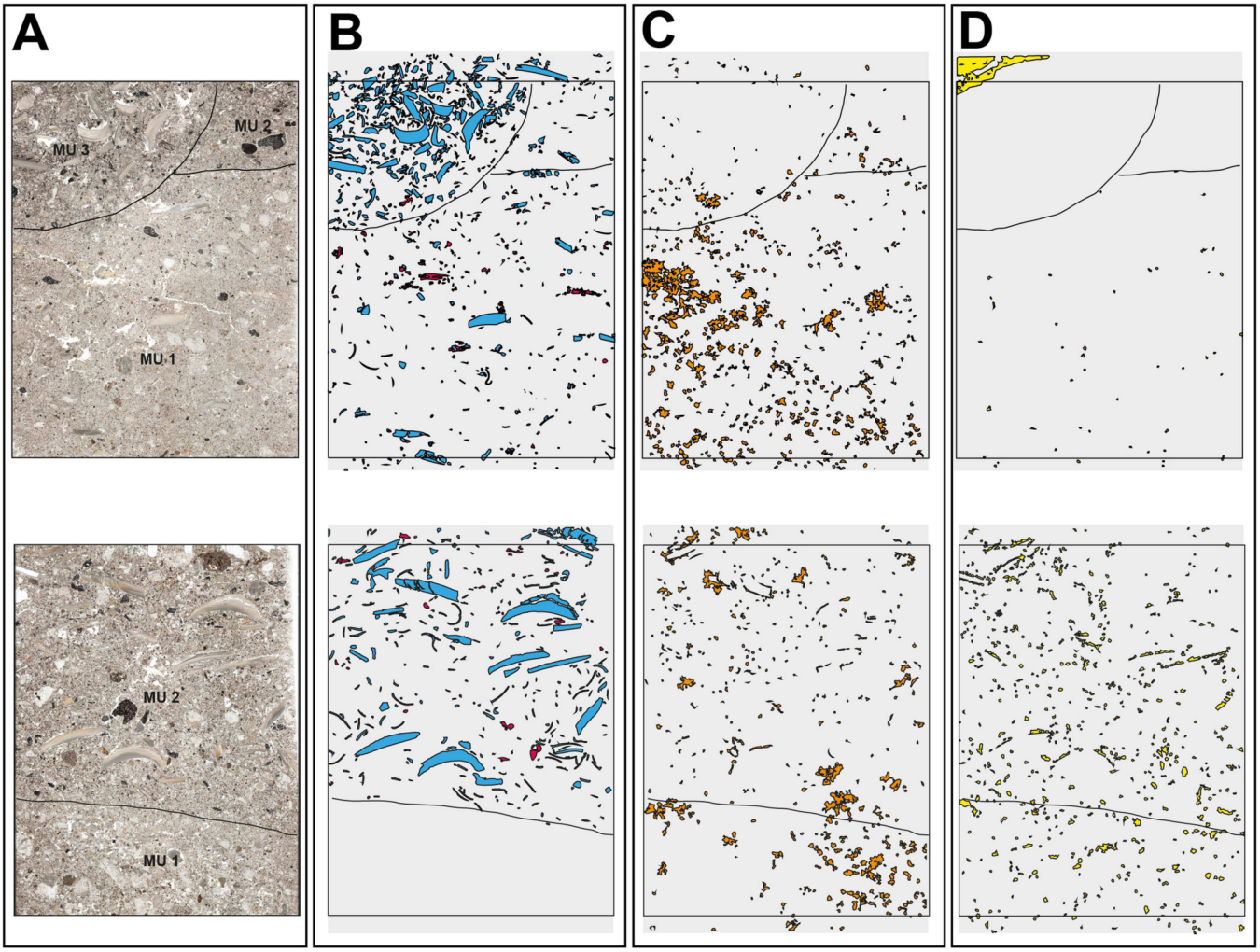

FIGURE 10 | Thin section scans and μXRF component maps of QJ-17-11, bottom to top QJ-17-11A and QJ-17-11B. (A) Scans with micro-units. (B) Shell (blue) and bone (pink) distribution. (C) Halite (orange) distribution. (D) Gypsum (yellow) distribution.

the most prominent pedofeature is the formation of gypsum crystals and nodules. The larger nodules in the groundmass are mostly composed of lenticular-tabular sparitic gypsum.

MU2 is marked by an increase in clay and silt aggregates, resulting in an enaulic c/f-related distribution and granular microstructure (Figure 12B). This MU has a weakly stipple-speckled b-fabric related to the presence of clays. Rock fragments compose the coarse fraction. No anthropogenic material is included. Pedofeatures are similar to MU1, with gypsum crystal and nodule formation. We observe a slight increase in the formation of gypsum nodules with lenticular-tabular crystals.

MU3 comprises the first archaeological layer in this area, as indicated by the calcium distribution in this thin section (Figure 9B). It is limited to the top of the thin section (MU3 and MU4) and correlates with the presence of shell in the archaeological layers. MU3 is similar in terms of groundmass and fabric to MU2, but the coarse fraction now also contains sand-sized, burnt marine shell fragments and sand-sized fragments of charcoal. A few, highly weathered and fractured bone fragments can be identified microscopically. The bone fragments are small, sand-sized, and in the XRF maps are visible as very small fragments of bone, which is indicative of the very poor preservation of bone at the site (Figure 9B). Silt-sized charred organic matter contributes to the fine fraction. In MU3, we also observe a slaking crust, indicative of an originally waterlain deposit that here is not in situ but reworked (Figure 12C). Gypsum formation in MU3 remains similar to MU2 with a very slight increase in gypsum formation (Figure 9D).

MU4 differs from MU3 by a more separated granular microstructure and the presence of channels. The contact of MU4 is a rounded cut through MU3 and into MU2 with a connecting channel that is infilled with MU4 material through MU3. Gypsum formation and inclusion of anthropogenic material remain the same.

The XRF map of the gypsum confirms the microscopic observations for MU2 to MU4. Most of the sulphur is in larger crystals or nodules. Towards the top, smaller crystals increase between the larger nodules. Invisible under the microscope, but visualized in the XRF maps, we observe that halite is present throughout the thin section except in MU1, where the groundmass consists of large clasts, and except for MU4 (Figure 9C). In MU4, little halite is present in crumbs, randomly distributed in the MU (Figure 9C).

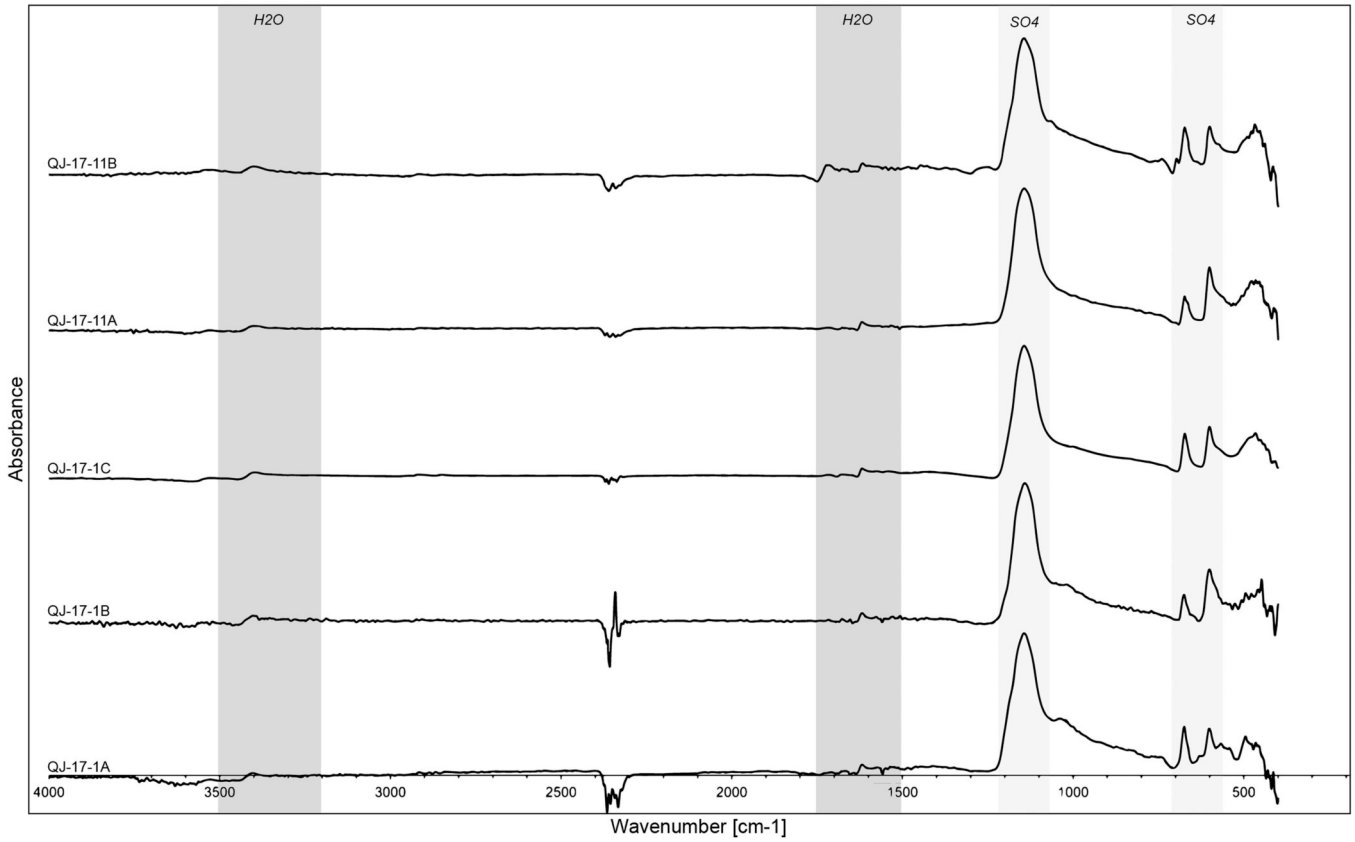

FIGURE 11 | μFTIR spectra of selected gypsum nodules from each thin section. Light grey-shaded areas are SO_4 peaks, present in both gypsum and anhydrite (Chukanov 2014). v_2 (SO_4) peaks around 500 cm^{-1} indicative of gypsum, but spectral resolution is poor < 550 cm^{-1}. Dark grey-shaded areas are H_2O peaks that are only present in gypsum (Chukanov 2014).

4.2.1.2 | *Thin Section QJ-17-1B*

This thin section derives from the same block sample as QJ-17-1C, directly above the previous sample. The first MU (MU1) in this thin section is very similar to MU4 of QJ-17-1C, with a granular microstructure with channels, gypsum crystals and nodules, and broken and weathered burnt shell, charcoal, and bone fragments. The bottom of the thin section indicates a higher amount of gypsum in the sediment, visible as many larger crystals or nodules throughout MU1 and MU2 (Figure 9D).

MU2 appears similar to MU1 at first glance, but the amount of coarse sand-sized coarse fraction, as well as that of the clay and silt aggregates, decreases slightly. The gypsum formations remain the same as in MU1, with crystals and nodules formed of randomly oriented lenticular-tabular crystals. The microstructure is intergrain-granular and less open than in MU1. Anthropogenic contributions, such as shell, bone, and charcoal, remain the same. The biggest difference between MU1 and MU2 is visualized in the XRF map. Halite is present throughout the thin section except where we observe large clasts in the groundmass, and except for MU1, where the feature from QJ-17-1C continues, creating a sharp boundary to MU2.

Atop MU2, MU3 is marked by more prominent changes in the size and distribution of materials, though the overall composition (in terms of types of material) remains the same. While the content of clay and silt aggregates further decreases, the coarse fraction increases in size with more fine gravel-sized clasts present, both in the geogenic and the anthropogenic components (rock fragments and charcoal pieces). The gypsum content decreases, and when present, the nodules and crystals within are smaller, which is confirmed by the XRF map.

The halite distribution in MU3 is especially noteworthy. First, we observe halite forming within the cracks of larger shell fragments (Figures 9C and 12E). Second, bigger charcoal pieces contain halite within the cell tissue as well as in the pores, as shown in the XRF map, while petrographic analysis of the same pieces reveals that the growth of the halite has contributed to in situ fragmentation (Figure 9C). The distribution of the halite within some charcoal pieces shows a concentration of the mineral within the outer zone, and its absence in the centre. This indicates a process of cementation in the pieces proceeding from outside to inside. This process may also correlate with the degree of burning, as these same larger charcoal pieces are not always fully charred but may exhibit an unburnt centre. An overall lack of halite in the area with larger clasts also displays a slight sloping of the surface of MU3.

Above MU3, MU4 exhibits a decrease in the size of coarse fraction components compared to MU3. Here, the most significant change is that, besides sand-sized burnt shell fragments, now also unburnt and larger fragments of shell are frequently present. Shell, charcoal, and bone are all broken and weathered (Figure 12D). The gypsum content remains similar to MU3, with mostly single crystals or small sand-sized nodules visible in these micro-units, indicating fewer and smaller gypsum crystals

TABLE 2 | Summary of micromorphology results, archaeological interpretation.

		Micromorphology			
			Main components		
TS depth (masl)	TS/MU	Groundmass and fabric	Coarse fraction > 20 μm	Fine fraction < 20 μm	Archaeological observations and interpretation
37.48–37.39	QJ-17-1C/1	*Colour*: *c/f rel. distribution*: por-mon-en *Microstructure*: single grain/ intergrain *b-fabric*: undiff. (st.-sp., gr-st.) *Voids*: complex packing *Pedofeatures*: NaCl impregnation (▪ ▪ ▪ ▪), gypsum crystals and nodules (▪ ▪), dusty clay cappings	**Geogenic** *Rock fragments*: granite, ms-cs, (▪ ▪ ▪ ▪ ▪) andesite, ms-cs, (▪ ▪) quarzite, ms-cs, (▪ ▪ ▪) *Mineral grains*: quartz, fs-ms, (▪ ▪ ▪ ▪) magnetite, fs-ms, (▪ ▪ ▪) feldspars, fs-ms, (▪ ▪) mica, fs-cs (▪ ▪) amphiboles, ms, (▪ ▪) **Anthropogenic** None **Biogenic** none	**Geogenic** clay/silt aggregates (▪) **Anthropogenic** None **Biogenic** None	• Sterile substratum • Mostly aeolian deposition
	QJ-17-1C/2	*Colour*: *c/f rel. distribution*: en *Microstructure*: granular *b-fabric*: cryst. (st.-sp.) *Voids*: complex packing *Pedofeatures*: NaCl impregnation (▪ ▪ ▪ ▪ ▪), gypsum crystals and nodules (▪ ▪ ▪), dusty clay cappings	**Geogenic** *Rock fragments*: granite, ms-cs, (▪ ▪ ▪) andesite, ms-cs, (▪ ▪) quarzite, ms-cs, (▪ ▪ ▪) *Mineral grains*: quartz, fs-ms, (▪ ▪ ▪) magnetite, fs-ms, (▪ ▪ ▪) feldspars, fs-ms, (▪ ▪) mica, fs-cs, (▪ ▪) amphiboles, ms, (▪ ▪) **Anthropogenic** None **Biogenic** none	**Geogenic** clay/silt aggregates (▪ ▪ ▪ ▪ ▪) **Anthropogenic** None **Biogenic** none	• Sterile substratum • Reworked slaking crust → alluvial deposition and post-depositional disturbance
	QJ-17-1C/3	*Colour*: *c/f rel. distribution*: en *Microstructure*: granular *b-fabric*: cryst. (st.-sp.) *Voids*: complex packing *Pedofeatures*: NaCl impregnation (▪ ▪ ▪ ▪ ▪), gypsum crystals and	**Geogenic** *Rock fragments*: granite, ms-cs, (▪ ▪ ▪) andesite, ms-cs, (▪ ▪) quarzite, ms-cs, (▪ ▪ ▪) *Mineral grains*: quartz, fs-ms, (▪ ▪ ▪) magnetite, fs-ms, (▪ ▪ ▪)	**Geogenic** clay/silt aggregates (▪ ▪ ▪ ▪) **Anthropogenic** charred organic matter (▪ ▪ ▪) **Biogenic** none	• First archaeological occupation layer • Small combustion residues → domestic area where hearth-related activities took place

(Continues)

TABLE 2 | (Continued)

TS depth (masl)	TS/MU	Micromorphology			Archaeological observations and interpretation
		Groundmass and fabric	Main components: Coarse fraction > 20 μm	Main components: Fine fraction < 20 μm	
		nodules (▪ ▪ ▪), dusty clay cappings	feldspars, fs-ms, (▪ ▪) mica, fs-cs, (▪) amphiboles, ms, (▪ ▪) **Anthropogenic** shell (marine), fs-ms (▪ ▪ ▪), burnt charcoal, fs-cs (▪ ▪ ▪), broken *bone*, ms (▪ ▪), burnt or weathered **Biogenic** none		• Absence of large burnt fragments or well-defined hearth feature → maintenance activities?
	QJ-17-1C/4	*Colour*: ■ *c/f rel. distribution*: en *Microstructure*: granular (v.open) *b-fabric*: cryst. (undiff., st.-sp.) *Voids*: complex packing, channels *Pedofeatures*: NaCl impregnation (▪), gypsum crystals and nodules (▪ ▪ ▪), dusty clay cappings	**Geogenic** *Rock fragments*: granite, ms-cs, (▪ ▪ ▪) andesite, ms-cs, (▪ ▪) quarzite, ms-cs (▪ ▪ ▪) *Mineral grains*: quartz, fs-ms, (▪ ▪ ▪) magnetite, fs-ms, (▪ ▪ ▪) feldspars, fs-ms, (▪ ▪) mica, fs-cs, (▪) amphiboles, ms, (▪ ▪) **Anthropogenic** shell (marine), fs-ms (▪ ▪ ▪), burnt, snapped charcoal, fs-cs, (▪ ▪ ▪), broken *bone*, ms, (▪ ▪), burnt or weathered, reworked, broken **Biogenic** none	**Geogenic** clay/silt aggregates (▪ ▪ ▪ ▪) **Anthropogenic** charred organic matter (▪ ▪ ▪) **Biogenic** none	• Small combustion residues → domestic area where hearth-related activities took place • Absence of large burnt fragments or well-defined hearth feature → maintenance activities? • Reworked material! Bioturbation • Material overall similar to layer above and below, but more open structure and effect on pedofeatures
37.56–37.47	QJ-17-1B/1	*Colour*: ■ *c/f rel. distribution*: en-por *Microstructure*: granular/intergrain *b-fabric*: st.-sp. (undiff., cryst.) *Voids*: complex packing, channels *Pedofeatures*: NaCl impregnation, (▪), gypsum crystals and nodules (▪ ▪ ▪), impure clay cappings	**Geogenic** *Rock fragments*: granite, ms-cs, (▪ ▪ ▪) andesite, ms-cs, (▪ ▪) quarzite, ms-cs, (▪ ▪ ▪) *Mineral grains*: quartz, fs-ms, (▪ ▪ ▪) magnetite, fs-ms, (▪ ▪ ▪) feldspars, fs-ms, (▪ ▪) mica, fs-cs, (▪)	**Geogenic** clay/silt aggregates (▪ ▪ ▪ ▪) **Anthropogenic** charred organic matter (▪ ▪ ▪) **Biogenic** none	• Small combustion residues → domestic area where hearth-related activities took place • Absence of large burnt fragments or well-defined hearth feature → maintenance activities? • Reworked material! Bioturbation

(Continues)

TABLE 2 | (Continued)

TS depth (masl)	TS/MU	Micromorphology			Archaeological observations and interpretation
		Groundmass and fabric	Main components		
			Coarse fraction > 20 μm	Fine fraction < 20 μm	
			amphiboles, ms, (▪ ▪) **Anthropogenic** shell (marine), fs-ms (▪ ▪ ▪), burnt, snapped charcoal, fs-cs, (▪ ▪ ▪), broken bone, ms, (▪ ▪), burnt or weathered, reworked, broken **Biogenic** none		• Material overall similar to layer above and below, but more open structure and effect on pedofeatures • Same as 1C/4
	QJ-17-1B/2	*Colour*: *c/f rel. distribution*: en-por *Microstructure*: granular/intergrain *b-fabric*: st.-sp. (undiff., cryst.) *Voids*: complex packing *Pedofeatures*: NaCl impregnation (▪ ▪ ▪ ▪ ▪), gypsum crystals and nodules (▪ ▪ ▪), dusty clay cappings	**Geogenic** *Rock fragments*: granite, ms-cs, (▪ ▪ ▪) andesite, ms-cs, (▪ ▪) quarzite, ms-cs, (▪ ▪ ▪) *Mineral grains*: quartz, fs-ms, (▪ ▪ ▪) magnetite, fs-ms, (▪ ▪ ▪) feldspars, fs-ms, (▪ ▪) mica, fs-cs (▪) amphiboles, ms, (▪ ▪) **Anthropogenic** shell (marine), fs-ms, (▪ ▪ ▪), burnt, snapped charcoal, fs-cs, (▪ ▪ ▪), broken bone, ms, (▪ ▪), burnt or weathered, reworked, broken **Biogenic** none	**Geogenic** clay/silt aggregates (▪ ▪ ▪) **Anthropogenic** charred organic matter (▪ ▪ ▪) **Biogenic** none	• Small combustion residues → domestic area where hearth- related activities took place • Absence of large burnt fragments or well-defined hearth feature → maintenance activities? • Similar to 1C/3
	QJ-17-1B/3	*Colour*: *c/f rel. distribution*: en-por *Microstructure*: granular/intergrain *b-fabric*: st.-sp. (undiff., cryst.) *Voids*: complex packing *Pedofeatures*: NaCl impregnation (▪ ▪ ▪ ▪ ▪), gypsum crystals and nodules (▪)	**Geogenic** *Rock fragments*: granite, ms-fg, (▪ ▪ ▪) andesite, ms-cs, (▪ ▪) quarzite, ms-cs, (▪ ▪ ▪) *Mineral grains*: quartz, fs-ms, (▪ ▪ ▪) magnetite, fs-ms, (▪ ▪ ▪) feldspars, fs-ms, (▪ ▪) mica, fs-cs, (▪)	**Geogenic** clay/silt aggregates (▪ ▪) **Anthropogenic** charred organic matter (▪ ▪) **Biogenic** none	• Change to larger fragments, both in rock and anthropogenic component (especially charcoal) • Yet, mostly burnt anthropogenic material

(Continues)

TABLE 2 | (Continued)

TS depth (masl)	TS/MU	Micromorphology			Archaeological observations and interpretation
		Groundmass and fabric	Main components: Coarse fraction > 20 μm	Main components: Fine fraction < 20 μm	
			amphiboles, ms, (▪ ▪) **Anthropogenic** shell (marine), fs-fg, (▪ ▪ ▪), burnt, snapped charcoal, fs-fg, (▪ ▪ ▪), broken, not fully charred bone, ms, (▪ ▪), burnt or weathered, reworked, broken **Biogenic** none		
	QJ-17-1B/4	*Colour*: *c/f rel. distribution*: por-en *Microstructure*: granular/intergrain *b-fabric*: undiff. (cryst.) *Voids*: complex packing *Pedofeatures*: NaCl impregnation (▪ ▪ ▪ ▪ ▪), gypsum crystals and nodules (▪)	**Geogenic** *Rock fragments*: granite, ms-cs, (▪ ▪ ▪) andesite, ms-cs, (▪ ▪) quarzite, ms-cs, (▪ ▪ ▪) *Mineral grains*: quartz, fs-ms, (▪ ▪ ▪) magnetite, fs-ms, (▪ ▪ ▪) feldspars, fs-ms, (▪ ▪) mica, fs-cs, (▪) amphiboles, ms, (▪ ▪) **Anthropogenic** shell (marine), fs-fg, (▪ ▪ ▪), burnt and unburnt, snapped charcoal, fs-cs, (▪ ▪ ▪ ▪), broken bone, ms, (▪ ▪ ▪), burnt or weathered, reworked, broken **Biogenic** none	**Geogenic** clay/silt aggregates (▪ ▪) **Anthropogenic** charred organic matter (▪ ▪ ▪) **Biogenic** none	• Still mostly burnt anthropogenic material • Less coarse fragments again, but overall larger and more anthropogenic input than in 1c/3 and 1B/2
37.61–37.55	QJ-17-1A/1	*Colour*: *c/f rel. distribution*: por-en *Microstructure*: granular/intergrain *b-fabric*: st.-sp. *Voids*: complex packing *Pedofeatures*: NaCl impregnation (▪ ▪ ▪ ▪ ▪), gypsum crystals and nodules (▪), impure clay cappings and coatings	**Geogenic** *Rock fragments*: granite, ms-cs, (▪ ▪ ▪) andesite, ms-cs, (▪ ▪) quarzite, ms-cs, (▪ ▪ ▪) *Mineral grains:* quartz, fs-ms, (▪ ▪ ▪ ▪) magnetite, fs-ms, (▪ ▪ ▪) feldspars, fs-ms, (▪ ▪)	**Geogenic** clay/silt aggregates (▪ ▪) **Anthropogenic** charred organic matter (▪) micrite (from shell weathering) (▪ ▪) **Biogenic** None	• Scatter of larger, mostly unburnt shell, some small burnt shell, fewer charcoal pieces

(Continues)

TABLE 2 | (Continued)

TS depth (masl)	TS/MU	Micromorphology			Archaeological observations and interpretation
		Groundmass and fabric	Main components		
			Coarse fraction > 20 μm	Fine fraction < 20 μm	
			mica, fs-cs, (▪ ▪) amphiboles, ms, (▪ ▪) **Anthropogenic** shell (marine), fs-fg, (▪ ▪ ▪), burnt and unburnt, snapped charcoal, fs-ms, (▪ ▪), broken bone, fs, (▪), weathered, reworked, broken **Biogenic** Biopellets (insects?), fs, (▪)		
36.92–36.83	QJ-17-11B/1	*Colour*: *c/f rel. distribution*: en-por-mon *Microstructure*: single grain/ intergrain *b-fabric*: undiff. *Voids*: complex packing *Pedofeatures*: NaCl impregnation (▪ ▪), gypsum crystals and nodules (▪ ▪)	**Geogenic** *Rock fragments*: granite, ms-cs, (▪ ▪ ▪ ▪ ▪) andesite, ms-cs, (▪ ▪) quarzite, ms-cs, (▪ ▪ ▪) *Mineral grains*: quartz, fs-ms, (▪ ▪ ▪ ▪) magnetite, fs-ms, (▪ ▪ ▪) feldspars, fs-ms, (▪ ▪) mica, fs-cs, (▪ ▪) amphiboles, ms, (▪ ▪) **Anthropogenic** None **Biogenic** none	**Geogenic** clay/silt aggregates (▪) **Anthropogenic** None **Biogenic** none	• Sterile substratum
	QJ-17-11B/2	*Colour*: *c/f rel. distribution*: en *Microstructure*: intergrain *b-fabric*: st.-sp. *Voids*: complex packing *Pedofeatures*: NaCl impregnation (▪ ▪), gypsum crystals and nodules (▪ ▪)	**Geogenic** *Rock fragments*: granite, ms-cs, (▪ ▪ ▪) andesite, ms-cs, (▪ ▪) quarzite, ms-cs, (▪ ▪ ▪) *Mineral grains*: quartz, fs-ms, (▪ ▪ ▪) magnetite, fs-ms, (▪ ▪ ▪) feldspars, fs-ms, (▪ ▪) mica, fs-cs, (▪ ▪) amphiboles, ms, (▪ ▪) **Anthropogenic**	**Geogenic** clay/silt aggregates (▪ ▪ ▪) **Anthropogenic** charred organic matter (▪ ▪) **Biogenic**	• Scatter of large, mostly unburnt shell, some small burnt shell, few charcoal pieces

(Continues)

TABLE 2 | (Continued)

TS depth (masl)	TS/MU	Micromorphology			Archaeological observations and interpretation
		Groundmass and fabric	Main components		
			Coarse fraction > 20 μm	Fine fraction < 20 μm	
			shell (marine), cs-g, (▪ ▪ ▪ ▪), unburnt, snapped, oriented charcoal, fs-cs, (▪ ▪), broken bone, ms, (▪ ▪), weathered, reworked, broken **Biogenic** Terrestrial gastropod shell, cs, (▪)		
37.00–36.91	QJ-17-11A/1	*Colour*: *c/f rel. distribution*: mon-por-en *Microstructure*: single grain/ intergrain *b-fabric*: undiff. (st.-sp.) *Voids*: complex packing, channels *Pedofeatures*: NaCl impregnation (▪ ▪ ▪), gypsum crystals and nodules (▪)	**Geogenic** *Rock fragments*: granite, ms-cs, (▪ ▪ ▪ ▪) andesite, ms-cs, (▪ ▪) quarzite, ms-cs, (▪ ▪ ▪) *Mineral grains*: quartz, fs-ms, (▪ ▪ ▪ ▪) magnetite, fs-ms, (▪ ▪ ▪) feldspars, fs-ms, (▪ ▪) mica, fs-cs, (▪ ▪) amphiboles, ms, (▪ ▪) **Anthropogenic** shell (marine), cs-g, (▪ ▪ ▪), unburnt, snapped, oriented charcoal, fs-cs, (▪ ▪), broken bone, ms-cs, (▪ ▪ ▪), weathered, reworked, broken, oriented **Biogenic** none	**Geogenic** clay/silt aggregates (▪) **Anthropogenic** charred organic matter (▪ ▪) **Biogenic** none	• Scatter of larger, mostly unburnt shell, some small burnt shell, fewer charcoal pieces, but overall reduction in size and amount to 1B/2 • Middle of MU almost layer of fragmented bone
	QJ-17-11A/2	*Colour*: *c/f rel. distribution*: en-por-mon *Microstructure*: intergrain *b-fabric*: undiff. (st.-sp., cryst.) *Voids*: complex packing, channels *Pedofeatures*: NaCl impregnation (▪)	**Geogenic** *Rock fragments*: granite, ms-cs, (▪ ▪ ▪) andesite, ms-cs, (▪ ▪) quarzite, ms-cs, (▪ ▪ ▪) *Mineral grains*: quartz, fs-ms, (▪ ▪ ▪ ▪) magnetite, fs-ms, (▪ ▪ ▪) feldspars, fs-ms, (▪ ▪) mica, fs-cs, (▪ ▪) amphiboles, ms, (▪ ▪) **Anthropogenic**	**Geogenic** clay/silt aggregates (▪) **Anthropogenic** charred organic matter (▪ ▪ ▪) **Biogenic** none	• Mostly combustion related/burnt anthropogenic material • Comparable to 1C/3, 1B/2 and 1C/4

(Continues)

TABLE 2 | (Continued)

TS depth (masl)	TS/MU	Micromorphology			Archaeological observations and interpretation
		Groundmass and fabric	Main components		
			Coarse fraction > 20 μm	Fine fraction < 20 μm	
			shell (marine), ms-g, (▪ ▪ ▪), burnt and unburnt, snapped charcoal, fs-cs, (▪ ▪), broken, not fully charred bone, ms, (▪ ▪), burnt, weathered, reworked, broken **Biogenic** none		
	QJ-17-11A/3	*Colour*: ■ *c/f rel. distribution*: mon-por-en *Microstructure*: intergrain (open) *b-fabric:* st.-sp. (undiff., cryst.) *Voids*: complex packing *Pedofeatures*: NaCl impregnation (▪)	**Geogenic** *Rock fragments*: granite, ms, (▪ ▪ ▪) andesite, ms-cs, (▪ ▪) quarzite, ms-cs, (▪ ▪ ▪) *Mineral grains*: quartz, fs-ms, (▪ ▪ ▪ ▪) magnetite, fs-ms, (▪ ▪ ▪) feldspars, fs-ms, (▪ ▪) mica, fs-cs, (▪ ▪) amphiboles, ms, (▪ ▪) **Anthropogenic** shell (marine), cs-g, (▪ ▪ ▪ ▪ ▪), burnt and unburnt, snapped charcoal, fs-cs, (▪ ▪ ▪ ▪), broken, not fully charred bone, ms, (▪ ▪), burnt, weathered, reworked, broken **Biogenic** Unburnt wood fragment, fg, (▪)	**Geogenic** clay/silt aggregates (▪) **Anthropogenic** charred organic matter (▪ ▪ ▪ ▪) micrite (from shell weathering) (▪ ▪) **Biogenic** None	• Completely unoriented mix of larger unburnt shell fragments, smaller burnt shell fragments and small charcoal • Midden/dumping

Abbreviations: cryst. = crystallitic; cs = coarse sand; en = enaulic; fg = fine gravel; fs = fine sand; gr.-st. = grano-striated; mon = monic; ms = medium sand; MU = Micro Unit; por = porphyric; st.-sp. = stipple speckled; TS = thin section; undiff. = undifferentiated, (▪) = very few; (▪ ▪) = few; (▪ ▪ ▪) = common; (▪ ▪ ▪ ▪) = frequent; (▪ ▪ ▪ ▪ ▪) = dominant (like Bullock et al. 1985, but relative amount).

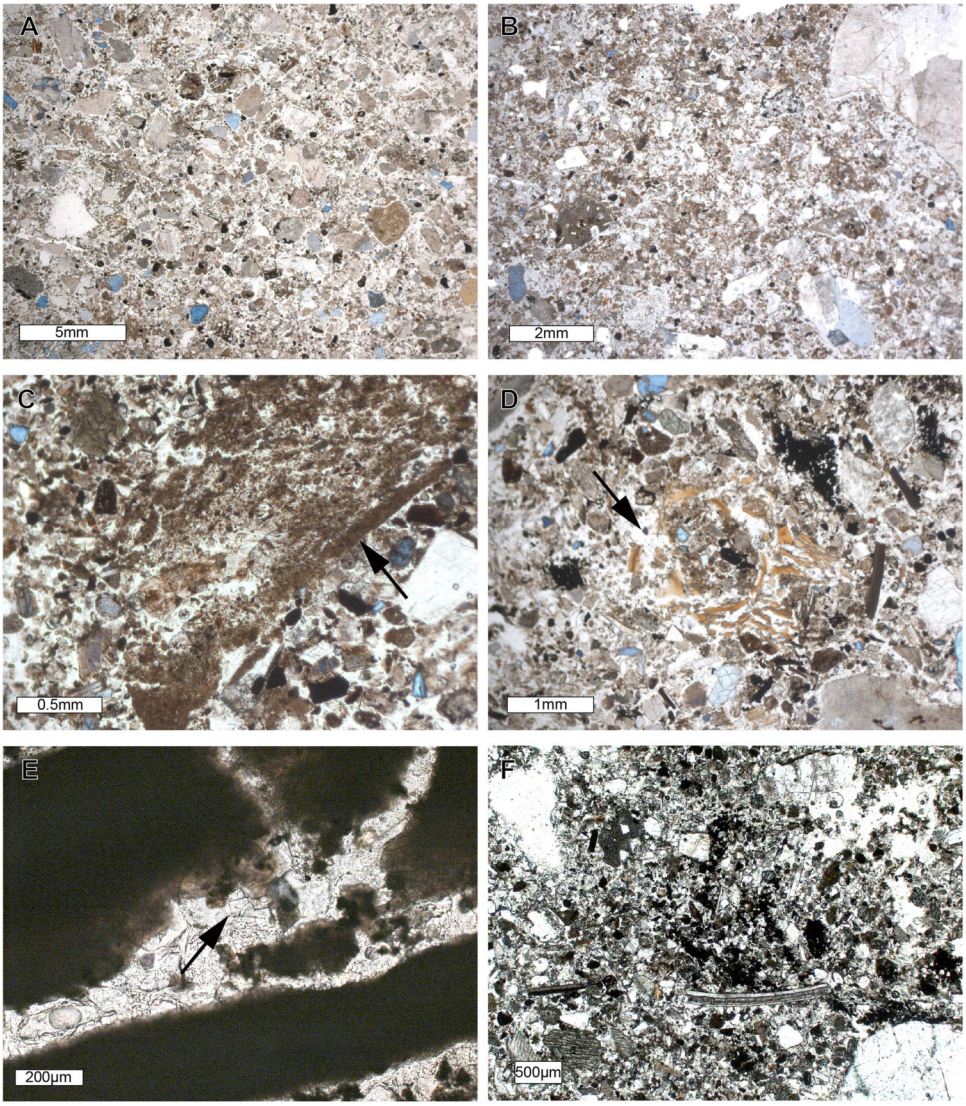

FIGURE 12 | Photomicrographs of QJ-17-1. (A) QJ-17-1C MU1 with sandy groundmass in PPL. (B) QJ-17-1C MU2 with an increase in silt aggregates in PPL. (C) QJ-17-1C MU3 with reworked slaking crust (arrow) in PPL. (D) QJ-17-1C MU4 with weathered fish vertebra (arrow) in PPL. (E) QJ-17-1B, burnt shell with halite forming in weathering cracks, barely visible (arrow) in PPL. (F) QJ-17-1A with shell, charred organic matter in groundmass in PPL.

forming. We can also witness halite present within some of the large charcoal fragments.

Overall, microscopically, as well as in the XRF display, the amount of shell fragments is slightly increasing in this thin section compared to QJ-17-1C, just as the size of the shell fragments is increasing from MU1 and MU2 to MU3 and MU4 throughout this thin section. Bone is visible as dispersed, small fragments throughout the thin section, especially highlighted by the XRF maps.

4.2.1.3 | *Thin Section QJ-17-1A*

This thin section encompasses the top layer of block sample QJ-17-1. This thin section shows only one MU, MU1 (Figure 12F). The amount of charcoal, both in the coarse fraction and in the fine fraction, decreases compared to the previous thin section, resulting in a lighter colour of the sediment. Shell is present—both burnt and unburnt—and larger pieces appear horizontally oriented. The amount of gypsum further decreases to the lowest in the sequence, no larger nodules are formed, and crystals are small sand-sized (Figure 9D). Halite is also present throughout the thin section, similar to the two thin sections before (Figure 9C). However, we also notice a lack of halite at the centre top of the sample, as well as on top, and beneath a large shell piece. We also observe salt forming within the cracks of larger shell fragments. The calcium content in this thin section is mostly linked to shell fragments. There are some bone accumulations visible that are dispersing into the groundmass. When comparing the phosphorus accumulations to the halite distribution, we observe that there is also a high halite concentration present in the areas in which we see bone.

4.2.2 | *Micromorphology Block QJ-17-11*

4.2.2.1 | *Thin Section QJ-17-11B*

This thin section derives from the bottom of block sample QJ-17-11 and includes the deepest archaeological layers in Area 1.

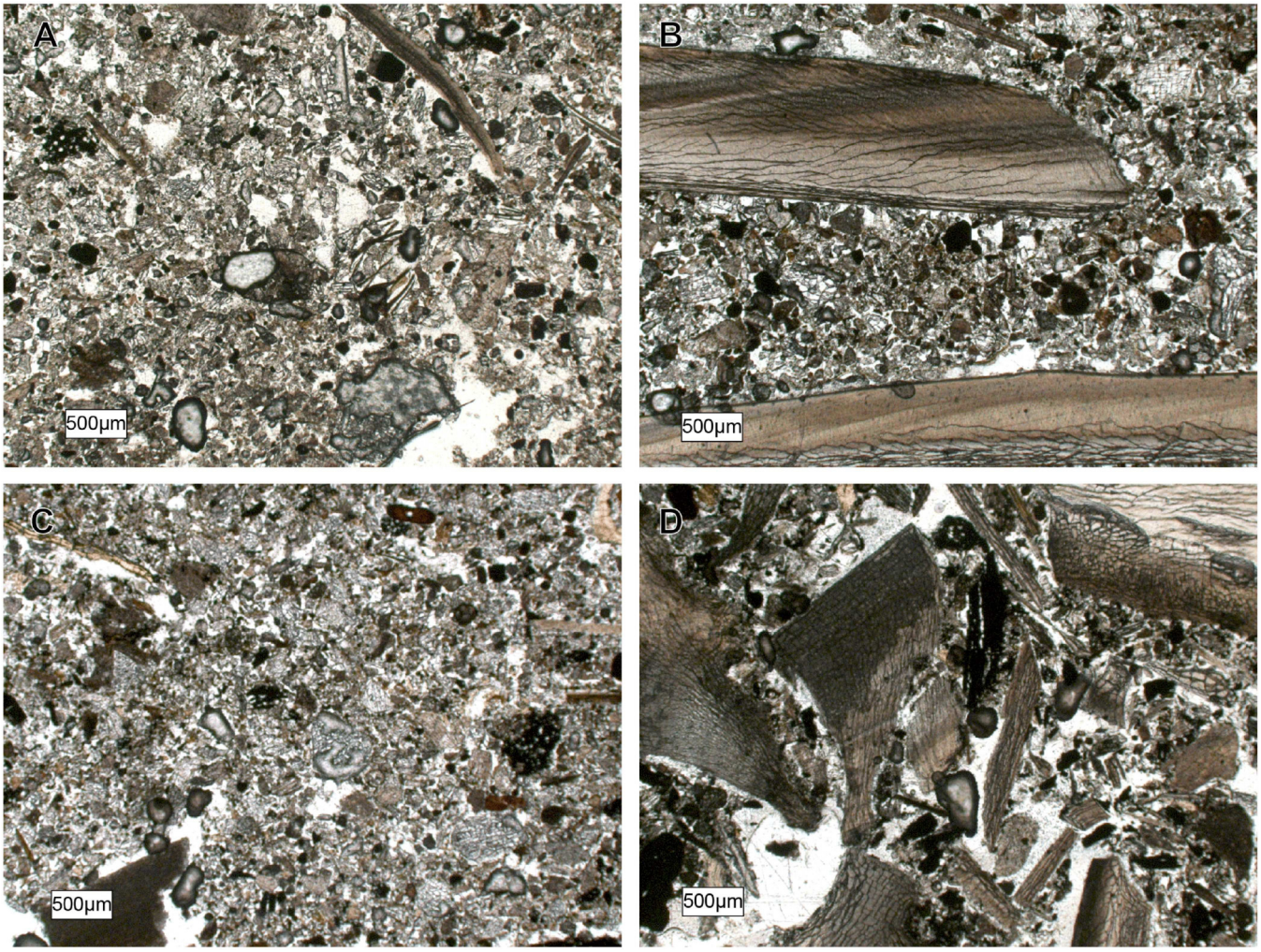

FIGURE 13 | Photomicrographs of QJ-17-11. (A) QJ-17-11B with transition from archaeological sterile MU1 to MU2 with shell and charcoal in PPL. (B) QJ-17-11A MU1 with large, horizontally oriented shell fragments in PPL. (C) QJ-17-11A MU2 with a mix of shell, charred organic matter, and bone fragments. (D) QJ-17-11A MU3 with loosely packed, unoriented shell matrix with some charred matter.

QJ-17-11B comprises two MUs, the lower one, MU1, being the archaeologically sterile sublayer.

In MU1, we see similarities to QJ-17-1C MU1 with a mix of different rock fragments of varying sand sizes (Figures 1 and 13A). In contrast to the transition from MU1 to MU2 in sample QJ-17-1C, however, there is no gradual fining to a clay/silt aggregate-dominated unit in the sterile layer in QJ-17-11B (Figure 13A). We observe some clay and silt aggregates in MU1, but not in the same abundance as in Area 2. There is a slight fining of material at the transition from MU1 to MU2 with a decrease of the very coarse sand fraction, but it is subtle.

Overlying MU1, we encounter MU2, the earliest archaeological deposit in Area 1. Compared to MU1, MU2 exhibits an increase in the amount of clay and silt aggregates. The coarse fraction composition remains similar, but with fewer very coarse rock fragments. The anthropogenic components are dominated by frequent large shell fragments that do not appear to be burned and are in horizontal orientation (Figure 13B). Larger pieces of shell are often broken or snapped in place. The shell fragments are mostly large, though some smaller fragments are also visible through the elemental mapping. Charcoal is also frequent, and we observe some weathering and breakage of the fragments, too. However, it is not as disintegrated and broken into silt-sized fragments as, for example, in QJ-17-1B. The largest piece of charcoal does not appear to be fully charred. There is also some bone found in this MU. The bone fragments are weathered and broken, but do not appear burnt. In the XRF maps, the surface of the bone fragments appears smoother, and the fragments are not as fragmented, indicating a slightly better preservation in some of those fragments than in the thin sections before. Besides a marine shell, we also find a terrestrial gastropod shell in this sample.

Regarding pedofeatures in this sample, we observe gypsum formation as lenticular-tabular crystals and nodules. Some of those gypsum pedofeatures, though also found randomly throughout the groundmass, appear to be concentrated on top of larger clasts in the groundmass (i.e., cappings), which is also shown in the XRF map (Figure 10D). There is no difference in gypsum formation between MU1 and MU2. Also, in the XRF maps, we observe a consistent distribution of gypsum throughout this sample that is mostly visible as larger crystals and nodules and some small crystals (Figure 10D). There does

not appear to be a positive correlation between gypsum and halite formation, but the minerals are also not mutually exclusive. Halite is also distributed throughout the thin section, but there are randomly distributed areas with higher concentrations, and other areas where there is still a noticeable amount, but less halite is present. Halite is oftentimes aggregated around shell fragments. Some shell fragments, especially in the top left of the thin section, exhibit almost a coating of halite, as well as halite within the fractures of the shell fragments (Figure 10C).

4.2.2.2 | Thin Section QJ-17-11A

Sample QJ-17-11A derives from the same slab as QJ-17-11B, above the previous sample. It encompasses the subsequent archaeological layers in this unit. In total, we observe three distinct MUs.

MU1 is overall very similar to MU2 of QJ-17-11B. The main differences lie within the abundance of anthropogenic components, as well as the decrease in the abundance of clay and silt aggregates in the geogenic fine fraction. We observe a decrease in large oriented, unburnt marine shell, but an increase of small burnt shell fragments compared to MU1, resulting in a mix of burnt and unburnt shell but in general lower shell content. The amount and state of preservation of charcoal are comparable to MU2 of QJ-17-11B. One of the most significant changes is in the amount of bone. Bone pieces are mostly visible as very small fragments dispersed in the groundmass throughout the thin section, but the XRF map also visualizes a horizontal concentration in the centre of the thin section (middle of MU1). This unit contains the most bone that we see in any sample from QJ-280. It appears mostly unburnt. Gypsum is present in MU1 as very few nodules and some crystal growths, but the formations are relatively small. In MU1, we notice many aggregated accumulations of halite and an especially large concentration in the centre left of the thin section (Figure 10C).

Conformably overlying MU1, with a gradational transition, we see MU2 as a layer of mixed burnt materials. We observe an increase in charcoal pieces and fine charred organic matter, as well as mostly burnt shell fragments that are weathered, reworked, and broken, with generally no orientation of larger clasts (Figure 13C). Bone fragments are small broken fragments and range from unburnt to burnt, with variation in temperatures based on their optical properties such as colour in PPL and birefringence in XPL (Villagran et al. 2017). There are relatively few coarse rock fragments.

MU3 starkly contrasts visually with the other MUs in this thin section. The contact between MU2 and MU3 is abrupt, sharp, and not horizontal. This contact is a cut, as MU3 cuts through the previous micro-units. MU3 is a layer dominated by large, unburnt, completely unoriented marine shell fragments (Figure 13D). In the finer sand size fraction, burnt, weathered (into micrite) shell is also present (Villagran et al. 2017).

The XRF maps indicate a high calcium content that is linked to a mix of larger and finer shell fragments (Figure 10B). Bone, burnt to different temperatures, charcoal fragments, and one unburnt wood fragment are intermixed in MU3. In the fine fraction, silt-sized charred organic matter is an important contribution. In MU2 and MU3, the amount of gypsum further decreases. Only a few, predominantly microcrystalline, gypsum formations can be found in the groundmass, and there are no larger gypsum nodules. In MU2 and MU3, we observe a decrease in halite content and overall smaller specks become more prevalent compared to larger accumulations.

5 | Discussion

5.1 | Site Formation—Deposition of Sediments and (Paleo-)Landscape

Understanding regional drivers of geomorphic change in the Atacama region is important for disentangling site formation processes. Hartley et al. (2005) and Ortega et al. (2019) suggest that the morphodynamics of coastal alluvial fans in the Atacama region are controlled by climate, the latter pointing out the role of ENSO events in alluvial fan activity. Therefore, ENSO rainfall events, together with the seasonal character of the feeder channels in our study area, are the main drivers of transport and deposition on the coastal alluvial fan. From this, we can deduce a reduced fan activity during the peak aridity of the Middle Holocene, and increased activity and material transport and deposition during wetter phases, such as the CAPE II event during the Terminal Pleistocene and intense El Niño rainfall events during the Holocene. Especially in arid settings, a mix of depositional processes (debris flows, hyperconcentrated flows, sheet flows) is expected, which can occur even within a single intense rainfall event, which creates a highly complex fan system (Cabré et al. 2020; Lehmkuhl et al. 2018; Walk 2020).

The site is located close to the fan apex, which formed within the incised channel region of the system. Prior to human occupation, we observe evidence of clast-rich deposits, indicative of a high-energy depositional regime. We also observe sand deposits, demonstrating some lower energy deposition. The presence of volcanic ash in the Area 2 north wall profile demonstrates that, besides deposition by alluvial activity, volcanic deposition also contributed to landscape formation. Incision of the ash suggests erosional events, such as gullying on the fan surface.

Right before the first occupation layers, we observe lateral variation in the geogenic components between the two excavated areas, with Area 2 exhibiting a higher amount of silt aggregates compared to the sand-dominated matrix in Area 1. These differences reflect micro-regional variations in deposition. The silty deposit may reflect a sheetflow deposit (S. E. Hogg 1982) that has been reworked.

In the first occupation layers, we observe mostly finer (< gravel-sized) geogenic components. We detect no evidence for erosion by water or in situ emplacement of waterlain deposits within the occupation layers. We suggest that geogenic components were likely introduced via aeolian processes. If alluvial action occurred, the flow regime was so low that it did not result in erosion.

The anthropogenic impacts on the modern-day landscape do not allow for direct statements about the morphostratigraphy of the coastal alluvial fan directly surrounding the archaeological site. However, the excavation profiles and thin sections from the deposits at QJ-280 allow us to refine our understanding of the

site setting before and during human occupation. While the modern-day disturbances at QJ-280 preclude statements on diachronic changes and the morphostratigraphy of the coastal alluvial fan beyond the site itself, comparison to coastal alluvial fan systems in the broader region (Walk et al. 2022, 2023) suggests that changes in the location of the active channel caused the differences observed at the site. It is likely that the site preservation is due to its location on an older surface as opposed to the active channel.

5.2 | Post-Deposition: Taphonomy, Pedogenesis, and Paleoenvironment

Focusing on the preserved deposits at QJ-280, we observe several post-depositional processes that affect the archaeological and natural materials at the site. Most of these processes are related to the setting of the site on the arid coast of southern Peru. Most prominently, we observe the formation of salt minerals (halite and gypsum).

5.2.1 | Taphonomy

Most of the anthropogenic components exhibit taphonomic changes. Shell and bone are sometimes snapped, mostly without angular movement of the fragments. Here, it does not necessarily indicate human activity such as trampling (Aldeias and Bicho 2016; Rentzel et al. 2017). Rather, the microscopic observations (Figures 12 and 13) and μXRF maps indicate halite and gypsum crystals formation in the cracks of the shells and bone fragments (Figures 9 and 10). Therefore, we suggest that the formation of salt crystals is one driver leading to the breakage and fragmentation of the faunal remains at the site. The charcoal fragments, too, are affected by this process. The μXRF scans show larger pieces of charcoal almost completely indurated by halite (Figure 9C). Salt action or haloturbation (as defined in Zinelabedin et al. 2025, 258) in the sediment is therefore a major process at the site that has (negatively) affected the preservation of archaeological materials.

As stated, we attempted to resolve this issue by soaking indurated sediment in water to recover cemented artefacts during the 2017 excavations. However, the provenience resolution of those finds is not comparable to screen-recovered or even in situ finds. Further, fragile materials like the charcoal fragments that were impregnated with salts may physically disintegrate when the salts dissolve.

These processes are an issue not only at QJ-280 but also at other archaeological sites along the hyper-arid coast where similar pedogenic processes can be expected.

In fact, similar salt action (terminology varies, some common terms are: induration/indurated sediment, *caliche*, cementation) at archaeological sites has been described at other coastal sites along the South American Pacific coast (in latitudes ranging at least 12°S–25°S)—impacting those excavations. The site of Cerro Los Chivateros on the coast of central Peru was excavated in the 1960s and was described as a deposit that consists of salt-impregnated, indurated soil (R. Berger et al. 1965). At Quebrada Cruz de Hueso (Punta Negra, Department of Lima, Peru), a concretion compacted by salt has been described (Ugarte 2008, 47). Excavation was stopped at 12 cm below the surface due to the induration. Benfer (1990, 288) reports that at the site of Paloma (Chilca valley, Peru), different periods within the stratigraphic sequence were capped by *caliche* caused by intensified moisture. Further, Benfer (1990, 288) points out a temporal factor of the *caliche* formation, as a series of wet years may suffice to impregnate materials. At Quebrada de la Vaca (Department of Arequipa, Peru) indurated sediment has been reported from test Trench 2 (Riddell 2007, 187). The slope of a midden feature is also indurated by salt (Riddell 2007, 187). Indurated deposits are also known from Quebrada Maní in Chile. At QM12, the presence of salt-cemented soil horizons, the authors describe as what is locally known as *caliche*, has been described as 'highly indurated salic and gypsic horizons' after Ericksen (1981) (Latorre et al. 2013, 27). Gypsum formation is also reported at the site of Zapatero in Chile (Power et al. 2022; Villagran et al. 2021).

5.2.2 | Pedogenesis and Paleoenvironment

Salt action appears to be a major pedogenic process at QJ-280. At QJ-280, we observe differences in halite and gypsum formation, as well as variations between the excavation areas. To explain these differences, it is important to understand the origin and depositional history of the salts.

On the arid coast of southern Peru, we expect Aridisol soil formation processes, typical of a dry climate with low humus content and precipitation of translocated salts, and/or, for example, gypsum or carbonates in salic, gypsic, or calcic horizons (Ericksen 1981; Holliday 2004; Schaetzl and Anderson 2005; Voigt et al. 2020). In general, possible sources of pedogenic salts include the in situ weathering of bedrock, aerosols from the Pacific Ocean, salares, or atmospheric dust (Ericksen 1981; Rech et al. 2003; Voigt et al. 2020). However, in the coastal region, Rech et al. (2003) demonstrate that close to the ocean (within 50 km, below 800 masl), over 50% of the analysed soluble salts derive from marine aerosols. On the arid coast, these saline materials mostly precipitated from dry fallout and from condensate droplets formed by low clouds, fog, and dew, particularly in winter, as a surface formation (Ericksen 1981). Eventually, the salts are leached and translocated to deeper soil levels through fog and occasional rainfall (Ericksen 1981). Accordingly, a major source for the soluble salts at QJ-280 is likely marine aerosols.

In the studied mineral formations at the site, halite precipitation did not exhibit clear diachronic changes. But there are differences between the two excavation areas. In Area 2, halite impregnates all of the sediment, with the exception of the section with bioturbation (Figure 9C). This observation, based on the μXRF maps, can be confirmed by field observations. Sampling QJ-17-1 was only possible by using a chisel and hammer due to the hardened nature of the complete block. In contrast, in Area 1, we observe a more 'patchy' halite formation (Figure 10C). Halite formed around (and in) shells and was randomly distributed in the groundmass. Only in QJ-17-11A (MU3 and MU4) is there a decrease that may be correlated with specific micro-units. QJ-17-1 should be seen as an extreme case of halite cementation. The sample was intentionally placed to capture the observed 'induration', extending vertically in the stratigraphic sequence, whereas laterally, the induration was expressed as an undulating subsurface layer in which the

deposits did not seem to be completely cemented, more similar to Area 1 (Figure 8).

In contrast, the gypsum formation at the site exhibits some temporal variation. A peak in gypsum formation is expressed in an overall higher amount, larger crystal growths and nodules of gypsum in the sequence in QJ-17-1C (MU3 and MU4) and QJ-17-1B (MU1 and MU2). These variations are, at least to a certain degree, related to past paleoclimatic conditions. This allows us to use the presence of pedofeatures, mainly the gypsum formation, as a proxy for past climate, complementing established archaeological climate proxies (Sandweiss 2003; Sandweiss et al. 2020).

What is the explanation for this phase of intensified gypsum precipitation? Villagran et al. (2021) correlate larger gypsum growths with lenticular crystals with slower formation associated with relatively more moisture, whereas microcrystalline gypsum formations are used as a proxy for drier conditions based on higher evaporation and more rapid crystal formation (Poch et al. 2010). Therefore, the intensified gypsum formation at Quebrada Jaguay may represent slightly moister conditions during times of precipitation. Further, besides marine aerosols, additional sources for gypsum, such as Andean precipitation and regional evaporite deposits (I. A. Berger and Cooke 1997), as well as organic matter decay (Villagran et al. 2021), have been reported. These sources may contribute to gypsum precipitation at the site. As gypsum formation may also be influenced by the anthropogenic (organic-rich midden) deposits contained in the sequence, gypsum observations should not be used as a climate proxy on their own but rather complement other climate data.

It is difficult to control for the chronology of these processes. The archaeological layers in which the minerals precipitated are at least partially dated to the Terminal Pleistocene/Early Holocene transition. The pedogenic translocation and precipitation processes, however, may have occurred later. After deposition on the surface (i.e., from marine aerosols), mineral precipitation occurs in the subsurface through translocation, within the penetration depth of soil moisture at the wetting front (Amit and Yaalon 1996; Aref 2003; Schaetzl and Anderson 2005).

Attempting to disentangle the relative timing of these processes, we suggest that sediments were first cemented by halite, with some gypsum precipitation occurring simultaneously with the halite precipitation, as indicated by the moderate gypsum formation throughout. This is likely a syndepositional process occurring at the surface (Amit and Yaalon 1996). After the deposition and initial induration with halite, bioturbation occurred, resulting in the desalinization in the disturbed area. The phase of increased gypsum precipitation post-dates the initial halite impregnation and the bioturbation, which is indicated by the intensified gypsum formation occurring independently of the previously described alterations to the deposit (Figure 9). This suggests that the main phase of gypsum formation dates to the Holocene, not the Pleistocene. Following Villagran et al. (2021) and Poch et al. (2010), this main phase, characterized by slightly larger crystals, suggests formation under relatively wetter conditions. Carré et al. (2021) show that compared to the Middle Holocene with the Holocene ENSO minimum (HEM) (3–6 ka), the Early Holocene (11.7–8.2 ka) exhibited reduced SST and a higher ENSO variance, which in turn resulted in more *garúa* (coastal fog) and more rainfall events, creating relatively wetter conditions. Amit and Yaalon (1996) emphasize the differences in gypsum and halite formations as a function of depth relative to the surface and maturity of soil development (time). Evidence for the Late Holocene is missing, as no deposit is preserved at Quebrada Jaguay, so these variables are unknown at QJ-280. Therefore, we can only hypothesize the intensified gypsum formation formed during the relatively more humid Early Holocene, allowing for (1) leaching, and (2) precipitation of larger crystals and nodules.

Another question is: Why does the main phase of intensive gypsum formation post-date the salt formation, since we hypothesize that both the halite and sulphur have the same main source (Ericksen 1981; Rech et al. 2003)? There are some differences between the salt minerals. Due to differences in solubility and permeability, differences in precipitation between halite (highly soluble/deep leaching) and gypsum (less soluble/mean wetting depth) are expected (Amit et al. 1993; Amit and Yaalon 1996; Schaetzl and Anderson 2005). Besides sea spray, gypsum is also a common mineral byproduct of the decay of organic matter from (shell) middens (Villagran et al. 2021), as well as other geological sources can contribute as a gypsum source (I. A. Berger and Cooke 1997). While natural biogenic input at the site is low, the site, while exhibiting a differentiated picture of use during the Terminal Pleistocene, exhibits a rather extensive (in Area 1 and Area 2) capping with an organic shell midden deposit during the Holocene. This deposit may be an additional gypsum source. Villagran et al. (2021) show that weathering processes of shell and bone, together with sulphates from organic matter decay, favour gypsum formation.

Besides precipitation through geogenic sources, halite formation at the site may be influenced by the archaeological deposit. For example, salt minerals are a known component in plant ashes, and evidence for combustion is ubiquitous at the site (Canti 2003). Further, vast amounts of marine resources like shell brought to the site may also have influenced the halite content in the deposit. This would presuppose higher halite concentrations on-site than contemporaneous deposits off-site. However, the presence of indurated sediment off-site suggests that marine aerosols are likely a main source of salt impregnation, as proposed by Rech et al. (2003). Andrus et al. (2000) demonstrate that off-site induration cannot be attributed to salt formation alone, also indicating clay weathering processes. We do not have dated off-site reference samples that would allow for comparison of contemporaneous sediment. In synthesis, we observe (1) lateral variation within the site, (2) lateral variation between the site and off-site, (3) diachronic variation within the site, and (4) temporal, climatic, and depth-dependent pedogenic processes controlling induration dynamics. These factors highly complicate a final interpretation. A more in-depth, landscape-scale approach to soil formation in this setting, similar to Voigt et al. (2020) and Walk et al. (2023), may yield further information on these issues.

Ultimately, these questions cannot be answered unequivocally, considering that the majority of the Holocene deposits are missing due to modern disturbances. Yet, trying to understand the processes behind features, natural and anthropogenic alike, helps in the interpretation of the archaeological record at QJ-280 and other coastal sites exhibiting similar formations.

The indurated sediment has previously been used as a chronostratigraphic marker at QJ-280 (McInnis 1999; Reitz et al. 2016, 2017; Tanner 2001). However, there is no demonstrated positive correlation between salt induration, especially halite, and any single MU. We interpret the salt impregnation as the result of pedogenic processes, such as water and mineral precipitation, percolation and translocation processes down the sequence in relation to the (paleo-)surface, and subject to subsequent post-depositional alterations such as bioturbation. The induration that we encountered in 2017 does not encompass one specific archaeological layer, micro-unit, or occupation surface; therefore, we do not recommend the use of indurated sediment as a chronostratigraphic marker. However, in 1999 in Sector II (Area 1), Sandweiss's team recorded a thick coherent indurated level with indications of formation while a post and panel house was standing. This indurated level was not preserved or encountered in our work, so we cannot assess its use as a chronostratigraphic marker.

5.2.3 | *Bioturbation*

Besides taphonomic and pedogenetic processes, another focus of the micromorphological analysis was on the impact of bioturbation at the site. Most prominently we observed and sampled a krotovina in block sample QJ-17-1 that is present in thin sections QJ-17-1B (MU4) and QJ-17-1C (MU1). These micro-units encompass the krotovina and are characterized by a granular microstructure with channels, but otherwise appear similar to the surrounding sediments—under the microscope. However, the scan of the block sample (Supporting Information S1: SM1) indicates that the sediment of krotovina infilling differs from the surrounding deposit. Further, the μXRF scans exhibit the most significant difference. The bioturbated area is almost completely desalinated, except for a few, randomly oriented specs of halite.

Why is the bioturbation desalinated? One possible answer would be that, originally, the sediment within the krotovina was also impregnated by salt and through the bioturbation process, the halite was dissolved. Another option is that the krotovina was infilled with material from elsewhere in the site that had not been cemented with halite to the degree that the surrounding sediment has. This would imply sediment transport through the archaeological deposit, which can potentially impact the integrity of the find. Based on the observations from the scans, where we can observe macroscopic differences between infilling and surrounding material, the latter option appears more likely.

What does this observation imply for archaeological interpretations? Evidence for bioturbation at QJ-280 is indicated by the presence of small-scale channels, which are typically attributed to insects and other soil mesofauna, but also by a large krotovina, usually attributed to larger animals, that can move material through the deposit (Bocek 1986; Courty et al. 1989; Stein 1983). One concern is that vertical krotovinas can also mimic circular, anthropogenic features. Especially at QJ-280, where circular features were interpreted as postmolds of early residential structures (Jones et al. 2019; Sandweiss et al. 1998; Tanner 2001), the presence of bioturbation suggests that such features require further analysis to distinguish between bioturbation and anthropogenic activity. However, Sandweiss (e.g. 2014) found a piece of wood interpreted as a post fragment in situ in one of the holes, confirming that at least some of the holes (which form a coherent pattern for a structure) were postmolds.

5.3 | Outlook: Archaeological Interpretations and Human Behaviours

Though this paper focuses on the overall site setting and formation, the analysed thin sections also provide insights into early human activities at QJ-280.

5.3.1 | *Anthropogenic Components*

We observe differences between the two areas, as well as between the different micro-units of each thin section, supporting inferences pertaining to lateral and diachronic variation in the deposition of materials. Villagran (2014) has highlighted that the processes associated with shell mound deposition may reveal insights beyond simple 'waste deposition'. Beyond the differential accumulation of deposits at QJ-280, anthropogenically derived components at the site include charred organic matter, bone fragments, and shell valves.

5.3.1.1 | *Charred Organic Matter*

The charred organic matter is visible both as very fine matter distributed through the sediment, leading to a dark colour of the sediment (in the field used to define 'features', e.g., Feature 17–20), or as larger charcoal fragments. Part of the organic material was likely introduced to the site as fuel for maintaining fires and building hearths, for example, for cooking, while other charred remains could be identified as comestible taxa (Furlotte 2024).

5.3.1.2 | *Bone*

Recovered bone fragments derive from fish and small mammals (Reitz et al. 2016 2017) (Figure 12, see Villagran et al. 2017 for comparison). However, bones visible in the thin section samples are usually very small (fine sand-sized to small gravel-sized), complicating identification. Some of the bone appears thermally altered at 'lower' temperatures (beige-brown colour scale), with a small portion appearing to have been exposed to high enough temperatures to calcine bone (Ellingham et al. 2015; Stiner et al. 1995; Villagran et al. 2017). Much of the bone is broken in situ and distributed into the groundmass—a result of the salt action induced taphonomy. Further, disintegrating and very low-density bone may hint at the presence of fish bone when compared to reference micrographs of fish bone (Villagran et al. 2017).

5.3.1.3 | *Shell*

Shell valves display the most variation in composition, ranging from sand-sized pieces to near-complete valves. The smallest pieces appear altered into micrite, which indicates burning. However, larger chunks of shell rarely show signs of complete burning, except for the occasional observed burned rim.

Villagran et al. (2011) and Balbo et al. (2010) argue that shells with low fragmentation and sub-horizontal distribution represent waste discard outside of the living spaces, indicating a single tossing event (Villagran 2019). This description fits the

observations from Area 1 in thin sections QJ-17-11B (MU2) and QJ-17-11A (MU1), as well as in Area 2 in sample QJ-17-1A, where the anthropogenic input of the earliest occupation layer is dominated by large and mostly unburnt (i.e., not visually thermally altered), horizontally oriented shells with low fragmentation and some larger charcoal pieces. In these samples, the shell content is relatively low, with no shell-supported matrix but a sandy/geogenic matrix, which may point towards a more peripheral position within the dwelling site.

When it comes to interpreting burned shell, it is important to bear in mind that different signatures are expected depending on the applied cooking practices (Aldeias et al. 2019). Some cooking practices may leave the shells unaltered, and some shell consumption may not involve cooking at all (Aldeias et al. 2019). Complete burning (and transformation into micrite) of shells, however, can be used as an indicator for tossing of the shells directly into the fire or for the shells being part of the substrate beneath the fire (Aldeias et al. 2019; Villagran 2014).

5.3.2 | *Combustion, Maintenance, and Deposition*

The three observed anthropogenic components (charcoal, bone, and shell) can all be related to combustion practices and are expected in combustion features. However, Aldeias et al. (2019) argue that with shell cooking practices, we may not always expect to find 'intact' combustion features because different practices, such as building a fire above the shells, will result in dispersed and swept combustion features in which we observe a disconnection among fire, residues, and deposits rather than intact hearths (sensu (Mentzer 2012). Further, Aldeias et al. (2019) propose that visible combustion features that resemble in situ hearths may be related to cooking practices like building the fire below the shells. Therefore, the presence of completely burned shell fragments mixed with other combusted material likely indicates a fireplace, rather than a roasting hearth (Aldeias et al. 2019), and/or a swept combustion feature where only smaller fragments are preserved (Miller et al. 2010).

In the Area 2 samples, QJ-17-1C (MU3) and QJ-17-1B (MU2-4), and Area 1 sample QJ-17-11A (MU2), the mostly small and completely burned fragments of shell and finely dispersed charred organic matter suggest these areas were used as a fireplace, and/or maintained by cleaning out the combustion structures. In QJ-17-1B (MU3) larger charcoal pieces, together with larger rock fragments, suggests non-thorough cleaning, or proximity to the centre of a hearth (Miller et al. 2010).

In sample QJ-17-11A (MU3), components are mixed, including some burnt and unburnt shell intermingled with bone within a clast-supported matrix, suggesting dumping or tossing into a midden (Aldeias and Bicho 2016; Miller et al. 2010; Shillito et al. 2011; Villagran 2019). There are no micro-laminations and no sedimentary breaks visible within MU4, from which we can infer that the deposit visible in MU4 of QJ-17-11A was likely tossed in a single and rapidly deposited event (Aldeias and Bicho 2016; Duarte et al. 2019).

5.3.3 | *Use of Space and Occupation*

Overall, the microstratigraphic analysis provides evidence for differentiated uses of space at QJ-280. Such spatial variability can be linked to site maintenance and spatial organization, contrasting the living spaces and refuse or waste disposal areas.

The first occupation layer in Area 1 suggests an activity area used for peripheral refuse and waste disposal, as indicated by the low fragmentation and sub-horizontal distribution of the shell. In later periods, there is a shift towards a possible living space with an increase in anthropogenic components and charred material. This layer is later overprinted by refuse or dumping deposits, which are a mixed and unoriented shell-matrix deposit.

In Area 2, the earliest occupation layers represent a living space, with indications of fire maintenance and sparse waste disposal, suggesting site maintenance. Friesem et al. (2024) suggest that a critical threshold for people to maintain a dwelling site is about two weeks of occupation. This observation is supported by the previously suggested seasonal occupation of the site during the austral summer when freshwater is available in the *quebrada* and isotopic data from the shell midden (Gruver 2018; Sandweiss et al. 1998). In the Holocene deposits that were still available for study in Area 2 in 2017, there is a shift towards more of a refuse deposit, similar to Area 1. The profile photograph (Figure 8A) demonstrates how the occupation layers become capped with shell, following a shift in use of space from primary occupation to a tossing area, as described by Balbo et al. (2010) at Tunel VII.

Overall, the anthropogenic signatures observed in the microstratigraphy are best explained by relatively rapid, short-lived events rather than prolonged occupations. Considering that a one-time tossing event may build up a few decimetres of midden deposit, the deposits at QJ are very shallow and do not point towards a prolonged use of the same space. However, microstratigraphic observations suggest that lateral shifts of dwelling areas on the terrace are likely. Villagran et al. (2011) further demonstrate that substantial spatial variation within a deposit can occur even within a single context—in their case, within one hut.

Hence, it is important to note that these statements are specific to the locality of the samples. Though our sampling strategy represents key areas identified in the 2017 excavations, it is possible––and likely––that there are more lateral variations present at the site that have not been captured by the two block samples but are suggested by comparing the 1996 and 2017 excavations. Especially in the later, Holocene deposits, we observe a definite increase in what appears to be dumped shell valve deposits (similar to MU4 in QJ-17-11A). However, comparison of the 1996 and 2017 stratigraphic profiles reveals the loss of most of the Holocene deposits due to present-day mining activities in the quebrada, especially the use of heavy earth-moving machinery on the terrace.

Still, interpretations from the five thin sections highlight the potential of a micro-contextual approach to contribute to our understanding of activities and occupation intensity at QJ-280. Future work focused on field-identified anthropogenic features, such as a hearth, pits, and postholes, may prove a promising approach to further understand human behaviours at QJ-280.

6 | Conclusion

We applied a multi-method approach, combining micromorphology, μXRF, and μFTIR to develop a formation model

for Quebrada Jaguay 280, a Pleistocene–Holocene site on the southern Peruvian coast. With this, we combine a wide range of microscopic approaches on the micro-scale but also tie these micro-results into landscape-scale observations. Thereby, we critically test existing hypotheses pertaining to forager behaviour within the framework of the site setting. Our results demonstrate the potential of a micro-contextual approach for revealing new information about the stratigraphy, about taphonomic and formation processes, and about aspects of human activity, including site use, maintenance, and occupation intensity.

At the macro-scale, geomorphological observations reveal that prior to human occupation, the location of the site was situated within the active fan system. During human occupation, we suggest that the active system had shifted further away from the site, evidenced by a lack of deposition (or erosion) by water, ultimately favouring preservation of the archaeological site. However, modern gravel and sand mining of the quebrada channel and bulldozing of the terrace surface do not allow for specifications about the morphostratigraphy of the coastal alluvial fan surrounding the archaeological site.

On the micro-scale, using a range of microanalytical methods, it was possible to identify several sedimentary components, depositional agents, and spatiotemporal changes in the deposit of the archaeological site. Perhaps the most notable stratigraphic feature was the formation of an 'indurated layer', which has been recognized at QJ-280, as well as across various desert-coastal sites in the region. A key observation of this study is that salt formation does not relate to specific occupation phases or micro-units but forms by pedogenic processes. The induration is not an appropriate chronostratigraphic marker for the parts of the site preserved for study in 2017, although these differ significantly from what was found in the 1990s.

The combination of micromorphology and μXRF further allowed us to address methodological issues of optical petrography, as the combined approach allows us to map and better understand the relationship between halite and gypsum formation, which are difficult to observe using optical petrography alone. Halite and gypsum formation appear as a syndepositional process of coastal fog precipitation, incorporating marine aerosols, on the surface that is affected by post-depositional translocation processes. Further, we identify paleoclimatic links in the gypsum formation that suggest intensified gypsum formation during relatively more humid phases.

The combined micromorphological and μXRF data demonstrate that the part of Area 2 covered by our sample likely served first as a living space, later shifting to a refuse area, while the part of Area 1 covered by our sample exhibits indicators of a refuse area almost throughout. Further, the observations at the micro-scale from Area 2 indicate possible site maintenance, suggesting a more intensively used area. The thickness of the shell deposits also provides insights into the likely duration of site use, specifically, the relatively shallow contexts suggest that site areas were not used longer than a few weeks at a time, an observation consistent both with Sandweiss et al.'s (1998) predictions of seasonal site use and Gruver (2018) corroborating isotopic evidence from the site's surf clams.

The behavioural observations from QJ-280 have important implications for early coastal archaeology in western South America. While the site was used repeatedly from at least the Terminal Pleistocene to Middle Holocene, it likely served as a temporary camp in a wider settlement system. However, supporting this interpretation will require additional insights from botanical, lithic, and faunal analyses, as well as further geoarchaeological investigations focused on samples from anthropogenic features.

Author Contributions

Sarah A. Meinekat: conceptualization, data curation, formal analysis, investigation, methodology, validation, visualization, writing – original draft, writing – review and editing. **Emily B. P. Milton:** writing – review and editing. **Daniela P. Osorio:** writing – review and editing. **Susan M. Mentzer:** methodology, writing – review and editing. **Christopher E. Miller:** resources, supervision, writing – review and editing. **Daniel H. Sandweiss:** writing – review and editing. **Kurt Rademaker:** funding acquisition, project administration, resources, supervision, writing – review and editing.

Acknowledgements

Excavations at Quebrada-Jaguay 280 were authorized by the Peruvian Ministry of Culture (Resolución Directoral Nacional 205-2017). We thank Co-PI Cecilia Mauricio. The National Science Foundation (Grant BCS-1659015 to K.R.) funded the fieldwork and laboratory analyses. Additionally, the Deutsche Forschungsgemeinschaft (DFG) funded the purchase of the FTIR (M 1748/1-1). Open Access funding enabled and organized by Projekt DEAL.

Endnotes

[1] ka = thousands of calibrated years ago using SHCal20 (A. G. Hogg et al. 2020).

References

Abbott, M. B., B. B. Wolfe, A. P. Wolfe, et al. 2003. "Holocene Paleohydrology and Glacial History of the Central Andes Using Multiproxy Lake Sediment Studies." *Palaeogeography, Palaeoclimatology, Palaeoecology* 194, no. 1: 123–138. https://doi.org/10.1016/S0031-0182(03)00274-8.

Abele, G. 1990. "Salzkrusten, salzbedingte Solifluktion und Steinsalzkarst in der nordchilenisch-peruanischen Wüste." *Mainzer Geographische Studien* 34: 23–46.

Acosta, H., M. Oviedo, J. Rodríguez, and A. Alván. 2010a. "Actividad tectónica del sistema de fallas Cincha-Lluta Incapuquio durante la evolución de la cuenca Arequipa en el Jurásico." *Congreso Peruano de Geología* 15: 742–745.

Acosta, H., M. Oviedo, J. Rodríguez, and A. Alván. 2010b. "Mapa geológico y perfiles del Cuadrángulo de Ocoña (33p-I, 33p-II, 33p-III and 33p-IV) [Map].

Aldeias, V., and N. Bicho. 2016. "Embedded Behavior: Human Activities and the Construction of the Mesolithic Shellmound of Cabeço da Amoreira, Muge, Portugal." *Geoarchaeology* 31, no. 6: 530–549. https://doi.org/10.1002/gea.21573.

Aldeias, V., S. Gur-Arieh, R. Maria, P. Monteiro, and P. Cura. 2019. "Shell We Cook It? An Experimental Approach to the Microarchaeological Record of Shellfish Roasting." *Archaeological and Anthropological Sciences* 11, no. 2: 389–407. https://doi.org/10.1007/s12520-016-0413-1.

Alván, A., and H. von Eynatten. 2014. "Sedimentary Facies and Stratigraphic Architecture in Coarse-Grained Deltas: Anatomy of the Cenozoic Camaná Formation, Southern Peru (16°25′ S to 17°15′ S)." *Journal of South American Earth Sciences* 54: 82–108. https://doi.org/10.1016/j.jsames.2014.04.008.

Alván, A., H. von Eynatten, I. Dunkl, and A. Gerdes. 2015. "Zircon U–Pb Geochronology and Heavy Mineral Composition of the Camaná Formation, Southern Peru: Constraints on Sediment Provenance and Uplift of the Coastal and Western Cordilleras." *Journal of South American Earth Sciences* 61: 14–32. https://doi.org/10.1016/j.jsames.2015.02.008.

Amit, R., and D. H. Yaalon. 1996. "The Micromorphology of Gypsum and Halite in Reg Soils—The Negev Desert, Israel." *Earth Surface Processes and Landforms* 21, no. 12: 1127–1143. https://doi.org/10.1002/(SICI)1096-9837(199612)21:12<1127::AID-ESP656>3.0.CO;2-G.

Amit, R., R. Gerson, and D. H. Yaalon. 1993. "Stages and Rate of the Gravel Shattering Process by Salts in Desert Reg Soils." *Geoderma* 57, no. 3: 295–324. https://doi.org/10.1016/0016-7061(93)90011-9.

Andrus, C. F. T., D. E. Crowe, and D. H. Sandweiss. 2000. "Anthropogenic Induration of Sediments at the Terminal Pleistocene Peruvian Site Quebrada Jaguay." Geological Society of America Meeting Program A276, Boulder, CO.

Aref, M. A. M. 2003. "Classification and Depositional Environments of Quaternary Pedogenic Gypsum Crusts (Gypcrete) From East of the Fayum Depression, Egypt." *Sedimentary Geology* 155, no. 1: 87–108. https://doi.org/10.1016/S0037-0738(02)00162-8.

Armijo, R., R. Lacassin, A. Coudurier-Curveur, and D. Carrizo. 2015. "Coupled Tectonic Evolution of Andean Orogeny and Global Climate." *Earth-Science Reviews* 143: 1–35. https://doi.org/10.1016/j.earscirev.2015.01.005.

Baker, P. A., and S. C. Fritz. 2015. "Nature and Causes of Quaternary Climate Variation of Tropical South America." *Quaternary Science Reviews* 124: 31–47.

Baker, P. A., G. O. Seltzer, S. C. Fritz, et al. 2001. "The History of South American Tropical Precipitation for the Past 25,000 Years." *Science* 291, no. 5504: 640–643. https://doi.org/10.1126/science.291.5504.640.

Balbo, A., X. S. Villagran, M. Madella, A. Vila, and J. Estevez. 2010. "An Experimental Approach for Archeological Soil Micromorphology: Building a Model for Site Taphonomy in Coastal Shell Middens of the Beagle Channel (Argentina)." *Geophysical Research Abstracts* 12: 2906.

Benfer, R. A. 1990. "The Preceramic Period Site of Paloma, Peru: Bioindications of Improving Adaptation to Sedentism." *Latin American Antiquity* 1, no. 4: 284–318. https://doi.org/10.2307/971812.

Beresford-Jones, D., A. G. Pullen, O. Q. Whaley, et al. 2015. "Re-Evaluating the Resource Potential of Lomas Fog Oasis Environments for Preceramic Hunter–Gatherers Under Past ENSO Modes on the South Coast of Peru." *Quaternary Science Reviews* 129: 196–215. https://doi.org/10.1016/j.quascirev.2015.10.025.

Berger, I. A., and R. U. Cooke. 1997. "The Origin and Distribution of Salts on Alluvial Fans in The Atacama Desert, Northern Chile." *Earth Surface Processes and Landforms* 22, no. 6: 581–600. https://doi.org/10.1002/(SICI)1096-9837(199706)22:6<581::AID-ESP714>3.0.CO;2-4.

Berger, R., G. J. Fergusson, and W. F. Libby. 1965. "UCLA Radiocarbon Dates IV." *Radiocarbon* 7: 336–371. https://doi.org/10.1017/S0033822200037310.

Betancourt, J. L., C. Latorre, J. A. Rech, J. Quade, and K. A. Rylander. 2000. "A 22,000-Year Record of Monsoonal Precipitation From Northern Chile's Atacama Desert." *Science* 289, no. 5484: 1542–1546. https://doi.org/10.1126/science.289.5484.1542.

Bird, B. W., M. B. Abbott, D. T. Rodbell, and M. Vuille. 2011. "Holocene Tropical South American Hydroclimate Revealed From a Decadally Resolved Lake Sediment δ18O Record." *Earth and Planetary Science Letters* 310, no. 3: 192–202. https://doi.org/10.1016/j.epsl.2011.08.040.

Blair, T., and J. McPherson. 2009. "Processes and Forms of Alluvial Fans." In *Geomorphology of Desert Environments*, edited by A. J. Parsons and A. D. Abrahams, 413–467. Springer.

Bocek, B. 1986. "Rodent Ecology and Burrowing Behavior: Predicted Effects on Archaeological Site Formation." *American Antiquity* 51, no. 3: 589–603. https://doi.org/10.2307/281754.

Bullock, P., N. Fedoroff, and A. Jongerius. 1985. *Handbook for Soil Thin Section Description*. Waine Research Publications. https://research.wur.nl/en/publications/handbook-for-soil-thin-section-description.

Bush, M. B., B. C. S. Hansen, D. T. Rodbell, et al. 2005. "A 17 000-year History of Andean Climate and Vegetation Change From Laguna de Chochos, Peru." *Journal of Quaternary Science* 20, no. 7/8: 703–714. https://doi.org/10.1002/jqs.983.

Bustamante, M. G., F. W. Cruz, M. Vuille, et al. 2016. "Holocene Changes in Monsoon Precipitation in the Andes of NE Peru Based on δ18O Speleothem Records." *Quaternary Science Reviews* 146: 274–287. https://doi.org/10.1016/j.quascirev.2016.05.023.

Cabré, A., G. Aguilar, A. E. Mather, V. Fredes, and R. Riquelme. 2020. "Tributary-Junction Alluvial Fan Response to an ENSO Rainfall Event in the El Huasco Watershed, Northern Chile." *Progress in Physical Geography: Earth and Environment* 44, no. 5: 679–699. https://doi.org/10.1177/0309133319898994.

Canti, M. G. 2003. "Aspects of the Chemical and Microscopic Characteristics of Plant Ashes Found in Archaeological Soils." *CATENA, Achievements in Micromorphology* 54, no. 3: 339–361. https://doi.org/10.1016/S0341-8162(03)00127-9.

Carrè, M., I. Bentaleb, M. Fontugne, and D. Lavallee. 2005. "Strong El Niño Events During the Early Holocene: Stable Isotope Evidence From Peruvian Sea Shells." *Holocene* 15, no. 1: 42–47. https://doi.org/10.1191/0959683605h1782rp.

Carré, M., J. P. Sachs, S. Purca, et al. 2014. "Holocene History of ENSO Variance and Asymmetry in the Eastern Tropical Pacific." *Science* 345, no. 6200: 1045–1048. https://doi.org/10.1126/science.1252220.

Carré, M., P. Braconnot, M. Elliot, et al. 2021. "High-Resolution Marine Data and Transient Simulations Support Orbital Forcing of ENSO Amplitude Since the Mid-Holocene." *Quaternary Science Reviews* 268: 107125. https://doi.org/10.1016/j.quascirev.2021.107125.

Chauchat, C. 2006. "Prehistoria de la costa norte del Perú: El Paijanense de Cupisnique." Institut français d'études andines, Patronato Huacas del Valle Moche.

Cheng, H., A. Sinha, F. W. Cruz, et al. 2013. "Climate Change Patterns in Amazonia and Biodiversity." *Nature Communications* 4, no. 1: 1411. https://doi.org/10.1038/ncomms2415.

Chukanov, N. V. 2014. *Infrared Spectra of Mineral Species: Extended Library*. Springer Netherlands Imprint: Springer.

Cosentino, N. J., T. E. Jordan, L. A. Derry, and J. P. Morgan. 2015. "87Sr/86Sr in Recent Accumulations of Calcium Sulfate on Landscapes of Hyperarid Settings: A Bimodal Altitudinal Dependence for Northern Chile (19.5°S–21.5°S)." *Geochemistry, Geophysics, Geosystems* 16, no. 12: 4311–4328. https://doi.org/10.1002/2015GC005954.

Courty, M. A., P. Goldberg, and R. Macphail. 1989. *Soils and Micromorphology in Archaeology*. Cambridge University Press.

Cross, S. L., P. A. Baker, G. O. Seltzer, S. C. Fritz, and R. B. Dunbar. 2000. "A New Estimate of the Holocene Lowstand Level of Lake Titicaca, Central Andes, and Implications for Tropical Palaeohydrology." *Holocene* 10, no. 1: 21–32. https://doi.org/10.1191/095968300671452546.

de Haas, T., D. Ventra, P. E. Carbonneau, and M. G. Kleinhans. 2014. "Debris-Flow Dominance of Alluvial Fans Masked by Runoff Reworking and Weathering." *Geomorphology* 217: 165–181. https://doi.org/10.1016/j.geomorph.2014.04.028.

Dillehay, T. D., D. Bonavia, S. L. Goodbred, M. Pino, V. Vásquez, and T. R. Tham. 2012. "A Late Pleistocene Human Presence at Huaca Prieta, Peru, and Early Pacific Coastal Adaptations." *Quaternary Research* 77, no. 3: 418–423. https://doi.org/10.1016/j.yqres.2012.02.003.

Dillehay, T. D., J. Rossen, G. Maggard, K. Stackelbeck, and P. Netherly. 2003. "Localization and Possible Social Aggregation in the Late Pleistocene and Early Holocene on the North Coast of Perú." *Quaternary International* 109–110: 3–11. https://doi.org/10.1016/S1040-6182(02)00198-2.

Dillon, M., M. Nakazawa, and S. Leiva. 2003. *The Lomas Formations of Coastal Peru: Composition and Biogeographic History*. Vol. 43, 1–9. Feild Museum of Natural History.

Dillon, M., S. Leiva González, M. Zapata, P. Lezama, and V. Quipuscoa Silvestre. 2011. "Floristic Checklist of the Peruvian Lomas Formations." *Arnaldoa* 18: 7–32.

Duarte, C., E. Iriarte, M. Diniz, and P. Arias. 2019. "The Microstratigraphic Record of Human Activities and Formation Processes at the Mesolithic Shell Midden of Poças de São Bento (Sado Valley, Portugal)." *Archaeological and Anthropological Sciences* 11, no. 2: 483–509. https://doi.org/10.1007/s12520-017-0519-0.

Ekdahl, E. J., S. C. Fritz, P. A. Baker, C. A. Rigsby, and K. Coley. 2008. "Holocene Multidecadal- to Millennial-Scale Hydrologic Variability on the South American Altiplano." *Holocene* 18, no. 6: 867–876. https://doi.org/10.1177/0959683608093524.

Ellingham, S. T., T. J. Thompson, M. Islam, and G. Taylor. 2015. "Estimating Temperature Exposure of Burnt Bone—A Methodological Review." *Science & Justice* 55, no. 3: 181–188. https://doi.org/10.1016/j.scijus.2014.12.002.

Engel, F.-A. 1981. *Prehistoric Andean Ecology: Man Settlement and Environment in the Andes: Volume II: The Deep South*. Humanities Press.

Ericksen, G. E. 1981. "Geology and Origin of the Chilean Nitrate Deposits." Professional Paper 1188, 37. U.S. Geological Survey. https://doi.org/10.3133/pp1188.

Fick, S. E., and R. J. Hijmans. 2017. "Worldclim 2: New 1-km Spatial Resolution Climate Surfaces for Global Land Areas." *International Journal of Climatology* 37, no. 12: 4302–4315. https://doi.org/10.1002/joc.5086.

Friesem, D. E., N. Lavi, S. Lew-Levy, and A. H. Boyette. 2024. "Mobility, Site Maintenance and Archaeological Formation Processes: An Ethnoarchaeological Perspective." *Journal of Anthropological Archaeology* 74: 101588. https://doi.org/10.1016/j.jaa.2024.101588.

Furlotte, B. A. 2024. "Hunting for the Gathering: Terminal Pleistocene and Early Holocene Plant Resource Exploitation at the Quebrada Jaguay (QJ-280) Site, Southern Coastal Peru." Master Thesis, University of Saskatchewan. https://hdl.handle.net/10388/15768.

Garreaud, R. D., M. Vuille, R. Compagnucci, and J. Marengo. 2009. "Present-Day South American Climate." *Palaeogeography, Palaeoclimatology, Palaeoecology* 281, no. 3: 180–195. https://doi.org/10.1016/j.palaeo.2007.10.032.

GEBCO Bathymetric Compilation Group. 2023. "GEBCO 2023 Grid—A Continuous Terrain Model of the Global Oceans and Land [Dataset]." NERC EDS British Oceanographic Data Centre NOC. https://doi.org/10.5285/f98b053b-0cbc-6c23-e053-6c86abc0af7b.

Goldberg, P., and F. Berna. 2010. "Micromorphology and Context." *Quaternary International, Geoarchaeology and Taphonomy* 214, no. 1: 56–62. https://doi.org/10.1016/j.quaint.2009.10.023.

Goudie, A. S., E. Wright, and H. A. Viles. 2002. "The Roles of Salt (Sodium Nitrate) and Fog in Weathering: A Laboratory Simulation of Conditions in the Northern Atacama Desert, Chile." *Catena* 48, no. 4: 255–266. https://doi.org/10.1016/S0341-8162(02)00028-0.

Grosjean, M., L. Núñez, I. Cartajena, and B. Messerli. 1997. "Mid-Holocene Climate and Culture Change in the Atacama Desert, Northern Chile." *Quaternary Research* 48, no. 2: 239–246. https://doi.org/10.1006/qres.1997.1917.

Gruver, S. 2018. "Occupational Seasonality and Paleoenvironmental Reconstruction at Quebrada Jaguay 280." Master thesis, Northern Illinois University. https://huskiecommons.lib.niu.edu/allgraduatethesesdissertations/7082.

Haaland, M. M., M. Czechowski, F. Carpentier, M. Lejay, and B. Vandermeulen. 2019. "Documenting Archaeological Thin Sections in High-Resolution: A Comparison of Methods and Discussion of Applications." *Geoarchaeology* 34, no. 1: 100–114. https://doi.org/10.1002/gea.21706.

Hartley, A. J., A. E. Mather, E. Jolley, and P. Turner. 2005. "Climatic Controls on Alluvial-Fan Activity, Coastal Cordillera, Northern Chile." *Geological Society, London, Special Publications* 251, no. 1: 95–116. https://doi.org/10.1144/GSL.SP.2005.251.01.08.

Hillyer, R., B. G. Valencia, M. B. Bush, M. R. Silman, and M. Steinitz-Kannan. 2009. "A 24,700-yr Paleolimnological History From the Peruvian Andes." *Quaternary Research* 71, no. 1: 71–82. https://doi.org/10.1016/j.yqres.2008.06.006.

Hogg, A. G., T. J. Heaton, Q. Hua, et al. 2020. "SHCal20 Southern Hemisphere Calibration, 0-55,000 Years Cal BP." *Radiocarbon* 62, no. 4: 759–778. https://doi.org/10.1017/RDC.2020.59.

Hogg, S. E. 1982. "Sheetfloods, Sheetwash, Sheetflow, Or...?" *Earth-Science Reviews* 18, no. 1: 59–76. https://doi.org/10.1016/0012-8252(82)90003-4.

Holliday, V. T. 2004. *Soils in Archaeological Research*. Oxford University Press.

Houston, J. 2006. "Evaporation in the Atacama Desert: An Empirical Study of Spatio-Temporal Variations and Their Causes." *Journal of Hydrology* 330, no. 3: 402–412. https://doi.org/10.1016/j.jhydrol.2006.03.036.

Houston, J., and A. J. Hartley. 2003. "The Central Andean West-Slope Rainshadow and Its Potential Contribution to the Origin of Hyper-Aridity in the Atacama Desert." *International Journal of Climatology* 23, no. 12: 1453–1464. https://doi.org/10.1002/joc.938.

Jackson, D., C. Méndez, R. Seguel, A. Maldonado, and G. Vargas. 2007. "Initial Occupation of the Pacific Coast of Chile During Late Pleistocene Times." *Current Anthropology* 48: 725–731. https://doi.org/10.1086/520965.

Jones, K. B., G. W. L. Hodgins, and D. H. Sandweiss. 2019. "Radiocarbon Chronometry of Site QJ-280, Quebrada Jaguay, a Terminal Pleistocene to Early Holocene Fishing Site in Southern Peru." *Journal of Island and Coastal Archaeology* 14, no. 1: 82–100. https://doi.org/10.1080/15564894.2017.1338316.

Keefer, D. K., S. D. deFrance, M. E. Moseley, J. B. Richardson, D. R. Satterlee, and A. Day-Lewis. 1998. "Early Maritime Economy and El Niño Events at Quebrada Tacahuay, Peru." *Science* 281, no. 5384: 1833–1835. https://doi.org/10.1126/science.281.5384.1833.

Lambeck, K., H. Rouby, A. Purcell, Y. Sun, and M. Sambridge. 2014. "Sea Level and Global Ice Volumes From the Last Glacial Maximum to the Holocene." *Proceedings of the National Academy of Sciences* 111, no. 43: 15296–15303. https://doi.org/10.1073/pnas.1411762111.

Latorre, C., C. M. Santoro, P. C. Ugalde, et al. 2013. "Late Pleistocene Human Occupation of the Hyperarid Core in the Atacama Desert, Northern Chile." *Quaternary Science Reviews* 77: 19–30.

Lehmkuhl, F., V. Nottebaum, and D. Hülle. 2018. "Aspects of Late Quaternary Geomorphological Development in the Khangai Mountains and the Gobi Altai Mountains (Mongolia)." *Geomorphology* 312: 24–39. https://doi.org/10.1016/j.geomorph.2018.03.029.

Lehner, B., and G. Grill. 2013. "Global River Hydrography and Network Routing: Baseline Data and New Approaches to Study the World's Large River Systems." *Hydrological Processes* 27, no. 15: 2171–2186. https://doi.org/10.1002/hyp.9740.

Liebmann, B., and C. R. Mechoso. 2011. "The South American Monsoon System." In *The Global Monsoon System*, Vol. 5, 137–157. World Scientific.

Llagostera, A., R. Weisner, G. Castillo, M. Cervellino, and M. Costa-Junquiera. 2000. "El complejo Huentelauquen bajo una perspectiva macroespacial y multidisciplinaria." *Contribuciones Arqueologicas Museo Regional de Atacama* 1, no. 5: 461–480.

Londono, A. C., S. D. de France, and M. E. LeBlanc. 2024. "Coastal Paleolandscapes of Far Southern Peru: Implications for Late Pleistocene

Human Settlement." *Journal of Island and Coastal Archaeology* 19, no. 1: 211–228. https://doi.org/10.1080/15564894.2022.2030826.

Maggard, G. J. 2010. "Late Pleistocene-Early Holocene Colonization and Regionalization in Northern Perú: Fishtail and Paiján Complexes of the Lower Jequtepeque Valley." Doctoral Dissertations, University of Kentucky. https://uknowledge.uky.edu/cgi/viewcontent.cgi?article=1090&context=gradschool_diss.

Maldonado, A., J. L. Betancourt, C. Latorre, and C. Villagran. 2005. "Pollen Analyses From a 50 000-yr Rodent Midden Series in the Southern Atacama Desert (25° 30′ S)." *Journal of Quaternary Science* 20, no. 5: 493–507. https://doi.org/10.1002/jqs.936.

Mallol, C., and S. M. Mentzer. 2017. "Contacts Under the Lens: Perspectives on the Role of Microstratigraphy in Archaeological Research." *Archaeological and Anthropological Sciences* 9, no. 8: 1645–1669. https://doi.org/10.1007/s12520-015-0288-6.

Marcazzan, D., and S. A. Meinekat. 2022. "Creating Qualitative Datasets in Geoarchaeology: An Easy-Applicable Description Template for Archaeological Thin Section Analysis Using Stoops 2003." *MethodsX* 9: 101663. https://doi.org/10.1016/j.mex.2022.101663.

McInnis, H. 1999. "Subsistence and Maritime Adaptations at Quebrada Jaguay, Camaná, Peru: A FAUNAL Analysis." PhD Thesis, University of Maine. https://scholar.google.com/scholar?cluster=8179533489966797093&hl=en&oi=scholarr.

Mentzer, S. M. 2012. "Microarchaeological Approaches to the Identification and Interpretation of Combustion Features in Prehistoric Archaeological Sites." *Journal of Archaeological Method and Theory* 21: 616–668.

Mentzer, S. M. 2017. "Micro XRF." In *Archaeological Soil and Sediment Micromorphology*, edited by C. Nicosia and G. Stoops, 1st ed. 431–440. Wiley. https://doi.org/10.1002/9781118941065.ch41.

Miller, C. E., N. J. Conard, P. Goldberg, and F. Berna. 2010. "Dumping, Sweeping and Trampling: Experimental Micromorphological Analysis of Anthropogenically Modified Combustion Features." *Palethnologie. Archéologie et Sciences Humaines* 2, no. 2: 25–37. https://doi.org/10.4000/palethnologie.8197.

Milton, E. B. P., N. D. Stansell, H. Bocherens, A. Brownlee, D. Chala-Aldana, and K. Rademaker. 2022. "Examining Surface Water δ18O and δ2H Values in the Western Central Andes: A Watershed Moment for Anthropological Mobility Studies." *Journal of Archaeological Science* 146: 105655. https://doi.org/10.1016/j.jas.2022.105655.

Ministerio del Ambiente (MINAM). 2018. "Mapa Nacional de Ecosistemas." https://geoservidor.minam.gob.pe/recursos/intercambio-de-datos/.

Moreno, A., C. M. Santoro, and C. Latorre. 2009. "Climate Change and Human Occupation in the Northernmost Chilean Altiplano Over the Last Ca. 11 500 Cal. A BP." *Journal of Quaternary Science* 24, no. 4: 373–382.

Morrissey, P., S. M. Mentzer, and S. Wurz. 2023. "The Stratigraphy and Formation of Middle Stone Age Deposits in Cave 1B, Klasies River Main Site, South Africa, With Implications for the Context, Age, and Cultural Association of the KRM 41815/SAM-AP 6222 Human Mandible." *Journal of Human Evolution* 183: 103414. https://doi.org/10.1016/j.jhevol.2023.103414.

Nester, P. L., E. Gayó, C. Latorre, T. E. Jordan, and N. Blanco. 2007. "Perennial Stream Discharge in the Hyperarid Atacama Desert of Northern Chile During the Latest Pleistocene." *Proceedings of the National Academy of Sciences* 104, no. 50: 19724–19729. https://doi.org/10.1073/pnas.0705373104.

Nicosia, C., and G. Stoops. 2017. *Archaeological Soil and Sediment Micromorphology*. Wiley.

Núñez, L., I. Cartajena, and M. Grosjean. 2013. "Archaeological Silence and Ecorefuges: Arid Events in the Puna of Atacama During the Middle Holocene." *Quaternary International, Human Populations and Environments During the Middle Holocene in the South-Central Andes* 307: 5–13. https://doi.org/10.1016/j.quaint.2013.04.028.

Núñez, L., M. Grosjean, and I. Cartajena. 2002. "Human Occupations and Climate Change in the Puna de Atacama, Chile." *Science* 298: 821–824.

Ortega, C., G. Vargas, M. Rojas, et al. 2019. "Extreme ENSO-Driven Torrential Rainfalls at the Southern Edge of the Atacama Desert During the Late Holocene and Their Projection Into the 21th Century." *Global and Planetary Change* 175: 226–237. https://doi.org/10.1016/j.gloplacha.2019.02.011.

Palacios, D., C. R. Stokes, F. M. Phillips, et al. 2020. "The Deglaciation of the Americas During the Last Glacial Termination." *Earth-Science Reviews* 203: 103113. https://doi.org/10.1016/j.earscirev.2020.103113.

Pfeiffer, M., C. Latorre, C. M. Santoro, et al. 2018. "Chronology, Stratigraphy and Hydrological Modelling of Extensive Wetlands and Paleolakes in the Hyperarid Core of the Atacama Desert During the Late Quaternary." *Quaternary Science Reviews* 197: 224–245. https://doi.org/10.1016/j.quascirev.2018.08.001.

Poch, R. M., O. Artieda, J. Herrero, and M. Lebedeva-Verba. 2010. "Gypsic Features." In *Interpretation of Micromorphological Features of Soils and Regoliths*, edited by G. Stoops, V. Marcelino and F. Mees, 195–216. Elsevier.

Power, X., L. Sitzia, S. Yrarrázaval, et al. 2022. "Ritual Stone-Built Architecture and Shell Midden Foundation: A Semisubterranean Structure in Hyperarid Atacama Desert Coast, Northern Chile." *Geoarchaeology* 37, no. 1: 198–226. https://doi.org/10.1002/gea.21857.

Pueyo, J. J., A. Sáez, S. Giralt, et al. 2011. "Carbonate and Organic Matter Sedimentation and Isotopic Signatures in Lake Chungará, Chilean Altiplano, During the Last 12.3 Kyr." *Palaeogeography, Palaeoclimatology, Palaeoecology* 307, no. 1: 339–355. https://doi.org/10.1016/j.palaeo.2011.05.036.

Quade, J., J. A. Rech, J. L. Betancourt, et al. 2008. "Paleowetlands and Regional Climate Change in the Central Atacama Desert, Northern Chile." *Quaternary Research* 69, no. 3: 343–360. https://doi.org/10.1016/j.yqres.2008.01.003.

Rademaker, K. 2024. "Updated Peru Archaeological Radiocarbon Database, 20,000–7000 14C BP." *Quaternary International* 703: 32–48. https://doi.org/10.1016/j.quaint.2024.01.012.

Rademaker, K., M. D. Glascock, B. Kaiser, D. Gibson, D. R. Lux, and M. G. Yates. 2013. "Multi-Technique Geochemical Characterization of the Alca Obsidian Source, Peruvian Andes." *Geology* 41: 779–782. https://doi.org/10.1130/G34313.1.

Rademaker, K., M. D. Glascock, D. A. Reid, E. Zuñiga, and G. R. M. Bromley. 2022. "Comprehensive Mapping and Compositional Analysis of the Alca Obsidian Source, Peru." *Quaternary International* 619: 56–71. https://doi.org/10.1016/j.quaint.2021.11.029.

Ramirez, E., G. Hoffmann, J. D. Taupin, et al. 2003. "A New Andean Deep Ice Core From Nevado Illimani (6350 m), Bolivia." *Earth and Planetary Science Letters* 212, no. 3: 337–350. https://doi.org/10.1016/S0012-821X(03)00240-1.

Rech, J. A., B. S. Currie, G. Michalski, and A. M. Cowan. 2006. "Neogene Climate Change and Uplift in the Atacama Desert, Chile." *Geology* 34, no. 9: 761–764. https://doi.org/10.1130/G22444.1.

Rech, J. A., J. Quade, and W. S. Hart. 2003. "Isotopic Evidence for the Source of Ca and S in Soil Gypsum, Anhydrite and Calcite in the Atacama Desert, Chile." *Geochimica et Cosmochimica Acta* 67, no. 4: 575–586. https://doi.org/10.1016/S0016-7037(02)01175-4.

Reitz, E. J., H. E. McInnis, D. H. Sandweiss, and S. D. deFrance. 2016. "Terminal Pleistocene and Early Holocene Fishing Strategies at Quebrada Jaguay and the Ring Site, Southern Perú." *Journal of Archaeological Science: Reports* 8: 447–453. https://doi.org/10.1016/j.jasrep.2016.05.035.

Reitz, E. J., H. E. McInnis, D. H. Sandweiss, and S. D. deFrance. 2017. "Variations in Human Adaptations During the Terminal Pleistocene and Early Holocene at Quebrada Jaguay (QJ-280) and the Ring Site, Southern Perú." *Journal of Island and Coastal Archaeology* 12, no. 2: 224–254. https://doi.org/10.1080/15564894.2016.1172381.

Rentzel, P., C. Nicosia, A. Gebhardt, D. Brönnimann, C. Pümpin, and K. Ismail-Meyer. 2017. "Trampling, Poaching and the Effect of Traffic." In *Archaeological Soil and Sediment Micromorphology*, 281–297. John Wiley & Sons, Ltd.

Riddell, F. A. 2007. "Archaeological Recovery at Quebrada de la Vaca, Chala, Peru." *Andean Past* 8, no. 1: 16.

Rigsby, C. A., J. P. Bradbury, P. A. Baker, S. M. Rollins, and M. R. Warren. 2005. "Late Quaternary Palaeolakes, Rivers, and Wetlands on the Bolivian Altiplano and Their Palaeoclimatic Implications." *Journal of Quaternary Science* 20, no. 7–8: 671–691. https://doi.org/10.1002/jqs.986.

Rüegg, W. 1952. "The Camana Formation and Its Bearing on the Andean Post-Orogenic Uplift." *Bulletin Der Vereinigung Schweiz. Petroleum-Geologen Und -Ingenieure* 19, no. 57: 7. https://doi.org/10.5169/seals-186193.

Salazar, D., C. Arenas, P. Andrade, et al. 2018. "From the Use of Space to Territorialisation During the Early Holocene in Taltal, Coastal Atacama Desert, Chile." *Quaternary International, Mobility and Use of Space in Late Pleistocene South America: Discussing Early Human Regional Trajectories* 473: 225–241. https://doi.org/10.1016/j.quaint.2017.09.035.

Salazar, D., P. Andrade, C. Borie, et al. 2013. "New Sites of the Huentelauquén Cultural Complex in the Coast of Taltal." *Taltalia* 5, no. 6: 9–19.

Sandweiss, D. H. 2003. "Terminal Pleistocene Through Mid-Holocene Archaeological Sites as Paleoclimatic Archives for the Peruvian Coast." *Palaeogeography, Palaeoclimatology, Palaeoecology* 194, no. 1: 23–40. https://doi.org/10.1016/S0031-0182(03)00270-0.

Sandweiss, D. H. 2008. "Early Fishing Societies in Western South America." In *The Handbook of South American Archaeology*, edited by H. Silverman and W. H. Isbell, 145–156. Springer.

Sandweiss, D. H. 2014. "Early Coastal South America." In *The Cambridge World Prehistory*, edited by C. Renfrew and P. Bahn, 1058–1074. Cambridge University Press. https://doi.org/10.1017/CHO9781139017831.071.

Sandweiss, D. H., and K. M. Rademaker. 2011. "El poblamiento del sur peruano: Costa y sierra." *Boletín de Arqueología PUCP* no. 15: 275–293. https://doi.org/10.18800/boletindearqueologiapucp.201101.010.

Sandweiss, D. H., B. Ojeda, J. Roque, and A. Cano. 1999. "Pescadores paleoíndios del Perú." *Investigación y Ciencia* 277: 55–61.

Sandweiss, D. H., C. F. T. Andrus, A. R. Kelley, K. A. Maasch, E. J. Reitz, and P. B. Roscoe. 2020. "Archaeological Climate Proxies and the Complexities of Reconstructing Holocene El Niño in Coastal Peru." *Proceedings of the National Academy of Sciences* 117, no. 15: 8271–8279. https://doi.org/10.1073/pnas.1912242117.

Sandweiss, D. H., H. McInnis, R. L. Burger, et al. 1998. "Quebrada Jaguay: Early South American Maritime Adaptations." *Science* 281, no. 5384: 1830–1832. https://doi.org/10.1126/science.281.5384.1830.

Schaetzl, R. J., and S. Anderson. 2005. *Soils: Genesis and Geomorphology*. Cambridge University Press.

Seltzer, G., D. Rodbell, and S. Burns. 2000. "Isotopic Evidence for Late Quaternary Climatic Change in Tropical South America." *Geology* 28, no. 1: 35–38. https://doi.org/10.1130/0091-7613(2000)28<35:IEFLQC>2.0.CO;2.

Shillito, L.-M., W. Matthews, M. J. Almond, and I. D. Bull. 2011. "The Microstratigraphy of Middens: Capturing Daily Routine in Rubbish at Neolithic Çatalhöyük, Turkey." *Antiquity* 85, no. 329: 1024–1038.

Stackelbeck, K. 2008. "Adaptational Flexibility and Processes of Emerging Complexity: Early to Mid-Holocene Foragers in the Lower Jequetepeque Valley, Northern Peru." University of Kentucky Doctoral Dissertations. https://uknowledge.uky.edu/gradschool_diss/583.

Stein, J. K. 1983. "Earthworm Activity: A Source of Potential Disturbance of Archaeological Sediments." *American Antiquity* 48, no. 2: 277–289. https://doi.org/10.2307/280451.

Stiner, M. C., S. L. Kuhn, S. Weiner, and O. Bar-Yosef. 1995. "Differential Burning, Recrystallization, and Fragmentation of Archaeological Bone." *Journal of Archaeological Science* 22, no. 2: 223–237. https://doi.org/10.1006/jasc.1995.0024.

Stoops, G. 2003. "Guidelines for the Analysis and Description of Soil and Regolith Thin Sections." Soil Science Society of America. http://hdl.handle.net/1854/LU-285112.

Stoops, G. 2021. "Guidelines for Analysis and: Description of Soil and Regolith Thin Sections." Soil Science Society of America. https://www.scribd.com/document/755877173/19994.

Stoops, G., F. Mees, and V. Marcelino. 2010. *Interpretation of Micromorphological Features of Soils and Regoliths*. Elsevier.

Stothert, K. E. 1985. "The Preceramic Las Vegas Culture of Coastal Ecuador." *American Antiquity* 50, no. 3: 613–637. https://doi.org/10.2307/280325.

Tanner, B. R. 2001. "Lithic Analysis of Chipped Stone Artifacts Recovered From Quebrada Jaguay, Peru." The University of Maine. https://digitalcommons.library.umaine.edu/etd/667.

Thompson, L. G. 1998. "A 25,000-Year Tropical Climate History From Bolivian Ice Cores." *Science* 282, no. 5395: 1858–1864. https://doi.org/10.1126/science.282.5395.1858.

Thompson, L. G., E. Mosley-Thompson, M. E. Davis, et al. 1995. "Late Glacial Stage and Holocene Tropical Ice Core Records From Huascarán, Peru." *Science* 269, no. 5220: 46–50. https://doi.org/10.1126/science.269.5220.46.

Thouret, J.-C., G. Wörner, Y. Gunnell, B. Singer, X. Zhang, and T. Souriot. 2007. "Geochronologic and Stratigraphic Constraints on Canyon Incision and Miocene Uplift of the Central Andes in Peru." *Earth and Planetary Science Letters* 263, no. 3/4: 151–166. https://doi.org/10.1016/j.epsl.2007.07.023.

Ugarte, J. 2008. "En Medio Del Desierto Tradicion Paijanense en el sur de Lima." Arqueología de La Costa Centro Sur Peruana, AVQI edicion, 39–61.

van Breukelen, M. R., H. B. Vonhof, J. C. Hellstrom, W. C. G. Wester, and D. Kroon. 2008. "Fossil Dripwater in Stalagmites Reveals Holocene Temperature and Rainfall Variation in Amazonia." *Earth and Planetary Science Letters* 275, no. 1: 54–60. https://doi.org/10.1016/j.epsl.2008.07.060.

Viles, H. A., and A. S. Goudie. 2007. "Rapid Salt Weathering in the Coastal Namib Desert: Implications for Landscape Development." *Geomorphology* 85, no. 1: 49–62. https://doi.org/10.1016/j.geomorph.2006.03.025.

Villagran, X. S. 2014. "A Redefinition of Waste: Deconstructing Shell and Fish Mound Formation Among Coastal Groups of Southern Brazil." *Journal of Anthropological Archaeology* 36: 211–227. https://doi.org/10.1016/j.jaa.2014.10.002.

Villagran, X. S. 2019. "The Shell Midden Conundrum: Comparative Micromorphology of Shell-Matrix Sites From South America." *Journal of Archaeological Method and Theory* 26, no. 1: 344–395. https://doi.org/10.1007/s10816-018-9374-2.

Villagran, X. S., A. L. Balbo, M. Madella, A. Vila, and J. Estevez. 2011. "Stratigraphic and Spatial Variability in Shell Middens: Microfacies Identification at the Ethnohistoric Site Tunel VII (Tierra del Fuego, Argentina)." *Archaeological and Anthropological Sciences* 3, no. 4: 357–378. https://doi.org/10.1007/s12520-011-0074-z.

Villagran, X. S., C. Flores, and L. Olguín, et al. 2021. "Microstratigraphy and Faunal Records from a Shell Midden on the Hyperarid Coast of the Atacama Desert (Taltal, Chile)." In *South American Contributions to World Archaeology*, edited by M. Bonomo and S. Archila, 249–281. Springer International Publishing.

Villagran, X. S., D. J. Huisman, S. M. Mentzer, C. E. Miller, and M. M. Jans. 2017. "Bone and Other Skeletal Tissues." In *Archaeological Soil and Sediment Micromorphology*, edited by C. Nicosia and G. Stoops, 9–38. John Wiley & Sons, Ltd.

Vining, B. R., B. A. Steinman, M. B. Abbott, and A. Woods. 2019. "Paleoclimatic and Archaeological Evidence From Lake Suches for Highland Andean Refugia During the Arid Middle-Holocene." *Holocene* 29, no. 2: 328–344. https://doi.org/10.1177/0959683618810405.

Voigt, C., S. Klipsch, D. Herwartz, G. Chong, and M. Staubwasser. 2020. "The Spatial Distribution of Soluble Salts in the Surface Soil of the Atacama Desert and Their Relationship to Hyperaridity." *Global and Planetary Change* 184: 103077. https://doi.org/10.1016/j.gloplacha.2019.103077.

Walk, J. 2020. Alluvial Fans Along the Coastal Atacama Desert—Landforms, Processes, and Evolution [RWTH Aachen University]. In *Dissertation: Rheinisch-Westfälische Technische Hochschule Aachen* (p. pages 1 Online-Ressource (xvii, 165 Seiten): Illustrationen, Diagramme). RWTH Aachen University. https://doi.org/10.18154/RWTH-2020-06003.

Walk, J., G. Stauch, M. Reyers, et al. 2020. "Gradients in Climate, Geology, and Topography Affecting Coastal Alluvial Fan Morphodynamics in Hyperarid Regions – The Atacama Perspective." *Global and Planetary Change* 185: 102994. https://doi.org/10.1016/j.gloplacha.2019.102994.

Walk, J., M. Bartz, G. Stauch, A. Binnie, H. Brückner, and F. Lehmkuhl. 2022. "Weathering Under Coastal Hyperaridity – Late Quaternary Development of Spectral, Textural, and Gravelometric Alluvial Fan Surface Characteristics." *Quaternary Science Reviews* 277: 107339. https://doi.org/10.1016/j.quascirev.2021.107339.

Walk, J., P. Schulte, M. Bartz, et al. 2023. "Pedogenesis at the Coastal Arid-Hyperarid Transition Deduced From a Late Quaternary Chronosequence at Paposo, Atacama Desert." *Catena* 228: 107171. https://doi.org/10.1016/j.catena.2023.107171.

Wurz, S., R. Pickering, and S. M. Mentzer. 2022. "U-Th Dating, Taphonomy, and Taxonomy of Shell Middens at Klasies River Main Site Indicate Stable and Systematic Coastal Exploitation by MIS 5c-d." *Frontiers in Earth Science* 10: 1001370. https://doi.org/10.3389/feart.2022.1001370.

Zinelabedin, A., J. Mohren, M. Wierzbicka-Wieczorek, T. J. Dunai, S. Heinze, and B. Ritter. 2025. "Haloturbation in the Northern Atacama Desert Revealed by a Hidden Subsurface Network of Calcium Sulfate Wedges." *Earth Surface Dynamics* 13, no. 2: 257–276. https://doi.org/10.5194/esurf-13-257-2025.

Supporting Information

Additional supporting information can be found online in the Supporting Information section.

SM 1.1 Columns left to right: 1) Scanned slab of sample QJ-17-1 with thin sections QJ-17-1A, QJ-17-1B and QJ-17-1C displaying micro-units placed on the block sample. 2) XRF scan of thin sections QJ-17-1A, QJ-17-1B and QJ-17-1C showing sulphur. 3) XRF scan of thin sections QJ-17-1A, QJ-17-1B and QJ-17-1C showing sodium and chloride. 4) XRF scan of thin sections QJ-17-1A, QJ-17-1B and QJ-17-1C showing aluminium, phosphor, calcium, and iron. **SM 1.2** Columns left to right: 1) Scanned slab of sample QJ-17-11 with thin sections QJ-17-11A and QJ-17-11B displaying micro-units placed on the block sample. 2) XRF scan of thin sections QJ-17-11A and QJ-17-11B showing sulphur. 3) XRF scan of thin sections QJ-17-1A and QJ-17-1B showing sodium and chloride. 4) XRF scan of thin sections QJ-17-1A and QJ-17-1B showing aluminium, phosphor, calcium, and iron.